frontiers | Research Topics

# Recent advances in the molecular genetics of glioma

**Edited by**
Pawel Buczkowicz and Caroline Chung

**Published in**
Frontiers in Genetics

ISSN 1664-8714
ISBN 978-2-8325-5484-5
DOI 10.3389/978-2-8325-5484-5

## About Frontiers

Frontiers is more than just an open access publisher of scholarly articles: it is a pioneering approach to the world of academia, radically improving the way scholarly research is managed. The grand vision of Frontiers is a world where all people have an equal opportunity to seek, share and generate knowledge. Frontiers provides immediate and permanent online open access to all its publications, but this alone is not enough to realize our grand goals.

## Frontiers journal series

The Frontiers journal series is a multi-tier and interdisciplinary set of open-access, online journals, promising a paradigm shift from the current review, selection and dissemination processes in academic publishing. All Frontiers journals are driven by researchers for researchers; therefore, they constitute a service to the scholarly community. At the same time, the *Frontiers journal series* operates on a revolutionary invention, the tiered publishing system, initially addressing specific communities of scholars, and gradually climbing up to broader public understanding, thus serving the interests of the lay society, too.

## Dedication to quality

Each Frontiers article is a landmark of the highest quality, thanks to genuinely collaborative interactions between authors and review editors, who include some of the world's best academicians. Research must be certified by peers before entering a stream of knowledge that may eventually reach the public - and shape society; therefore, Frontiers only applies the most rigorous and unbiased reviews. Frontiers revolutionizes research publishing by freely delivering the most outstanding research, evaluated with no bias from both the academic and social point of view. By applying the most advanced information technologies, Frontiers is catapulting scholarly publishing into a new generation.

## What are Frontiers Research Topics?

Frontiers Research Topics are very popular trademarks of the *Frontiers journals series*: they are collections of at least ten articles, all centered on a particular subject. With their unique mix of varied contributions from Original Research to Review Articles, Frontiers Research Topics unify the most influential researchers, the latest key findings and historical advances in a hot research area.

Find out more on how to host your own Frontiers Research Topic or contribute to one as an author by contacting the Frontiers editorial office: frontiersin.org/about/contact

# Recent advances in the molecular genetics of glioma

**Topic editors**

Pawel Buczkowicz — PhenoTips, Canada

Caroline Chung — University of Texas MD Anderson Cancer Center, United States

**Citation**

Buczkowicz, P., Chung, C., eds. (2024). *Recent advances in the molecular genetics of glioma*. Lausanne: Frontiers Media SA. doi: 10.3389/978-2-8325-5484-5

# Table of contents

frontiers | Frontiers in Genetics

TYPE Editorial
PUBLISHED 17 July 2024
DOI 10.3389/fgene.2024.1435186



OPEN ACCESS

EDITED AND REVIEWED BY
Anton A. Buzdin,
European Organisation for Research and Treatment of Cancer, Belgium

*CORRESPONDENCE
Caroline Chung,
cchung3@mdanderson.org

RECEIVED 19 May 2024
ACCEPTED 29 May 2024
PUBLISHED 17 July 2024

CITATION
Chung C and Buczkowicz P (2024), Editorial: Recent advances in the molecular genetics of glioma.
*Front. Genet.* 15:1435186.
doi: 10.3389/fgene.2024.1435186



# Editorial: Recent advances in the molecular genetics of glioma

Caroline Chung[1]* and Pawel Buczkowicz[2]

[1]Department of Radiation Oncology, University of Texas MD Anderson Cancer Center, Houston, TX, United States, [2]PhenoTips, Toronto, ON, Canada

KEYWORDS

**molecular genetics, cancer genetics, glioma, immunotherapy, brain tumor, brain cancer, neuro-oncology**

Editorial on the Research Topic
Recent advances in the molecular genetics of glioma

Gliomas, a varied and deadly group of central nervous system tumors of glial origin, are the leading cause of cancer-related death among females between 0 and 19 years and males between 0 and 39 years of age (Ostrom et al., 2022; Wang et al., 2022), highlighting the urgent need for effective diagnostic and therapeutic strategies. The molecular genetics of gliomas represent one of the most challenging and dynamic frontiers in modern oncology. Understanding the molecular genetics of glioma has become paramount in the pursuit of effective therapeutic strategies. Advances in molecular profiling have identified key genetic alterations driving gliomagenesis, offering new opportunities for targeted therapies. Single gene-targets, including mutations in genes such as EGFR, IDH, and TP53, have been extensively studied for their roles in glioma pathogenesis (Cheng and Guo, 2019; Khayari et al., 2022). Innovative treatments, including small molecule inhibitors, monoclonal antibodies, and gene editing technologies are being explored to selectively inhibit oncogenic pathways and disrupt tumor growth (Huang et al., 2022; Chen et al., 2024; Stitzlein et al., 2024). Precision medicine approaches targeting specific genetic aberrations hold promise for personalized treatment strategies tailored to individual glioma subtypes. This Research Topic highlights ten groundbreaking articles that delve into the complex molecular genetics of gliomas, including three key avenues of leveraging the genomic and molecular information for therapeutic interventions: single-targets, pan-targets, and immunotherapy.

Dysregulation of gene expression has long been correlated with the molecular landscape of gliomas. In this Research Topic, several manuscripts explore expression profiles of glioma and correlate them to prognosis. Zhao et al. uncovered a <1% mutation rate in *KIF23* using RNA sequencing and Whole-Exome Sequencing (WES) when screening 319 glioma samples. Subsequent gene-set enrichment analysis (GSEA) and review of copy number alterations (CNAs) deduced from WES data, the authors concluded that overexpression of *KIF23* was correlated with tumor samples having amplifications of the genetic region encompassing that gene, and the overexpression was positively correlated with WHO tumor grade and a worse overall survival. The analysis of gene expression of *ANXA1* in glioma by Zhang et al. utilizing three public data sources suggested the overexpression of this gene is associated with poor prognosis and that the elevated expression was an independent prognostic factor in glioma. Liu et al. identified elevated *ESPL1* expression in glioma using GSEA and

correlated the findings to poor overall survival. The authors performed *in silico* analysis of potential drug targets using CMap, identifying antimycin A, thioguanosine, and zidovudine as potential small-molecules inhibitors of this gene's signaling pathway. In a meta-analysis of four glioma datasets (TCGA, CGGA, GSE6011 and Rembrandt) by Zhou et al., high level expression of GAS2L3 was associated with higher grade tumor and shorter overall survival. Yang et al. found that centromeric protein A (CENP-A), a protein involved in chromosomal segregation during cell division, was upregulated in gliomas and high CENP-A levels were associated with high grade, response to therapy and shorter overall survival.

In contrast to their high-grade counterparts, low-grade glioma (LGG), which are categorized as WHO Grade I or II, pose different challenges driven by biological processes highlighted in three articles included in this Research Topic. Shi et al. conducted gene expression profiling of 433 LGG patients available in the TCGA database, identifying *JAG1* overexpression and Notch pathway activation as indicators of poorer prognosis and immune response in LGG. Implications of E3-related gene signatures in LGG was investigated by Tan *et al.* who identified *AURKA, MAP3K1, PCGF2, PRKN, TLE3, TRIM17,* and *TRIM34* as part of an E3-related prognostic signature and its role in LGG prognosis and tumor immune microenvironment cell infiltration. Lin et al. investigated six autophagy-related genes (BAG1, PTK6, EEF2, PEA15, ITGA6, and MAP1LC3C) to construct an autophagy-related prognostic risk model in LGG that was validated as an independent risk predictor for survival. These studies emphasize the crucial importance of gene expression profiles in understanding glioma prognosis and shaping therapeutic strategies.

To leverage the genomic and molecular information for therapeutic intervention, while single gene-targeted therapies have shown efficacy in subsets of glioma patients, the inherent heterogeneity within tumors often leads to therapeutic resistance and disease progression. Pan-targeted approaches aim to overcome this challenge by simultaneously inhibiting multiple signaling pathways involved in glioma progression. Multi-targeted kinase inhibitors, epigenetic modulators, and combination therapies are being developed to comprehensively disrupt tumor cell survival and proliferation. By targeting interconnected signaling networks, pan-targeted therapies offer the potential for synergistic effects and improved clinical outcomes in glioma patients. The need for combination therapy is blatantly apparent in the most aggressive and inoperable subtypes of glioma, those affecting the brainstem such as Diffuse Intrinsic Pontine Glioma (DIPG). Due to an intact blood-brain-barrier and unique molecular profile, these tumors have unique treatment challenges.

Immunotherapy has emerged as a promising approach across many solid tumors including for the treatment of gliomas. Strategies such as immune checkpoint inhibitors, chimeric antigen receptor T (CAR-T) cell therapy, and peptide vaccines are being investigated to enhance anti-tumor immune responses. By modulating immune checkpoints or directly engaging immune effector cells, immunotherapy offers a novel paradigm for glioma management, aiming to overcome immunosuppressive mechanisms within the tumor microenvironment. Lin et al. review the most recent advances in emerging technologies such as Magnetic Resonance guided Focused Ultrasound (MRgFUS) and various immunotherapy treatments such as cancer vaccines, autologous cell transfer therapy, CAR-T cell therapy, and immune checkpoint blockers for DIPG. Regarding immune related biomarkers, long noncoding RNAs (lncRNAs), which are noncoding RNAs that are more than 200 nucleotides in length without significant protein-coding function have been shown that these are immune-related and are prognostic.

In summary, the complex and heterogeneous molecular genetics of gliomas pose both daunting challenges and exciting opportunities ripe for therapeutic exploration. Immunotherapy, single gene-targets, and pan-targets represent distinct yet complementary strategies in the pursuit of more effective and personalized treatments for glioma patients. Ongoing research is imperative to unravel the intricate genetic and molecular mechanisms driving glioma development and resistance, paving the way for groundbreaking interventions that could dramatically improve patient survival, outcomes, and quality of life.

## Author contributions

CC: Conceptualization, Writing–original draft, Writing–review and editing. PB: Conceptualization, Writing–original draft, Writing–review and editing.

## Funding

The author(s) declare that no financial support was received for the research, authorship, and/or publication of this article.

## Conflict of interest

Author PB was employed by PhenoTips.

The remaining author declares that the research was conducted in the absence of any commercial or financial relationships that could be construed as a potential conflict of interest.

The author(s) declared that they were an editorial board member of Frontiers, at the time of submission. This had no impact on the peer review process and the final decision.

## Publisher's note

# References

Chen, X., Cui, Y., and Zou, L. (2024). Treatment advances in high-grade gliomas. *Front. Oncol.* 14, 1287725. doi:10.3389/fonc.2024.1287725

Cheng, F., and Guo, D. (2019). MET in glioma: signaling pathways and targeted therapies. *J. Exp. Clin. Cancer Res.* 38 (1), 270. doi:10.1186/s13046-019-1269-x

Huang, W., Hao, Z., Mao, F., and Guo, D. (2022). Small molecule inhibitors in adult high-grade glioma: from the past to the future. *Front. Oncol.* 12, 911876. doi:10.3389/fonc.2022.911876

Khayari, A., Bouchmaa, N., Taib, B., Wei, Z., Zeng, A., and El Fatimy, R. (2022). Metabolic rewiring in glioblastoma cancer: EGFR, IDH and beyond. *Front. Oncol.* 12, 901951. doi:10.3389/fonc.2022.901951

Ostrom, Q. T., Price, M., Ryan, K., Edelson, J., Neff, C., Cioffi, G., et al. (2022). CBTRUS statistical report: pediatric brain tumor foundation childhood and adolescent primary brain and other central nervous system tumors diagnosed in the United States in 2014-2018. *Neuro Oncol.* 24 (Suppl. 3), iii1–iii38. doi:10.1093/neuonc/noac161

Stitzlein, L. M., Adams, J. T., Stitzlein, E. N., Dudley, R. W., and Chandra, J. (2024). Current and future therapeutic strategies for high-grade gliomas leveraging the interplay between epigenetic regulators and kinase signaling networks. *J. Exp. Clin. Cancer Res.* 43 (1), 12. doi:10.1186/s13046-023-02923-7

Wang, G. M., Cioffi, G., Patil, N., Waite, K. A., Lanese, R., Ostrom, Q. T., et al. (2022). Importance of the intersection of age and sex to understand variation in incidence and survival for primary malignant gliomas. *Neuro Oncol.* 24 (2), 302–310. doi:10.1093/neuonc/noab199

frontiers in Genetics

ORIGINAL RESEARCH
published: 30 March 2021
doi: 10.3389/fgene.2021.649270

# Elevated GAS2L3 Expression Correlates With Poor Prognosis in Patients With Glioma: A Study Based on Bioinformatics and Immunohistochemical Analysis

*Yan Zhou[1†], Limin Zhang[1†], Sirong Song[1†], Lixia Xu[2], Yan Yan[3], Haiyang Wu[1], Xiaoguang Tong[2,4*] and Hua Yan[2,4*]*

*[1] Clinical College of Neurology, Neurosurgery and Neurorehabilitation, Tianjin Medical University, Tianjin, China, [2] Tianjin Key Laboratory of Cerebral Vascular and Neurodegenerative Diseases, Tianjin Neurosurgical Institute, Tianjin Huanhu Hospital, Tianjin, China, [3] Department of Clinical Laboratory, Tianjin Huanhu Hospital, Tianjin, China, [4] Department of Neurosurgery, Tianjin Huanhu Hospital, Tianjin, China*

OPEN ACCESS

**Edited by:**
*Stefan Gaubatz, Biocenter, University of Wuerzburg, Germany*

**Reviewed by:**
*Parik Kakani, Indian Institute of Science Education and Research, Bhopal, India*
*Gabriella D'Orazi, G. D'Annunzio University of Chieti-Pescara, Italy*

***Correspondence:**
*Hua Yan*
*yanhua20042007@sina.com*
*Xiaoguang Tong*
*tongxg@yahoo.com*

*[†] These authors have contributed equally to this work*

**Specialty section:**
*This article was submitted to Cancer Genetics and Oncogenomics, a section of the journal Frontiers in Genetics*

**Received:** *04 January 2021*
**Accepted:** *22 February 2021*
**Published:** *30 March 2021*

**Citation:**
*Zhou Y, Zhang L, Song S, Xu L, Yan Y, Wu H, Tong X and Yan H (2021) Elevated GAS2L3 Expression Correlates With Poor Prognosis in Patients With Glioma: A Study Based on Bioinformatics and Immunohistochemical Analysis. Front. Genet. 12:649270. doi: 10.3389/fgene.2021.649270*

**Background:** Growth arrest–specific 2 like 3 (GAS2L3) is a cytoskeleton-associated protein that interacts with actin filaments and tubulin. Abnormal GAS2L3 expression has been reported to be associated with carcinogenesis. However, the biological role of GAS2L3 in glioma remains to be determined.

**Methods:** The transcriptome level of GAS2L3 and its relationship with clinicopathological characteristics were analyzed among multiple public databases and clinical specimens. Bioinformatics analyses were conducted to explore biological functions and prognostic value of GAS2L3 in glioma.

**Results:** GAS2L3 was substantially expressed in glioma, and high GAS2L3 expression correlated with shorter overall survival time and poor clinical variables. Gene set enrichment analysis (GSEA), single-sample gene-set enrichment analysis, and CIBERSORT algorithm analyses showed that GAS2L3 expression was closely linked to immune-related pathways, inflammatory activities, and immune cell infiltration. Moreover, GAS2L3 was synergistic with T cell–inflamed gene signature, immune checkpoints, T-cell receptor diversities, and neoantigen numbers.

**Conclusion:** This study suggests that GAS2L3 is a prognostic biomarker for glioma, providing a reference for further study of the potential role of GAS2L3 in the immunomodulation of glioma.

**Keywords: GAS2L3, glioma, bioinformatics, biomarker, tumor microenvironment**

## INTRODUCTION

Worldwide, gliomas account for approximately 40–50% of all neoplasms of the central nervous system (CNS) (Ostrom et al., 2018). Although advances in glioma treatment have been achieved in the past decades, the therapeutic efficacy, especially on glioblastoma (GBM), is still limited (5-year survival are approximately only 5.5%) (Omuro and DeAngelis, 2013). The molecular

mechanisms underlying tumor development and progression are poorly understood, and the lack of specific markers for tumor type or disease stage further impedes the current understanding and treatments of glioma.

The growth arrest–specific 2 (GAS2) family, consisting of four related proteins (GAS2, GAS2L1, GAS2L2, and GAS2L3), participate in cross-linking of actin and microtubule filaments in interphase and in growth-arrested cells (Goriounov et al., 2003; Stroud et al., 2011). Unlike members, GAS2L3 mRNA expression in resting cells is extremely low, whereas the expression level gradually increases when the cell reenters the cell cycle and reaches a peak in the G2/M phase (Wolter et al., 2012). The loss of GAS2L3 and overexpression studies have implicated GAS2L3 in cytokinesis, chromosome segregation, and abscission (Pe'Er et al., 2013). Recently, it has been reported that GAS2L3 was dysregulated in various tumor cells. Shi et al. (2020) reported that GAS2L3 was significantly related to the deterioration of overall survival (OS) and disease-free survival in hepatocellular carcinoma. Seidl et al. (2010) reported that GAS2L3 was downregulated after incubation with highly cytotoxic α-emitter immunoconjugates in gastric cancer cells. However, the role of GAS2L3 in glioma has not been reported.

Here, we investigated the association between GAS2L3 gene expression and glioma clinical characteristics using data from public databases and clinical samples from our institution. Additionally, its potential roles in immune response and immune infiltration of tumor microenvironment (TME) were analyzed. Our results could potentially reveal new targets and strategies for glioma diagnosis and treatment.

# MATERIALS AND METHODS

## Dataset Selection

The mRNA level of GAS2L3 in different cancer types was confirmed by the Oncomine database. In glioma, gene expression and relevant clinical data of patients were obtained from five cancer datasets. The Cancer Genome Atlas (TCGA) (Wang et al., 2016) dataset was used as a discover set, whereas the Chinese Glioma Genome Atlas (CGGA) (Yan et al., 2012), the GSE16011 (from Gene Expression Omnibus database) (Gravendeel et al., 2009), and the Repository of Molecular Brain Neoplasia Data (REMBRANDT) (Madhavan et al., 2009) as validation sets. Additionally, we enrolled a total of 127 glioma patients from the department of neurosurgery, Huanhu Hospital (Tianjin, China), as the external validation set. All patients signed an informed consent form. The study protocol was approved by Huanhu Hospital Ethics Committee (Tianjin, China).

## Immunohistochemistry

Tumor tissues were surgically excised and were immediately fixed in 10% neutral buffered formalin for 24 h and then embedded in paraffin. Tissue slides were prepared and deparaffinized by baking in oven 60°C for 1 h. Then, antigen unmasking was done in boiling container with sodium citrate buffer for 20 min. Goat serum was used for blocking. Slides were then stained with GAS2L3 rabbit polyclonal antibody (1:400, bioss, BS-23297R) overnight at 4°C, and secondary antibodies were incubated for 1 h at room temperature. Positive or negative staining of GAS2L3 was independently evaluated by two experienced pathologists, and samples were divided into two groups: low expression group, including negative (−) and weak (+) staining, and high expression group, including moderate (++) and strong (+++) staining (Xiao et al., 2015).

## Bioinformatics Analysis

The examination of tumor/normal differential expression analysis of GAS2L3 in TCGA was performed by GEPIA, an interactive web server containing 8,587 normal samples from the GTEx database (Tang et al., 2019). The correlation between GAS2L3 expression and various clinical characteristics was analyzed and plotted using beeswarm R package. Kaplan–Meier curve, receiver operating characteristic (ROC) curve, and area under the ROC curve (AUC) were graphed using survival, survminer, and ROC packages. Univariate and multivariate Cox analyses were performed to compare the impact of GAS2L3 expression on the OS alongside with other clinical variables. The bioinformatics analyses were performed utilizing R software v3.6.3. All R packages were downloaded from CRAN[1] and Bioconductor[2].

## Meta-Analysis

We performed a meta-analysis to assess the overall prognostic value of GAS2L3 in glioma patients among four datasets. Combined hazard ratio (HR) and 95% confidence interval (CI) were used to measure the effect size. The heterogeneity among datasets was assessed by the $Q$ test ($I^2$ statistics). The random-effects model was used to minimize the influence of heterogeneity, whereas $I^2 > 50\%$ or $P < 0.10$; otherwise, the fixed-effects model would be applied. The meta-analysis was conducted in STATA 15 software.

## Comprehensive Correlation Analysis in Tumor Immunity

In the discovery cohort, gene set enrichment analysis (GSEA) (Subramanian et al., 2005) was conducted to identify Gene Ontology (GO) and Kyoto Encyclopedia of Genes and Genomes (KEGG) pathways, which showed statistically significant differences between high and low GAS2L3 expression cohorts. The annotated gene sets of c5.all.v7.2.symbols.gmt and c2.cp.kegg.v7.2.symbols.gmt in the MSigDB were selected in GSEA version 4.0 software. The false discovery rate < 0.25 and normal $P < 0.05$ were used as thresholds. The single-sample GSEA (ssGSEA) was used to analyze the RNA-seq data of 29 important immune signatures from each glioma sample in the form of ssGSEA scores. The signatures for immune cell types were obtained from previous publications (Bindea et al., 2013; Liu et al., 2018; Zhou et al., 2020). Furthermore, 22 types of tumor-infiltrating immune cells [tumor-infiltrating lymphocytes (TILs)] in glioma microenvironment were assessed based on CIBERSORT deconvolution algorithm (Newman et al., 2015).

[1]http://cran.r-project.org/

[2]http://bioconductor.org/

The gene expression signature of 22 TILs was obtained from the CIBERSORT platform[3].

The T cell–inflamed gene signature, obtained from a previously report (Ayers et al., 2017), was calculated by gene set variation analysis (GSVA). Then, we calculated the expression levels of programmed cell death ligand 1 (PD-L1) and other immune checkpoints in sample with GAS2L3-low and -high. Gene indel mutations and single-nucleotide variants are prone to result in major histocompatibility complex–binding neoantigens, which can be recognized by immune cells. The neoantigen load for each patient from the discovery cohort was obtained from a previous paper (Schumacher and Schreiber, 2015). The T-cell receptor (TCR) diversities of patients from the discovery cohort, which were measured using the Shannon entropy, were obtained from a previous report (Thorsson et al., 2018).

## Statistical Analysis

Patients with missing information were excluded from the corresponding analysis. Mann–Whitney *U* and Kruskal–Wallis test were used to analyze the relationship between GAS2L3 mRNA expression and the clinical features of glioma. For GAS2L3 protein expression, $\chi^2$ test was employed. The proportions of TILs between GAS2L3 expression-low and -high subtypes were compared using the Mann–Whitney *U* test. The statistical analyses were performed utilizing R software v3.6.3 and GraphPad Prism 7. All statistical tests were two-sided. $P < 0.05$ was used to determine the significance level.

# RESULTS

## Preparation of Datasets

A total of 2,604 cases (including 41 non-tumor samples) from discovery and validation datasets were included in this study. The characteristics of the glioma patients in these five datasets were concluded in **Table 1**. Patients' detailed information of Huanhu dataset is shown in **Supplementary Table 1**.

**TABLE 1 |** Characteristics of patients in TCGA, CGGA, GSE16011, REMBRANDT, and Huanhu datasets.

| Characteristic | TCGA | CGGA | GSE16011 | REMBRANDT | Huanhu |
|---|---|---|---|---|---|
| **Total** | 703 | 1,018 | 284 | 472 | 127 |
| **Age (years)** | | | | | |
| ≥52 | 263 | 191 | 133 | | 45 |
| <52 | 407 | 558 | 143 | | 82 |
| **Gender** | | | | | |
| Male | 651 | 442 | 184 | 221 | 77 |
| Female | 460 | 307 | 92 | 126 | 50 |
| **Grade** | | | | | |
| I | | | 8 | 2 | |
| II | 249 | 218 | 24 | 98 | 39 |
| III | 265 | 240 | 85 | 85 | 35 |
| IV | 596 | 291 | 159 | 130 | 53 |
| **Histology** | | | | | |
| Pilocytic astrocytoma | | | 8 | | |
| Astrocytoma | 194 | 150 | 29 | 147 | 28 |
| Oligodendroglioma | 191 | 76 | 52 | 67 | 46 |
| Oligoastrocytoma | 130 | 232 | 28 | | |
| Glioblastoma | 596 | 291 | 159 | 219 | 53 |
| Mixed glioma | | | | 11 | |
| **IDH1 mutation** | | | | | |
| Yes | 91 | 410 | 81 | | 87 |
| No | 34 | 339 | 140 | | 40 |
| **1p19q codeleted** | | | | | |
| Yes | | 155 | 110 | | |
| No | | 594 | 45 | | |
| **KPS** | | | | | |
| <80 | 151 | | 82 | | |
| ≥80 | 584 | | 182 | | |

## GAS2L3 Transcript Levels in Different Databases

First, the mRNA levels of GAS2L3 in different cancers were analyzed in Oncomine database. Relative to control specimens, GAS2L3 was significantly upregulated in brain and CNS, breast cancer, gastric cancer, kidney cancer, and pancreatic cancer, but downregulated in leukemia (**Figure 1A**). These results suggest that the high expression of GAS2L3 is common in various types of cancer.

In glioma, GAS2L3 mRNA expression data from TCGA and 207 normal samples from the GTEx project were analyzed based on GEPIA, and we found that GAS2L3 was significantly upregulated in GBM and had a relative increased expression in lower-grade glioma compared to normal samples (**Figure 1B**). The differential expression was also confirmed in validation datasets (**Figures 1C,D**). Additionally, the expression levels of other GAS2 members in glioma were also analyzed by GEPIA, but no upregulation was found compared with the control group (**Supplementary Figure 1**).

For protein expression level, immunohistochemistry (IHC) staining indicated that 67.7% (86/127) of glioma tissues had high GAS2L3 expression. Representative slides are displayed in **Figure 1E** and **Supplementary Figure 1**. Taken together, GAS2L3 was highly expressed at both transcriptional and proteomic levels in glioma tissues.

## GAS2L3 Is Associated With Clinicopathological Features of Glioma

Because of the heterogeneity of glioma (Lapointe et al., 2018), the mRNA expression data were analyzed according to the World Health Organization (WHO) grade, histology, age, isocitrate dehydrogenase 1 (IDH1) mutation, and other features. In TCGA, CGGA, GSE16011, and Rembrandt datasets, the expression of GAS2L3 was the highest in the grade IV compared with the low-grade tumors (**Figure 2A**). Besides, GAS2L3 expression increased in higher histopathologic malignancies (**Figure 2B**). As for age and IDH1 mutation status, the higher expression level of GAS2L3 was detected in patients older than 41 years and those with wild-type IDH1 in TCGA, CGGA, and GSE16011 datasets (**Figures 2C,D**). Then, we quantified the protein level of GAS2L3

[3]https://cibersortx.stanford.edu/

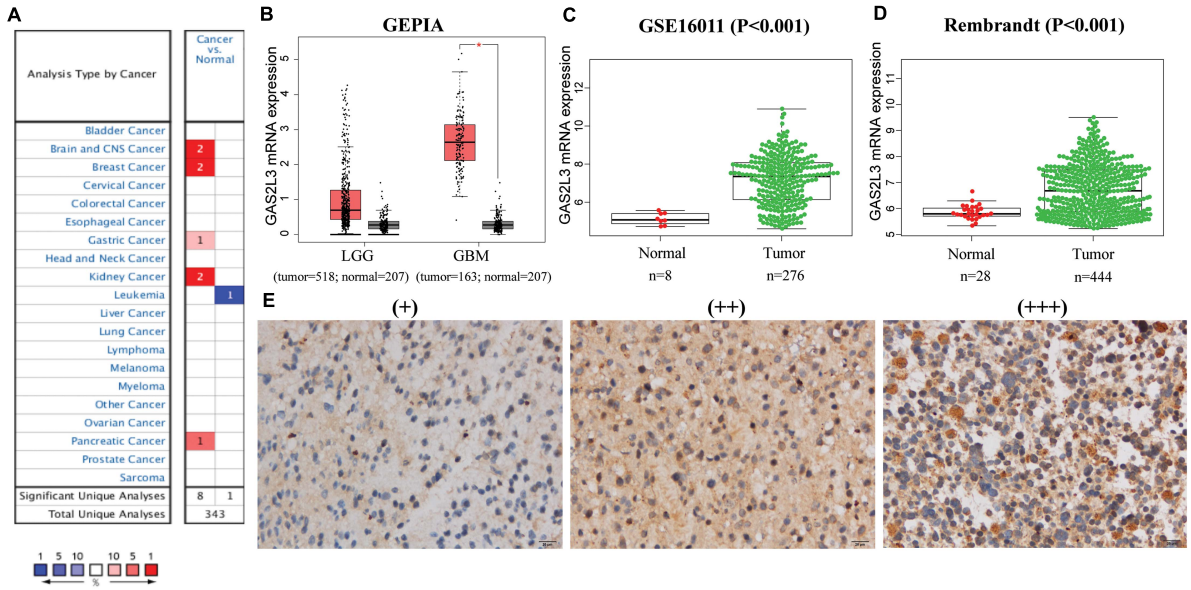


**FIGURE 1 |** The mRNA and protein expression levels of GAS2L3. **(A)** GAS2L3 expression level in cancers in Oncomine database: the left box in red indicates the number of datasets with GAS2L3 overexpression, and the right box in blue indicates the number of datasets with GAS2L3 hypoexpression after comparing cancerous and normal tissues. **(B–D)** TCGA (based on GEPIA), GSE16011, and REMBRANDT datasets support the findings that indicate GAS2L3 upregulation in glioma (*$P < 0.05$). **(E)** GAS2L3 protein expression was detected in glioma tissues from Huanhu dataset.

in Huanhu cohort by IHC staining. GAS2L3 was highly expressed in advanced grades and histopathologic types and wild-type IDH1, although no association was found between GAS2L3 expression and age (**Figure 2E**). Additionally, some other clinical characteristics [1p19q codeletion status, Karnofsky Performance Status (KPS), chemotherapy, radiotherapy, gender and recurrent status] were also analyzed (**Supplementary Figure 2**). These results indicated that high expression of GAS2L3 predicted high malignant glioma.

## GAS2L3 Predicts Worse Survival in Glioma

To investigate the prognostic value of GAS2L3 expression, patients were divided into low or high groups based on the median expression value. Kaplan–Meier plots demonstrated that high level of GAS2L3 expression was correlated with unfavorable OS of glioma patients in different datasets (**Figures 3A–D**). ROC analysis showed that GAS2L3 could be a good predictor of 1-year (AUC = 0.842), 3-year (AUC = 0.843), and 5-year survival (AUC = 0.838) (**Figure 3E**). These results were validated in other datasets (**Figures 3F–H**).

## Cox Regression Analysis and Meta-Analysis

To further explore the prognostic value of GAS2L3, univariate and multivariate Cox regression analyses were conducted in both TCGA and CGGA datasets. In TCGA cohort, the univariate analysis showed that patients with GAS2L3-high expression had worse OS (HR = 2.50, 95% CI [2.08–3.01], $P < 0.001$) (**Figure 4A**). Besides, clinical characteristics, age (HR = 1.06, 95% CI [1.05–1.08]), grade (HR = 4.71, 95% CI [3.51–6.34]), histological type (HR = 1.71, 95% CI[1.42–2.06]), and KPS (HR = 0.952, 95% CI [0.940–0.964]) also correlated significantly with poor survival (all with $P < 0.001$). After adjusting for other clinicopathologic characteristics, the multivariate analysis revealed that GAS2L3 expression remained independently associated with OS (**Figure 4B**, HR = 1.77, 95% CI [1.38–2.27], $P < 0.001$). These results were also validated in CGGA cohort (**Figures 4C,D**), demonstrating that GAS2L3 expression is an independent prognostic factor of glioma.

As no published studies have focused on the prognostic role of GAS2L3 expression in glioma, an integrated meta-analysis of four datasets was carried out to assess the overall prognostic value of GAS2L3 in glioma patients (**Figure 4E**). The pooled HR (HR = 1.48, 95% CI [1.30–1.67]) using the random-effects model suggested that a higher expression level of GAS2L3 significantly predicted poorer OS in patients with glioma. However, heterogeneity was found ($I^2 = 74.9\%$, $P = 0.008$), which may be partly attributed to the differences of Cox regression analyses for HR, sequencing methods, or countries among patients in four datasets.

## GAS2L3-Related Immune and Inflammatory Pathways

Patients with high GAS2L3 expression had a short OS time, suggesting that GAS2L3 may be involved in the initiation and the progression of glioma. Then, we performed GSEA to identify GO and KEGG signaling pathways, which were enriched in GAS2L3-high expression phenotype in TCGA. The GO analysis showed that a set of pathways, especially those related to

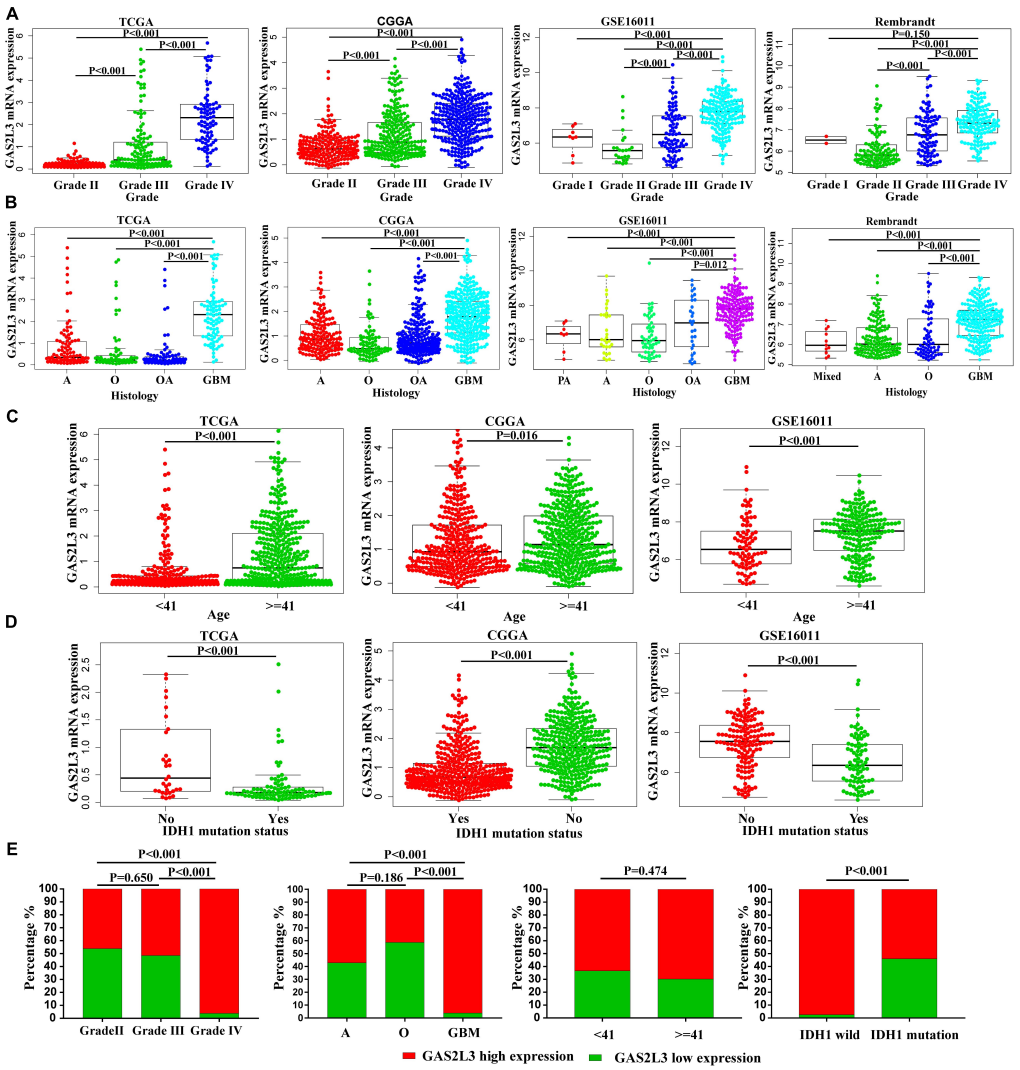


**FIGURE 2 |** Associations between GAS2L3 expression and clinicopathologic variables in different datasets. **(A)** WHO grade, **(B)** histological type; PA: pilocytic astrocytoma, A: astrocytoma, O: oligodendroglioma, OA: oligoastrocytoma, mixed: mixed histological type, GBM: glioblastoma, **(C)** age (years), **(D)** IDH1 mutation status, **(E)** the differential protein expression of GAS2L3 in samples from Huanhu dataset by IHC method.

immunity, was enriched, including regulation of innate immune response, regulation of lymphocyte migration, regulation of B cell–mediated immunity, immune response to tumor cell, and so on. Meanwhile, immune-related pathways, such as leukocyte transendothelial migration, TCR signaling pathway, and toll-like receptor signaling pathway, were also enriched in a cohort with GAS2L3-high by KEGG analysis (**Figure 5A**). These results indicated that GAS2L3 may play an essential role in the immune microenvironment of glioma.

## The Relationship Between GAS2L3 and Immune Infiltration and Activities

To better comprehend the role of GAS2L3 in immune activities, we used the ssGSEA to explore the relationship between GAS2L3 and activities or enrichment levels of immune cells and functions, based on the 29 well-established immune-associated gene sets (Bindea et al., 2013; Liu et al., 2018; Zhou et al., 2020). As the heatmap showed (**Figure 5B**), some immune cell types, such as $CD8^+$ T, macrophages, T helper cells, regulatory T cells (Tregs), immature dendritic cells (iDCs), and plasmacytoid dendritic cells (pDCs), were infiltrated in glioma samples with GAS2L3-high, whereas natural killer cells (NK cells) had an opposite trend. Additionally, some immune-associated functions also had positive correlations with GAS2L3 expression. The marker genes of antigen-presenting cells (APCs) costimulation, APC coinhibition, chemokine receptor (CCR), immune checkpoint, cytolytic activity, human leukocyte antigen, inflammation promoting, major histocompatibility complex class I, parainflammation, T-cell costimulation, T-cell coinhibition, and types I and II interferon (IFN) responses were more

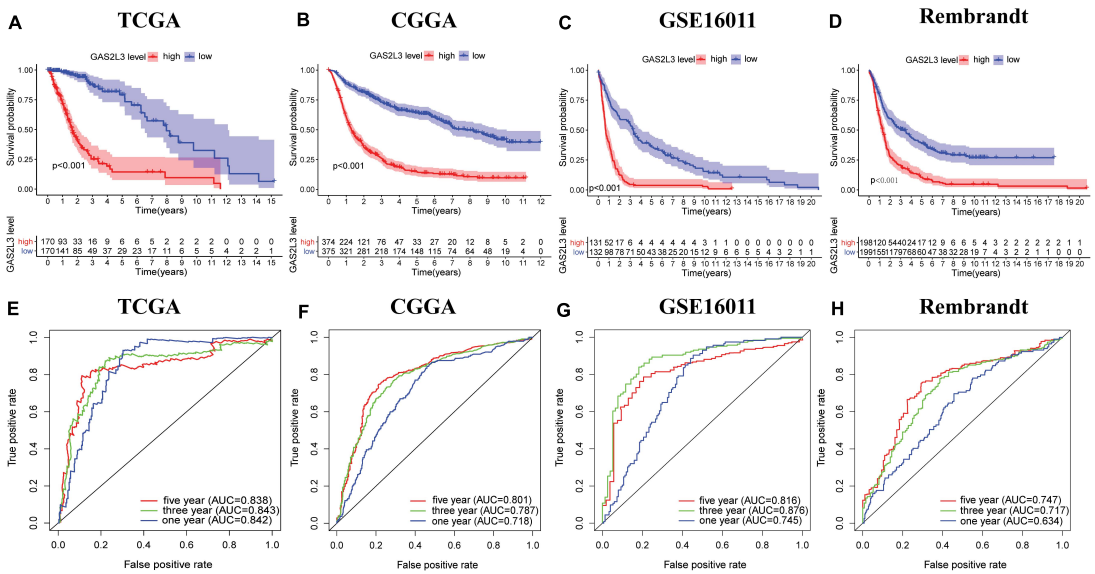


**FIGURE 3 |** Associations between GAS2L3 expression and prognosis of patients in different datasets. **(A–D)** Kaplan–Meier estimated of overall survival between groups harboring different GAS2L3 expression. **(E–H)** Time-dependent ROC curves of overall survival at 1, 3, and 5 years.

highly expressed in samples with GAS2L3-high than in those with GAS2L3-low.

As TILs play an essential pathophysiological role in the development of glioma (Domingues et al., 2016), we systematically estimated the proportions of 22 TILs in TCGA glioma samples based on CIBERSORT algorithm (Newman et al., 2015). The results showed the TIL subsets had significantly different proportions in different GAS2L3 expression cohorts (**Figure 5C**). Coincided with ssGSEA analysis, we observed that $CD8^+$ T cells, Tregs, $\gamma\delta$ T cells, neutrophils, and macrophages M0, M1, and M2 were enriched in GAS2L3-high cohort. Nevertheless, monocytes, NK cells activated, mast cells activated, and eosinophils were enriched in the GAS2L3-low cohort. These results indicated that GAS2L3 has a close relationship with immunomodulation of glioma.

## GAS2L3 Is a Predictive Marker for Response of Immunotherapy

Traditional therapies combined with immunotherapies, such as immune checkpoint inhibitors and chimeric antigen receptor T cells, have gained promising results in multiple tumor treatments (Abril-Rodriguez and Ribas, 2017). Several studies have explored the usage of immunotherapy against glioma (Suryadevara et al., 2015); however, the therapeutic efficacy was still less than satisfactory. Here, we investigated the potential of patients with different GAS2L3 expression to respond to anti–programmed cell death 1 (PD-1) therapy. As **Figure 6A** showed, the T cell–inflamed signature, a predictor of responses to anti–PD-1 therapy in various types of cancer (Ayers et al., 2017), was significantly enriched in tumors with GAS2L3-high based on GSEA analysis. The T cell–inflamed signature score calculated by GSVA was also higher in GAS2L3-high tumors (**Figure 6B**). Patients with higher PD-L1 expression tend to gain more clinical benefits from anti–PD-1 therapy (Ayers et al., 2017). Here, we found that GAS2L3 had positive associations with PD-L1, B7-H3, and other immune checkpoints (**Figure 6C**). The TCR diversity and neoantigen numbers, also known to be predictive markers for anti–PD-1 therapy (Tumeh et al., 2014), were similarly higher in tumors with GAS2L3-high (**Figures 6D,E**). In conclusion, GAS2L3 can help to predict response of antitumor immunotherapy.

# DISCUSSION

Glioma is the most prevalent and lethal primary brain tumors in adults (Ostrom et al., 2018). Because of the limited improvements in the treatment of glioma, new therapeutic methods are urgently needed. A variety of indicators, such as genetic aberrations and tumor environment, have been reported to participate in the development and progression of glioma (Molinaro et al., 2019). The potential roles of GAS2 family in tumorigenesis of liver cancer (Zhu et al., 2015), leukemia (Kong et al., 2020), recurrent colorectal cancer (Chang et al., 2016), or lung adenocarcinoma (Murugesan et al., 2018) have been explored. However, the prognostic value of GAS2L3 in glioma still remains unclear. In this study, we evaluated the expression level and prognostic value of GAS2L3 in glioma based on public databases and clinical specimens. We observed that GAS2L3 was significantly upregulated in glioma that was associated with malignant behavior. Our Cox regression models showed that a high level of GAS2L3 expression correlated with shorter patients' survival time. Meta-analysis containing patients from four public databases further established the critical role of high GAS2L3 expression in the adverse prognosis of glioma patients. Functional enrichment analysis illustrated that GAS2L3

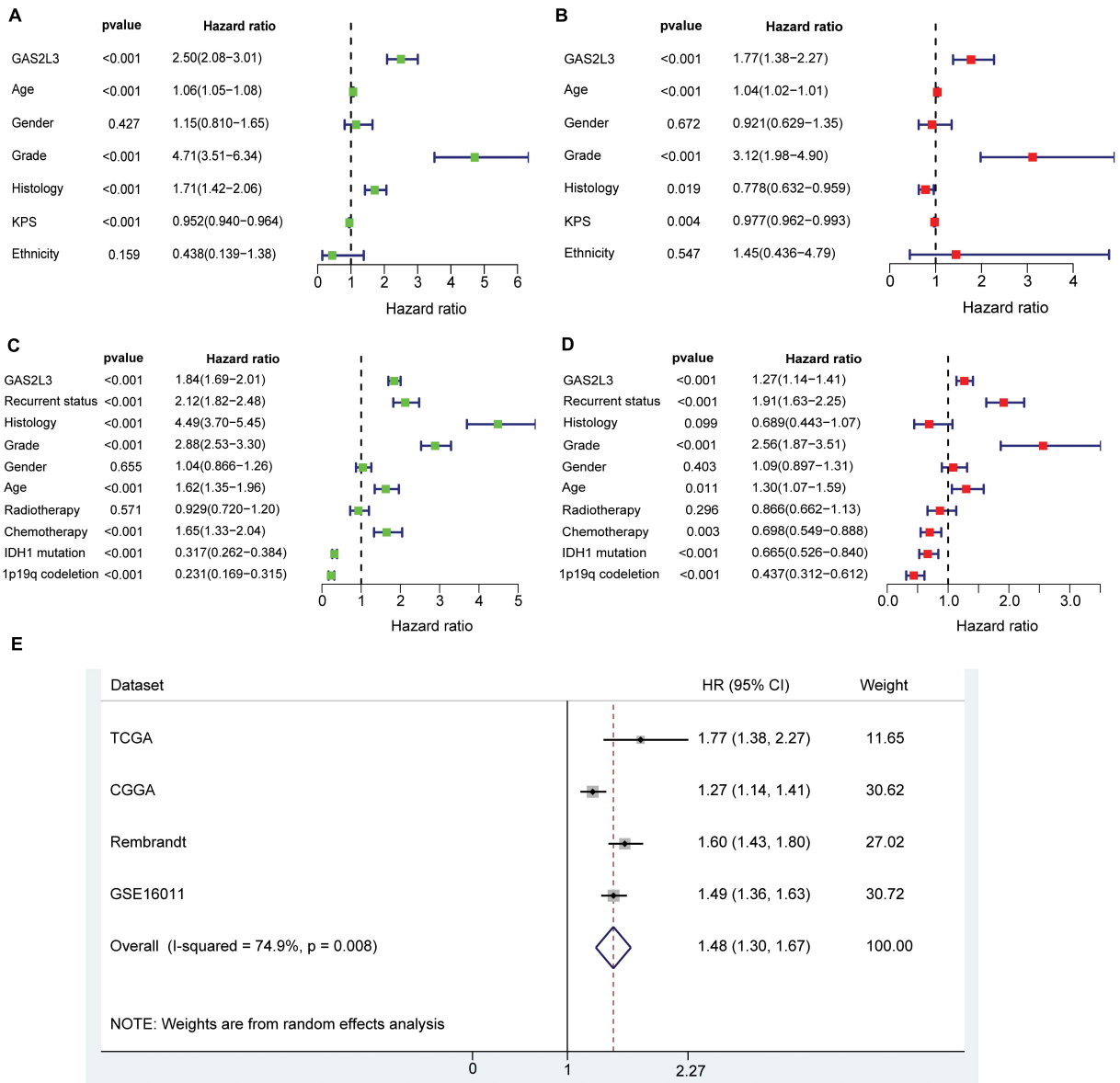


**FIGURE 4 |** Univariate and multivariate Cox regression analyses regarding OS in TCGA dataset **(A,B)** and CGGA validation dataset **(C,D)**. Precise forest plots were graphed, respectively. **(E)** Forest plot of a meta-analysis of high GAS2L3 expression with worse OS in glioma patients from four datasets.

was significantly involved in plenty of immune-related pathways, such as regulation of lymphocyte migration, TCR signaling pathway, and immune response to tumor cell.

Studies have shown that the TME, especially immune microenvironment, has a great impact on the development of cancers (Li et al., 2017; Wang et al., 2017). However, the functions of GAS2L3 in the TME have not been reported. Here, we employed two different methods (ssGSEA analysis and CIBERSORT algorithm) to investigate the impact of GAS2L3 on infiltration of immune cells in glioma. ssGSEA showed that GAS2L3 was positively correlated with the infiltration of various immune cell types, including T cells [$CD8^+$ T cells, T helper cell 1 [$T_H1$] cells, $T_H2$ cells, PD-L1], macrophages, iDCs, and pDCs, whereas NK cells had an opposite trend. CIBERSORT algorithm further revealed that GAS2L3 impacted the proportions of 22 TILs in glioma. Patients with different level of GAS2L3 expression had significant differences in the proportion of immune infiltration. For example, the proportions of $CD8^+$ T cells, Tregs, γδ T cells, neutrophils, and macrophages M0, M1, and M2 were higher in the group with GAS2L3-high, which were coincided with the ssGSEA analysis. The infiltration of DCs, the classical APCs, can help present tumor-associated antigens to T cells (Gardner and Ruffell, 2016). The increase of $CD8^+$ T cells can secrete various cytokines and generate cytolytic activity to enhance the antitumor immunity (Andre et al., 2018). The priming of $CD8^+$ cytotoxic T lymphocytes generally requires

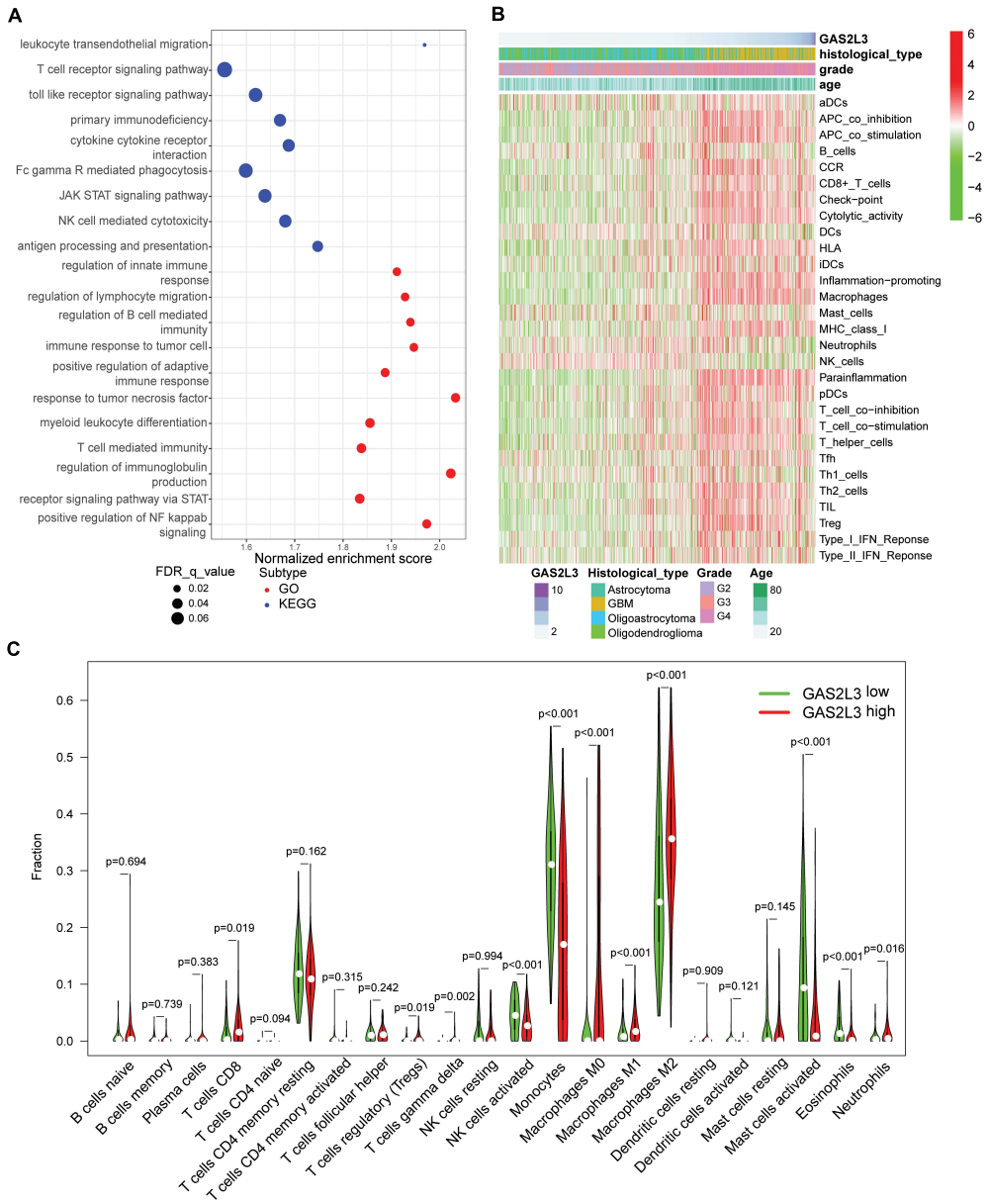


**FIGURE 5 |** GAS2L3-related inflammatory activities and immune infiltration in TCGA. **(A)** GO and KEGG pathway analysis. **(B)** Heatmaps displaying GAS2L3 expression, clinicopathological parameters, and 29 well-established immune-associated gene sets based on ssGSEA method. **(C)** The different proportions of 22 TILs in glioma samples based on CIBERSORT algorithm.

the participation of $CD4^+$ T-helper lymphocytes (Schoenberger et al., 1998). GAS2L3 also upregulated the infiltration of Tregs, which maintain a balance to fight diseases and at the same time prevent damage to healthy tissues (Schoenberger et al., 1998; Maghazachi, 2003). It has been reported that macrophages have a double effect on the development of tumor (Wang et al., 2015). M1 macrophages participate in antigen presentation and immune surveillance by secreting proinflammatory chemokines, whereas M2 macrophages exert inhibitory function (Chen et al., 2019). Through the ssGSEA analysis, we also found GAS2L3 may upregulate the level of CCRs and IFN (both types I and II), which are critical for immune cell recruitment and $CD8^+$ T cell activation (Balkwill, 2004; Farhood et al., 2019). Consequently, GAS2L3 may play a critical role in regulating TME in glioma by participating in cellular and humoral immunity.

In the last decade, immune checkpoint inhibitors have shown remarkable success in treating various tumors (Abril-Rodriguez and Ribas, 2017). However, because of the substantial heterogeneity of tumor cells, the efficacy of immunotherapies was less than satisfactory in glioma (Suryadevara et al., 2015). Identifying those who may respond to immunotherapies will certainly help glioma patients gain more clinical benefits from

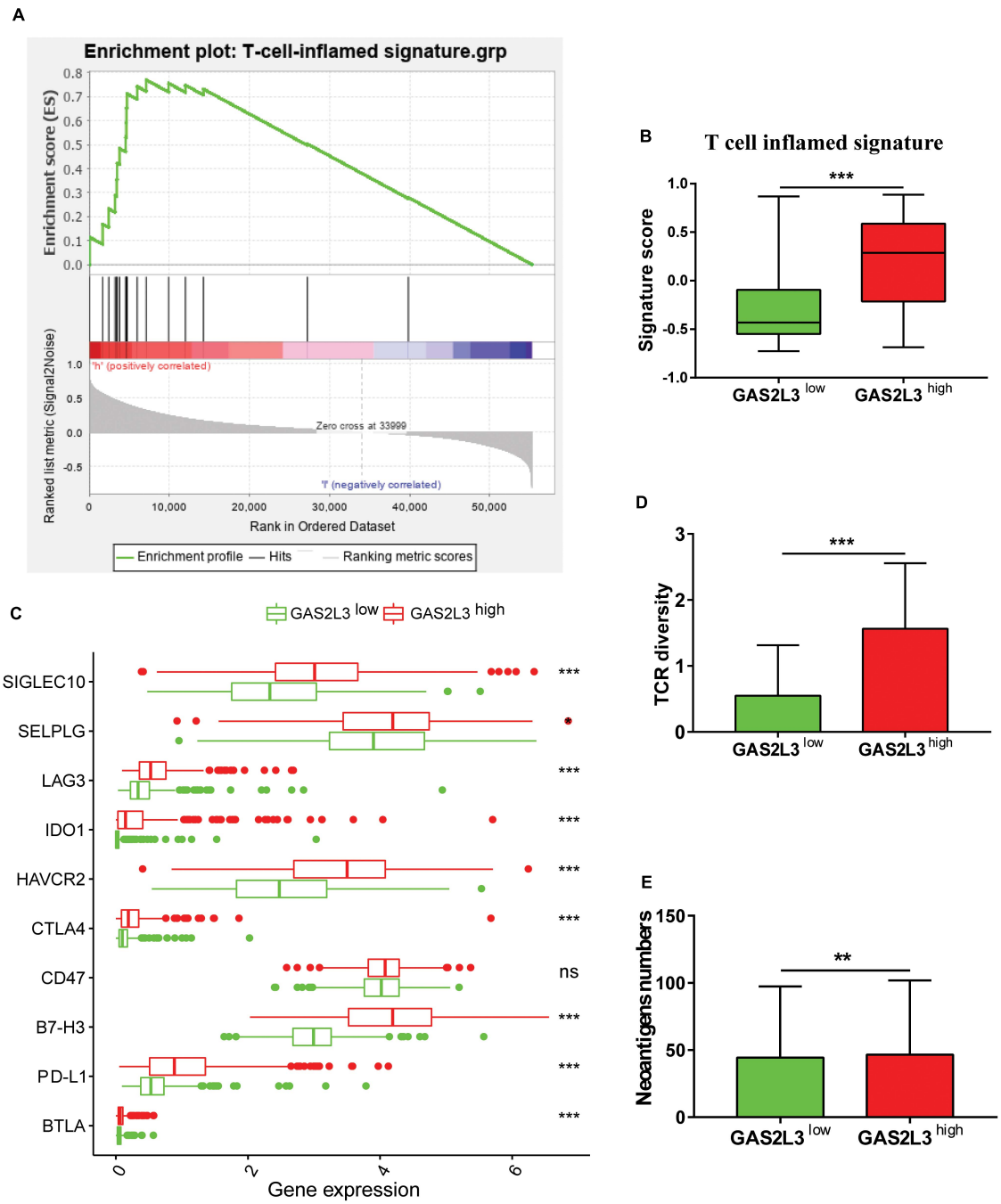


**FIGURE 6 |** GAS2L3-high and -low tumors exhibit features of anti–PD-1 responsiveness. **(A)** GSEA of the T-cell–inflamed gene signature in GAS2L3-high and -low tumors. **(B)** T-cell–inflamed gene signature scores in GAS2L3-high and -low groups. **(C)** GAS2L3 was synergistic with PD-L1 and other immune checkpoints. **(D)** T-cell receptor (TCR) diversity in GAS2L3-high and -low tumors. **(E)** Neoantigen numbers in GAS2L3-high and -low tumors. ns, not significant (*$P < 0.05$, **$P < 0.01$, ***$P < 0.001$).

anti–PD-1 therapy. In this study, we employed several predictive markers for anti–PD-1 therapy, which have been discussed in multiple types of cancer. We found that the T cell–inflamed signature, PD-L1 expression, the TCR diversity, and neoantigen numbers were significantly enriched in tumors with GAS2L3-high. In conclusion, it makes sense that GAS2L3 in combination with these biomarkers may help identify patients who have a higher likelihood of response to immunotherapies.

The current study had some limitations. First, heterogeneity was found in our meta-analysis, and we could hardly explain its source. Thus, more clinical research projects are needed for further elucidation. Second, the mechanisms by which

GAS2L3 may play an important role in the immunomodulation of the glioma microenvironment need further experimental verification. Third, more data are needed to prove the efficacy of the combination of GAS2L3 target and immunotherapies.

In summary, multicenter data showed that GAS2L3 was upregulated in advanced glioma and was related to adverse clinical outcomes. We found that GAS2L3 was involved in numerous immune activities and immune cell infiltration. It makes sense to combine anti-GAS2L3 and anti–PD-1 therapies to amplify the efficacy of treatments typically used in isolation. Taken together, GAS2L3 may act as a potential biomarker of prognosis and therapeutic target for glioma.

## DATA AVAILABILITY STATEMENT

The original contributions presented in the study are included in the article/**Supplementary Material**, further inquiries can be directed to the corresponding authors.

## ETHICS STATEMENT

All patients signed an informed consent form. The study protocol was approved by Tianjin Huanhu Hospital Ethics Committee (Tianjin, China).

## AUTHOR CONTRIBUTIONS

YZ, LX, and HY: study design. YZ, LZ, SS, and HW: data collection. YZ, LZ, YY, and HW: data analysis and interpretation. YZ, HW, XT, and HY: writing, review, polishing, and revision of the manuscript.

## FUNDING

This study was funded by Tianjin Municipal Science and Technology Commission (No. 20JCQNJC00410) and National Natural Science Foundation of China (No. 81972349).

## ACKNOWLEDGMENTS

We gratefully acknowledge contributions from Tianjin Huanhu Hospital and TCGA and other databases.

## SUPPLEMENTARY MATERIAL

The Supplementary Material for this article can be found online at: https://www.frontiersin.org/articles/10.3389/fgene.2021.649270/full#supplementary-material

## REFERENCES

Abril-Rodriguez, G., and Ribas, A. (2017). SnapShot: immune checkpoint inhibitors. *Cancer Cell* 31, 848–848.e1.

Andre, P., Denis, C., Soulas, C., Bourbon-Caillet, C., Lopez, J., Arnoux, T., et al. (2018). Anti-NKG2A mAb is a checkpoint inhibitor that promotes anti-tumor immunity by unleashing both T and NK cells. *Cell* 175, 1731–1743.e13.

Ayers, M., Lunceford, J., Nebozhyn, M., Murphy, E., Loboda, A., Kaufman, D. R., et al. (2017). IFN-gamma-related mRNA profile predicts clinical response to PD-1 blockade. *J. Clin. Invest.* 127, 2930–2940. doi: 10.1172/jci91190

Balkwill, F. (2004). Cancer and the chemokine network. *Nat. Rev. Cancer* 4, 540–550. doi: 10.1038/nrc1388

Bindea, G., Mlecnik, B., Tosolini, M., Kirilovsky, A., Waldner, M., and Obenauf, A. C. (2013). Spatiotemporal dynamics of intratumoral immune cells reveal the immune landscape in human cancer. *Immunity* 39, 782–795. doi: 10.1016/j.immuni.2013.10.003

Chang, C. C., Huang, C. C., Yang, S. H., Chien, C. C., Lee, C. L., and Huang, C. J. (2016). Data on clinical significance of GAS2 in colorectal cancer cells. *Data Brief* 8, 82–86. doi: 10.1016/j.dib.2016.05.010

Chen, P., Zhao, D., Li, J., Liang, X., Li, J., and Chang, A. (2019). Symbiotic macrophage-glioma cell interactions reveal synthetic lethality in PTEN-null glioma. *Cancer Cell* 35, 868–884.e6.

Domingues, P., Gonzalez-Tablas, M., Otero, A., Pascual, D., Miranda, D., and Ruiz, L. (2016). Tumor infiltrating immune cells in gliomas and meningiomas. *Brain Behav. Immun.* 53, 1–15. doi: 10.1016/j.bbi.2015.07.019

Farhood, B., Najafi, M., and Mortezaee, K. (2019). CD8(+) cytotoxic T lymphocytes in cancer immunotherapy: a review. *J. Cell. Physiol.* 234, 8509–8521. doi: 10.1002/jcp.27782

Gardner, A., and Ruffell, B. (2016). Dendritic cells and cancer immunity. *Trends Immunol.* 37, 855–865.

Goriounov, D., Leung, C. L., and Liem, R. K. (2003). Protein products of human Gas2-related genes on chromosomes 17 and 22 (hGAR17 and hGAR22) associate with both microfilaments and microtubules. *J. Cell Sci.* 116(Pt 6), 1045–1058. doi: 10.1242/jcs.00272

Gravendeel, L. A., Kouwenhoven, M. C., Gevaert, O., de Rooi, J. J., Stubbs, A. P., and Duijm, J. E. (2009). Intrinsic gene expression profiles of gliomas are a better predictor of survival than histology. *Cancer Res.* 69, 9065–9072. doi: 10.1158/0008-5472.can-09-2307

Kong, Y., Zhao, S., Tian, H., and Hai, Y. (2020). GAS2 promotes cell proliferation and invasion and suppresses apoptosis in pediatric T-cell acute lymphoblastic leukemia and activates wnt/beta-catenin pathway. *Onco Targets Ther.* 13, 1099–1108. doi: 10.2147/ott.s236854

Lapointe, S., Perry, A., and Butowski, N. A. (2018). Primary brain tumours in adults. *Lancet* 392, 432–446. doi: 10.1016/s0140-6736(18)30990-5

Li, G., Qin, Z., Chen, Z., Xie, L., Wang, R., and Zhao, H. (2017). Tumor microenvironment in treatment of glioma. *Open Med.* 12, 247–251. doi: 10.1515/med-2017-0035

Liu, Z., Li, M., Jiang, Z., and Wang, X. (2018). A comprehensive immunologic portrait of triple-negative breast cancer. *Transl. Oncol.* 11, 311–329. doi: 10.1016/j.tranon.2018.01.011

Madhavan, S., Zenklusen, J. C., Kotliarov, Y., Sahni, H., Fine, H. A., and Buetow, K. (2009). Rembrandt: helping personalized medicine become a reality through integrative translational research. *Mol. Cancer Res.* 7, 157–167. doi: 10.1158/1541-7786.mcr-08-0435

Maghazachi, A. A. (2003). G protein-coupled receptors in natural killer cells. *J. Leukoc. Biol.* 74, 16–24. doi: 10.1189/jlb.0103019

Molinaro, A. M., Taylor, J. W., Wiencke, J. K., and Wrensch, M. R. (2019). Genetic and molecular epidemiology of adult diffuse glioma. *Nat. Rev. Neurol.* 15, 405–417. doi: 10.1038/s41582-019-0220-2

Murugesan, S. N., Yadav, B. S., Maurya, P. K., Chaudhary, A., Singh, S., and Mani, A. (2018). Expression and network analysis of YBX1 interactors for identification of new drug targets in lung adenocarcinoma. *J. Genomics* 6, 103–112. doi: 10.7150/jgen.20581

Newman, A. M., Liu, C. L., Green, M. R., Gentles, A. J., Feng, W., and Xu, Y. (2015). Robust enumeration of cell subsets from tissue expression profiles. *Nat. Methods* 12, 453–457. doi: 10.1038/nmeth.3337

Omuro, A., and DeAngelis, L. M. (2013). Glioblastoma and other malignant gliomas: a clinical review. *JAMA* 310, 1842–1850. doi: 10.1001/jama.2013.280319

Ostrom, Q. T., Gittleman, H., Truitt, G., Boscia, A., Kruchko, C., and Barnholtz-Sloan, J. S. (2018). CBTRUS statistical report: primary brain and other central nervous system tumors diagnosed in the United States in 2011-2015. *Neuro Oncol.* 20(Suppl._4), iv1–iv86.

Pe'Er, T., Lahmi, R., Sharaby, Y., Chorni, E., Noach, M., and Vecsler, M. (2013). Gas2l3, a novel constriction site-associated protein whose regulation is mediated by the APC/C Cdh1 complex. *PLoS One* 8:e57532. doi: 10.1371/journal.pone.0057532

Schoenberger, S. P., Toes, R. E., van der Voort, E. I., Offringa, R., and Melief, C. J. (1998). T-cell help for cytotoxic T lymphocytes is mediated by CD40-CD40L interactions. *Nature* 393, 480–483. doi: 10.1038/31002

Schumacher, T. N., and Schreiber, R. D. (2015). Neoantigens in cancer immunotherapy. *Science* 348, 69–74.

Seidl, C., Port, M., Apostolidis, C., Bruchertseifer, F., Schwaiger, M., Senekowitsch-Schmidtke, R., et al. (2010). Differential gene expression triggered by highly cytotoxic alpha-emitter-immunoconjugates in gastric cancer cells. *Invest. New Drugs* 28, 49–60. doi: 10.1007/s10637-008-9214-4

Shi, L., Shang, X., Nie, K., Lin, Z., Zheng, M., and Wang, M. (2020). Identification of potential crucial genes associated with the pathogenesis and prognosis of liver hepatocellular carcinoma. *J. Clin. Pathol.* doi: 10.1136/jclinpath-2020-206979 Online ahead of print.

Stroud, M. J., Kammerer, R. A., and Ballestrem, C. (2011). Characterization of G2L3 (GAS2-like 3), a new microtubule- and actin-binding protein related to spectraplakins. *J. Biol. Chem.* 286, 24987–24995. doi: 10.1074/jbc.m111.242263

Subramanian, A., Tamayo, P., Mootha, V. K., Mukherjee, S., Ebert, B. L., and Gillette, M. A. (2005). Gene set enrichment analysis: a knowledge-based approach for interpreting genome-wide expression profiles. *Proc. Natl. Acad. Sci. U.S.A.* 102, 15545–15550. doi: 10.1073/pnas.0506580102

Suryadevara, C. M., Verla, T., Sanchez-Perez, L., Reap, E. A., Choi, B. D., and Fecci, P. E. (2015). Immunotherapy for malignant glioma. *Surg. Neurol. Int.* 6(Suppl. 1), S68–S77.

Tang, Z., Kang, B., Li, C., Chen, T., and Zhang, Z. (2019). GEPIA2: an enhanced web server for large-scale expression profiling and interactive analysis. *Nucleic Acids Res.* 47, W556–W560.

Thorsson, V., Gibbs, D. L., Brown, S. D., Wolf, D., Bortone, D. S., and Yang Ou, T. H. (2018). The immune landscape of cancer. *Immunity* 48, 812–830.e14.

Tumeh, P. C., Harview, C. L., Yearley, J. H., Shintaku, I. P., Taylor, E. J., and Robert, L. (2014). PD-1 blockade induces responses by inhibiting adaptive immune resistance. *Nature* 515, 568–571.

Wang, A., Dai, X., Cui, B., Fei, X., Chen, Y., and Zhang, J. (2015). Experimental research of host macrophage canceration induced by glioma stem progenitor cells. *Mol. Med. Rep.* 11, 2435–2442. doi: 10.3892/mmr.2014.3032

Wang, Q., Hu, B., Hu, X., Kim, H., Squatrito, M., and Scarpace, L. (2017). Tumor Evolution of glioma-intrinsic gene expression subtypes associates with immunological changes in the microenvironment. *Cancer Cell* 32, 42–56.e6.

Wang, Z., Jensen, M. A., and Zenklusen, J. C. (2016). A practical guide to the cancer genome atlas (TCGA). *Methods Mol. Biol.* 1418, 111–141. doi: 10.1007/978-1-4939-3578-9_6

Wolter, P., Schmitt, K., Fackler, M., Kremling, H., Probst, L., and Hauser, S. (2012). GAS2L3, a target gene of the DREAM complex, is required for proper cytokinesis and genomic stability. *J. Cell Sci.* 125(Pt 10), 2393–2406. doi: 10.1242/jcs.097253

Xiao, Y., Yuan, Y., Zhang, Y., Li, J., Liu, Z., and Zhang, X. (2015). CMTM5 is reduced in prostate cancer and inhibits cancer cell growth in vitro and in vivo. *Clin. Transl. Oncol.* 17, 431–437. doi: 10.1007/s12094-014-1253-z

Yan, W., Zhang, W., You, G., Zhang, J., Han, L., and Bao, Z. (2012). Molecular classification of gliomas based on whole genome gene expression: a systematic report of 225 samples from the Chinese glioma cooperative group. *Neuro Oncol.* 14, 1432–1440. doi: 10.1093/neuonc/nos263

Zhou, X., Qiu, S., Nie, L., Jin, D., Jin, K., and Zheng, X. (2020). Classification of muscle-invasive bladder cancer based on immunogenomic profiling. *Front. Oncol.* 10:1429

Zhu, R., Mok, M. T., Kang, W., Lau, S. S., Yip, W. K., and Chen, Y. (2015). Truncated HBx-dependent silencing of GAS2 promotes hepatocarcinogenesis through deregulation of cell cycle, senescence and p53-mediated apoptosis. *J. Pathol.* 237, 38–49. doi: 10.1002/path.4554

**Conflict of Interest:** The authors declare that the research was conducted in the absence of any commercial or financial relationships that could be construed as a potential conflict of interest.

frontiers in Genetics

ORIGINAL RESEARCH
published: 03 May 2021
doi: 10.3389/fgene.2021.646929

# Mutation and Copy Number Alterations Analysis of KIF23 in Glioma

*Zheng Zhao[1†], Zheng Wang[2†], Zhao-Shi Bao[2], Wei-Zhen Gao[3], Yuan-Da Zhang[3], Ci-Jie Ruan[3], Tao Lv[3], Yong Wang[3] and Li-Hua Sun[3]**

[1] Beijing Neurosurgical Institute, Capital Medical University, Beijing, China, [2] Department of Neurosurgery, Beijing Tiantan Hospital, Capital Medical University, Beijing, China, [3] Department of Neurosurgery, Renji Hospital, Shanghai Jiao Tong University School of Medicine, Shanghai, China

In glioma, kinesin family member 23 (KIF23) is up-regulated and plays a vital role in oncogenesis. However, the mechanism underlying KIF23 overexpression in malignant glioma remains to be elucidated. This study aims to find potential causes of KIF23 high expression at genome level. To clarify this issue, we obtained point mutation and copy number alterations (CNAs) of KIF23 in 319 gliomas using whole-exome sequencing. Only two glioma samples with missense mutations in KIF23 coding region were identified, while 7 patients were detected with amplification of KIF23. Additional analysis showed that KIF23 amplification was significantly associated with higher expression of KIF23. Gene ontology analysis indicated that higher copy number of KIF23 was associated TNF-α signaling pathway and mitotic cell circle checkpoint, which probably caused by subsequent upregulated expression of KIF23. Moreover, pan-cancer analysis showed that gaining of copy number was significantly associated with higher expression of KIF23, consolidating our findings in glioma. Thus, it was deduced that elevated KIF23 expression in glioma tended to be caused by DNA copy number amplification, instead of mutation.

**Keywords: glioma, KIF23, malignancy, mutation, copy number alterations**

OPEN ACCESS

***Edited by:***
*Silvia R. Rogatto, University of Southern Denmark, Denmark*

***Reviewed by:***
*Mehdi Pirooznia, National Heart, Lung, and Blood Institute (NHLBI), United States*
*Nicoletta Coccaro, University of Bari Aldo Moro, Italy*

****Correspondence:***
*Li-Hua Sun*
*sunnyshine1984@126.com*

*† These authors have contributed equally to this work*

***Specialty section:***
*This article was submitted to Cancer Genetics and Oncogenomics, a section of the journal Frontiers in Genetics*

***Received:*** *06 January 2021*
***Accepted:*** *06 April 2021*
***Published:*** *03 May 2021*

***Citation:***
*Zhao Z, Wang Z, Bao Z-S, Gao W-Z, Zhang Y-D, Ruan C-J, Lv T, Wang Y and Sun L-H (2021) Mutation and Copy Number Alterations Analysis of KIF23 in Glioma. Front. Genet. 12:646929. doi: 10.3389/fgene.2021.646929*

## INTRODUCTION

Kinesin family member 23 (KIF23) is a nuclear protein and plays a key role in regulating cytokinesis (Nislow et al., 1992; Zhu et al., 2005; Liu and Erikson, 2007). It has been found to be dysregulated and act as an oncogene with prognostic value in various tumors (Kato et al., 2016b; Iltzsche et al., 2017; Li X. L. et al., 2019). Our previous study showed that KIF23 mRNA expression was positively correlated with glioma grade, and high KIF23 expression conferred poor survival in glioma, which was further validated by the TCGA, REMBRANDT, and GSE16011 database (Sun et al., 2016). These results indicated that dysregulated KIF23 may play an essential role in tumorigenesis and progression, but how KIF23 expression is upregulated in cancers remains unelucidated.

Previous study showed that in the tumors with up-regulated KIF23 expression, DNA mutation of KIF23 was detected in nearly half of tested human cancer types, and CNAs of KIF23 showed gain in 30% of tested tumors (Cerami et al., 2012). Besides, p.P916R mutation of KIF23 causes a rare hereditary form of dyserythropoietic anemia (CDA III) with predisposition to blood cancer

(Liljeholm et al., 2013), and they further demonstrated that overexpression of KIF23 in non-small-cell lung cancer might be caused by CNAs (Vikberg et al., 2017). The above studies indicated that KIF23 gene expression can be modulated either by DNA mutation or by CNAs. However, KIF23 mutation and CNAs status in glioma is unclear. Given the idea that KIF23 is a novel prognostic biomarker with potential therapeutic implications in glioma, it is valuable to investigate the mutation and CNAs status of KIF23 in glioma.

In this study, we screened for KIF23 DNA mutation and CNAs in 319 gliomas with DNA and RNA sequencing data, and demonstrated that elevated KIF23 expression in glioma was probably caused by DNA copy number amplification. In terms of the important role of KIF23 in tumorigenesis and malignant aggressive progression of glioma, further understanding of its functional mechanism and pathway should be investigated.

# MATERIALS AND METHODS

## RNA-Sequencing Data

Two independent RNA-seq datasets (mRNAseq_325 and mRNAseq_693) and paired clinical information were obtained from Chinese Glioma Genome Atlas (CGGA) database[1] (Zhao et al., 2021). In the two datasets, only samples with definite WHO classification were included for survival and grade expression pattern analysis. Thus, 321 glioma samples (103 WHO grade II, 79 WHO grade III and 139 WHO grade IV) of CGGA mRNAseq_325 dataset, 692 glioma samples (188 WHO grade II, 255 WHO grade III, and 249 WHO grade IV) of CGGA mRNAseq_693 dataset were enrolled for subsequent analysis.

## Whole-Exome Sequencing (WES) Data

Genomic DNA from tumor and matched blood sample was extracted and confirmed for high integrity by 1% agarose gel electrophoresis. The DNA was subsequently fragmented, quality-controlled, and then pair-end libraries were prepared. For whole exome sequencing, Agilent SureSelect kit v6 was used for target capture. Sequencing was done on Illumina Hiseq platform using 150 bp pair-end sequencing strategy. In total, 319 whole-exome sequencing data of glioma samples were obtained, which were also available at CGGA Network.

DNA sequencing data were then mapped to the reference human genome (UCSC hg19) using Burrows-Wheeler Aligner (version 0.7.12-r1039, bwa mem) (Li and Durbin, 2009) with default parameters. Then, SAMtools (version 1.2) (Li et al., 2009) and Picard (version 2.0.1, Broad Institute)[2] were used to sort the reads by coordinates and mark duplicates. Statistics such as sequencing depth and coverage were calculated based on the resultant BAM files. SAVI2 was used to identify somatic mutations (including single nucleotide variations and short insertion/deletions) as previously described (Wang et al., 2016; Hu et al., 2018). In this pipeline, SAMtools mpileup and bcftools were used to perform variant calling, then the preliminary variant list was filtered to remove positions with no sufficient sequencing depth, positions with only low-quality reads, and positions that are biased toward either strand. Somatic mutations were identified and evaluated by an Empirical Bayesian method. In particular, mutations with significantly higher allele frequency in tumors than that in normal control were selected. Additionally, CNVkit (version 0.9.4.dev0)(Talevich et al., 2016) was used to detect copy number changes from WES data.

## Gene Set Enrichment Analysis

Firstly, we obtain the KIF23 CNV status WES data from CGGA database[3] and Cancer Hallmarks associated geneset from GSEA website[4] version 7.2. By integrating the WES data and matched RNA-seq data, we calculated the fold change of gene expression for each gene between KIF23 with or without CNV. Next, we use R package GSVA (version 1.36.3) to do enrichment analysis in cancer hallmarks.

## Statistical Analysis

Statistical analysis was performed using SPSS Graduate Pack (version 16.0) and GraphPad Prism (version 5.0) statistical software. Descriptive statistics were shown as mean ± standard deviation. Student's t test, one-way ANOVA test were used to test the significance of differences. Overall survival time (OS) was calculated from the date of histological diagnosis until death or the last follow-up. Kaplan-Meier survival analysis was used to estimate the survival distributions, and log-rank test was used to assess the statistical significance between stratified survivals groups. Patients with KIF23 expression lower than median level of KIF23 was defined as low expression, while patients with higher than the median value or equal to the median one was defined as high expression. A two-sided $p$ value $< 0.05$ was considered statistically significant.

# RESULTS

## KIF23 Expression Is Positively Correlated With Tumor Grade and Confers Poor Survival in Glioma

To validate the results of our previous study (Sun et al., 2016), we analyzed KIF23 expression pattern using CGGA mRNAseq_325 and mRNAseq_693 datasets. We got the similar results that KIF23 expression was the highest in grade IV glioma group, while had the lowest expression in grade II glioma group ($p < 0.001$) (**Figures 1A,B**). Besides, we also found that patients with high KIF23 expression (median survival in CGGA_mRNAseq_325 dataset is 386 days, and CGGA mRNAseq_693 dataset is 530 days) had a significantly worse overall survival compared to those with low KIF23 expression (median survival in CGGA mRNAseq_693 dataset is 3174 days, and CGGA mRNAseq_693 dataset is 2982 days) ($p < 0.001$) (**Figures 1C,D**).

[1] http://www.cgga.org.cn

[2] http://broadinstitute.github.io/picard/

[3] http://cgga.org.cn

[4] http://www.gsea-msigdb.org/gsea/index.jsp

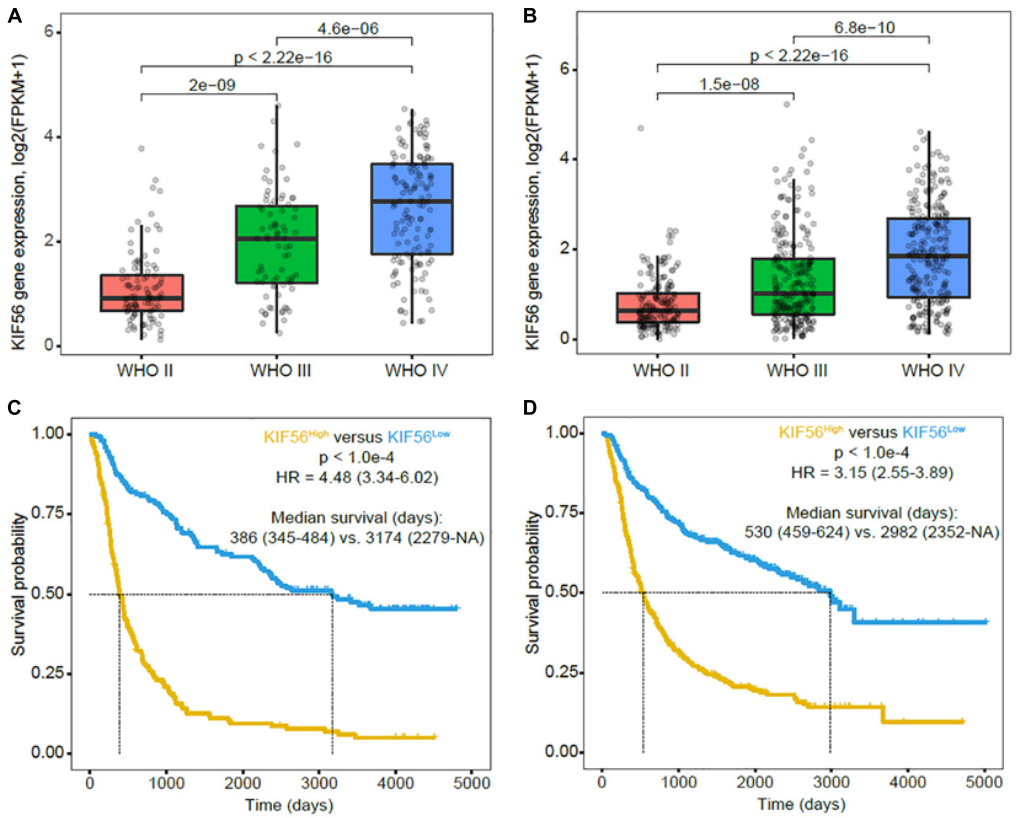


**FIGURE 1 |** KIF23 expression pattern and prognostic value in CGGA RNA sequence database. **(A,B)** KIF23 expression is positively correlated with tumor grade. **(C,D)** High KIF23 confers a poor survival in glioma patients. High group, patients with higher KIF23 expression than the median value or equal to the median one. Low group, patients with lower KIF23 level than the median one.

## Mutation Analysis of KIF23 in Glioma

Tumor DNA from 319 glioma patients were available for calling mutations, as shown in **Figure 2**. The mutation rate of IDH1 and TP53 was 53% and 48%, respectively. However, KIF23 mutation rate was less than 1% (**Figure 2A**). Only two case-specific missense mutations were detected, including non-synonymous change 69733357 G > A in Case104 and 69728081 C > T in Case241 (**Table 1**). Our results showed that patients with KIF23 mutation (median survival is 530 days) had a significantly worse overall survival compared to those without KIF23 mutation (median survival is 2982 days) ($p = 0.025$) (**Figure 2B**).

## CNAs Analysis of KIF23 in Glioma

CNAs were analyzed from the above WES data with 319 samples. We defined log ratio > 0.25 as Amplification group ($n = 11$), log ratio < -0.25 as Deletion group ($n = 40$), others as Wildtype group ($n = 268$). As shown in **Figure 3A**, KIF23 expression was the highest in Amplification group. Though

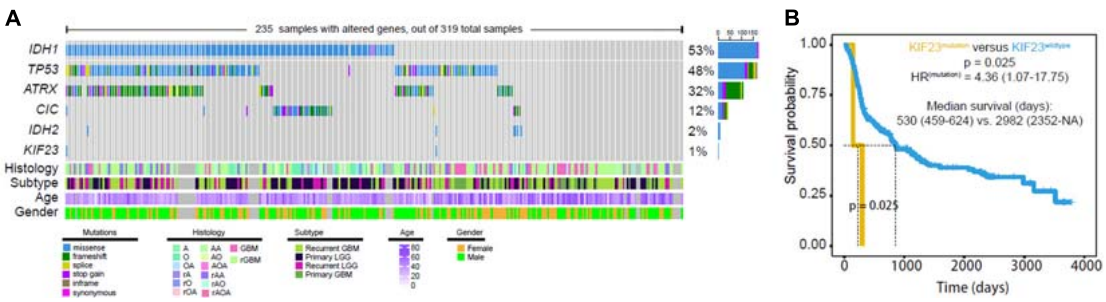


**FIGURE 2 |** Mutation analysis was done in 319 glioma samples. Only two case-specific missense mutations were detected were detected **(A)** although mutation of KIF23 showed worse overall survival **(B)**.

**TABLE 1 |** Case-specific non-synonymous mutation of KIF23 in 2 glioma samples.

| Sample ID | Cancer type | Chromosome | Mutation position | Reference allele | Variant allele | AA change |
|---|---|---|---|---|---|---|
| Case104 | Recurrent GBM | 15 | 69733357 | G | A | G773D |
| Case 241 | Recurrent GBM | 15 | 69728081 | C | T | P415S |

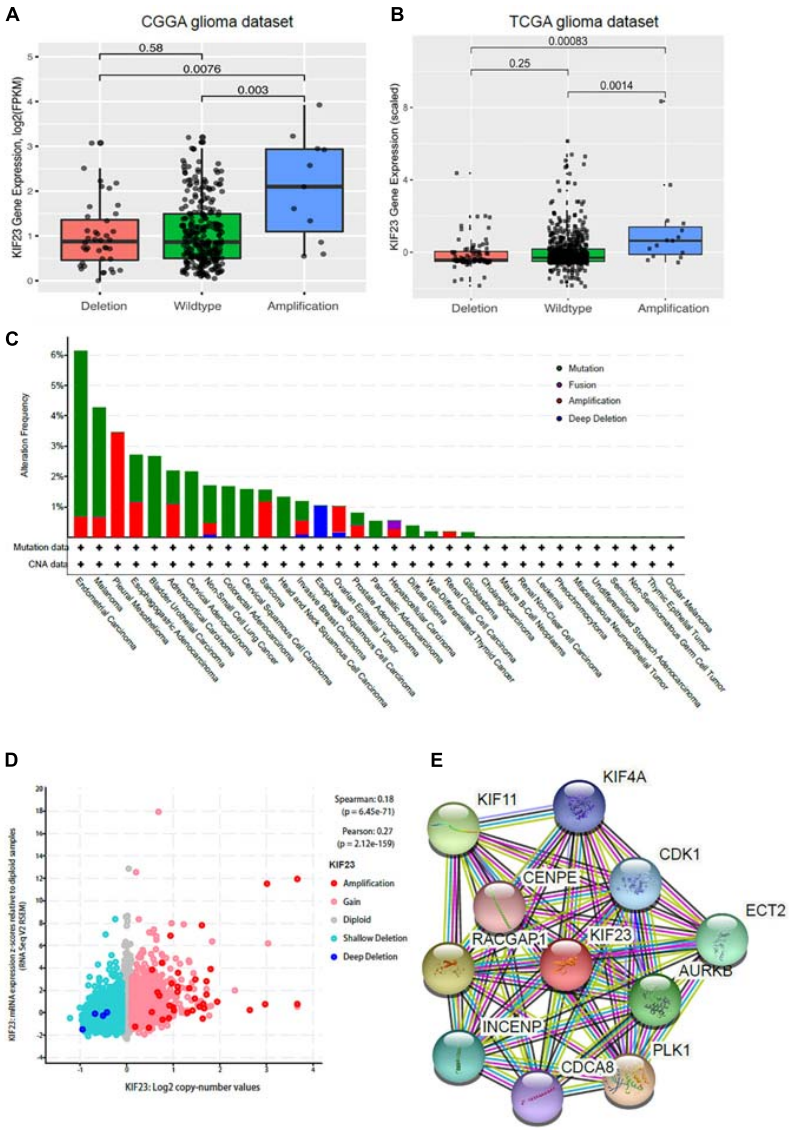


**FIGURE 3 |** CNAs analysis was done in 319 glioma samples. KIF23 expression was highest in copy number amplification group in CGGA dataset **(A)** and further validated in TCGA dataset **(B)**. Copy number alteration as universally occurred in various cancers **(C)** and gaining of copy number was significantly associated with higher expression of KIF23 **(D)**. Network analysis revealed that KIF23 was tightly involved in mitosis **(E)**.

there's no significant difference between Deletion group and Wildtype group, KIF23 in Wildtype group still showed relatively higher expression than that in Deletion group. The expression pattern was also independently validated in TCGA dataset (**Figure 3B**). Furthermore, we explored other focal CNAs in both low- and high-expression of KIF23 groups. We identified several significantly well-characterized genetic alterations in the case with high KIF23 expression (**Table 2**), such as PTEN loss ($p$ value = 7.37e-8), CDKN2A loss ($p$ value = 4.04e-12), CDKN2B loss ($p$ value = 9.44e-12), KIT gain ($p$ value = 3.33e-7), PDGFRA gain ($p$ value = 5.06e-7), MET gain ($p$ value = 1.30-04) and CDK6 gain ($p$ value = 3.06e-04). Furthermore, we explore the KIF23 CNVs in Pan-cancer levels from TCGA datasets. Our results showed that KIF23 CNVs occurred in various human cancers (**Figure 3C**), including endometrial carcinoma, melanoma and gliomas, suggesting KIF23 as a critical role in pan-cancer. Moreover, pan-cancer analysis showed that gaining of copy number was significantly associated with higher expression

**TABLE 2 |** Significant CNA events between KIF67 high expression and low expression groups.

| Alteration | Alt in $exp^{high}$ | Alt in $exp^{low}$ | WT in $exp^{high}$ | WT in $exp^{low}$ | *P* value |
|---|---|---|---|---|---|
| PTEN_loss | 90 | 42 | 70 | 117 | 7.37e-08 |
| CDKN2A_loss | 104 | 42 | 56 | 117 | 4.04e-12 |
| CDKN2B_loss | 104 | 43 | 56 | 116 | 9.44e-12 |
| KIT_gain | 46 | 11 | 114 | 148 | 3.33e-07 |
| PDGFRA_gain | 47 | 12 | 113 | 147 | 5.06e-07 |
| MET_gain | 58 | 27 | 102 | 132 | 1.30e-04 |
| CDK6_gain | 51 | 23 | 109 | 136 | 3.06e-04 |

of KIF23, consolidating our findings in glioma (**Figure 3D**). Network analysis revealed that KIF23 was tightly involved in mitosis, by interacting actively with genes such as CDK1 and CDCA8 (**Figure 3E**).

## Amplification of KIF23 Is a Negative Prognosticator for Glioma Patients

Since higher expression of KIF23 was negatively associated with overall survival with patients, we further investigated the prognostic value of KIF23 amplification with 319 glioma samples. As what was expected (**Figure 4**), patient with copy number gaining of KIF23 showed significantly worse survival than those without KIF23 amplification (log-rank test, *p* value = 0.033). This result was in consistence with the prognostic value of KIF23 high expression, which consolidates the role of KIF23 in glioma pathophysiology processes.

## Higher Copy Number of KIF23 Is Significantly Associated With TNF-α Signaling Pathway and Cellular Mitotic Activities

To explore the underlying mechanism of amplification of KIF23, we conducted gene ontology analysis for KIF23 copy number variation. Enrichment analysis revealed that KIF23 copy number positively associated genes tended to be associated with active cell biological process (**Figure 5A**), including TNF-α signaling pathway (**Figure 5B**), and G2M checkpoint (**Figure 5C**). These results indicated that higher copy number of KIF23 was involved with active immune activities and mitotic cellular activities, which further suggested more malignant biological processes. This is consistent with what we have found in the analysis of expression of KIF23, consolidating the malignant role of KIF23 in glioma.

# DISCUSSION

KIF23, also known as MKLP1 (mitotickinesin-like protein-1), is a member of kinesin-like motor protein superfamily. The protein encoded by KIF23 contains the kinesin superfamily motor domain at the N-terminal region. The domain mainly localizes in the interzone of mitotic spindles and acts as a plus-end-directed

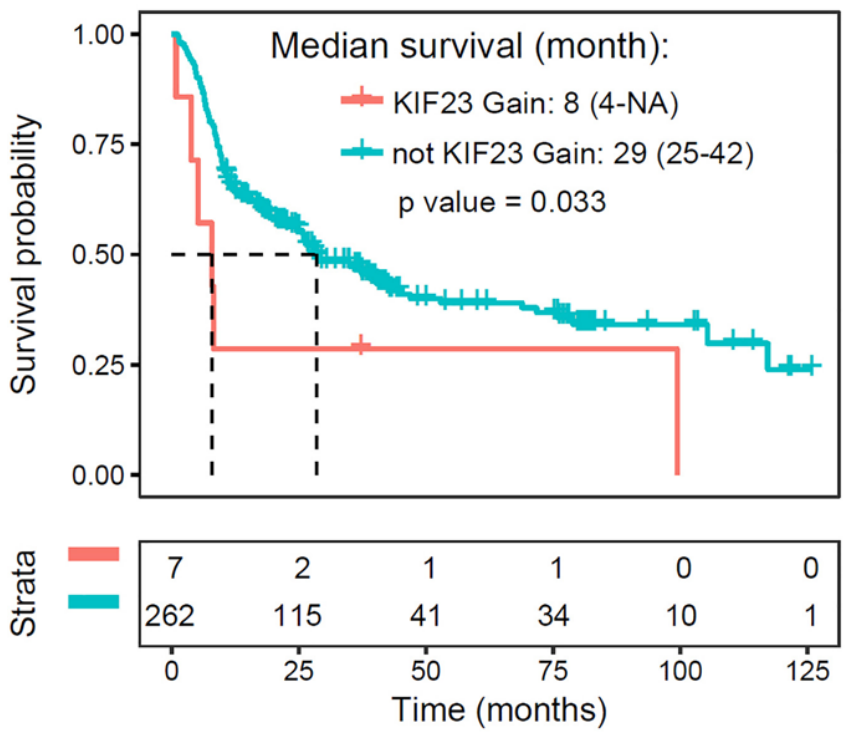


**FIGURE 4 |** Amplification of KIF23 is a negative prognosticator for glioma patients.

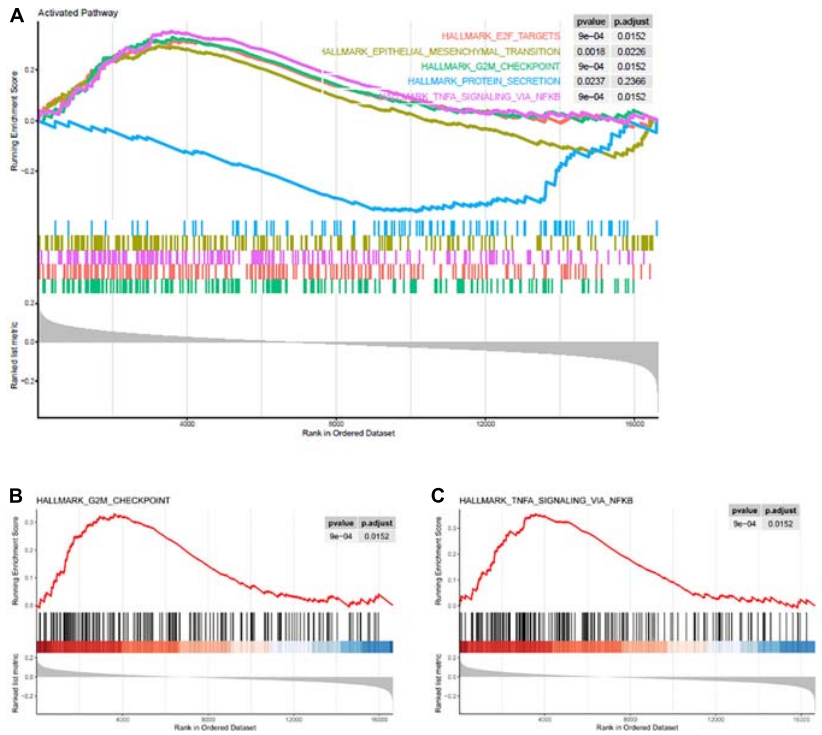


**FIGURE 5 |** Higher copy number of KIF23 was associated with active cell biological process **(A)**, including TNF-α signaling pathway **(B)**, and mitotic cell circle checkpoint **(C)**.

motor enzyme that moves along anti-parallel microtubules (Nislow et al., 1992). KIF23 has been identified as a key regulator of cytokinesis for its essential role in spindle midbody formation (Zhu et al., 2005; Liu and Erikson, 2007). Antagonism of KIF23 expression causes cell growth inhibition, and the formation of enlarged cell bodies with binuclear/multinuclear in many tumor cells (Liu et al., 2004; Takahashi et al., 2011; Kato et al., 2016b), probably due to the cell cycle arrest which further caused mitosis failure.

It seems that elevated of KIF23 expression is a common event in various human cancers. KIF23 was reported to be overexpressed in pancreatic ductal adenocarcinoma (Gao et al., 2020), malignant pleural mesothelioma (Kato et al., 2016a), lung cancer (Kato et al., 2016b; Ye et al., 2017), breast cancer (Zou et al., 2014), hepatocellular carcinoma (HCC) (Sun et al., 2015; Cheng et al., 2020), gastric cancer (Li X. L. et al., 2019; Liang et al., 2020), and ovarian cancer (Li T. et al., 2019; Hu et al., 2020). Interestingly, most studies also showed that patients with higher KIF23 expression had worse prognosis survival compared to these with lower KIF23 expression (Kato et al., 2016b; Ye et al., 2017; Li T. et al., 2019; Li X. L. et al., 2019). All these studies indicated that KIF23 plays as an oncogene in cancers. In glioma, KIF23 was also showed to be up-regulated compared to normal brain samples, and inhibition of KIF23 suppressed the proliferation of glioma cells both *in vivo* and *in vitro*. Furthermore, high KIF23 expression also conferred poor survival in glioma patients (Takahashi et al., 2011; Zhao et al., 2018). However, these two studies only employed 11 and 54 glioma samples, respectively. To further validate the above results, we investigated KIF23 expression pattern and its relationship with clinical features in glioma based on 305 samples from CGGA whole genome mRNA expression microarray data in our previous study. The analysis showed that: (1) KIF23 expression was positively correlated with tumor malignancy (grade, wild-type IDH1, G3, and Mesenchymal subtype preference), (2) patients with higher expression of KIF23 had a shorter survival time than those with lower KIF23 expression, and (3) KIF23 was an independent prognostic biomarker for glioma patients. We also demonstrated that reduction of KIF23 expression significantly suppressed U87MG cells proliferation *in vitro* and intracranial tumor growth *in vivo*, as well as prolonged intracranial glioma mice's overall survival days (Sun et al., 2016). All these researches indicated the potential value of KIF23 as therapeutic target in tumors. Thus, it is urgent and valuable to clarify the signaling pathway of KIF23, as well as the reason which caused its abnormal expression.

One study assumed that mutation in the CHR of KIF23 promoter may cause increased KIF23 expression (Fischer et al., 2013). In another study, Vikberg et al. (2017) employed a mutation screening of the KIF23 in 15 non-small-cell lung cancer (NSCLC) cases with elevated expression level of KIF23, however,

none of the examined samples had the mutation in the CHR of KIF23 by using sanger sequencing and single nucleotide polymorphism (SNP)-array. Interestingly, by assessment of CNAs in these samples, they concluded the elevated level of KIF23 might be due to additional copy of chromosome 15. In other researches, KIF23 p.R671W mutation was detected in one family with colorectal cancer (DeRycke et al., 2013). Melanoma cells derived from metastatic lesions patients also found KIF23 mutation by whole-exome sequencing and SNP array profiling (Cifola et al., 2013). Furthermore, KIF23 mutation was detected in about half of 38 tested tumor types (20 out of 38 were confirmed with elevated KIF23 expression). Additionally, CNAs analysis showed that gain in three out of ten tumors, loss in two type of cancer and five tumors confirmed with both gain and loss (Cerami et al., 2012; Vikberg et al., 2017). Based on the hypothesis that the presence of activating somatic mutation or CNAs may cause KIF23 overexpression, we first evaluated the KIF23 expression pattern and prognosis value in CGGA 325 and 693 RNA sequencing database. The results showed that KIF23 expression was positively correlated with tumor grade. Moreover, higher KIF23 expression conferred poor survival, which was consistent with our previous study (Sun et al., 2016). In order to investigate KIF23 somatic mutation and CNAs in glioma, we then screened the 319 glioma samples by using whole-exome sequencing analysis from CGGA database. However, only two case-specific non-synonymous mutations were detected. KIF23 mutation rate was less than 1% in our dataset. Next, we classified the 319 gliomas into CNAs Deletion group, Wildtype group, and Amplification group according to the log ratio. Then, the KIF23 gene expression was calculated, and a positive correlation was detected between KIF23 FPKM expression values and CNA. CNAs associated gene ontology revealed that KIF23 amplification was involved with active immune response and mitotic cell activities, which was consistent with the function of KIF23 expression in our previous paper. These results indicated that DNA copy number amplification may potentially contribute to elevated KIF23 expression in glioma while the biological effects of nucleotide mutation in KIF23 warrants additional investigation.

## DATA AVAILABILITY STATEMENT

The original contributions presented in the study are included in the article/supplementary material, further inquiries can be directed to the corresponding author.

## AUTHOR CONTRIBUTIONS

L-HS, ZZ, and ZW contributed to study concept and design. ZZ, ZW, Z-SB, W-ZG, and Y-DZ contributed to acquisition of data. C-JR, TL, and YW contributed to analysis and interpretation of data. L-HS, ZZ, and ZW contributed to draft of the manuscript. All authors contributed to the article and approved the submitted version.

## FUNDING

The study was funded by National Natural Science Foundation of China (Nos. 81302183 and 81902528), National Natural Science Foundation of China (NSFC)/Research Grants Council (RGC) Joint Research Scheme (81761168038), and Beijing Municipal Administration of Hospitals' Mission Plan (SML20180501, 2018.03-2022.02).

## ACKNOWLEDGMENTS

We would like to thank Hua Huang and Chengyin Liu from Beijing Neurosurgical Institute for collecting tumor samples and clinical follow-up. Furthermore, we appreciate the generosity of TCGA for sharing the huge amount of genetic sequencing data.

## REFERENCES

Cerami, E., Gao, J., Dogrusoz, U., Gross, B. E., Sumer, S. O., Aksoy, B. A., et al. (2012). The cBio cancer genomics portal: an open platform for exploring multidimensional cancer genomics data. *Cancer Discov* 2, 401–404. doi: 10.1158/2159-8290.CD-12-0095

Cheng, C., Wu, X., Shen, Y., and Li, Q. (2020). KIF14 and KIF23 Promote Cell Proliferation and Chemoresistance in HCC Cells, and Predict Worse Prognosis of Patients with HCC. *Cancer Manag Res* 12, 13241–13257. doi: 10.2147/CMAR.S285367

Cifola, I., Pietrelli, A., Consolandi, C., Severgnini, M., Mangano, E., Russo, V., Bellis, G.D., & Battaglia, C., et al. (2013). Comprehensive genomic characterization of cutaneous malignant melanoma cell lines derived from metastatic lesions by whole-exome sequencing and SNP array profiling. *PLoS One* 8:e63597. doi: 10.1371/journal.pone.0063597

DeRycke, M. S., Gunawardena, S., Middha, S., Asmann, Y., Schaid, D., McDonnell, S., Riska, S., Eckloff, B., et al. (2013). Identification of novel variants in colorectal cancer families by high-throughput exome sequencing. *Cancer Epidemiol Biomarkers Prev* 22, 1239–1251. doi: 10.1158/1055-9965.EPI-12-1226

Fischer, M., Grundke I, Sohr S, Quaas M, Hoffmann S, Knörck A., et al. (2013). p53 and cell cycle dependent transcription of kinesin family member 23 (KIF23) is controlled via a CHR promoter element bound by DREAM and MMB complexes. *PLoS One* 8:e63187. doi: 10.1371/journal.pone.0063187

Gao, C. T., Ren, J., Yu, J., Li, S., Guo, X., and Zhou, Y. (2020). KIF23 enhances cell proliferation in pancreatic ductal adenocarcinoma and is a potent therapeutic target. *Ann Transl Med* 8, 1394. doi: 10.21037/atm-20-1970

Hu, H., Mu, Q., Bao, Z., Chen, Y., and Jiang, T. (2018). Mutational Landscape of Secondary Glioblastoma Guides MET-Targeted Trial in Brain Tumor. *Cell* 175, 1665-1678 e18. doi: 10.1016/j.cell.2018.09.038

Hu, Y., Zheng, M., Wang, C., Wang, S., Gou, R., Liu, O., et al. (2020). Identification of KIF23 as a prognostic signature for ovarian cancer based on large-scale sampling and clinical validation. *Am J Transl Res* 12, 4955–4976. doi: 10.21203/rs.2.23036/v1

Iltzsche, F., Simon, K., Stopp, S., Pattschull, G., Francke, S., Wolter, P., et al. (2017). An important role for Myb-MuvB and its target gene KIF23 in a mouse model of lung adenocarcinoma. *Oncogene* 36, 110–121. doi: 10.1038/onc.2016.181

Kato, T., Lee, D., Wu, L., Patel, P., Young, A., Wada, H., et al. (2016a). Kinesin family members KIF11 and KIF23 as potential therapeutic targets in malignant pleural mesothelioma. *Int J Oncol* 49, 448–456. doi: 10.3892/ijo.2016.3566

Kato, T., Wada, H., Patel, P., Hu, H. P., Lee, D., Ujiie, H., et al. (2016b). Overexpression of KIF23 predicts clinical outcome in primary

lung cancer patients. *Lung Cancer* 92, 53–61. doi: 10.1016/j.lungcan.2015.11.018

Liu, X., Zhou, T., Kuriyama, R., and Erikson, R. L. (2004). Molecular interactions of Polo-like-kinase 1 with the mitotic kinesin-like protein CHO1/MKLP-1. *J Cell Sci* 117 (Pt 15), 3233–3246. doi: 10.1242/jcs.01173

Liu, X., and Erikson, R. L. (2007). The nuclear localization signal of mitotic kinesin-like protein Mklp-1: effect on Mklp-1 function during cytokinesis. *Biochem Biophys Res Commun* 353, 960–964. doi: 10.1016/j.bbrc.2006.12.142

Li, T., Li, Y., Gan, Y., Tian, R., Wu Q, Shu, G., et al. (2019). Methylation-mediated repression of MiR-424/503 cluster promotes proliferation and migration of ovarian cancer cells through targeting the hub gene KIF23. *Cell Cycle* 18, 1601–1618. doi: 10.1080/15384101.2019.1624112

Li, X. L., Ji, Y.-M., Song, R., Li, X.-N., and Guo, L.-S. N. (2019). KIF23 Promotes Gastric Cancer by Stimulating Cell Proliferation. *Dis Markers* 2019, 9751923. doi: 10.1155/2019/9751923

Li, H., Handsaker, B., Wysoker, A., Fennell, T., Ruan, J., Homer, N., et al. (2009). The Sequence Alignment/Map format and SAMtools. *Bioinformatics* 25, 2078–2079. doi: 10.1093/bioinformatics/btp352

Li, H., and Durbin, R. (2009). Fast and accurate short read alignment with Burrows-Wheeler transform. *Bioinformatics* 25, 1754–1760. doi: 10.1093/bioinformatics/btp324

Liang, W. T., Liu, X. F., Huang, H. B., Gao, Z. M., and Li, K. (2020). Prognostic significance of KIF23 expression in gastric cancer. *World J Gastrointest Oncol,* . 12, 1104–1118. doi: 10.4251/wjgo.v12.i10.1104

Liljeholm, M., Irvine, A. F., Vikberg, A. L., Norberg, A., Month, S., Sandström, H., et al. (2013). Congenital dyserythropoietic anemia type III (CDA III) is caused by a mutation in kinesin family member, KIF23. *Blood* 121, 4791–4799. doi: 10.1182/blood-2012-10-461392

Nislow, C., Lombillo, V. A., Kuriyama, R., and McIntosh, J. R. (1992). A plus-end-directed motor enzyme that moves antiparallel microtubules in vitro localizes to the interzone of mitotic spindles. *Nature* 359, 543–547. doi: 10.1038/359543a0

Sun, L., Zhang, C., Yang, Z., Wu, Y., Wang, H., Bao, Z., et al. (2016). KIF23 is an independent prognostic biomarker in glioma, transcriptionally regulated by TCF-4. *Oncotarget* 7, 24646–24655. doi: 10.18632/oncotarget.8261

Sun, X., Jin, Z., Song, X., Wang, J., Li, Y., Qian, X., et al. (2015). Evaluation of KIF23 variant 1 expression and relevance as a novel prognostic factor in patients with hepatocellular carcinoma. *BMC Cancer* 15:961. doi: 10.1186/s12885-015-1987-1

Talevich, E., Shain, A. H., Botton, T., and Bastian, B. C. (2016). CNVkit: Genome-Wide Copy Number Detection and Visualization from Targeted DNA Sequencing. *PLoS Computational Biology* 12, doi: 10.1371/journal.pcbi.1004873

Takahashi, S., Fusaki, N., Ohta, S., Iwahori, Y., Iizuka, Y., Inagawa, K., et al. (2011). Downregulation of KIF23 suppresses glioma proliferation. *J Neurooncol* 106, 519–529. doi: 10.1007/s11060-011-0706-2

Vikberg, A. L., Vooder, T., Lokk, K., Annilo, T., and Golovleva, I. (2017). Mutation analysis and copy number alterations of KIF23 in non-small-cell lung cancer exhibiting KIF23 over-expression. *Onco Targets Ther* 10, 4969–4979. doi: 10.2147/OTT.S138420

Wang, J., Cazzato, E., Ladewig, E., Frattini, V., Rosenbloom, D. I., Zairis, S., et al. (2016). Clonal evolution of glioblastoma under therapy. *Nat Genet* 48, 768–776. doi: 10.1038/ng.3590

Ye, L., Li, H., Zhang, F., Lv, T., Liu, H., and Song, Y. (2017). [Expression of KIF23 and Its Prognostic Role in Non-small Cell Lung Cancer: Analysis Based on the Data-mining of Oncomine]. *Zhongguo Fei Ai Za Zhi* 20, 822–826.

Zhu, C., Bossy-Wetzel, E., and Jiang, W. (2005). Recruitment of MKLP1 to the spindle midzone/midbody by INCENP is essential for midbody formation and completion of cytokinesis in human cells. *Biochem J* 389 (Pt 2), 373–381. doi: 10.1042/BJ20050097

Zhao, C., X-B Wang, Y-H Zhang, Y-M Zhou, Q Yin, W-C Yao. (2018). MicroRNA-424 inhibits cell migration, invasion and epithelial-mesenchymal transition in human glioma by targeting KIF23 and functions as a novel prognostic predictor. *Eur Rev Med Pharmacol Sci* 22, 6369–6378.

Zhao, Z., Zhang, K., Wang, Q., Li, G., Zeng, F., Zhang, Y., et al. (2021). Chinese Glioma Genome Atlas (CGGA): A Comprehensive Resource with Functional Genomic Data from Chinese Gliomas. *Genomics Proteomics Bioinformatics* doi: 10.1016/j.gpb.2020.10.005

Zou, J. X., Duan, Z., Wang, J., Sokolov, A., Xu, J., Chen, C., et al. (2014). Kinesin family deregulation coordinated by bromodomain protein ANCCA and histone methyltransferase MLL for breast cancer cell growth, survival, and tamoxifen resistance. *Mol Cancer Res* 12, 539–549. doi: 10.1158/1541-7786.MCR-13-0459

**Conflict of Interest:** The authors declare that the research was conducted in the absence of any commercial or financial relationships that could be construed as a potential conflict of interest.

frontiers in Genetics

ORIGINAL RESEARCH
published: 14 June 2021
doi: 10.3389/fgene.2021.678436

# Development of an Immune-Related LncRNA Prognostic Signature for Glioma

*Yudong Cao[1], Hecheng Zhu[2], Jun Tan[1], Wen Yin[1], Quanwei Zhou[1], Zhaoqi Xin[1], Zhaoping Wu[1], Zhipeng Jiang[1], Youwei Guo[1], Yirui Kuang[1], Can Li[1], Ming Zhao[2], Xingjun Jiang[1]*, Jiahui Peng[3]* and Caiping Ren[4]**

[1] Department of Neurosurgery, Xiangya Hospital, Central South University, Changsha, China, [2] Changsha Kexin Cancer Hospital, Changsha, China, [3] Department of Medical Ultrasonics, Seventh Affiliated Hospital of Sun Yat-sen University, Shenzhen, China, [4] Key Laboratory for Carcinogenesis of Chinese Ministry of Health, School of Basic Medical Science, Cancer Research Institute, Central South University, Changsha, China

OPEN ACCESS

**Edited by:**
Valerio Costa,
Institute of Genetics and Biophysics, Consiglio Nazionale delle Ricerche (CNR), Italy

**Reviewed by:**
Antonio Federico,
Tampere University, Finland
Antonella Iuliano,
Telethon Institute of Genetics and Medicine (TIGEM), Italy

***Correspondence:**
Xingjun Jiang
jiangxj@csu.edu.cn
Jiahui Peng
pengjiahui511@126.com
Caiping Ren
rencaiping@csu.edu.cn

**Specialty section:**
This article was submitted to Cancer Genetics and Oncogenomics, a section of the journal Frontiers in Genetics

**Received:** 10 March 2021
**Accepted:** 29 April 2021
**Published:** 14 June 2021

**Citation:**
Cao Y, Zhu H, Tan J, Yin W, Zhou Q, Xin Z, Wu Z, Jiang Z, Guo Y, Kuang Y, Li C, Zhao M, Jiang X, Peng J and Ren C (2021) Development of an Immune-Related LncRNA Prognostic Signature for Glioma. Front. Genet. 12:678436. doi: 10.3389/fgene.2021.678436

**Introduction:** Glioma is the most common primary cancer of the central nervous system with dismal prognosis. Long noncoding RNAs (lncRNAs) have been discovered to play key roles in tumorigenesis in various cancers, including glioma. Because of the relevance between immune infiltrating and clinical outcome of glioma, identifying immune-related lncRNAs is urgent for better personalized management.

**Materials and methods:** Single-sample gene set enrichment analysis (ssGSEA) was applied to estimate immune infiltration, and glioma samples were divided into high immune cell infiltration group and low immune cell infiltration group. After screening differentially expressed lncRNAs in two immune groups, least absolute shrinkage and selection operator (LASSO) Cox regression analysis was performed to construct an immune-related prognostic signature. Additionally, we explored the correlation between immune infiltration and the prognostic signature.

**Results:** A total of 653 samples were appropriate for further analyses, and 10 lncRNAs were identified as immune-related lncRNAs in glioma. After univariate Cox regression and LASSO Cox regression analysis, six lncRNAs were identified to construct a prognostic signature for glioma, which could be taken as independent prognostic factors in both univariate and multivariate Cox regression analyses. Moreover, risk score was significantly correlated with all the 29 immune-related checkpoint expression ($p < 0.05$) in ssGSEA except neutrophils ($p = 0.43$).

**Conclusion:** The study constructed an immune-related prognostic signature for glioma, which contributed to improve clinical outcome prediction and guide immunotherapy.

**Keywords: glioma, lncRNA, immune signature, TCGA, risk score**

# INTRODUCTION

Glioma is one of the most common primary brain tumors and accounts for greater than 70% of malignant brain tumors (Ostrom et al., 2016), presenting only a 5-year survival rate of 30 to 70% in low-grade glioma patients and less than 5% in the most malignant glioblastoma patients (Gousias et al., 2009; Ostrom et al., 2014). Although advances have been made in glioma treatment, including mass surgical resection, radiotherapy, and chemotherapy, the prognosis and survival rate of glioma patients are still unsatisfactory (Stupp et al., 2009; Wu et al., 2019). Unlike traditional therapeutic strategies of curbing cancer cell proliferation and invasion, more and more research reveals the importance of the tumor microenvironment (TME) in glioma development and progression. TME composed of cancer cells and noncancerous cell types is a complex system, including endothelial cells, pericytes, fibroblasts, and immune cells (Quail and Joyce, 2013). As many as 30 to 50% of the cells in gliomas are microglia or macrophages, and tumor-associated microglia and macrophages (TAMs) within the brain tend to be protumorigenic and accumulate as higher as tumor grade (Komohara et al., 2008; Hambardzumyan et al., 2016). Other immune cells, such as dendritic cells, also play an essential role in cancer immune therapy in recent years (Anguille et al., 2014). Therefore, screening reliable immune predictors and prognostic indicators to improve the prognosis of glioma and guide the individual treatment strategies is warranted.

Long noncoding RNAs (lncRNAs) are noncoding RNAs with more than 200 nucleotides in length without significant protein-coding function (Wilusz et al., 2009). Despite their limited expression levels, growing evidence has revealed that lncRNAs could regulate gene expression at epigenetic, transcriptional, and posttranscriptional levels or directly modulate protein activity (Orom et al., 2010; Augoff et al., 2012; Liu et al., 2015; Wang et al., 2016). LncRNAs have been confirmed to play an oncogenic or suppressive role in tumor growth and metastasis including glioma (Sun et al., 2013). For example, lncRNA CASC2 negatively regulates miR-21 to suppress cell growth of glioma, whereas lncRNA CRNDE promotes glioma cell growth and invasion through mTOR signaling (Kang et al., 2019). LncRNA SNHG18 can promote radioresistance of glioma cells by suppressing semaphorin5A16 (Zheng et al., 2016). In addition, lncRNA DANCR has been proved as a diagnostic marker or a potential therapeutic target for the treatment of glioma through regulating miR-135a-5p/BMI1 axis (Feng et al., 2020). Therefore, identifying immune-related lncRNA to predict the prognosis of glioma patients is of great importance for clinical diagnosis and treatment.

In the present study, we applied single-sample gene set enrichment analysis (ssGSEA), Estimation of STromal and Immune cells in MAlignant Tumor tissues using Expression data (ESTIMATE), and Cell type Identification By Estimating Relative Subsets Of RNA Transcripts (CIBERSORT) to classify the glioma patients by immune infiltration degree. Subsequently, we selected immune-related lncRNAs as well as differentially expressed between cancer and normal samples and used the least absolute shrinkage and selection operator (LASSO) Cox regression analysis to construct a prognosis-related risk model. It is hoped that this study will provide promising targets and stimulate new strategies in glioma patients.

# MATERIALS AND METHODS

## Data Sets and Grouping of Gliomas

The human glioma transcriptome with format of the FPKM (fragments per kilobase of per million) and corresponding clinical data were downloaded from The Cancer Genome Atlas (TCGA) database[1]. Twenty-nine immune data sets including immune cell types, immune-related pathways, and immune-related functions were obtained from the study by Bindea et al. (2013). According to the 29 immune data sets, the ssGSEA was used to calculate enrichment scores for each sample to establish immune-related term enrichment scores in glioma samples using the R packages "GSVA," "limma," and "GSEABase." According to the ssGSEA scores, glioma samples were divided into high and low immune cell infiltration groups using the R package "hclust."

## Verification of the Immune Grouping

Estimation of STromal and Immune cells in MAlignant Tumor tissues using Expression data and CIBERSORT were applied to validate the group divided by ssGSEA. ESTIMATE is a method that can deduce the stromal and immune cell proportion using gene expression profiles (Yoshihara et al., 2013). Based on this algorithm, tumor purity, ESTIMATE score, immune score, and stromal score of each glioma sample were calculated using "estimate" in R package. Clustering heatmap and statistical map between the two immune groups were shown using "pheatmap" and "ggpubr" in R package. In addition, human leukocyte antigen (HLA) and CD274 [programmed death 1 ligand [PD-L1]) expression were also compared between the two groups to verify the effect of ssGSEA grouping using "ggpubr" and "limma" in R package. CIBERSORT is another approach to characterize 22 types of immune infiltration cell composition using the deconvolution strategy (Newman et al., 2015). The CIBERSORT web tool[2] was used, and data with $p < 0.05$ were selected for further study. The proportions of immune cell types determined by CIBERSORT between the two groups were compared using the Kruskal–Wallis test to verify ssGSEA grouping again.

## Screen of Immune-Related LncRNAs

Ensembl database[3] was used to screen lncRNAs. All lncRNAs with false discovery rate (FDR) $< 0.05$ and $|\log2FC| \geq 0.5$ were defined as differentially expressed lncRNAs between the high and low immune cell infiltration groups using the "edgeR" package. To identify differentially expressed lncRNAs between the cancer group and the normal groups, gene expression data that included TCGA lower-grade glioma and glioblastoma (GBMLGG) gene expression RNAseq and The Genotype-Tissue Expression (GTEx) gene expression RNAseq were obtained from

[1]https://portal.gdc.cancer.gov

[2]https://cibersort.stanford.edu/

[3]https://www.ensembl.org/

the UCSC Xena website[4]. The two profiles were recomputed from raw RNA-Seq data by the UCSC Xena project based on a uniform pipeline and shown as log2($x$+1) transformed RSEM normalized count. After identifying the brain samples in GTEX, quantile normalization of gene expression combining TCGA and GTEx from UCSC Xena was performed using the "normalizeBetweenArrays" function in limma of R (Ritchie et al., 2015). The differentially expressed lncRNAs between the cancer and normal groups were selected using the "limma" package with FDR $< 0.05$ and $|\log2FC| \geq 0.5$. The lncRNAs selected in both two analyses were identified as immune-related lncRNA by Venn analysis.

## Construction and Validation of a Prognostic Immune-Related LncRNA Signature

Samples with follow-up time >30 days were kept, and univariate Cox regression analysis of continuous variables was performed by survival package in R with $p < 0.05$ as the criteria to select prognostic immune-related lncRNA. Then, we applied LASSO Cox analysis, a high-dimensional predictor regression method using 10-fold cross-validations, to construct an optimal risk signature model using the "glmnet" R package. The coefficients of the selected lncRNAs were calculated, and a risk score for each glioma patient was calculated using the following formula: risk score = $\sum_1^n \text{coefficient}\left(\text{lncRNAn}\right) \times$ expression (lncRNAn). According to the formula, the glioma patients were sorted into a high-risk group and a low-risk group with the median risk score as the cutoff.

To examine the performance of the prognostic immune-related lncRNA signature, the receiver operating characteristic (ROC) analysis was performed, and the area under the curve (AUC) was calculated using "survivalROC" package in Kaplan–Meier (K-M) analysis used to compare survival between the high- and low-risk groups by the log-rank test. To show the expression patterns of optimal immune-related lncRNAs between the high- and low-risk groups, principal components analysis (PCA) was applied with R using the "scatterplot3d" and "limma" package.

In addition, we also used univariate and multivariate Cox regression analyses to determine whether the signature could predict prognosis independently from clinical parameters, including age, gender, and grade. The grade of glioma was sorted by 2016 World Health Organization (WHO) classification.

## Correlation Between Immune Infiltration and Prognostic Signature

To further explore the relationship between the signature and TME, the correlation between risk scores and immune infiltration calculated by ssGSEA was calculated by Pearson correlation.

## Clinical Correlation and Functional Enrichment Analysis

We explored the relationship between the expression of each lncRNA in the signature and clinical WHO stage by Wilcoxon signed rank test. In addition, immune-related functional annotation (immune response and immune system process) was performed by GSEA to further explore the immune status between the high- and low-risk groups, and $p < 0.05$ was identified as statistically significant.

## Statistical Analysis

All statistical analyses were applied by R version 4.0.2 and corresponding packages. A two-tailed $p < 0.05$ was considered statistically significant, and FDR was calculated using Benjamini–Hochberg methods for multiple corrections to differential expression analyses results (Benjamini and Hochberg, 1995).

# RESULTS

## Construction and Verification of Glioma Groupings

A total of 693 glioma samples were downloaded from TCGA, and all of them were cancer samples. To evaluate infiltration of immune of each sample, ssGSEA was applied, and enrichment scores of the 29 immune-associated gene sets in the TME were obtained. According to the ssGSEA scores, glioma samples were hierarchically clustered into two groups, including the high immune cell infiltration group ($n = 151$) and the low immune cell infiltration group ($n = 542$; **Figure 1A**).

In the ESTIMATE algorithm, tumor purity, ESTIMATE score, immune score, and stromal score of each glioma sample were determined. Our results showed that tumor purity was significantly lower ($p < 0.001$) in high immune cell infiltration group than that in low immune cell infiltration group; ESTIMATE score, immune score, and stromal score were significantly higher ($p < 0.001$) in high immune cell infiltration group than those in low immune cell infiltration group (**Figure 1B**). In addition, the expression levels of the HLA family and CD274 (PD-L1) were significantly increasing in the high immune cell infiltration group than those in the low immune cell infiltration group, respectively ($p < 0.001$; **Figures 1C,D**). In the CIBERSORT algorithm, the high immune cell infiltration group showed higher proportion of immune cells than that in the low immune cell infiltration group (**Figure 1E**). Based on the above analysis, the immune grouping of the glioma samples was reasonable and feasible for subsequent analysis.

## Identification of LncRNAs Differentially Expressed in Two Classifications

In the 693 glioma samples from TCGA downloaded from the official website, 369 lncRNAs were differentially expressed between the high and low immune cell infiltration groups, including 179 up-regulated lncRNAs and 190 down-regulated lncRNAs in the high immune cell infiltration group (**Figure 2A**). We obtained 702 glioma samples (697 cancer samples and 5 paracancerous samples) and 1,152 normal brain samples on the UCSC Xena website. After merging the two databases from the

[4]https://xena.ucsc.edu/

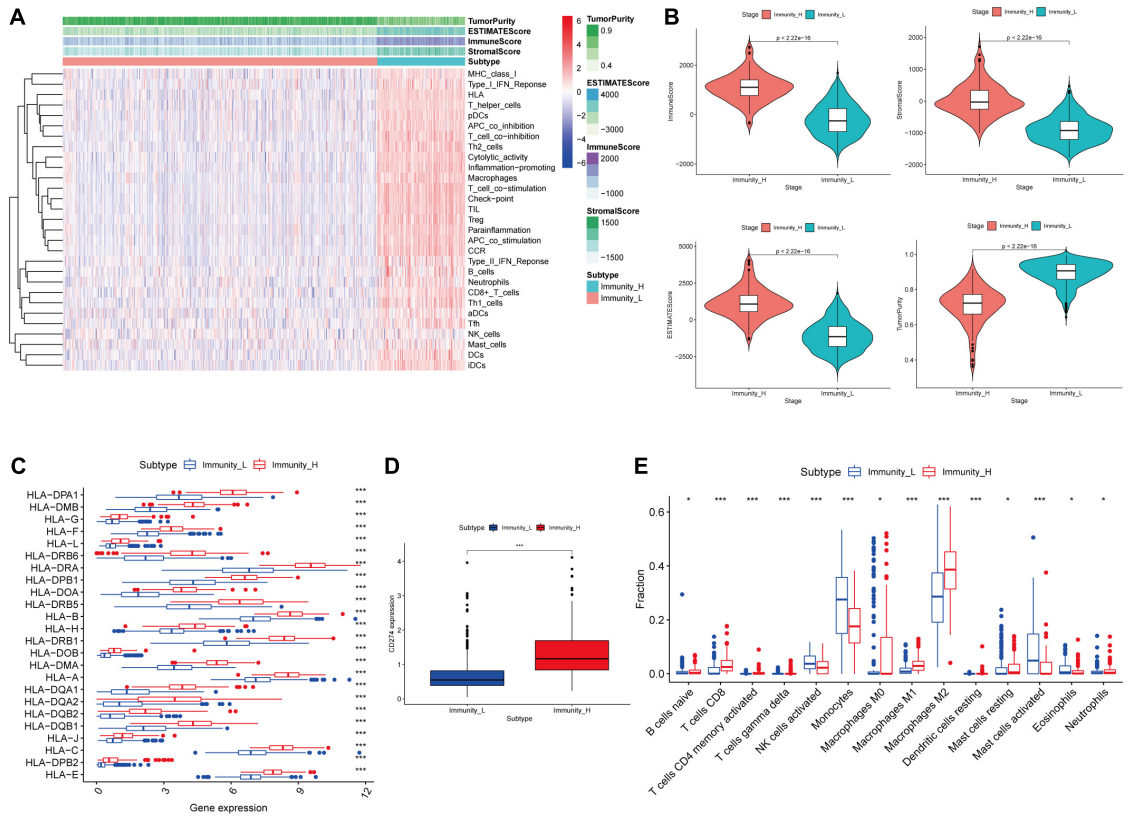


**FIGURE 1 |** Construction and validation of glioma grouping. **(A)** The display of tumor purity, ESTIMATE score, immune score, and stromal score of each sample gene calculated by ESTIMATE's algorithm between the high immune infiltration group and the low immune infiltration group. **(B)** The boxplot showed a statistical difference between the two groups in tumor purity, ESTIMATE score, immune score, and stromal score. **(C,D)** The expression of HLA family genes and CD274 between the two groups. **(E)** The proportion difference of immune cells calculated by CIBERSORT method between the two groups. "Immunity_H" and "Immunity_L" represent the high immune cell infiltration group and the low immune cell infiltration group, respectively; $^{*}p < 0.05$ and $^{***}p < 0.001$.

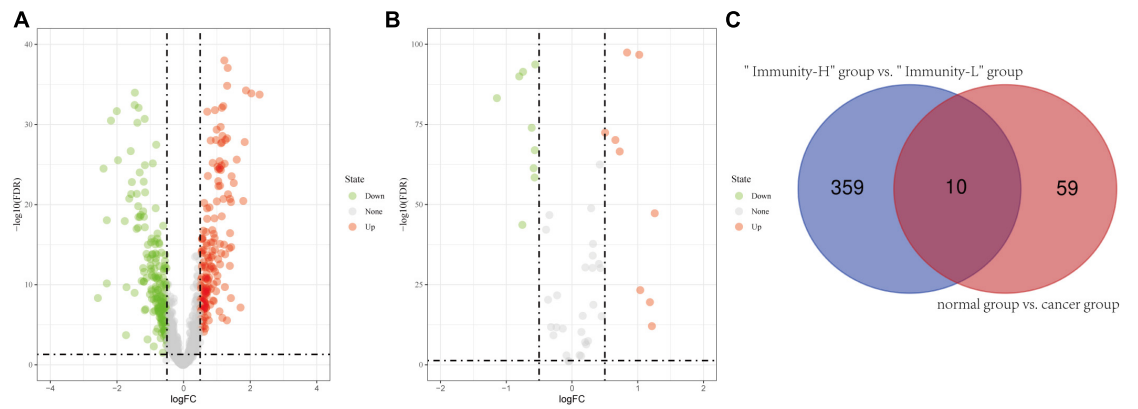


**FIGURE 2 |** Identification of differentially expressed lncRNAs. **(A)** Differentially expressed lncRNAs between the high immune infiltration group and the low immune infiltration group. **(B)** Differentially expressed lncRNAs between the cancer group and the normal group. **(C)** The intersection of differentially expressed lncRNAs is shown in the Venn diagram. "Immunity_H" and "Immunity_L" represent the high immune cell infiltration group and the low immune cell infiltration group, respectively.

UCSC Xena website, we identified 69 differentially expressed lncRNAs between the cancer and normal groups, including 34 up-regulated lncRNAs and 35 down-regulated lncRNAs in the cancer group compared to the normal group (**Figure 2B**). A two-way Venn analysis was then applied to select lncRNAs which were differentially expressed in both the high immune cell infiltration group compared with the low immune cell infiltration group and the cancer group compared with the normal group. Ultimately 10 lncRNAs were identified as immune-related lncRNAs in glioma (**Figure 2C**).

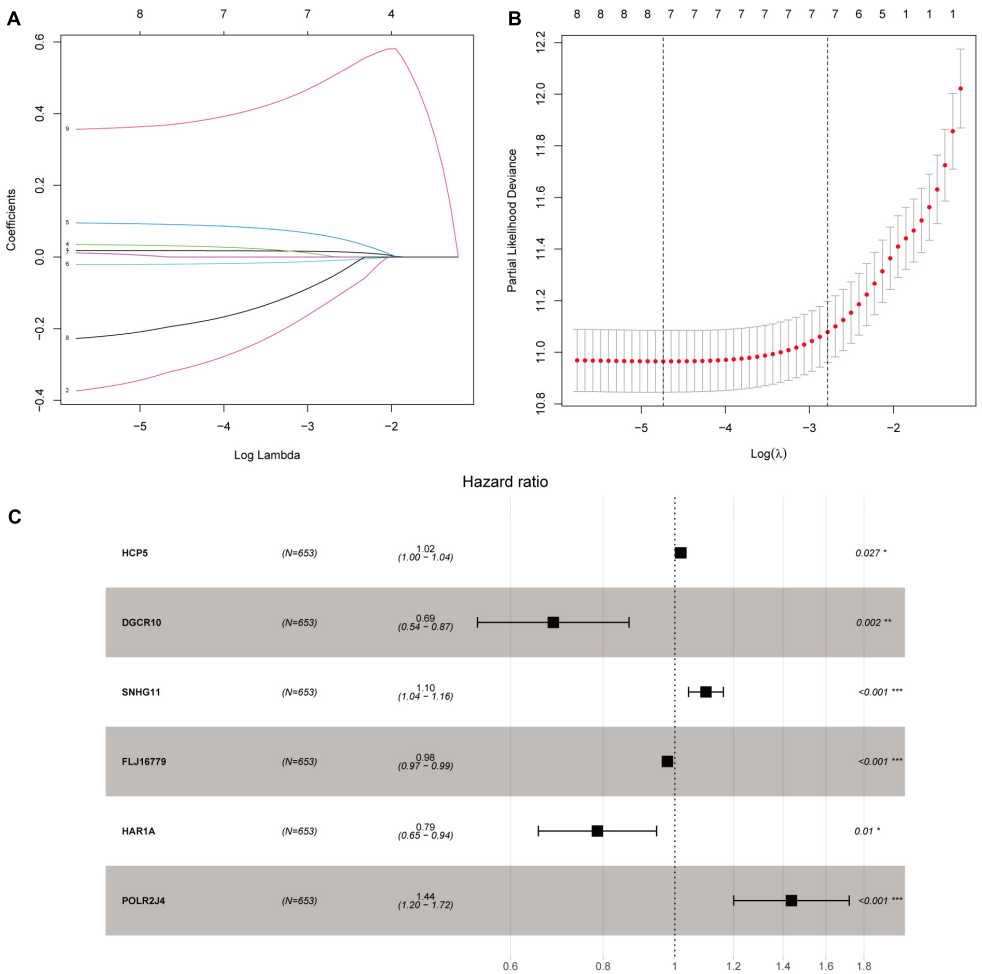


**FIGURE 3 |** Construction of an immune-related lncRNA prognostic risk score model. **(A)** LASSO Cox regression analysis of the nine prognostic lncRNAs. **(B)** Ten-round cross-validation was conducted for the optimal penalty parameter lambda. **(C)** Multivariate Cox regression analysis of immune-related lncRNAs. $^{*}p < 0.05$, $^{**}p < 0.01$, and $^{***}p < 0.001$.

## Construction and Validation of Immune-Related LncRNA Prognostic Signature

After screening data with eligible survival information, a total of 653 samples were available for further analyses. Univariate Cox regression analysis was used to screen lncRNA associated with the glioma patients' overall survival, and nine lncRNAs were selected. Then these nine lncRNAs were entered for LASSO regression analysis and multivariate Cox regression analysis (**Figures 3A,B**). Ultimately, six lncRNAs (HCP5, DGCR10, SNHG11, FLJ16779, HAR1A, and POLR2J4) were selected in this prognostic signature (**Table 1**) and the contribution of lncRNAs in the calculation formula is shown in **Figure 3C**. Therefore, a prognostic prediction model was developed based on the six lncRNAs as follows: risk score = $(0.0183) \times EXP_{HCP5} - (0.3778) \times EXP_{DGCR10} + (0.0968) \times EXP_{SNHG11} - (0.0229) \times EXP_{FLJ16779} - (0.2407) \times EXP_{HAR1A} + (0.3625) \times EXP_{POLR2J4}$. According to the risk score, glioma samples were divided into a low-risk group and a high-risk group with a median risk score as the threshold. HCP5, SNHG11, and POLR2J4 were highly expressed in the high-risk group, whereas DGCR10, FLJ16779, and HAR1A were highly expressed in the low-risk group (**Figure 4C**). The distribution of risk score and survival status is illustrated in **Figures 4A,B**.

**TABLE 1 |** The expression levels of these six lncRNAs.

| ID | Coefficient | HR | HR.95L | HR.95H | *p* value |
|---|---|---|---|---|---|
| HCP5 | 0.0183 | 1.0185 | 1.0021 | 1.0352 | 0.0273 |
| DGCR10 | −0.3778 | 0.6854 | 0.5415 | 0.8674 | 0.0017 |
| SNHG11 | 0.0968 | 1.1017 | 1.0436 | 1.1629 | 0.0005 |
| FLJ16779 | −0.0229 | 0.9773 | 0.9667 | 0.9881 | 4.10e-05 |
| HAR1A | −0.2407 | 0.7860 | 0.6541 | 0.9447 | 0.0103 |
| POLR2J4 | 0.3625 | 1.4369 | 1.2007 | 1.7196 | 7.61e-05 |

To evaluate the prediction model, the K-M curve revealed that the patients in the high-risk group showed a shorter survival time or lower survival probability compared to the low-risk group

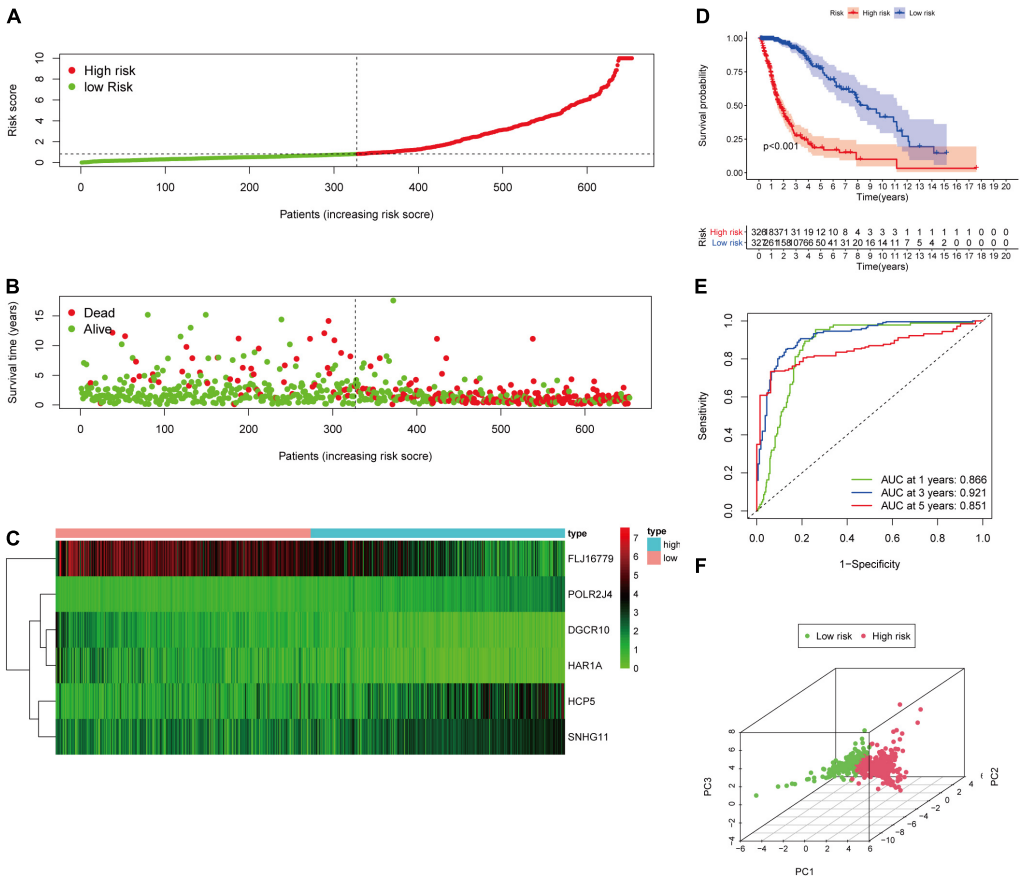


**FIGURE 4 |** Validation of the immune-related lncRNA prognostic risk score model. **(A)** The distribution of risk score. **(B)** The distribution of patients' survival time and status. **(C)** Heatmap of selected six immune-related lncRNAs of the classifier. **(D)** Kaplan–Meier curves of high-risk and low-risk score groups. **(E)** Time-dependent ROC analyses of the identified immune-related risk signature. **(F)** PCA analysis based on six survival-related immune lncRNAs.

(**Figure 4D**) with 1-, 3-, and 5-year AUC values of 0.866, 0.921, and 0.851, respectively (**Figure 4E**). The PCA result of the six immune-related lncRNAs is shown in the figure and indicated a significant distinction of the samples after risk score clustering between precorrection and postcorrection (**Figure 4F**).

## Independent Prognostic Analysis of the Immune-Related LncRNA Prognostic Signature

Considering that the prognosis of patients with glioma is associated with clinical characteristics such as age, gender, and pathological stage, univariate and multivariate Cox regression analyses were conducted. The results showed that the immune-related lncRNA prognostic signature could be taken as independent prognostic factors, as well as age and grade in both univariate and multivariate Cox regression analyses (**Figures 5A,B**). The contribution of each independent factor is presented in the nomogram (**Figures 5C,E**), and it revealed that the grade was the leading factor for predicting nomogram. Then we divided the glioma samples into glioblastoma multiforme (grade 4) and non–glioblastoma multiforme (grades 2 and 3). The nomogram in non–glioblastoma multiforme showed that risk score was the leading predicted factor with the grade as inferior impact (**Figures 5D,F**).

## Correlation Between Immune Checkpoint Expression and the Risk Score

Pearson correlation analysis between immune checkpoint expression and the risk score revealed that risk score was significantly correlated with all the 29 immune-related checkpoint expression ($p < 0.05$) in ssGSEA except neutrophils ($p = 0.43$). The relationship is partly displayed in **Figure 6**.

## Clinical Correlation and GSEA Functional Enrichment Analysis

We found that all lncRNAs in the signature were significantly different in different grades (**Figure 7**). In addition, GSEA suggested that immune response term and immune system process term significantly enriched in the high-risk group compared to the low-risk group (**Figures 8A,B**).

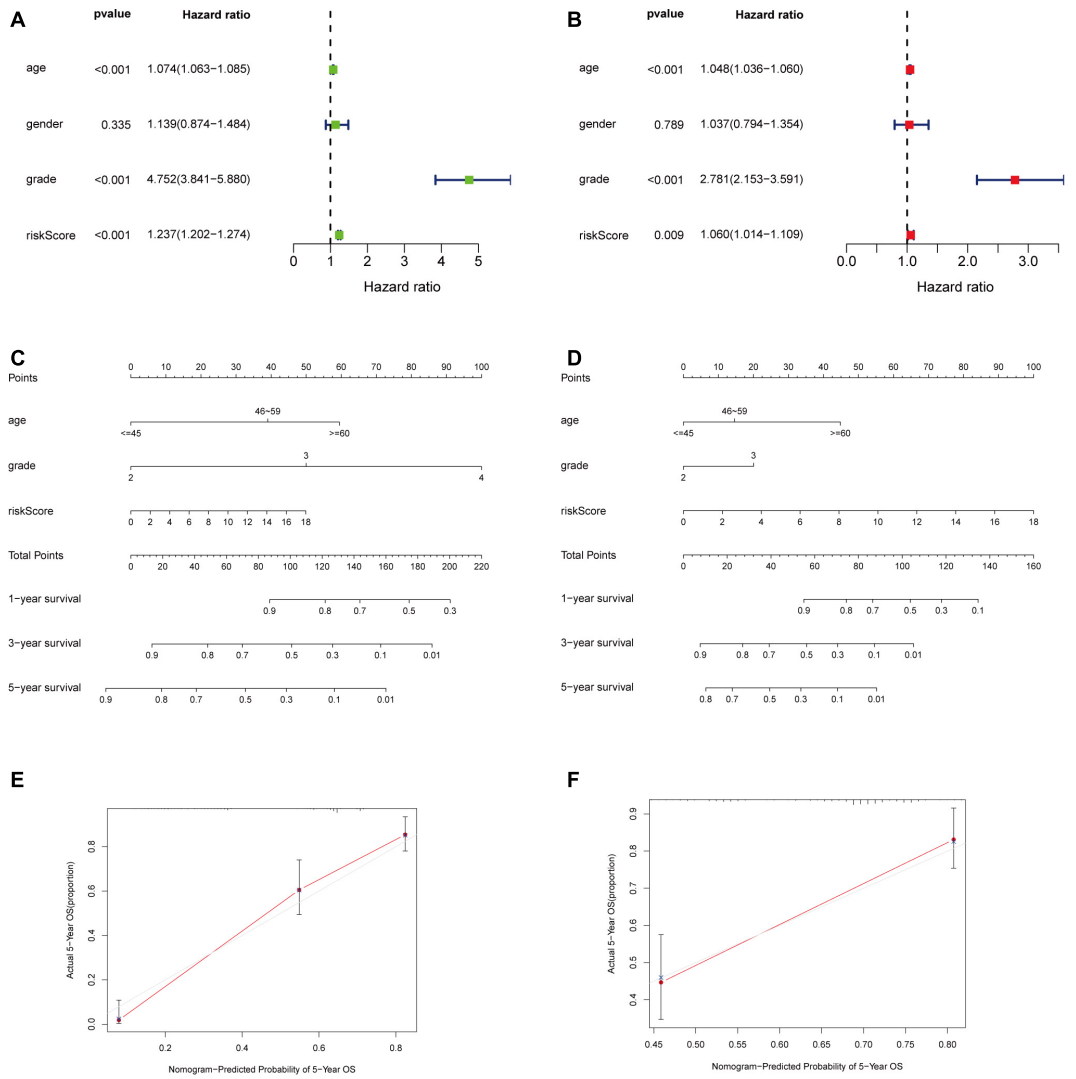


**FIGURE 5 |** Independent prognostic analysis of the immune-related lncRNA prognostic signature. The univariate **(A)** and multivariate **(B)** Cox regression analysis of risk score, age, gender, and grade. A nomogram to quantitatively predict 1-, 3-, and 5-year survival for all the glioma patients **(C)** and non–glioblastoma multiforme patients **(D)** Calibration curves of the nomogram model for showing the consistency between predicted and actual survival in all the glioma patients **(E)** and non–glioblastoma multiforme patients **(F)**.

## DISCUSSION

Glioma is the most common primary cancer of the central nervous system. Despite advances in conventional therapy, the prognosis for most glioma patients remains dismal. Nowadays, increasing insight into immunotherapy suggests it may be recognized as an effective treatment alternative. Immunotherapy that aims at stimulating a specific and sustained antitumor response is taken as a promising therapeutic approach. Immunomonitoring can track the effects of immunotherapy upon the patient's immune system and accelerate the development of immunotherapeutic agents. Therefore, investigating potential biomarkers of clinical benefit that can efficiently reflect treatment efficacy is one of the primary goals of immunomonitoring in glioma immunotherapy trials (Lamano et al., 2016). Thus, in the present study, we constructed a 6-lncRNA prognostic signature related to immune infiltration.

For the first time, immune-related lncRNAs in glioma were identified by screening differentially expressed lncRNAs between the high and low immune cell infiltration groups, which was divided by ssGSEA and verified by ESTIMATE, the expression of HLA and CD724, and the algorithm of CIBERSORT. Similarly, the study by Shen et al. (2020) on immune-related lncRNA prognostic signature for breast cancer also identified immune cell infiltration group by ssGSEA and verified the groups by ESTIMATE and CIBERSORT, which confirmed the feasibility of the methods further, whereas previous studies in glioma identified immune-related lncRNAs by GSEA database or the molecular signature database. In addition, compared to previous studies, the lncRNAs in our

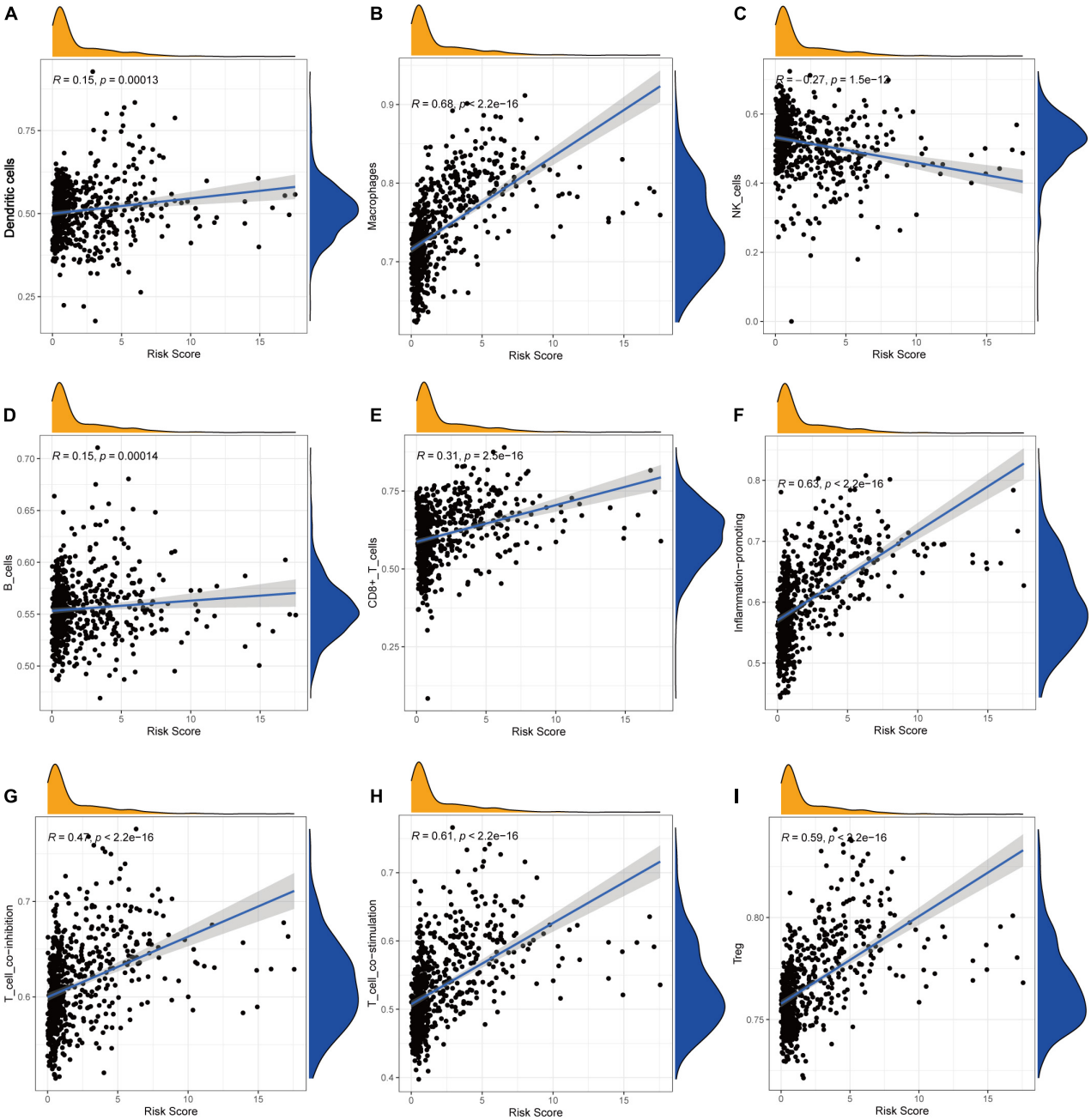


**FIGURE 6 |** Correlations between the risk score and infiltration abundances of immune cells and immune-related functions. **(A)** Dendritic cells, **(B)** macrophages, **(C)** NK cells, **(D)** B cells, **(E)** $CD8^+$ T cells, **(F)** inflammation promoting, **(G)** T-cell coinhibition, **(H)** T-cell costimulation, **(I)** Treg.

signature were not only immune-related but also differentially expressed between the cancer and normal groups (Tian et al., 2020; Xia et al., 2021). In this study, our signature achieved a satisfactory level of 1-, 3-, and 5-year AUC (0.866, 0.921, and 0.851, respectively), which outperformed Xia and colleagues' and Tian and colleagues' studies' 3-year AUC and was comparable with Tian and colleagues' study's 1- and 5-year AUCs. Moreover, we established a predicting nomogram combining age and grade to predict the survival of glioma patients more accurately and intuitively. When the samples were divided into glioblastoma (grade 4) and non–glioblastoma (grades 2 and 3), risk score was the dominant factor in the nomogram, indicating risk score was an excellent prognostic factor.

Long noncoding RNAs can be used as biomarkers to classify and predict tumors because they can display characteristic tissue-specific and cell-type–specific expression patterns (Deveson et al., 2017). Increasing evidence has shown that a specific lncRNA

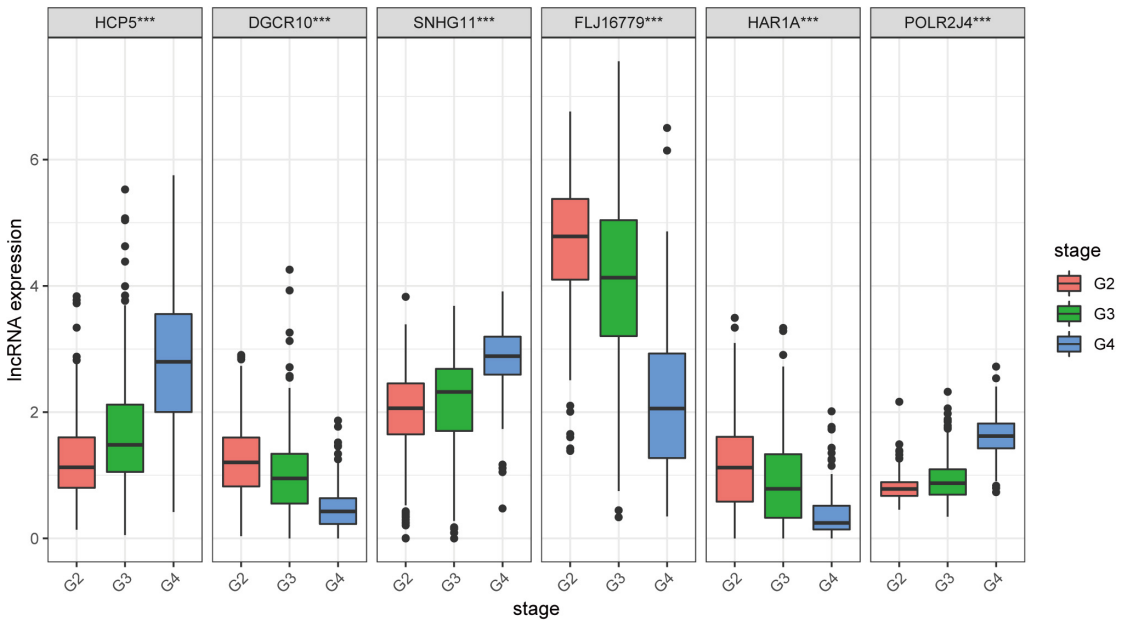


**FIGURE 7 |** Expression profile of six immune-related lncRNAs in the signature with different glioma grades.

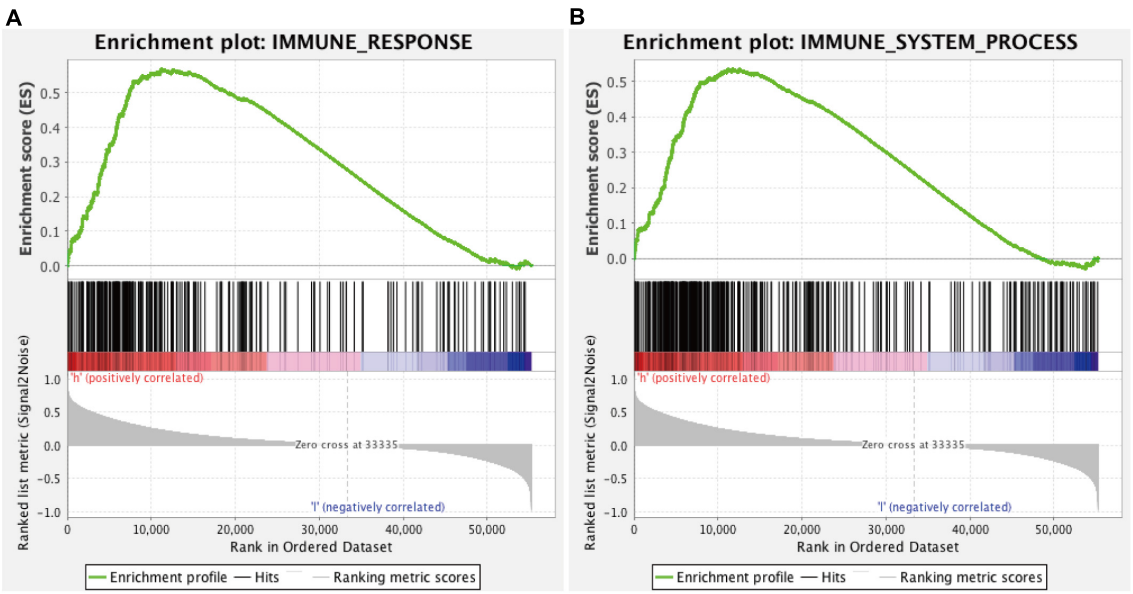


**FIGURE 8 |** GSEA for comparing immune response **(A)** and immune system process **(B)** between low- and high-risk groups.

plays a role in the onset and progression of various cancers, as well as tumorigenesis and progression in glioma (Huarte, 2015; Bhan et al., 2017). In our study, we extracted nine immune-related lncRNAs correlated with prognosis and differentially expressed in the cancer group compared to the normal group at the same time. After LASSO analysis and multivariate Cox regression analysis, six immune-related lncRNAs were selected to construct a prognostic signature. Most of them have been reported to be related to immune or participate in immune regulation in previous studies. HCP5 was mainly expressed in immune system cells and had an effect on autoimmunity (Li et al., 2018). Researches have indicated that HCP5 acted as an oncogene in glioma, and the expression of HCP5 increased with the level of grade of glioma (Zou and Chen, 2021). It is also reported that knockdown of HCP5 can inhibit proliferation, cell migration, and invasion, so as to promote apoptosis of glioma cells (Teng et al., 2016). SNHG11 was confirmed to express highly in glioblastoma compared to normal brain, and it could

promote proliferation, migration, and invasion via epithelial–mesenchymal transition by sponging miR154-5p (Geng et al., 2020). These findings are consistent with our findings that HCP5 and SNHG11 were highly expressed in the high-risk group. POLR2J4 has been reported as a composition of signature to predict the survival of cirrhotic hepatocellular carcinoma and recurrence-free hepatocellular carcinoma (Gu et al., 2019; Ma and Deng, 2019). It was also found to be a predictor of the risk for site-specific metastasis of breast cancer (Park et al., 2020). FLJ16779 was implicated in gastric carcinogenesis and progression via modulating energy metabolism (Wang et al., 2020). HAR1A was expressed specifically in Cajal–Retzius neurons in the developing human neocortex, and a previous study reported that HAR1A could act as a prognostic marker for isocitrate dehydrogenase mutant glioma (Pollard et al., 2006; Shi et al., 2019; Chen et al., 2020). However, no published studies have reported biological functions of DGCR10 so far, and further studies are needed to investigate its molecular characteristics.

Cancer tissues consist of not only malignant neoplastic cells but also immune cells, fibroblasts, endothelial cells, and an abundant collection of cytokines, chemokines, growth factors (Bremnes et al., 2011). Those components and their complicated interaction form the TME, and the various cellular compartments of the TME can critically regulate tumorigenesis, which is essential not only to tumor initiation, malignant progression, and metastasis but also to response to therapy (Klemm and Joyce, 2015). In TME, immune cells are the predominant host cells that are recruited to and activated (Bremnes et al., 2011). In myeloid lineage, TAM inhibition effects on blocking gliomagenesis and activated TAMs have confirmed the ability to regulate glioma stem cell pools within the brain. What is more, because of the plasticity of TAM, it may be feasible to develop strategies to reeducate macrophages to specifically adopt antitumor phenotypes in brain tumors, which are likely to be new immunotherapy methods. In lymphoid lineage, accumulated studies demonstrated that reprogramming of immunosuppressive T-cell subsets might boost antitumor immune responses in glioma or other brain tumors (Quail and Joyce, 2017). It is also an emerging field in cancer therapy to enhance T-cell activation via enabling costimulation primary in gliomas or brain metastases (Fecci et al., 2014; Cohen and Kluger, 2016). In this study, we found that six-lncRNA prognostic signature for glioma was associated with the infiltration of immune cell subtypes, which further verified the signature.

There were some limitations to the present study. First, it was a retrospective study, and prospective cohort studies are needed to further validate the results. Second, the biological functions of the six identified lncRNAs need comprehensive exploration and should be fully elucidated in *in vitro* and *in vivo* experiments, especially in terms of immune infiltration.

In conclusion, our study established a reliable immune-related prognostic signature. With further prospective validation, the signature may become therapeutic targets and offer biological information for personal treatment of glioma.

## DATA AVAILABILITY STATEMENT

Publicly available datasets were analyzed in this study. This data can be found here: the TCGA website (https://portal.gdc.cancer.gov) and the UCSC Xena website (https://xena.ucsc.edu/).

## AUTHOR CONTRIBUTIONS

XJ and JP conceived and designed the study. YC and JP wrote the manuscript. CR, JT, WY, QZ, ZX, and ZW analyzed the results. HZ, ZJ, YG, YK, CL, and MZ performed the image visualization. All authors contributed to the article and approved the submitted version.

## FUNDING

This study was supported by the National Natural Science Foundation of China (No. 81472355) and the Hunan Provincial Science and Technology Department (No. 2014FJ6006).

## REFERENCES

Anguille, S., Smits, E. L., Lion, E., van Tendeloo, V. F., and Berneman, Z. N. (2014). Clinical use of dendritic cells for cancer therapy. *Lancet Oncol.* 15, e257–e267. doi: 10.1016/s1470-2045(13)70585-0

Augoff, K., McCue, B., Plow, E. F., and Sossey-Alaoui, K. (2012). miR-31 and its host gene lncRNA LOC554202 are regulated by promoter hypermethylation in triple-negative breast cancer. *Mol. Cancer* 11:5. doi: 10.1186/1476-4598-11-5

Benjamini, Y., and Hochberg, Y. (1995). Controlling the false discovery rate: a practical and powerful approach to multiple testing. *J. R. Stat. Soc. Ser. B Methodol.* 57, 289–300. doi: 10.1111/j.2517-6161.1995.tb02031.x

Bhan, A., Soleimani, M., and Mandal, S. S. (2017). Long noncoding RNA and cancer: a new paradigm. *Cancer Res.* 77, 3965–3981. doi: 10.1158/0008-5472.Can-16-2634

Bindea, G., Mlecnik, B., Tosolini, M., Kirilovsky, A., Waldner, M., Obenauf, A. C., et al. (2013). Spatiotemporal dynamics of intratumoral immune cells reveal the immune landscape in human cancer. *Immunity* 39, 782–795. doi: 10.1016/j.immuni.2013.10.003

Bremnes, R. M., Al-Shibli, K., Donnem, T., Sirera, R., Al-Saad, S., Andersen, S., et al. (2011). The role of tumor-infiltrating immune cells and chronic inflammation at the tumor site on cancer development, progression, and prognosis: emphasis on non-small cell lung cancer. *J. Thorac. Oncol.* 6, 824–833. doi: 10.1097/JTO.0b013e3182037b76

Chen, Y., Guo, Y., Chen, H., and Ma, F. (2020). Long non-coding RNA expression profiling identifies a four-long non-coding RNA prognostic signature for isocitrate dehydrogenase mutant glioma. *Front. Neurol.* 11:573264. doi: 10.3389/fneur.2020.573264

Cohen, J. V., and Kluger, H. M. (2016). Systemic immunotherapy for the treatment of brain metastases. *Front. Oncol.* 6:49. doi: 10.3389/fonc.2016.00049

Deveson, I. W., Hardwick, S. A., Mercer, T. R., and Mattick, J. S. (2017). The dimensions, dynamics, and relevance of the mammalian noncoding transcriptome. *Trends Genet.* 33, 464–478. doi: 10.1016/j.tig.2017.04.004

Fecci, P. E., Heimberger, A. B., and Sampson, J. H. (2014). Immunotherapy for primary brain tumors: no longer a matter of privilege. *Clin. Cancer Res.* 20, 5620–5629. doi: 10.1158/1078-0432.Ccr-14-0832

Feng, L., Lin, T., Che, H., and Wang, X. (2020). Long noncoding RNA DANCR knockdown inhibits proliferation, migration and invasion of glioma by regulating miR-135a-5p/BMI1. *Cancer Cell Int.* 20:53. doi: 10.1186/s12935-020-1123-4

Geng, Y. B., Xu, C., Wang, Y., and Zhang, L. W. (2020). Long non-coding RNA SNHG11 promotes cell proliferation, invasion and migration in glioma by targeting miR-154-5p. *Eur. Rev. Med. Pharmacol. Sci.* 24, 4901–4908. doi: 10.26355/eurrev_202005_21179

Gousias, K., Markou, M., Voulgaris, S., Goussia, A., Voulgari, P., Bai, M., et al. (2009). Descriptive epidemiology of cerebral gliomas in northwest Greece and study of potential predisposing factors, 2005-2007. *Neuroepidemiology* 33, 89–95. doi: 10.1159/000222090

Gu, J. X., Zhang, X., Miao, R. C., Xiang, X. H., Fu, Y. N., Zhang, J. Y., et al. (2019). Six-long non-coding RNA signature predicts recurrence-free survival in hepatocellular carcinoma. *World J. Gastroenterol.* 25, 220–232. doi: 10.3748/wjg.v25.i2.220

Hambardzumyan, D., Gutmann, D. H., and Kettenmann, H. (2016). The role of microglia and macrophages in glioma maintenance and progression. *Nat. Neurosci.* 19, 20–27. doi: 10.1038/nn.4185

Huarte, M. (2015). The emerging role of lncRNAs in cancer. *Nat. Med.* 21, 1253–1261. doi: 10.1038/nm.3981

Kang, C. M., Bai, H. L., Li, X. H., Huang, R. Y., Zhao, J. J., Dai, X. Y., et al. (2019). The binding of lncRNA RP11-732M18.3 with 14-3-3 β/α accelerates p21 degradation and promotes glioma growth. *EBioMedicine* 45, 58–69. doi: 10.1016/j.ebiom.2019.06.002

Klemm, F., and Joyce, J. A. (2015). Microenvironmental regulation of therapeutic response in cancer. *Trends Cell Biol.* 25, 198–213. doi: 10.1016/j.tcb.2014.11.006

Komohara, Y., Ohnishi, K., Kuratsu, J., and Takeya, M. (2008). Possible involvement of the M2 anti-inflammatory macrophage phenotype in growth of human gliomas. *J. Pathol.* 216, 15–24. doi: 10.1002/path.2370

Lamano, J. B., Ampie, L., Choy, W., Kesavabhotla, K., DiDomenico, J. D., Oyon, D. E., et al. (2016). Immunomonitoring in glioma immunotherapy: current status and future perspectives. *J. Neurooncol.* 127, 1–13. doi: 10.1007/s11060-015-2018-4

Li, J., Zhu, Y., Wang, H., and Ji, X. (2018). Targeting long noncoding RNA in glioma: a pathway perspective. *Mol. Ther. Nucleic Acids* 13, 431–441. doi: 10.1016/j.omtn.2018.09.023

Liu, Y., Zhou, D., Li, G., Ming, X., Tu, Y., Tian, J., et al. (2015). Long non coding RNA-UCA1 contributes to cardiomyocyte apoptosis by suppression of p27 expression. *Cell Physiol. Biochem.* 35, 1986–1998. doi: 10.1159/000374006

Ma, L., and Deng, C. (2019). Identification of a novel four-lncRNA signature as a prognostic indicator in cirrhotic hepatocellular carcinoma. *PeerJ* 7:e7413. doi: 10.7717/peerj.7413

Newman, A. M., Liu, C. L., Green, M. R., Gentles, A. J., Feng, W., Xu, Y., et al. (2015). Robust enumeration of cell subsets from tissue expression profiles. *Nat. Methods* 12, 453–457. doi: 10.1038/nmeth.3337

Orom, U. A., Derrien, T., Beringer, M., Gumireddy, K., Gardini, A., Bussotti, G., et al. (2010). Long noncoding RNAs with enhancer-like function in human cells. *Cell* 143, 46–58. doi: 10.1016/j.cell.2010.09.001

Ostrom, Q. T., Bauchet, L., Davis, F. G., Deltour, I., Fisher, J. L., Langer, C. E., et al. (2014). The epidemiology of glioma in adults: a "state of the science" review. *Neuro Oncol.* 16, 896–913. doi: 10.1093/neuonc/nou087

Ostrom, Q. T., Gittleman, H., Xu, J., Kromer, C., Wolinsky, Y., Kruchko, C., et al. (2016). CBTRUS statistical report: primary brain and other central nervous system tumors diagnosed in the United States in 2009-2013. *Neuro Oncol.* 18(supple_5), v1–v75. doi: 10.1093/neuonc/now207

Park, S. B., Hwang, K. T., Chung, C. K., Roy, D., and Yoo, C. (2020). Causal Bayesian gene networks associated with bone, brain and lung metastasis of breast cancer. *Clin. Exp. Metastasis* 37, 657–674. doi: 10.1007/s10585-020-10060-0

Pollard, K. S., Salama, S. R., Lambert, N., Lambot, M. A., Coppens, S., Pedersen, J. S., et al. (2006). An RNA gene expressed during cortical development evolved rapidly in humans. *Nature* 443, 167–172. doi: 10.1038/nature05113

Quail, D. F., and Joyce, J. A. (2013). Microenvironmental regulation of tumor progression and metastasis. *Nat. Med.* 19, 1423–1437. doi: 10.1038/nm.3394

Quail, D. F., and Joyce, J. A. (2017). The microenvironmental landscape of brain tumors. *Cancer Cell* 31, 326–341. doi: 10.1016/j.ccell.2017.02.009

Ritchie, M. E., Phipson, B., Wu, D., Hu, Y., Law, C. W., Shi, W., et al. (2015). limma powers differential expression analyses for RNA-sequencing and microarray studies. *Nucleic Acids Res.* 43, e47. doi: 10.1093/nar/gkv007

Shen, Y., Peng, X., and Shen, C. (2020). Identification and validation of immune-related lncRNA prognostic signature for breast cancer. *Genomics* 112, 2640–2646. doi: 10.1016/j.ygeno.2020.02.015

Shi, Z., Luo, Y., Zhu, M., Zhou, Y., Zheng, B., Wu, D., et al. (2019). Expression analysis of long non-coding RNA HAR1A and HAR1B in HBV-induced hepatocullular carcinoma in Chinese patients. *Lab. Med.* 50, 150–157. doi: 10.1093/labmed/lmy055

Stupp, R., Hegi, M. E., Mason, W. P., van den Bent, M. J., Taphoorn, M. J., Janzer, R. C., et al. (2009). Effects of radiotherapy with concomitant and adjuvant temozolomide versus radiotherapy alone on survival in glioblastoma in a randomised phase III study: 5-year analysis of the EORTC-NCIC trial. *Lancet Oncol.* 10, 459–466. doi: 10.1016/S1470-2045(09)70025-7

Sun, Y., Wang, Z., and Zhou, D. (2013). Long non-coding RNAs as potential biomarkers and therapeutic targets for gliomas. *Med. Hypotheses* 81, 319–321. doi: 10.1016/j.mehy.2013.04.010

Teng, H., Wang, P., Xue, Y., Liu, X., Ma, J., Cai, H., et al. (2016). Role of HCP5-miR-139-RUNX1 feedback loop in regulating malignant behavior of glioma cells. *Mol. Ther.* 24, 1806–1822. doi: 10.1038/mt.2016.103

Tian, Y., Ke, Y. Q., and Ma, Y. (2020). Immune-Related lncRNA Correlated with Transcription Factors Provide Strong Prognostic Prediction in Gliomas. *J. Oncol.* 2020:2319194. doi: 10.1155/2020/2319194

Wang, Y., Zhang, H., and Wang, J. (2020). Discovery of a novel three-long non-coding RNA signature for predicting the prognosis of patients with gastric cancer. *J. Gastrointest. Oncol.* 11, 760–769. doi: 10.21037/jgo-20-140

Wang, Z., Zhang, X. J., Ji, Y. X., Zhang, P., Deng, K. Q., Gong, J., et al. (2016). The long noncoding RNA Chaer defines an epigenetic checkpoint in cardiac hypertrophy. *Nat. Med.* 22, 1131–1139. doi: 10.1038/nm.4179

Wilusz, J. E., Sunwoo, H., and Spector, D. L. (2009). Long noncoding RNAs: functional surprises from the RNA world. *Genes Dev.* 23, 1494–1504. doi: 10.1101/gad.1800909

Wu, Y., Song, Z., Sun, K., Rong, S., Gao, P., Wang, F., et al. (2019). A novel scoring system based on peripheral blood test in predicting grade and prognosis of patients with glioma. *Onco Targets Ther.* 12, 11413–11423. doi: 10.2147/OTT.S236598

Xia, P., Li, Q., Wu, G., and Huang, Y. (2021). An immune-related lncRNA signature to predict survival in glioma patients. *Cell Mol. Neurobiol.* 41, 365–375. doi: 10.1007/s10571-020-00857-8

Yoshihara, K., Shahmoradgoli, M., Martínez, E., Vegesna, R., Kim, H., Torres-Garcia, W., et al. (2013). Inferring tumour purity and stromal and immune cell admixture from expression data. *Nat. Commun.* 4:2612. doi: 10.1038/ncomms3612

Zheng, R., Yao, Q., Ren, C., Liu, Y., Yang, H., Xie, G., et al. (2016). Upregulation of long noncoding RNA small nucleolar RNA host gene 18 promotes radioresistance of glioma by repressing semaphorin 5A. *Int. J. Radiat. Oncol. Biol. Phys.* 96, 877–887. doi: 10.1016/j.ijrobp.2016.07.036

Zou, Y., and Chen, B. (2021). Long non-coding RNA HCP5 in cancer. *Clin. Chim. Acta* 512, 33–39. doi: 10.1016/j.cca.2020.11.015

**Conflict of Interest:** The authors declare that the research was conducted in the absence of any commercial or financial relationships that could be construed as a potential conflict of interest.

frontiers in Genetics

ORIGINAL RESEARCH
published: 26 August 2021
doi: 10.3389/fgene.2021.666106

# ESPL1 Is a Novel Prognostic Biomarker Associated With the Malignant Features of Glioma

*Zhendong Liu[1,2†], Xiaoyu Lian[3†], Xiuru Zhang[1†], Yongjie Zhu[4†], Wang Zhang[5], Jialin Wang[3], Hongbo Wang[4], Binfeng Liu[3], Zhishuai Ren[3], Mengjun Zhang[6], Mingyang Liu[1] and Yanzheng Gao[1,2*]*

[1] Department of Surgery of Spine and Spinal Cord, Henan Provincial People's Hospital, Henan International Joint Laboratory of Intelligentized Orthopedics Innovation and Transformation, Henan Key Laboratory for Intelligent Precision Orthopedics, People's Hospital of Zhengzhou University, People's Hospital of Henan University, Zhengzhou, China, [2] Department of Surgery of Spine and Spinal Cord, Microbiome Laboratory, Henan Provincial People's Hospital, People's Hospital of Zhengzhou University, People's Hospital of Henan University, Zhengzhou, China, [3] Zhengzhou University People's Hospital, Henan Provincial People's Hospital, Zhengzhou, China, [4] Henan University People's Hospital, Henan Provincial People's Hospital, Zhengzhou, China, [5] Department of Neurosurgery, The First Affiliated Hospital of Harbin Medical University, Harbin, China, [6] Harbin Medical University Cancer Hospital, Heilongjiang Provincial Cancer Hospital, Harbin, China

OPEN ACCESS

**Edited by:**
Pawel Buczkowicz,
PhenoTips, Canada

**Reviewed by:**
Ajay Chatrath,
University of Virginia, United States
Jozsef Dudas,
Innsbruck Medical University, Austria

***Correspondence:**
Yanzheng Gao
yanzhenggaohn@163.com

[†] These authors have contributed equally to this work

**Specialty section:**
This article was submitted to Cancer Genetics and Oncogenomics, a section of the journal Frontiers in Genetics

**Received:** 15 March 2021
**Accepted:** 04 August 2021
**Published:** 26 August 2021

**Citation:**
Liu Z, Lian X, Zhang X, Zhu Y, Zhang W, Wang J, Wang H, Liu B, Ren Z, Zhang M, Liu M and Gao Y (2021) ESPL1 Is a Novel Prognostic Biomarker Associated With the Malignant Features of Glioma. Front. Genet. 12:666106. doi: 10.3389/fgene.2021.666106

Research has confirmed that extra spindle pole bodies-like 1 (ESPL1), an etiological factor, promotes the malignant progression of cancers. However, the relationship between ESPL1 and glioma has not yet been demonstrated. The purpose of this study was to reveal the potential mechanisms of ESPL1-mediated malignant glioma progression. Gene expression data and detailed clinical information of glioma cases were obtained from multiple public databases. Subsequently, a series of bioinformatics analyses were used to elucidate the effects of ESPL1 on glioma. The results demonstrated that the mRNA and protein levels of ESPL1 in glioma were higher than those in normal brain tissues. In addition, ESPL1 expression was considerably associated with the clinical and pathological features of gliomas, such as World Health Organization grade, histology, and 1p19q co-deletion status. Importantly, ESPL1 reduced the overall survival (OS) of glioma patients and had prognostic value for gliomas. Gene set enrichment analysis (GSEA) indirectly revealed that ESPL1 regulates the activation of cancer-related pathways, such as the cell cycle and base excision repair pathways. In addition, we used the Connectivity Map (CMap) database to screen three molecular drugs that inhibit ESPL1: thioguanosine, antimycin A, and zidovudine. Finally, reverse transcription-quantitative polymerase chain reaction (RT-qPCR) was used to detect the expression levels of ESPL1 in glioma cell lines. This study plays an important role in revealing the etiology of glioma by revealing the function of ESPL1, providing a potential molecular marker for the diagnosis and treatment of glioma, especially low-grade glioma.

**Keywords: ESPL1, glioma, CGGA, TCGA, prognosis, biomarker**

## INTRODUCTION

Glioma is one of the most prevalent and tricky malignant intracranial tumors due to its infiltrative growth, high degree of malignancy, and unfavorable prognosis (Cordier et al., 2016). According to the 2016 World Health Organization (WHO) guidelines, gliomas are further classified into grades I–IV, of which grades I and II are low-grade gliomas and grades III and IV (glioblastoma, GBM) are high-grade gliomas (Wesseling and Capper, 2018). GBM is the most malignant type; the median survival time is still less than 2 years after maximum resection combined with radiotherapy and chemotherapy, with a 5-year survival rate of only 9.8% (Stupp et al., 2005, 2009). The prognosis of grades II and III gliomas was improved but was still not optimistic at 2 and 2–5 years, respectively (Bell et al., 2015). Although, worldwide, researchers have made significant efforts to facilitate early diagnosis and ensure comprehensive treatment of gliomas, patient prognosis is still not ideal due to its malignant biological characteristics, causing affliction to the families of the patients as well as a huge medical burden to society. One of the reasons for this situation might be the lack of reliable and effective biomarkers for early diagnosis and targeted treatment.

Extra spindle pole bodies-like 1 (ESPL1), a cysteine endopeptidase, plays a vital role in the stable binding between sister chromatids before anaphase and their timely separation during anaphase, which is the key to chromosome inheritance (Chestukhin et al., 2003; Schöckel et al., 2011). When ESPL1 is overactivated, it acts as an oncogene, making cells susceptible to aneuploidy induced by chromosomal mismatch as well as vulnerable to DNA damage and loss of key tumor suppressor gene sites associated with tumorigenesis and disease progression (Pati, 2008; Mukherjee et al., 2014). For example, the overexpression of separase in the mammary glands of mouse mammary tumor virus (MMTV)-ESPL1 mice leads to the occurrence of highly aneuploid breast cancer, which has a high degree of chromosomal instability and an invasive disease phenotype. In addition, Liu J. et al. (2020) showed that the abnormal expression of ESPL1 in endometrial cancer (EC) cells facilitates metastasis and invasion, thereby leading to poor prognosis of EC. ESPL1 also participates in the occurrence and development of other human cancers and is associated with reduced patient survival (Meyer et al., 2009). However, the regulatory mechanisms of ESPL1 in gliomas has not yet been studied. Based on the role of ESPL1 in other tumors, we speculate that ESPL1 might be associated with the clinical features and survival prognosis of glioma patients.

The major aim of this study was to evaluate the expression level, prognostic value, and biological function of ESPL1 based on glioma tissue samples from multiple databases. High expression of ESPL1 was observed at both the mRNA and protein levels by reverse transcription-quantitative polymerase chain reaction (RT-qPCR) and immunohistochemistry (IHC). Our results demonstrated that upregulation of ESPL1 is associated with poor prognosis in glioma patients. Therefore, it is reasonable to speculate that ESPL1 may represent a novel and reliable biomarker for glioma and may aid in the development of individualized treatment strategies.

## MATERIALS AND METHODS

### Data Collection

Gene expression profiling interactive analysis (GEPIA)[1] is a convenient and intuitive online public database established by Peking University (Tang et al., 2017). A variety of human tumor and corresponding normal tissue samples are freely available on the website. The database was used to detect the expression levels of ESPL1 in various tumors. The difference in target gene expression in tumor tissues can be obtained by inputting the target gene on the official website. In addition, we downloaded the GSE2223 dataset based on the GPL1833 platform, and the GSE4290 and GSE50161 datasets based on the GPL570 platform from Gene Expression Omnibus (GEO)[2] (Barrett et al., 2013). GSE2223 contains 50 glioma and 4 normal tissue samples; GSE50161 contains 34 glioma and 13 normal tissue samples; and GSE4290 contains 77 glioma and 23 normal tissue samples. Three different datasets obtained from the GEO database were used to analyze the changes in ESPL1 expression levels in glioma and control brain tissues. These operations were performed using the limma package in R software according to a cut-off standard ($p < 0.05$, logFC $> 1$) to complete the differential expression of ESPL1 in glioma and control brain tissues.

The Chinese Glioma Genome Atlas (CGGA)[3] is a public database that contains various types of high-throughput data and corresponding clinical information. By excluding data with incomplete clinical information, we obtained an RNA-seq dataset containing 748 glioma samples and gene microarray data containing 268 glioma samples. The Cancer Genome Atlas (TCGA)[4] is a credible database that primarily stores several human malignant tumors (Tomczak et al., 2015). We also searched for and obtained mRNA sequencing and clinical information of 653 human gliomas from the TCGA RNA-seq dataset. **Supplementary Tables 1–3** provide clinical information of the patients corresponding to the three CGGA RNA-seq, CGGA microarray, and TCGA RNA-seq datasets. The above three original datasets contain detailed data on clinical–molecular characteristics, survival time, and status of glioma patients; thus, they were used to analyze the impact of ESPL1 expression changes on prognosis, clinical–molecular characteristics, and diagnostic value of glioma patients. All these datasets were divided into high- and low-expression groups according to the median expression level of ESPL1 in all samples for subsequent analysis. Statistical significance set at $p < 0.05$ was considered meaningful.

The Human Protein Atlas (HPA)[5] is a comprehensive and diverse online data platform that contains information about human RNA and protein expression in various cancers (Uhlén et al., 2015; Thul et al., 2017; Uhlen et al., 2017; Thul and Lindskog, 2018). In this study, to detect changes in the expression level of ESPL1 protein in brain glioma tissue samples, we loaded

[1]http://gepia.cancer-pku.cn/index.html
[2]https://www.ncbi.nlm.nih.gov/geo/
[3]http://www.cgga.org.cn/
[4]https://portal.gdc.cancer.gov/
[5]http://www.proteinatlas.org/

ESPL1 into the database webpage to obtain its expression levels in normal brain, low-grade glioma, and high-grade glioma tissue samples. Therefore, we only observed changes in the ESPL1 protein levels among the groups.

## GSEA

Gene set enrichment analysis (GSEA) is a tool used to predict the function of target genes (Subramanian et al., 2005). We calibrated and normalized the CGGA RNA-seq, CGGA microarray, and TCGA RNA-seq datasets using limma software packages. According to the expression levels of ESPL1, it was divided into high and low expression groups. GSEA 4.0.2 jar software was used to explore the cell signaling pathways of ESPL1 in glioma patients. The number of gene permutations was set to 1000; "C2.cp.kegg.v7.4.symbols.gmt[curated]" was selected as the gene set database. The high expression group of ESPL1 was compared with the low expression group according to the cut-off standard. Values of $p < 0.05$ and FDR $< 0.25$ were regarded as statistically significant. Finally, the consistent results of the independent datasets are presented in the experimental results section.

## Connectivity Map Predicts Potential Therapeutic Drugs

Connectivity Map (CMap) is a drug research and development system founded by Harvard University and is a common tool for discovering the potential therapeutic effects of drugs (Lamb, 2007). In this study, we used the R language to screen for genes with co-expression relationships with ESPL1. We then selected 20 genes (10 positive and 10 negative) and uploaded them to the official website of CMap for analysis to obtain the corresponding small-molecule compounds. The obtained small-molecule drugs are regarded as valuable drugs according to $p < 0.001$ and enrichment $< -0.75$, which are presented in the Experimental Results section; the chemical structure formula of the final small-molecule drug as well as its 3D structure were obtained from the PubChem database.[6]

## Cell Culture and Reverse Transcription Quantitative Polymerase Chain Reaction Analysis

Human glioma cell lines (LN229, T98, and A172) and human-derived astrocytes (HA) were purchased from the Cell Bank of the Chinese Academy of Sciences (Shanghai, China). All cells were grown in incubators at 37°C and 5% carbon dioxide and were cultured in DMEM (HyClone, United States) supplemented with 10% FBS (Thermo Fisher Scientific, United States). To examine the expression levels of the three glioma cell lines (LN229, T98, and A172) and HA in ESPL1, total RNA was extracted from LN229, T98, A172, and HA cells using Tri-Reagent (Sigma, United States). Total RNA quality and quantity were determined using a NanoDrop One spectrophotometer (Thermo Fisher Scientific, United States), measuring 260/280 nm absorbance values. Subsequently, the cDNA was reverse transcribed from total RNA using the Transcriptor First Strand cDNA Synthesis kit (Novoprotein Scientific Inc., Shanghai, China). RT-qPCR was performed according to the guidelines for the FastStart Universal SYBR Green Master (ROX) (Novoprotein Scientific Inc., Shanghai, China). The results were quantified using QuantStudio software (Thermo Fisher Scientific, United States), following the manufacturer's instructions. GADPH was used as an internal reference. The primer sequences used in this study are listed in **Table 1**. Relative expression levels were determined using the $2^{-\Delta\Delta Ct}$ method. The expression level of ESPL1 was detected using the "$2^{-\Delta\Delta CT}$" method. Statistical differences were analyzed by unpaired *t*-test; values of $p < 0.05$, were considered statistically significant.

[6]https://pubchem.ncbi.nlm.nih.gov/

## Statistical Analysis

R (v.3.6.1) was used for statistical analysis. Cox regression was used to analyze the relationship between ESPL1 expression and the prognosis of glioma patients; the Kaplan–Meier method was used to create survival curves. Finally, the Wilcox or Kreskas test was utilized to explore the relationship between clinical molecular characteristics and ESPL1 expression in glioma patients. Differences were considered statistically significant at $^{*}p < 0.05$ or $^{**}p < 0.01$.

# RESULTS

## ESPL1 Is Highly Expressed in Glioma at Different Levels

Extra spindle pole bodies-like 1 expression in various tumors and matched normal tissues was assessed using the GEPIA online tool (**Figure 1A**); we observed that ESPL1 was abnormally highly expressed in a variety of malignant tumor tissues, including GBM, while the ESPL1 expression level of esophageal carcinoma (ESCA) was lower than that in normal tissues. Thereafter, to understand the changes in ESPL1 expression in glioma tissues at a deeper level, we performed analysis on three glioma-related GSE datasets (GSE2223, GSE4290, GSE50161) from the GEO database, including 40 normal brain and 161 glioma samples. As shown in **Figures 1B–D**, in these three datasets, the expression levels of ESPL1 in glioma tissues were significantly higher than those in corresponding normal tissues. To validate the above results, we further assessed the expression levels of ESPL1 in three glioma cell lines (T98, U251, and LN229) and in human astrocytes (HA) by RT-qPCR. The results revealed that ESPL1 was markedly overexpressed in glioma cell lines compared to that in HAs (**Figure 1E**).

**TABLE 1 |** Sequences of primers used for qRT-PCR analysis.

| Gene | Primer sequence (5′-3′) |
|---|---|
| ESPL1-F | GCCCTAAAACTTACAACAAA |
| ESPL1-R | AGACTCAAGCAAGAACAGAA |
| GAPDH-F | CAAGGTCATCCATGACAACTTTG |
| GAPDH-R | GTCCACCACCCTGTTGCTGTAG |

*F, forward; R, reverse.*

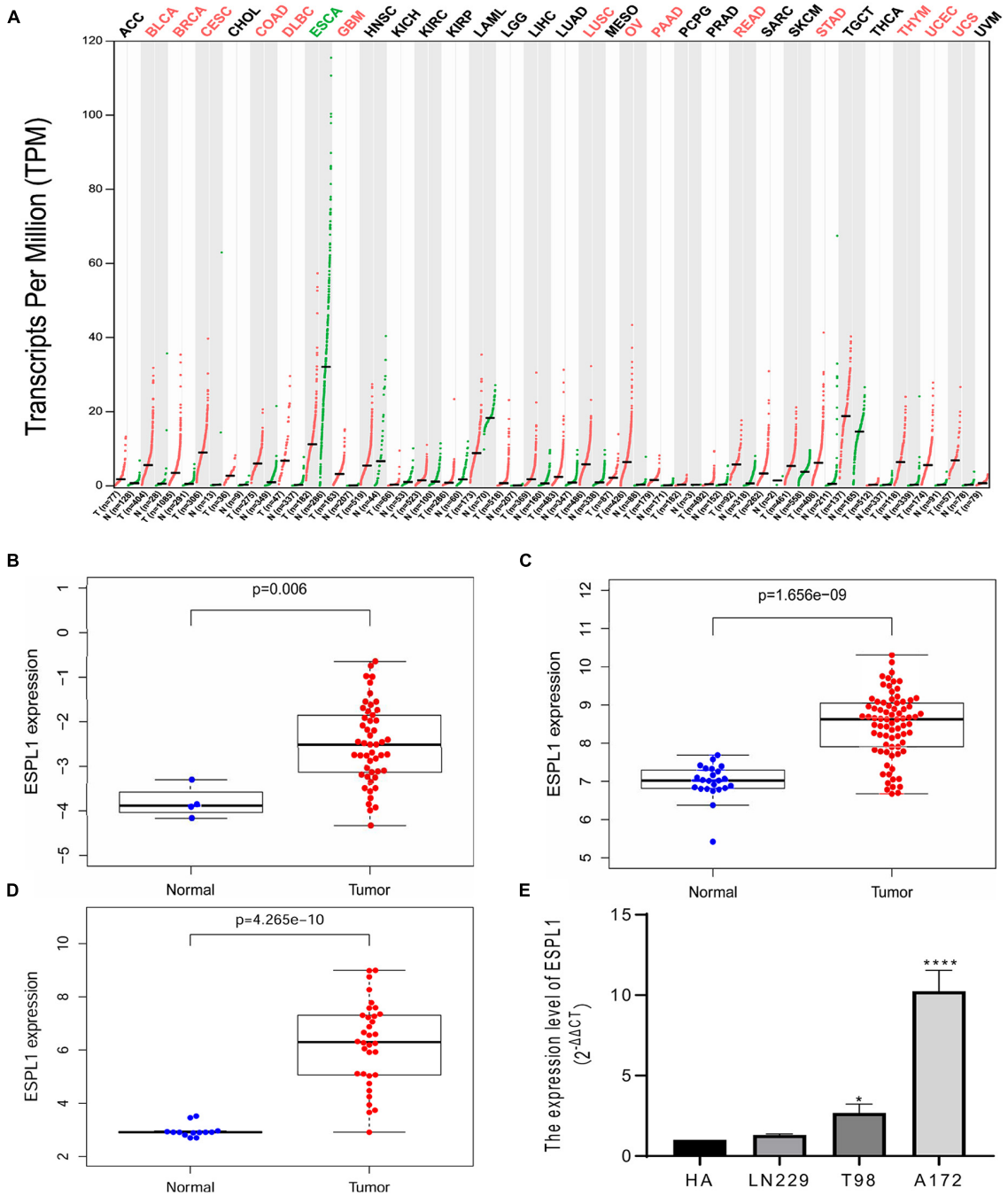


**FIGURE 1 |** Extra spindle pole bodies-like 1 expression in gliomas. **(A)** The expression of ESPL1 in a variety of malignant tumors. Red indicates that ESPL1 is higher than the corresponding normal control group, while green indicates that ESPL1 is highly expressed in the tumor. **(B)** ESPL1 expression in 50 gliomas and 4 normal brain tissues in GSE2223. The expression of ESPL1 in gliomas was significantly increased. **(C)** In the GSE4290 data, the expression of ESPL1 in 77 gliomas and 23 normal brain tissues was compared, and the expression of ESPL1 in gliomas increased. **(D)** Comparing 34 kinds of glioma tissue specimens with 13 normal brain tissue specimens in the GSE50161 data set, the expression level of ESPL1 in glioma tissue was significantly increased. **(E)** RT-qPCR experiments show that the expression level of ESPL1 in glioma cell lines (LN229, T98, and A172) is higher than that in human astrocytes. $^{*}p < 0.05$ and $^{****}p < 0.0001$.

## Overexpression of ESPL1 Leads to Poor Overall Survival in Glioma Patients

Next, to further examine the effects of abnormally high expression of ESPL1 on the prognosis of glioma, we analyzed three data cohorts: CGGA RNA-seq, CGGA microarray, and TCGA RNA-seq and created survival curves. As indicated in **Figures 2A–C**, high expression of ESPL1 in the three data cohorts consistently conveyed a significant reduction in patient

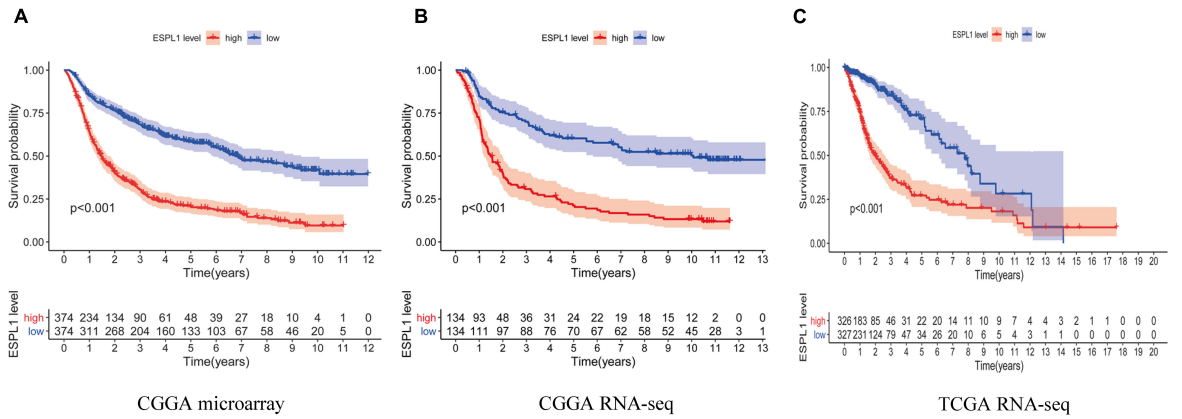


**FIGURE 2 |** The relationship between the difference of the expression level of ESPL1 and overall survival (OS). The red curve in the figure represents the ESPL1 high expression group, and the blue curve represents the ESPL1 low expression group. **(A)** CGGA RNA-seq dataset. **(B)** CGGA microarray dataset. **(C)** TCGA RNA-seq dataset.

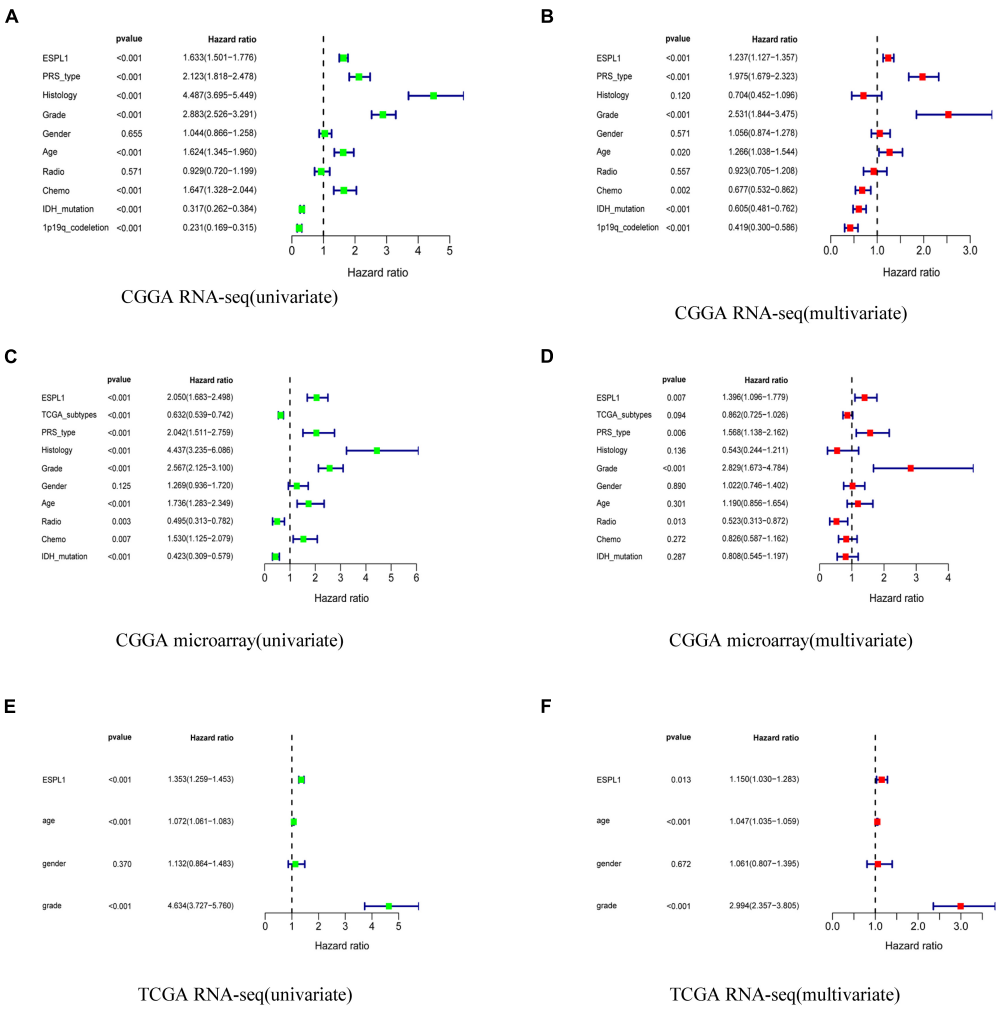


**FIGURE 3 |** Univariate analysis and multivariate analysis with Cox regression model. **(A)** Univariate analysis of CGGA RNA-seq database. **(B)** Multivariate analysis of CGGA RNA-seq database. **(C)** Univariate analysis of CGGA microarray database. **(D)** Multivariate analysis of CGGA microarray database. **(E)** Univariate analysis of TCGA RNA-seq database. **(F)** Multivariate analysis of TCGA RNA-seq database.

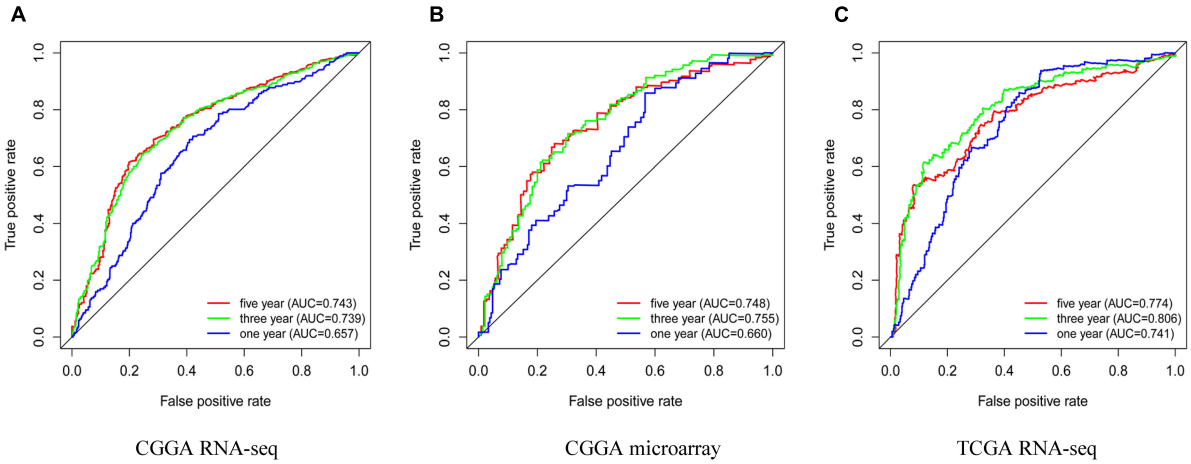


**FIGURE 4 |** Prognostic factors and risk assessment of glioma and the diagnostic value of ESPL1. **(A)** The receiver operating characteristic (ROC) curve in CGGA sequence. **(B)** ROC curve in CGGA microarray. **(C)** ROC curve in TCGA RNA-seq.

overall survival (OS) ($p < 0.001$). Because the prognosis of patients with high-grade gliomas and low-grade gliomas is significantly different, the tissue samples were further divided into high- and low-grade gliomas for KM survival analysis to explore the impact of ESPL1 on the prognosis of patients with different grades. The results showed that the change in ESPL1 expression level had no significant difference in the prognosis of high-grade glioma in three independent datasets (**Supplementary Figures 1–3B**). However, for the prognosis of low-grade gliomas, the increased expression of ESPL1 can indeed reduce the OS time of patients (**Supplementary Figures 1–3A**). The 2016 WHO grading standard for gliomas also included the molecular characteristics of gliomas in the classification of patients. Therefore, we divided patients into molecular groups to detect the impact of ESPL1 on the prognosis of patients between different molecular categories. The results showed that the increased expression of ESPL1 could significantly reduce the survival time of patients, whether in the IDH mutation group or wild-type group and whether accompanied by 1p19q codeletion or not (**Supplementary Figures 1C–E, 2C,D**). Although the abovementioned results were obtained from a large sample of 1669 gliomas in 3 data cohorts, whether high expression of ESPL1 represents an independent risk factor for glioma remains to be verified.

## ESPL1 Represents an Independent Risk Factor in Glioma Patients

To explore whether ESPL1 represents an independent risk factor for poor prognosis in gliomas, univariate, and multivariate Cox analyses were performed to verify the relationship between high expression of ESPL1 and the prognosis of gliomas. As shown in **Figure 3**, univariate Cox analysis demonstrated that increased ESPL1 expression in glioma was closely related to poor prognosis in CGGA RNA-seq (HR = 1.633), CGGA microarray (HR = 2.050), and TCGA RNA-seq (HR = 1.353). High-grade CGGA RNA-seq (HR = 2.883), CGGA microarray (HR = 2.567), and TCGA RNA-seq (HR = 4.634), in older patients in CGGA RNA-seq (HR = 1.624), CGGA microarray (HR = 1.736), and TCGA RNA-seq (HR = 1.072), and in the PRS type in CGGA RNA-seq (HR = 2.123) and CGGA microarray (HR = 2.042) (**Figures 3A,C,E**). At the same time, multivariate Cox analysis revealed that increased expression levels of ESPL1 represent a risk factor in CGGA RNA-seq (HR = 1.237), CGGA microarray (HR = 1.396), and TCGA RNA-seq (HR = 1.103), in older patients in CGGA RNA-seq (HR = 1.266) and TCGA RNA-seq (HR = 1.047), and in PRS type in CGGA RNA-seq (HR = 1.975) and CGGA microarray (HR = 1.568) (**Figures 3B,D,F**). Consistently, the above results demonstrated that ESPL1 can be regarded as an independent risk factor that conveys an unsatisfactory clinical prognosis.

## The Clinical Diagnostic Value of ESPL1

To determine whether high expression of ESPL1 has clinical diagnostic value for the prognosis of glioma, we used Cox regression and Kaplan–Meier methods to draw ROC curves of the CGGA RNA-seq, CGGA microarray, and TCGA RNA-seq cohorts (**Figures 4A–C**). In these three databases, the area under the curve (AUC) of 3- and 5-years were all greater than 0.7, indicating that ESPL1 has an appropriate diagnostic value. However, in the 1-year survival curve, except for the AUC of TCGA RNA-seq which was 0.741, the AUCs of CGGA RNA-seq and CGGA microarray were all less than 0.7. In addition, in the grading of gliomas, these independent datasets consistently showed that the expression level of ESPL1 has good diagnostic value for the prognosis of low-grade gliomas (**Supplementary Figures 4–6A**). However, in high-grade gliomas, only the TCGA RNA-seq dataset suggested a good diagnostic value for the prognosis of patients (**Supplementary Figures 4–6B**). It is worth noting that the expression level of ESPL1 has good diagnostic value among various molecular subtypes in the molecular typing of gliomas (**Supplementary Figures 4C–E, 5C,D**). In summary,

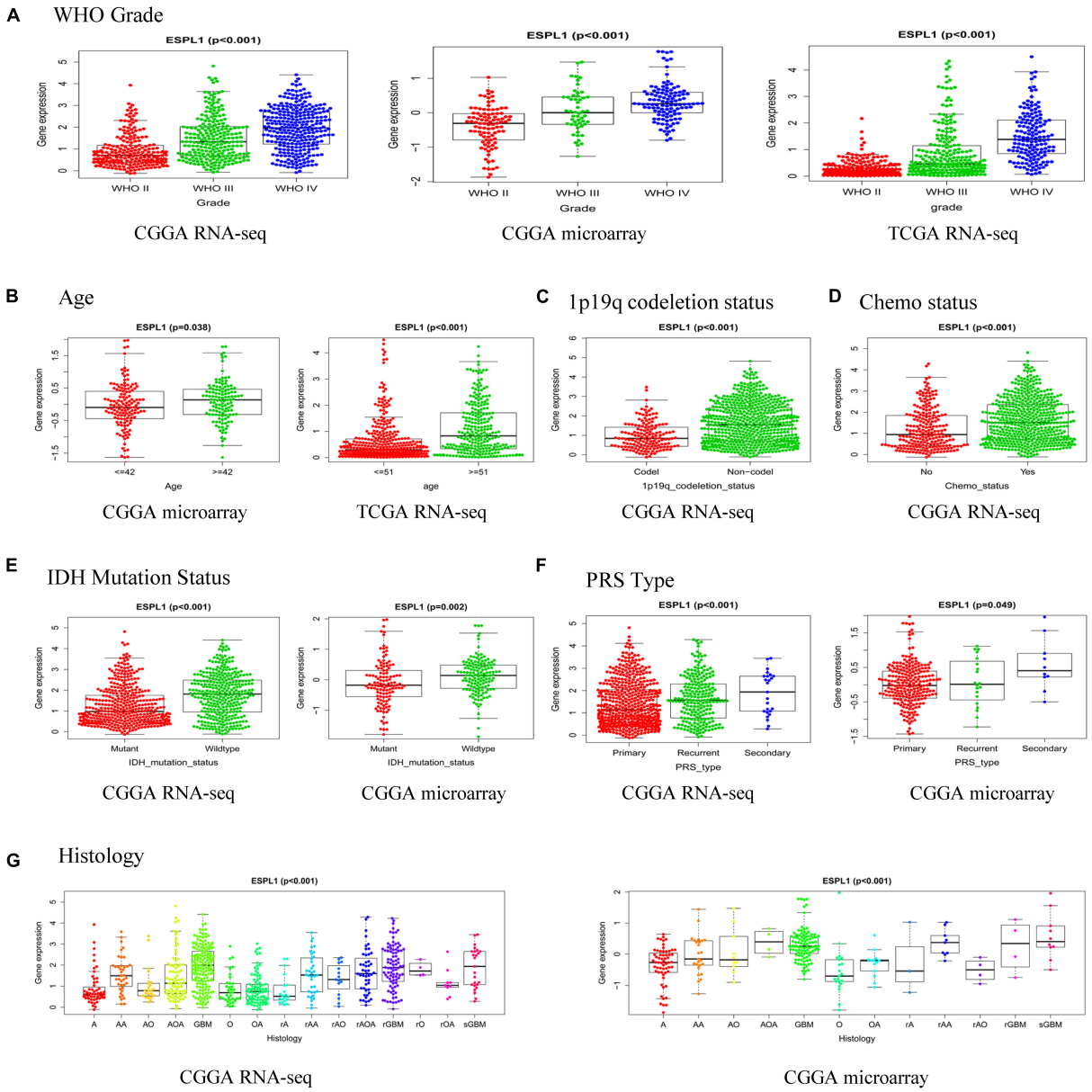


**FIGURE 5 |** Relationship between the expression of ESPL1 in glioma and clinicopathological characteristics in the CGGA RNA-seq, CGGA microarray, and TCGA RNA-seq datasets. **(A)** Grade. **(B)** Age. **(C)** 1p19q_codeletion status. **(D)** Chemotherapy status. **(E)** IDH mutation status. **(F)** PRS type. **(G)** Histology (A, astrocytoma; AA, anaplastic astrocytoma; AO, anaplastic oligodendroglioma; AOA, anaplastic oligoastrocytoma; GBM, glioblastoma; O, oligodendroglioma; OA, oligoastrocytoma; rA, relapse astrocytoma; rAA, relapse anaplastic astrocytoma; rAO, relapse anaplastic oligodendroglioma; rAOA, relapse anaplastic oligoastrocytoma; rGBM, relapse oligodendroglioma; rO, relapse oligodendroglioma; rOA, relapse oligoastrocytoma; sGBM, secondary relapse oligodendroglioma).

**TABLE 2 |** The gene set enriches the high ESPL1 expression phenotype.

| | CGGA RNA-seq | | | CGGA microarray | | | TCGA RNA-seq | | |
|---|---|---|---|---|---|---|---|---|---|
| **Gene set name** | **NES** | **NOM *p*-value** | **NOM *q*-value** | **NES** | **NOM *p*-value** | **NOM *q*-value** | **NES** | **NOM *p*-value** | **NOM *q*-value** |
| Homologous recombination | 1.745 | 0.009 | 0.116 | 1.760 | 0.011 | 0.382 | 1.984 | 0 | 0.006 |
| Cell cycle | 1.964 | 0 | 0.031 | 1.795 | 0.014 | 0.513 | 2.225 | 0 | 0.001 |
| Base excision repair | 1.840 | 0 | 0.082 | 1.645 | 0.045 | 0.550 | 1.956 | 0 | 0.008 |

*NES, normalized enrichment score; NOM, nominal. Gene sets with NOM p-value < 0.05 was considered as significantly enriched.*

these results indicate that ESPL1 has diagnostic significance for patients with glioma, especially for low-grade gliomas.

## Relationship Between ESPL1 Expression and Clinical Characteristics in Glioma Patients

To further investigate the relationship between ESPL1 and the clinical features of glioma patients, we used R software to analyze the three databases in detail. As presented in **Figure 5A**, high expression of ESPL1 was positively correlated with the WHO grade in the CGGA RNA-seq, CGGA microarray, and TCGA RNA-seq databases ($p < 0.001$). In the CGGA microarray and TCGA RNA-seq, the expression levels of ESPL1 were significantly associated with age (**Figure 5B**). In CGGA RNA-seq, expression levels of ESPL1 were significantly correlated with 1p19q co-deletion and chemotherapy status (**Figures 5C,D**, $p < 0.001$). In the two CGGA datasets, expression of ESPL1 was closely correlated with IDH mutation, PRS type, and histology (**Figures 5E–G**). These results demonstrate that the expression levels of ESPL1 are significantly related to diverse clinical characteristics in glioma patients.

## GSEA Identifies ESPL1-Related Signaling Pathways

These results suggest that ESPL1 plays an important role in the pathophysiology of glioma, but the underlying mechanism remains unclear. Therefore, we conducted GSEA analysis to determine whether ESPL1 is involved in tumor-related

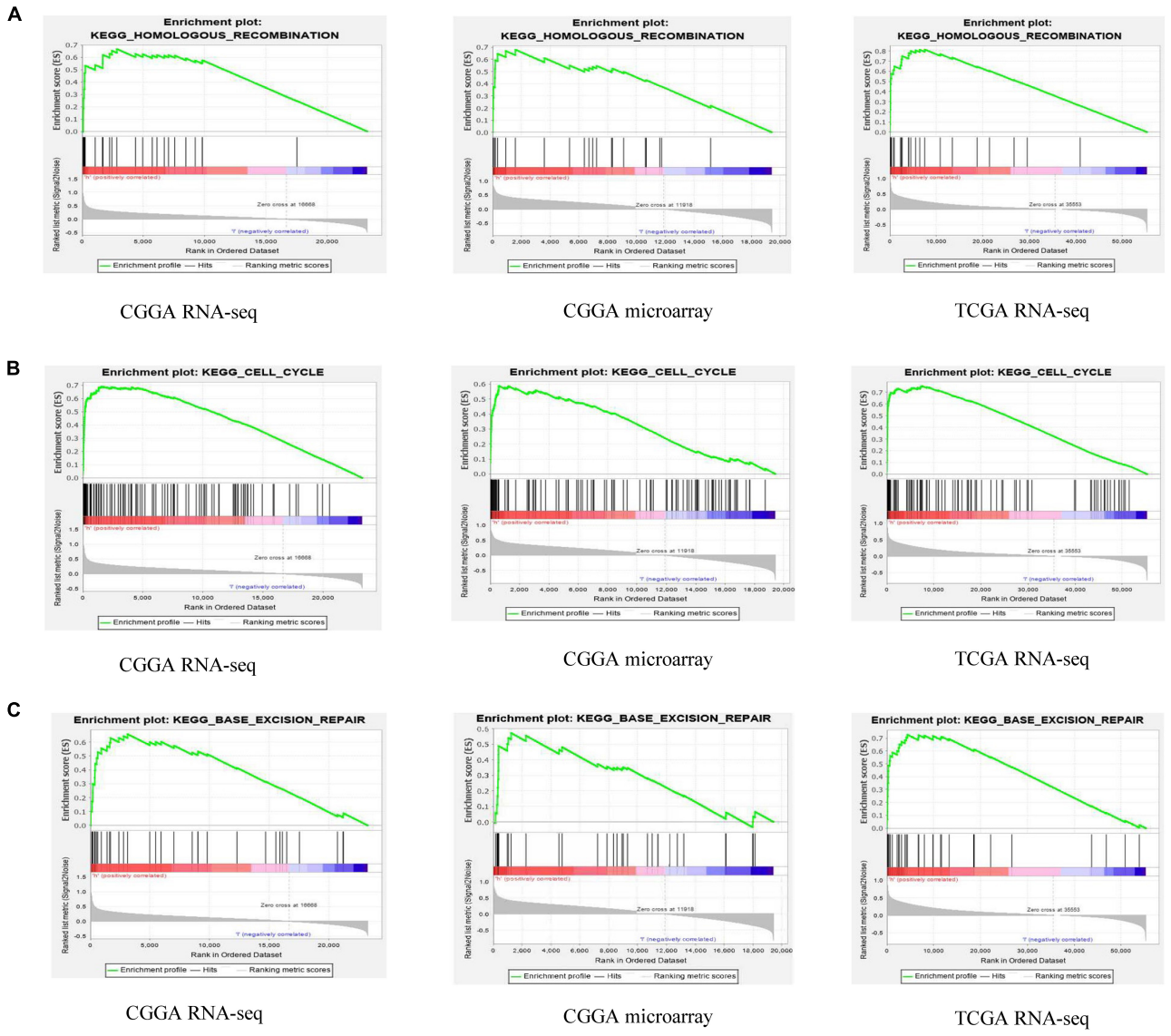


**FIGURE 6 |** Gene set enrichment analysis (GSEA) of ESPL1 in CGGA RNA-seq, CGGA microarray, and TCGA RNA-seq databases. The results of the three databases show that ESPL1 is associated with three pathways **(A–C)** homologous recombination, cell cycle, and base excision repair.

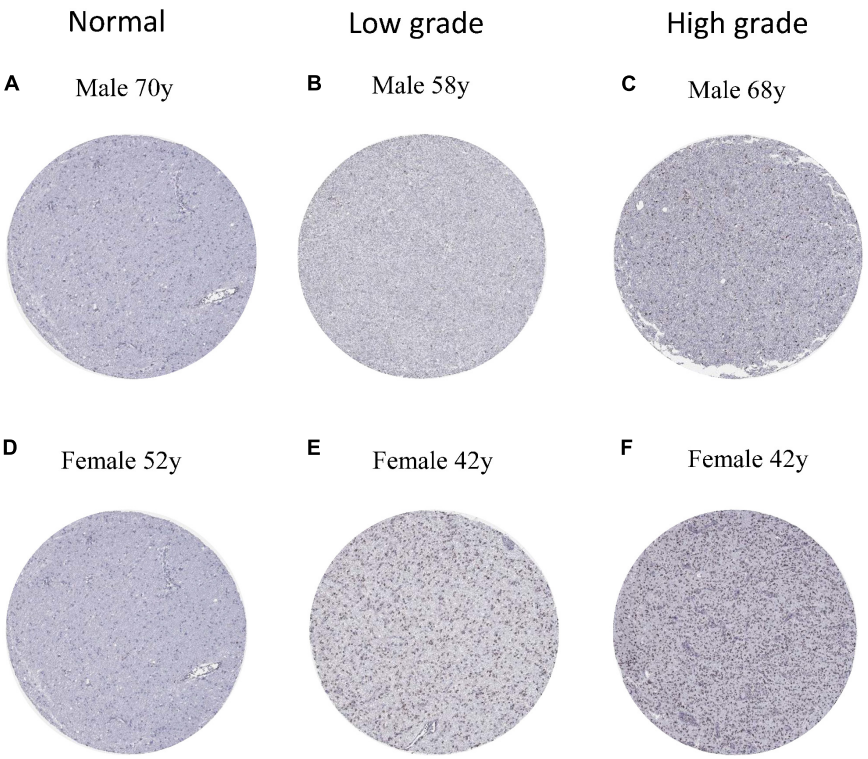


**FIGURE 7 |** Protein levels of ESPL1 in normal and glioma tissues by immunohistochemistry based on the Human Protein Atlas (staining: medium; intensity: moderate; quantity: >75%). **(A,D)** The expression of ESPL1 in normal brain tissues of men and women. **(B,E)** The expression status of ESPL1 in low-grade gliomas in men and women. **(C,F)** The expression status of ESPL1 in high-grade gliomas in men and women.

signaling pathways. The results demonstrated that homologous recombination, cell cycle, and base excision repair were differentially enriched with a high ESPL1 expression phenotype (**Table 2** and **Figure 6**).

## Immunohistochemistry of ESPL1

To verify the expression of ESPL1 in normal brain and glioma tissues at the protein level, we downloaded six immunohistochemical slices from the HPA[7] (two normal, two low-grade, and two high-grade), which were stained with HPA073188 (**Figures 7A–F**). Results showed that ESPL1 protein expression levels in glioma tissue samples were significantly higher than those in normal brains. Furthermore, there was a direct relationship between higher glioma grade and higher expression levels of ESPL1.

## Potential Drugs for the Treatment of Glioma Based on CMap Analysis

Through Pearson correlation analysis, we obtained 20 ESPL1-related genes using co-expression analysis. There were 10 genes (KIF2C, FAM64A, KIF20A, MKI67, ASPM, HJURP, KIF23, IQGAP3, TROAP, GTSE1) that were positively correlated and 10 (SPOCK2, LYNX1, CBX7, FBXW4, ADARB2, NEBL, MRVI1, SCN2B, ETNPPL, LDHD) that were negatively correlated (**Figures 8A,B**). We then uploaded these genes to CMap, which predicted three drugs that may harbor potential therapeutic effects on glioma: thioguanosine, antimycin A, and zidovudine (**Table 3**). The 2D and 3D structures of these small-molecule drugs are available from PubChem and are shown in **Figure 9**.

[7]https://www.proteinatlas.org/search/ESPL1

# DISCUSSION

In the field of oncology, several studies have demonstrated that ESPL is related to the malignant biological behavior of many human tumors, promoting the development and proliferation of tumor cells and leading to poor outcomes. For example, Finetti et al. (2014) reported that ESPL1 is an oncogenic driver of luminal B breast cancers and has a powerful prognostic value. Furthermore, Hu et al. (2020) found that an HBV S-integrated human ESPL1 fusion gene may potentially represent a biomarker for the early diagnosis of HCC in HBV-infected patients. In addition, it has been reported that enhanced ESPL1 expression might be the reason for the increased malignancy of non-small cell and small cell lung cancer, and that ESPL1 represents a potential target for molecular therapy of lung cancer (Zhang et al., 2016). Similar conclusions have been verified in other malignant tumors, such as rectal adenocarcinoma, bladder cancer, and prostate carcinoma (Zhang and Pati, 2017; Chen et al., 2019). However, there is no literature on

**A**

| Gene | Correlation coefficient | P-value |
|---|---|---|
| GTSE1 | 0.9 | 0 |
| TROAP | 0.891 | 0 |
| IQGAP3 | 0.89 | 0 |
| KIF23 | 0.866 | 1.22E-307 |
| HJURP | 0.854 | 5.02E-290 |
| ASPM | 0.844 | 7.56E-277 |
| MKI67 | 0.841 | 7.40E-273 |
| KIF20A | 0.837 | 8.42E-269 |
| FAM64A | 0.836 | 3.07E-267 |
| KIF2C | 0.835 | 1.72E-265 |
| LDHD | -0.51 | 1.29E-68 |
| ETNPPL | -0.495 | 4.18E-64 |
| SCN2B | -0.481 | 6.03E-60 |
| MRVI1 | -0.476 | 9.75E-59 |
| NEBL | -0.476 | 9.45E-59 |
| ADARB2 | -0.465 | 8.85E-56 |
| FBXW4 | -0.454 | 5.65E-53 |
| CBX7 | -0.451 | 3.20E-52 |
| LYNX1 | -0.451 | 3.57E-52 |
| SPOCK2 | -0.448 | 2.60E-51 |

**B**

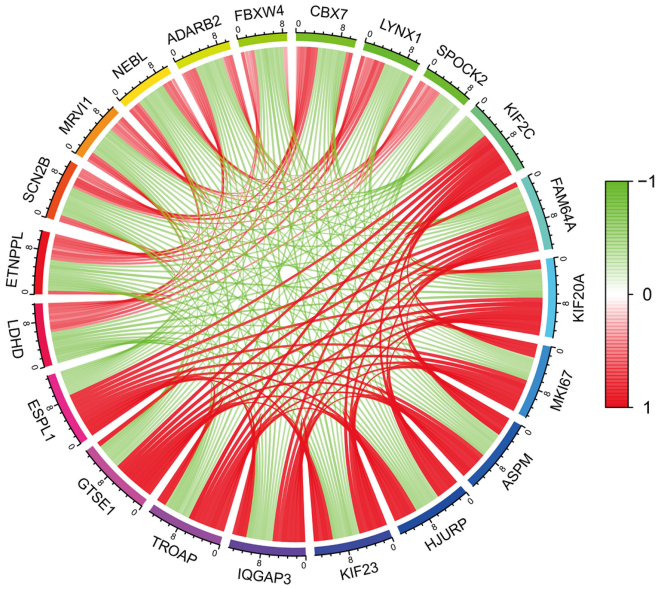


**FIGURE 8 |** It co-expresses the analysis results. **(A)** Some genes that have synergistic and antagonistic effects with ESPL1, including their names, correlation coefficient values, and *p*-values. **(B)** The expression relationship diagram of genes related to ESPL1.

the relationship between ESPL1 and glioma. Elucidating the expression levels of ESPL1 in glioma and its clinical relevance will help to establish a new therapeutic target to improve existing treatment methods.

In this study, we first assessed the expression levels of ESPL1 in glioma using the GEPIA, GEO, and HPA databases. The results demonstrated that ESPL1 expression in glioma tissues was elevated compared to that in normal brain tissues at both the mRNA and protein levels. In addition, univariate and multivariate Cox analyses demonstrated that ESPL1 expression might be a useful biomarker for glioma prognosis and that ROC analysis confirmed the diagnostic value of ESPL1 expression in glioma. Moreover, Kaplan–Meier curves for OS showed that higher expression of ESPL1 was related to worse outcomes in glioma patients, especially in patients with low-grade gliomas. Furthermore, the potential mechanism of these results might be linked to homologous recombination, cell cycle, and base excision repair, as indicated by the GSEA results. These signaling pathways have been shown to play key roles in the biological behavior of many tumors in terms of metastasis and proliferation, indicating the potential role of ESPL1 as a new therapeutic and prognostic biomarker in glioma (Pennington et al., 2014; Wallace, 2014; Gavande et al., 2016; Ouyang et al., 2016; Christenson and Antonarakis, 2018). However, the function of this gene is realized in multiple ways. Therefore, further studies on the mechanism of ESPL1 in glioma are needed to clarify and expand upon these findings.

The abnormal expression of many genes is related to the pathological mechanism and malignant progression of glioma (Guan et al., 2018; Wang et al., 2018; Feng et al., 2020; Liu Z. et al., 2020). To determine whether ESPL1 associates with other genes to promote the malignant development of glioma, we further analyzed its co-expression and identified genes with co-expression relationships with ESPL1, confirming ESPL1 as a cancer gene with abnormally high expression that promotes the malignant progression of glioma. These results indicate that high expression of GTSE1, TROAP, IQGAP3, KIF23, HJURP, ASPM, MIKI67, KIF20A, FAM64A, and KIF2C might be unfavorable for glioma prognosis, whereas high expression of LDHD, ETNPPL, SCN2B, MRVI1, NEBL, ADARB2, FBXW4, CBX7, LYNX1, and SPOCK2 may be beneficial for the prognosis of glioma. For example, Sun et al. (2016) revealed that overexpression of KIF23 leads to unfavorable clinical outcomes in glioma and might be a useful independent prognostic biomarker for glioma patients (Sun et al., 2016). On the other hand, it has been reported that reduced expression of ETNPPL is closely related to the progression of glioma, particularly in glioblastoma (González-García et al., 2020). These results are consistent with our analysis. These genes also indirectly suggest that ESPL1 may promote the pathological processes of glioma and affect the prognosis of glioma patients.

**TABLE 3 |** Three small molecule compounds identified as potential drugs for glioma treatment in CMap analysis.

| CMap name | Mean | *N* | Enrichment | *p*-Value |
|---|---|---|---|---|
| Thioguanosine | −0.706 | 4 | −0.944 | 0 |
| Antimycin A | −0.592 | 5 | −0.786 | 0.00084 |
| Zidovudine | −0.586 | 4 | −0.754 | 0.00734 |

*CMap, Connectivity Map.*

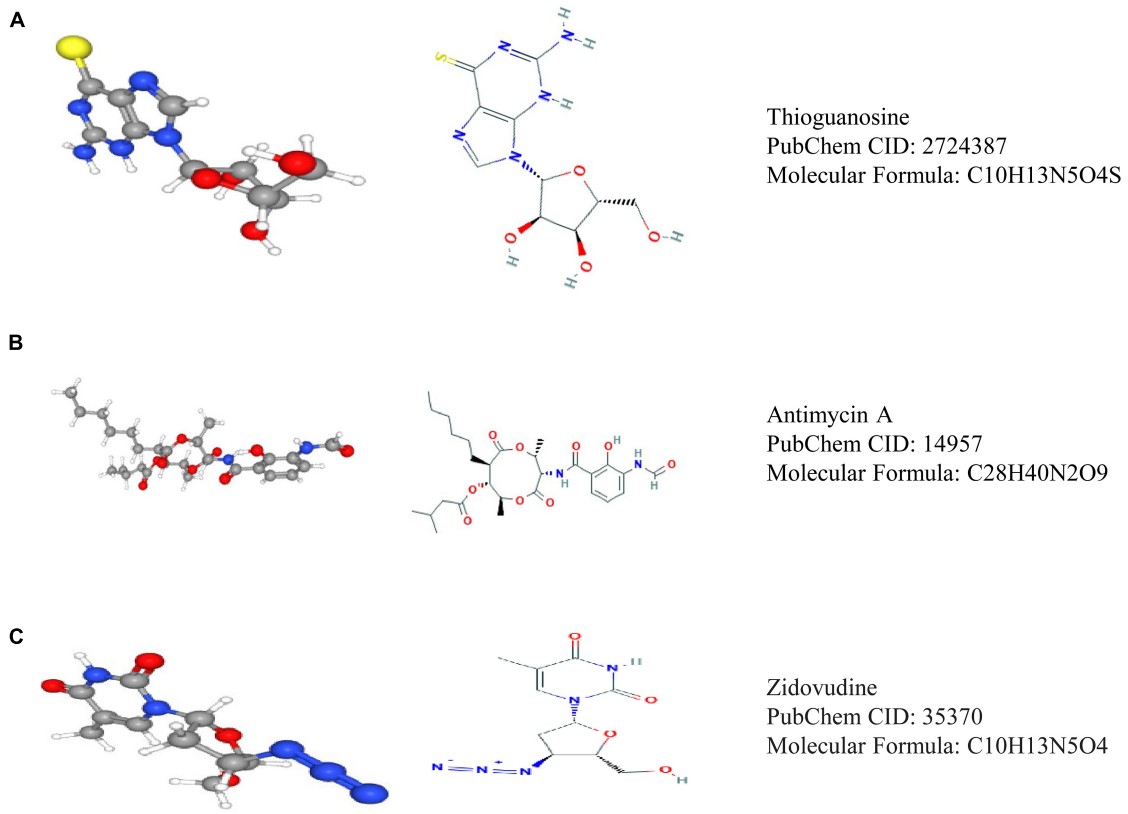


**FIGURE 9 |** Three drugs predicted by CMap analysis results. **(A)** Structure diagram of thioguanosine, structure formula, and ID. **(B)** Structure diagram of antimycin A, structure formula, and ID. **(C)** Structure diagram of zidovudine, structure formula, and ID.

Finally, the CMap database is an online platform for drug research and development. It can screen out drugs with potential therapeutic effects based on the change in gene expression level in the pathophysiological process of disease, so as to correct gene disorders and exert its therapeutic effects (Lamb et al., 2006). In this study, we screened three small-molecule drugs that may inhibit the occurrence and development of glioma through CMap analysis: thioguanosine, antimycin A, and zidovudine. The potential therapeutic effects of these small-molecule compounds on tumors have been described in the literature. For example, thioguanosine has been widely used in the treatment of acute leukemia (Evans and Relling, 1994). Subsequently, Kyritsis et al. (1996) demonstrated that chemotherapy with a combination of 6-thioguanine, procarbazine, lomustine, and hydroxyurea is effective for recurrent anaplastic gliomas (Kyritsis et al., 1996). In addition, as an antifungal drug, antimycin A was recently shown to inhibit the self-renewal ability of lung cancer stem cells by negatively regulating β-catenin signaling (Seipke et al., 2011; Yeh et al., 2013). Moreover, Wagner et al. (1997) revealed that zidovudine inhibits the activity of breast cancer. The above findings indicate that the small-molecule compounds inhibit tumor growth. However, these small-molecule drugs have not been reported to prevent anti-glioma cell proliferation. This study only provides an index to guide more researchers to pay attention to their potential value in the treatment of glioma. Drug repurposing can quickly understand the pharmacokinetics of drugs and evaluate their side effects, so that it can be applied to the first-line clinical practice (Ashburn and Thor, 2004; Boguski et al., 2009). For example, atorvastatin was considered to be a traditional classic antihyperlipidemic drug in the past, but it has been found to have a good therapeutic effect for chronic subdural hemorrhage in recent years (Jiang et al., 2018). Zidovudine has not been previously studied in the field of anti-glioma. However, it was later found that it can improve the sensitivity of glioma cells to radiotherapy, so as to play an anti-glioma therapeutic effect (Zhou et al., 2007). Therefore, these small-molecule drugs may have similar effects on glioma. Although there is no direct evidence that these compounds have an inhibitory effect on glioma, we have sufficient reason to support them as potentially effective drugs. However, additional studies are needed to examine their novel effects.

Although this study utilized multiple datasets with thousands of glioma samples for scientific analysis, revealing the mechanism of ESPL1 in glioma diagnosis and treatment will require additional studies. This study has several limitations. Since most of our data were from public databases, detailed treatment strategies were not available for each patient. However, it is precisely because of the multi-dataset fusion analysis that the statistical bias of race is reduced, which makes our results more reliable.

In summary, our results suggest that the overexpression of ESPL1 is closely related to poor prognosis in glioma patients. We believe that this study further improves our understanding of the pathogenesis of glioma and provides a novel and effective prognostic biomarker for gliomas, especially low-grade gliomas.

## DATA AVAILABILITY STATEMENT

The original contributions presented in the study are included in the article/**Supplementary Material**, further inquiries can be directed to the corresponding author/s.

## ETHICS STATEMENT

The authors are accountable for all aspects of the work (including full data access, integrity of the data and the accuracy of the data analysis) in ensuring that questions related to the accuracy or integrity of any part of the work are appropriately investigated and resolved. Procedures of this work were approved by Ethics Committee of Affiliated of Henan Provincial People's Hospital. The use of patient samples conformed to the declaration of Helsinki.

## AUTHOR CONTRIBUTIONS

ZL, XL, YZ, and YG contributed to experimental design and implementation. XZ, XL, WZ, HW, and ZR performed the experiments. ZL, MZ, JW, and ML analyzed the data. XL and BL drafted the manuscript. All authors read and approved the final manuscript.

## FUNDING

This work was supported by The Thousand Talents Plan of Central Plains (ZYQR201912122).

## ACKNOWLEDGMENTS

We would like to thank Editage (www.editage.cn) for English language editing.

## SUPPLEMENTARY MATERIAL

The Supplementary Material for this article can be found online at: https://www.frontiersin.org/articles/10.3389/fgene.2021.666106/full#supplementary-material

## REFERENCES

Ashburn, T. T., and Thor, K. B. (2004). Drug repositioning: identifying and developing new uses for existing drugs. *Nat. Rev. Drug Discov.* 3, 673–683. doi: 10.1038/nrd1468

Barrett, T., Wilhite, S. E., Ledoux, P., Evangelista, C., Kim, I. F., Tomashevsky, M., et al. (2013). NCBI GEO: archive for functional genomics data sets–update. *Nucleic Acids Res.* 41, D991–D995.

Bell, C., Dowson, N., Fay, M., Thomas, P., Puttick, S., Gal, Y., et al. (2015). Hypoxia imaging in gliomas with 18F-fluoromisonidazole PET: toward clinical translation. *Semin. Nucl. Med.* 45, 136–150. doi: 10.1053/j.semnuclmed.2014.10.001

Boguski, M. S., Mandl, K. D., and Sukhatme, V. P. (2009). Drug discovery. Repurposing with a difference. *Science* 324, 1394–1395.

Chen, Q., Hu, J., Deng, J., Fu, B., and Guo, J. (2019). Bioinformatics analysis identified key molecular changes in bladder cancer development and recurrence. *Biomed. Res. Int.* 2019:3917982.

Chestukhin, A., Pfeffer, C., Milligan, S., DeCaprio, J. A., and Pellman, D. (2003). Processing, localization, and requirement of human separase for normal anaphase progression. *Proc. Natl. Acad. Sci. U. S. A.* 100, 4574–4579. doi: 10.1073/pnas.0730733100

Christenson, E. S., and Antonarakis, E. S. (2018). PARP inhibitors for homologous recombination-deficient prostate cancer. *Expert Opin. Emerg. Drugs* 23, 123–133. doi: 10.1080/14728214.2018.1459563

Cordier, D., Krolicki, L., Morgenstern, A., and Merlo, A. (2016). Targeted radiolabeled compounds in glioma therapy. *Semin. Nucl. Med.* 46, 243–249. doi: 10.1053/j.semnuclmed.2016.01.009

Evans, W. E., and Relling, M. V. (1994). Mercaptopurine vs thioguanine for the treatment of acute lymphoblastic leukemia. *Leuk. Res.* 18, 811–814. doi: 10.1016/0145-2126(94)90160-0

Feng, X., Zhang, L., Ke, S., Liu, T., Hao, L., Zhao, P., et al. (2020). High expression of GPNMB indicates an unfavorable prognosis in glioma: combination of data from the GEO and CGGA databases and validation in tissue microarray. *Oncol. Lett.* 20, 2356–2368. doi: 10.3892/ol.2020.11787

Finetti, P., Guille, A., Adelaide, J., Birnbaum, D., Chaffanet, M., and Bertucci, F. (2014). ESPL1 is a candidate oncogene of luminal B breast cancers. *Breast Cancer Res. Treat.* 147, 51–59. doi: 10.1007/s10549-014-3070-z

Gavande, N. S., VanderVere-Carozza, P. S., Hinshaw, H. D., Jalal, S. I., Sears, C. R., Pawelczak, K. S., et al. (2016). DNA repair targeted therapy: the past or future of cancer treatment? *Pharmacol. Ther.* 160, 65–83. doi: 10.1016/j.pharmthera.2016.02.003

González-García, N., Nieto-Librero, A. B., Vital, A. L., Tao, H. J., González-Tablas, M., Otero, Á, et al. (2020). Multivariate analysis reveals differentially expressed genes among distinct subtypes of diffuse astrocytic gliomas: diagnostic implications. *Sci. Rep.* 10:11270.

Guan, X., Zhang, C., Zhao, J., Sun, G., Song, Q., and Jia, W. (2018). CMTM6 overexpression is associated with molecular and clinical characteristics of malignancy and predicts poor prognosis in gliomas. *EBioMedicine* 35, 233–243. doi: 10.1016/j.ebiom.2018.08.012

Hu, B., Huang, W., Wang, R., Zang, W., Su, M., Li, H., et al. (2020). High rate of detection of human ESPL1-HBV S fusion gene in patients with HBV-related liver cancer: a chinese case-control study. *Anticancer Res.* 40, 245–252. doi: 10.21873/anticanres.13946

Jiang, R., Zhao, S., Wang, R., Feng, H., Zhang, J., Li, X., et al. (2018). Safety and efficacy of atorvastatin for chronic subdural hematoma in chinese patients: a randomized clinicaltrial. *JAMA Neurol.* 75, 1338–1346. doi: 10.1001/jamaneurol.2018.2030

Kyritsis, A. P., Yung, W. K., Jaeckle, K. A., Bruner, J., Gleason, M. J., Ictech, S. E., et al. (1996). Combination of 6-thioguanine, procarbazine, lomustine, and hydroxyurea for patients with recurrent malignant gliomas. *Neurosurgery* 39, 921–926. doi: 10.1097/00006123-199611000-00006

Lamb, J. (2007). The connectivity map: a new tool for biomedical research. *Nat. Rev. Cancer* 7, 54–60. doi: 10.1038/nrc2044

Lamb, J., Crawford, E. D., Peck, D., Modell, J. W., Blat, I. C., Wrobel, M. J., et al. (2006). The connectivity map: using gene-expression signatures to connect small molecules, genes, and disease. *Science* 313, 1929–1935. doi: 10.1126/science.1132939

Liu, J., Wan, Y., Li, S., Qiu, H., Jiang, Y., Ma, X., et al. (2020). Identification of aberrantly methylated differentially expressed genes and associated pathways

in endometrial cancer using integrated bioinformatic analysis. *Cancer Med.* 9, 3522–3536. doi: 10.1002/cam4.2956

Liu, Z., Shen, F., Wang, H., Li, A., Wang, J., Du, L., et al. (2020). Abnormally high expression of HOXA2 as an independent factor for poor prognosis in glioma patients. *Cell Cycle* 19, 1632–1640. doi: 10.1080/15384101.2020.1762038

Meyer, R., Fofanov, V., Panigrahi, A., Merchant, F., Zhang, N., and Pati, D. (2009). Overexpression and mislocalization of the chromosomal segregation protein separase in multiple human cancers. *Clin. Cancer Res.* 15, 2703–2710. doi: 10.1158/1078-0432.ccr-08-2454

Mukherjee, M., Ge, G., Zhang, N., Edwards, D. G., Sumazin, P., Sharan, S. K., et al. (2014). MMTV-Espl1 transgenic mice develop aneuploid, estrogen receptor alpha (ERα)-positive mammary adenocarcinomas. *Oncogene* 33, 5511–5522. doi: 10.1038/onc.2013.493

Ouyang, Q., Xu, L., Cui, H., Xu, M., and Yi, L. (2016). MicroRNAs and cell cycle of malignant glioma. *Int. J. Neurosci.* 126, 1–9. doi: 10.3109/00207454.2015.1017881

Pati, D. (2008). Oncogenic activity of separase. *Cell Cycle* 7, 3481–3482. doi: 10.4161/cc.7.22.7048

Pennington, K. P., Walsh, T., Harrell, M. I., Lee, M. K., Pennil, C. C., Rendi, M. H., et al. (2014). Germline and somatic mutations in homologous recombination genes predict platinum response and survival in ovarian, fallopian tube, and peritoneal carcinomas. *Clin. Cancer Res.* 20, 764–775. doi: 10.1158/1078-0432.ccr-13-2287

Schöckel, L., Möckel, M., Mayer, B., Boos, D., and Stemmann, O. (2011). Cleavage of cohesin rings coordinates the separation of centrioles and chromatids. *Nat. Cell Biol.* 13, 966–972. doi: 10.1038/ncb2280

Seipke, R. F., Barke, J., Brearley, C., Hill, L., Yu, D. W., Goss, R. J., et al. (2011). A single streptomyces symbiont makes multiple antifungals to support the fungus farming ant *Acromyrmex octospinosus*. *PLoS One* 6:e22028. doi: 10.1371/journal.pone.0022028

Stupp, R., Hegi, M. E., Mason, W. P., van den Bent, M. J., Taphoorn, M. J., Janzer, R. C., et al. (2009). Effects of radiotherapy with concomitant and adjuvant temozolomide versus radiotherapy alone on survival in glioblastoma in a randomised phase III study: 5-year analysis of the EORTC-NCIC trial. *Lancet Oncol.* 10, 459–466. doi: 10.1016/s1470-2045(09)70025-7

Stupp, R., Mason, W. P., van den Bent, M. J., Weller, M., Fisher, B., Taphoorn, M. J., et al. (2005). Radiotherapy plus concomitant and adjuvant temozolomide for glioblastoma. *New Engl. J. Med.* 352, 987–996.

Subramanian, A., Tamayo, P., Mootha, V. K., Mukherjee, S., Ebert, B. L., Gillette, M. A., et al. (2005). Gene set enrichment analysis: a knowledge-based approach for interpreting genome-wide expression profiles. *Proc. Natl. Acad. Sci. U. S. A.* 102, 15545–15550. doi: 10.1073/pnas.0506580102

Sun, L., Zhang, C., Yang, Z., Wu, Y., Wang, H., Bao, Z., et al. (2016). KIF23 is an independent prognostic biomarker in glioma, transcriptionally regulated by TCF-4. *Oncotarget* 7, 24646–24655. doi: 10.18632/oncotarget.8261

Tang, Z., Li, C., Kang, B., Gao, G., Li, C., and Zhang, Z. (2017). GEPIA: a web server for cancer and normal gene expression profiling and interactive analyses. *Nucleic Acids Res.* 45, W98–W102.

Thul, P. J., Åkesson, L., Wiking, M., Mahdessian, D., Geladaki, A., Ait Blal, H., et al. (2017). A subcellular map of the human proteome. *Science* 356:eaal3321.

Thul, P. J., and Lindskog, C. (2018). The human protein atlas: a spatial map of the human proteome. *Protein Sci.* 27, 233–244. doi: 10.1002/pro.3307

Tomczak, K., Czerwińska, P., and Wiznerowicz, M. (2015). The cancer genome atlas (TCGA): an immeasurable source of knowledge. *Contemp. Oncol. (Pozn.)* 19, A68–A77.

Uhlén, M., Fagerberg, L., Hallström, B. M., Lindskog, C., Oksvold, P., Mardinoglu, A., et al. (2015). Proteomics. Tissue-based map of the human proteome. *Science* 347:1260419.

Uhlen, M., Zhang, C., Lee, S., Sjöstedt, E., Fagerberg, L., Bidkhori, G., et al. (2017). A pathology atlas of the human cancer transcriptome. *Science* 357:eaan2507.

Wagner, C. R., Ballato, G., Akanni, A. O., McIntee, E. J., Larson, R. S., Chang, S., et al. (1997). Potent growth inhibitory activity of zidovudine on cultured human breast cancer cells and rat mammary tumors. *Cancer Res.* 57, 2341–2345.

Wallace, S. S. (2014). Base excision repair: a critical player in many games. *DNA Repair (Amst)* 19, 14–26. doi: 10.1016/j.dnarep.2014.03.030

Wang, Z., Wang, Z., Zhang, C., Liu, X., Li, G., Liu, S., et al. (2018). Genetic and clinical characterization of B7-H3 (CD276) expression and epigenetic regulation in diffuse brain glioma. *Cancer Sci.* 109, 2697–2705. doi: 10.1111/cas.13744

Wesseling, P., and Capper, D. (2018). WHO 2016 classification of gliomas. *Neuropathol. Appl. Neurobiol.* 44, 139–150. doi: 10.1111/nan.12432

Yeh, C. T., Su, C. L., Huang, C. Y., Lin, J. K., Lee, W. H., Chang, P. M., et al. (2013). A preclinical evaluation of antimycin a as a potential antilung cancer stem cell agent. *Evid. Based Complement. Alternat. Med.* 2013:910451.

Zhang, C., Min, L., Zhang, L., Ma, Y., Yang, Y., and Shou, C. (2016). Combined analysis identifies six genes correlated with augmented malignancy from non-small cell to small cell lung cancer. *Tumour Biol.* 37, 2193–2207. doi: 10.1007/s13277-015-3938-5

Zhang, N., and Pati, D. (2017). Biology and insights into the role of cohesin protease separase in human malignancies. *Biol. Rev. Camb. Philos. Soc.* 92, 2070–2083. doi: 10.1111/brv.12321

Zhou, F. X., Liao, Z. K., Dai, J., Xiong, J., Xie, C. H., Luo, Z. G., et al. (2007). Radiosensitization effect of zidovudine on human malignant glioma cells. *Biochem. Biophys. Res. Commun.* 354, 351–356. doi: 10.1016/j.bbrc.2006.12.180

**Conflict of Interest:** The authors declare that the research was conducted in the absence of any commercial or financial relationships that could be construed as a potential conflict of interest.

**Publisher's Note:** All claims expressed in this article are solely those of the authors and do not necessarily represent those of their affiliated organizations, or those of the publisher, the editors and the reviewers. Any product that may be evaluated in this article, or claim that may be made by its manufacturer, is not guaranteed or endorsed by the publisher.

frontiers in Genetics

ORIGINAL RESEARCH
published: 13 October 2021
doi: 10.3389/fgene.2021.698284

# A Novel Six Autophagy-Related Genes Signature Associated With Outcomes and Immune Microenvironment in Lower-Grade Glioma

*Tao Lin[1†], Hao Cheng[2†], Da Liu[1†], Lei Wen[3], Junlin Kang[4], Longwen Xu[5], Changguo Shan[3], Zhijie Chen[1], Hainan Li[6], Mingyao Lai[3], Zhaoming Zhou[3], Weiping Hong[3], Qingjun Hu[3], Shaoqun Li[3], Cheng Zhou[7], Jiwu Geng[8]* and Xin Jin[1]**

[1]Department of Neurosurgery, Guangdong Sanjiu Brain Hospital, Guangzhou, China, [2]Department of Nasopharyngeal Carcinoma, The First People's Hospital of Chenzhou, Southern Medical University, Chenzhou, China, [3]Department of Oncology, Guangdong Sanjiu Brain Hospital, Guangzhou, China, [4]Department of Neurosurgery, Lanzhou University First Hospital, Lanzhou, China, [5]Department of Medical Oncology, The First Affiliated Hospital of Xi'an Jiaotong University, Xi'an, China, [6]Department of Pathology, Guangdong Sanjiu Brain Hospital, Guangzhou, China, [7]Department of Radiation Oncology, Nanfang Hospital, Southern Medical University, Guangzhou, China, [8]Guangdong Key Laboratory of Occupational Disease Prevention and Treatment/Guangdong Province Hospital for Occupational Disease Prevention and Treatment, Guangzhou, China

Since autophagy and the immune microenvironment are deeply involved in the tumor development and progression of Lower-grade gliomas (LGG), our study aimed to construct an autophagy-related risk model for prognosis prediction and investigate the relationship between the immune microenvironment and risk signature in LGG. Therefore, we identified six autophagy-related genes (BAG1, PTK6, EEF2, PEA15, ITGA6, and MAP1LC3C) to build in the training cohort ($n$ = 305 patients) and verify the prognostic model in the validation cohort ($n$ = 128) and the whole cohort ($n$ = 433), based on the data from The Cancer Genome Atlas (TCGA). The six-gene risk signature could divide LGG patients into high- and low-risk groups with distinct overall survival in multiple cohorts (all $p < 0.001$). The prognostic effect was assessed by area under the time-dependent ROC (t-ROC) analysis in the training, validation, and whole cohorts, in which the AUC value at the survival time of 5 years was 0.837, 0.755, and 0.803, respectively. Cox regression analysis demonstrated that the risk model was an independent risk predictor of OS (HR > 1, $p < 0.05$). A nomogram including the traditional clinical parameters and risk signature was constructed, and t-ROC, C-index, and calibration curves confirmed its robust predictive capacity. KM analysis revealed a significant difference in the subgroup analyses' survival. Functional enrichment analysis revealed that these autophagy-related signatures were mainly involved in the phagosome and immune-related pathways. Besides, we also found significant differences in immune cell infiltration and immunotherapy targets between risk groups. In conclusion, we built a powerful predictive signature and explored immune components (including immune cells and emerging immunotherapy targets) in LGG.

**Keywords: lower-grade glioma, gene signature, autophagy, immune microenvironment, immunotherapy**

OPEN ACCESS

***Edited by:***
*Tania Lee Slatter, University of Otago, New Zealand*

***Reviewed by:***
*Sven R. Kantelhardt, Johannes Gutenberg University Mainz, Germany*
*Fabricio Figueiró, Federal University of Rio Grande do Sul, Brazil*

****Correspondence:***
*Xin Jin*
*jinxin_12171@163.com*
*Jiwu Geng*
*1044161@qq.com*

*[†]These authors have contributed equally to this work*

***Specialty section:***
*This article was submitted to Cancer Genetics and Oncogenomics, a section of the journal Frontiers in Genetics*

***Received:*** *21 April 2021*
***Accepted:*** *22 September 2021*
***Published:*** *13 October 2021*

***Citation:***
*Lin T, Cheng H, Liu D, Wen L, Kang J, Xu L, Shan C, Chen Z, Li H, Lai M, Zhou Z, Hong W, Hu Q, Li S, Zhou C, Geng J and Jin X (2021) A Novel Six Autophagy-Related Genes Signature Associated With Outcomes and Immune Microenvironment in Lower-Grade Glioma. Front. Genet. 12:698284. doi: 10.3389/fgene.2021.698284*

## INTRODUCTION

Diffuse low-grade and intermediate-grade gliomas including WHO grades II and III, hereafter called lower-grade gliomas (LGG) (Cancer Genome Atlas Research et al., 2015). Lower-grade gliomas (LGG) constitute about 15 percent of all primary brain tumors that originate from glial cells, showing great heterogeneity in clinical outcomes (Ostrom et al., 2013; Zeng et al., 2018). So far, maximum surgery, subsequent-radiotherapy, and chemotherapy have been the standard treatment modalities for LGG (Soffietti et al., 2010). Although numerous efforts to prolong LGG patient survival, more than half of them develop and progress to treatment-resistant and aggressive high-grade glioma in the future (Claus et al., 2015). Hence, it is urgent to search for novel prognostic biomarkers and therapeutic targets of LGG. Several genetic biomarkers were incorporated into the 2016 WHO classification, including chromosome arms 1p and 19q codeletion, isocitrate dehydrogenase (IDH) mutation, and O-6-methylguanine-DNA methyltransferase (MGMT) methylation, to illuminate the histological characteristics and guide the therapeutic approach (Hartmann et al., 2010; Wick et al., 2013; Hainfellner et al., 2014; Louis et al., 2016). Although these widely utilized biomarkers in LGG have recently been discovered, the novel predictors of clinical outcomes or therapeutic targets for LGG are not fully unraveled.

Autophagy is a highly conserved lysosomal degradation process that is crucial for homeostasis, differentiation, development, and survival (Rabinowitz and White, 2010) and has been found involved in diverse pathologies, including cancer (Kondo et al., 2005). By self-degradation of damaged proteins and intracellular components, autophagy can suppress tumor initiation, thereby mitigating cell injury and suppressing chromosomal instability (Mathew et al., 2007; White et al., 2010). But, autophagy can also facilitate cancer proliferation by supplying nutritional substance in the context of hypoxic and innutritious surroundings (Guo et al., 2011). Mostly, autophagy is believed to impede cancer initiation and promote tumor progression (Trejo-Solis et al., 2018). In addition, autophagy can alter the tumor or stroma cell immunogenicity within the tumor microenvironment (TME) and the development of antitumor immunity through intertwining with pattern recognition receptor (PRR), cell death pathways, and inflammatory (Gerada and Ryan, 2020). Nevertheless, few studies have reported the impact on prognosis and the correlation with immune cells of autophagy in LGG.

In the study, we established a powerful prognostic signature based on six autophagy-related genes, and then a nomogram was built with the signature and traditional clinical parameters, to predict clinical outcomes and assist clinical procedures. Moreover, the association of autophagy-related genes signature with immune cells and emerging immune targets and was further analyzed.

## MATERIALS AND METHODS

### Data Collection and Processing

The level 3 RNA-seq expression profiles and corresponding clinicopathologic data including age, gender, grade, IDH mutation status, chemotherapy, radiotherapy of LGG patients were obtained from TCGA Lower Grade Glioma (LGG) of UCSC Xena (https://xenabrowser.net/). All patients were diagnosed with LGG, who were followed for more than 90 days and have complete clinical information. Overall, 433 patients of the LGG whole cohort met the screening rules. The patients were randomly separated into a training cohort ($n$ = 305) and a validation cohort ($n$ = 128) at a ratio of 7:3. mRNA Expression profiles used in normal brain tissues were downloaded from the Genome Tissue Expression (GTEx, https://gtexportal.org/home/datasets) (Consortium, 2015). To normalize expression data and eliminate the batch effects, the "sva" R package was used.

### Selection and Functional Enrichment of Autophagy-Related Genes

The "limma" R package was employed to select differentially expressed genes (DEGs) by comparing TCGA-LGG tissues and GTEX-brain normal tissues, with the included criteria (Adj. $p$ < 0.05 and $|\text{LogFC}| > 1$) (Ritchie et al., 2015). A volcano plot was used to visualize the DEGs. The 232 autophagy-related genes (ARGs) were extracted from the Human Autophagy Database (HADb, http://www.autophagy.lu/) (Moussay et al., 2011). The intersection of the DEGs and ARGs was selected as the significant differentially expressed autophagy-related genes (DE-ARGs) for further assessment and was then showed in Venn diagrams.

In the whole set, LGG patients were separated into two risk groups, low- and high-risk groups, according to the optimal risk cutoff obtained from the training set. To probe underlying functions of DE-ARGs and risk model, the biological process of GO and KEGG pathways analysis was performed and GESA was conducted to identify the critical altered signaling pathways between high- and low-risk groups, by the aid of the "clusterProfiler" package in R 3.6.3 (Yu et al., 2012). The "c2.cp.kegg.v7.0.symbols.gmt" KEGG gene set was adopted as reference. The nominal $p$-value (NOM-$P$) for gene sets <0.05, the absolute normalized enrichment score ($|\text{NES}|$) > 1.8 and the false discovery rate (FDR) <0.05 were confirmed as threshold.

### Construction and Validation of the Risk Model Based on Autophagy-Related Genes

Performing univariate Cox regression analysis in the "survival" R package, 13 of 53 DE-ARGs in the training cohort was identified with prognosis significance (all $p < 0.05$) (Linden and Yarnold, 2017). The least absolute shrinkage and selection operator (LASSO) (Friedman et al., 2010) analysis was utilized to establish the risk model. The prognostic risk score model according to a combination of LASSO coefficient and the corresponding normalized expression level was built in the following equation: risk score = sum (the normalized expression level of each gene × corresponding LASSO coefficient). Subsequently, a risk score was computed for each patient. All patients were stratified into the low-risk and high-risk groups based on the optimum cutoff of risk score (risk score = −7.009) counted by ROC curve using the "survminer" package in

R (**Supplementary Figure S1**). Next, a KM plot based on log-rank test was applied to measure the survival difference between patients with high- and low-risk groups. The prognostic capacity of the ARG-based signature was investigated by using Harrell's concordance index (C-index), time-dependent receiver operating characteristic (ROC) curve, and Principal component analysis (PCA) with the R packages "survcomp," "survivalROC," and " scatterplot3d" (Harrell et al., 1996; Mächler and Ligges, 2003; Alba et al., 2017). Then, the prognostic effect of the signature established by the training set was verified in the validation cohort and the whole cohort using some similar methods.

Moreover, to evaluated whether the predictive capacity of the prognostic risk model could be independent of other clinic factors (including age, gender, WHO grade, radiotherapy, chemotherapy, and IDH status) for patients with LGG, univariate Cox regression and multivariate Cox regression analyses were applied in the TCGA training cohort, the validation cohort, and the whole cohort. Next, by using "rms," "foreign," and "survival" R packages, we established a nomogram comprising of traditional clinical factors and risk score based on the multivariate Cox regression analysis. The prognostic effect of the prognostic nomogram was examined by Harrell's concordance index (C-index), time-dependent ROC curve, and calibration plots of the nomogram for 3 and 5 years OS plotted to assess the coincidence of actual observed rates with the predicted survival probability. Time-dependent ROC analyses were performed by the "timeROC" R package.

## Associations Between Immune Components and Autophagy-Related Genes Signature

To identify the potential association between the signature and immune components, both emerging immune targets and tumor-infiltrating immune cells were included. The list of potential immunotherapy targets involved in innate and adaptive immune processes was extracted from a recent review (Burugu et al., 2018). We Compared the target gene expression between different risk groups. CIBERSORT algorithm, a novel deconvolution algorithm, uses 547 reference gene expression values for estimating enrichment of different immunocyte subpopulations (Newman et al., 2015). Our study applied the CIBERSORT algorithm to examine the abundance of 22 infiltrating immune cells in the high-risk and low-risk group in the whole cohort. Utilizing the Monte-Carlo sampling, the deconvolution $p$-values of samples were computed to offer reliability in the assessment. Patients with $p < 0.05$ were considered to be high reliability of the inferred cell composition. Therefore, samples with a $p$ value of <0.05 were retained for subsequent analysis. The expression profiles of TCGA-LGG patients were put on the CIBERSORT web tool (http://cibersort.stanford.edu/) for analysis with the default signature matrix at 1,000 permutations.

## Statistical Analysis

All data analyses were done on software R (version 3.6.3). The student's t-test and chi-square test were used to determine that whether there is a difference in clinical parameters between the training cohort and validation cohort and to evaluate the association between clinical characteristics and the risk score. Kaplan–Meier survival analysis was used to compare the prognosis between risk groups. The significantly independent prognostic factors in LGG were identified using univariate and multivariate Cox regression. The predictive capacity of the signature and other clinical parameters was determined by ROC curves. A nomogram was constructed with the "rms" package in R, by using multivariate Cox analysis. The C-index and calibration plot with the bootstrap method were performed to evaluate the predictive power of the nomogram. A $p$ value <0.05 is considered statistically significant.

# RESULTS

## Identification of Differentially Expressed Autophagy-Related Genes and Enrichment Analysis

RNA-seq expression data and clinical information of 529 lower-grade glioma tissue samples were obtained from TCGA, and 1,035 non-tumor samples were selected from GTEX. Of those patients, a total of 433 LGG patients who were followed for more than 3 months and had complete clinical data were analyzed in the study. After analyzing the TCGA-LGG expression data using limma, 7,143 DEGs were found between LGG and normal tissues and showed in the volcano plots (**Figure 1A**). Venn diagrams revealed that the intersection of fifty-three significant DE-ARGs were used for further analysis (**Figure 1B**).

Next, we performed functional enrichment analysis to identify risk pathways and biological functions associated with the DE-ARGs. Go enrichment analysis revealed that the biological process of the DE-ARGs were significantly enriched in terms of autophagy-related processes; the cellular component of the DE-ARGs were significantly enriched in the terms autophagosome membrane, autophagosome and vacuolar membrane and the molecular function of the DE-ARGs were significantly enriched in the terms ubiquitin and ubiquitin–like protein ligase binding, and cyclin–dependent protein serine/threonine kinase inhibitor activity (**Figure 1C**). In addition, KEGG enrichment analysis showed that the DE-ARGs were mainly involved in cancer-related pathways, Autophagy–animal and Mitophagy–animal (**Figure 1D**).

## Establishment of an Autophagy-Related Model for Survival Prediction in the The Cancer Genome Atlas Lower-Qrade Qliomas Training Cohort

According to the screening conditions, we randomly separated 433 patients in TCGA-LGG into a training dataset ($n = 305$) and a validation dataset ($n = 128$), using the "caret" package. The chi-square test demonstrated no significant difference in basic clinical factors between the two datasets (**Table 1**). Moreover, the clinicopathological parameters of LGG patients based on risk

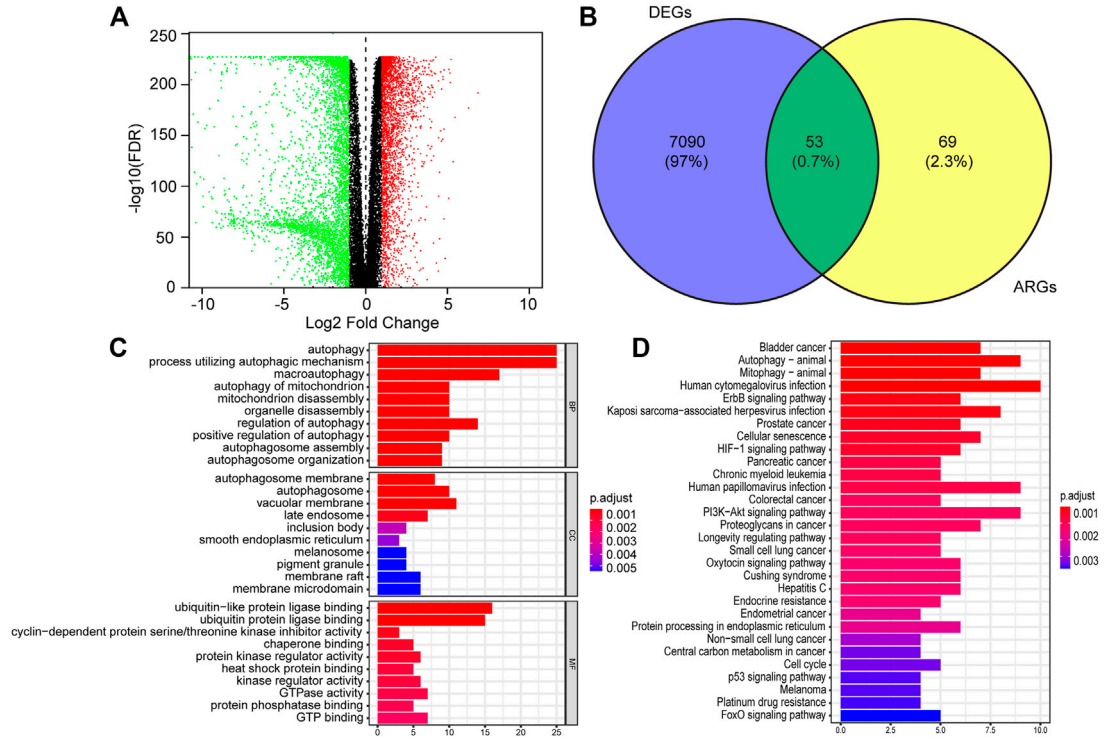


**FIGURE 1 |** Identification of differentially expressed autophagy-related genes (DE-ATGs) in low grade glioma (LGG) and enrichment analysis. **(A)** Volcano plot of DEGs in 529 tumor tissues of The Cancer Genome Atlas (TCGA) dataset and 1,035 normal samples from The Genotype-Tissue Expression (GTEx). The vertical axis indicates the–log [adjusted *p* value (adj. *p* value)], and the horizontal axis indicates the log2 [fold change (FC)]. The red dots represent upregulated genes, and the green dots represent downregulated genes (adj. *p* value <0.01 and |log2(FC)| > 1). **(B)** Venn diagram showing the 53 DE-ARGs (the intersection of the DEGs and ARGs). **(C)** Biological processes (BP), Cellular components (CC) and Molecular functions (MF) enriched in the DE-ARGs. **(D)** Kyoto Encyclopedia of Genes and Genomes (KEGG) pathways enriched in the DE-ARGs.

**TABLE 1 |** Demographics and clinicopathological data of 433 LGG patients from the TCGA database.

| Clinical variables | Total set number (%) | Training set number (%) | Validating set number (%) | *p* Value |
|---|---|---|---|---|
| Age at diagnosis | | | | |
| <40 | 237 (54.73) | 159 (52.13) | 78 (60.94) | 0.1155 |
| ≥40 | 196 (45.27) | 146 (47.87) | 50 (39.06) | |
| Gender | | | | |
| FEMALE | 197 (45.5) | 135 (44.26) | 62 (48.44) | 0.4899 |
| MALE | 236 (54.5) | 170 (55.74) | 66 (51.56) | |
| Grade | | | | |
| G2 | 206 (47.58) | 141 (46.23) | 65 (50.78) | 0.4473 |
| G3 | 227 (52.42) | 164 (53.77) | 63 (49.22) | |
| Radiotherapy | | | | |
| NO | 159 (36.72) | 113 (37.05) | 46 (35.94) | 0.9126 |
| YES | 274 (63.28) | 192 (62.95) | 82 (64.06) | |
| Chemotherapy | | | | |
| NO | 182 (42.03) | 134 (43.93) | 48 (37.5) | 0.258 |
| YES | 251 (57.97) | 171 (56.07) | 80 (62.5) | |
| IDH status | | | | |
| Mutation | 353 (81.52) | 246 (80.66) | 107 (83.59) | 0.5598 |
| Wild | 80 (18.48) | 59 (19.34) | 21 (16.41) | |

signature constructed below was also examined (**Supplementary Table S2**). After univariate Cox regression analysis, 13 significantly prognosis-associated genes were identified in the training cohort of 305 LGG patients. These significant genes entered into LASSO COX regression analyses, and the regression coefficient was determined. As a result, the six most important

**TABLE 2 |** Six survival-related autophagy-related gene in the signature associated with overall survival in the TCGA-training set.

| ID | uniCox regression | | | | LASSO |
|---|---|---|---|---|---|
| | HR | Low 95% CI | High 95% CI | *p* value | Coefficient |
| BAG1 | 0.060069 | 0.023310698 | 0.154791644 | 5.78E-09 | –0.773344244 |
| PTK6 | 0.175985 | 0.084795649 | 0.365238271 | 3.11E-06 | –0.200973447 |
| EEF2 | 0.362671 | 0.241460173 | 0.544727587 | 1.02E-06 | –0.162054564 |
| PEA15 | 0.335272 | 0.238622505 | 0.471066233 | 3.00E-10 | –0.463926374 |
| ITGA6 | 3.111707 | 1.844873426 | 5.248445579 | 2.08E-05 | 0.056506153 |
| MAP1LC3C | 2.274053 | 1.794350072 | 2.881999107 | 1.07E-11 | 0.322322447 |

genes were identified as BAG Cochaperone 1 (BAG1), Protein Tyrosine Kinase 6 (PTK6), Eukaryotic Translation Elongation Factor 2 (EEF2), Proliferation and Apoptosis Adaptor Protein 15 (PEA15), Integrin Subunit Alpha 6 (ITGA6), and Microtubule Associated Protein 1 Light Chain 3 Gamma 5 (MAP1LC3C). An autophagy-related LGG risk score was constructed through a linear combination of the expression values of the six autophagy-related genes adjusted by the LASSO regression coefficient. The risk score = −0.7733 × expression level of BAG1-0.2010 × expression level of PTK6-0.1621 × expression level of EEF2-0.4639 × expression level of PEA15 + 0.0565 × expression level of ITGA6 + 0.3223 × expression level of MAP1LC3C. The risk score for each patient was calculated according to this equation (**Table 2**).

Subsequently, we computed the risk score for each LGG patient in the training cohort. The cutoff risk score (−7.009) was counted using the "survminer" package in the TCGA-LGG training cohort. All LGG patients were then separated into low- (risk score < −7.009) and high-risk (risk score ≥ −7.009) groups (**Figure 2D**). Kaplan–Meier survival analysis showed that patients in high-risk group were associated with a relatively poor OS as than those in the low-risk group (log-rank $p$ = 1.554e-15, **Figure 2A**). The heatmap showed that six prognostic expression profiles between two risk groups (**Figure 2C**). Besides, multivariate Cox regression analysis demonstrated that the risk score could independently predict OS after adjusting for various clinicopathologic parameters in the training cohort (**Table 3**). ROC analysis of 5 years overall survival was applied to examine the predictive capacity of the six-gene prognostic risk model. Moreover, the 5 years AUC of risk model was 0.837, which was markedly higher than that of age (AUC = 0.684), gender (AUC = 0.538), WHO grade (AUC = 0.700), radiotherapy (AUC = 0.671), IDH status (AUC = 0.293), and chemotherapy (AUC = 0.616), indicating that it has a more robust prediction of clinical outcome than the other clinical parameters (**Figure 2B**).

## Testing the Signature in the Validation Cohort and the Whole Cohort

The validation dataset and the whole dataset were used to predict OS and demonstrate the predictive capacity of the risk model. The risk score in each LGG patient from the validation cohort was calculated based on the formula. Then, we divided the validation cohort into a high-risk group ($n$ = 44) and a low-risk group ($n$ = 84) depending on the optimal risk cutoff value in the training cohort (risk score = −7.009, **Figure 3D**). Kaplan-Meier analysis indicated that patients in the high-risk group had a poorer prognosis compared to those in the low-risk group (log-rank $p$ = 7.382e-05, **Figure 3A**). The heatmap displayed that six autophagy-related expression profiles between low- and high-risk groups in the validation cohort (**Figure 3C**). Besides, univariate and multivariate analysis revealed that the risk score was significantly associated with OS after adjustment for other clinical parameters such as age, gender, grade, radiotherapy, chemotherapy, and IDH status (**Table 3**). Moreover, The ROC curves for 5 years overall survival indicated that the risk score has the best predictive capacity of OS (AUC = 0.755) among the clinical parameters (**Figure 3C**).

We then further demonstrated the prognostic predictive capacity of the six autophagy-related genes signature in the whole dataset and achieved similar findings. As shown in **Figure 4D**, the optimal risk cutoff value in the training cohort was adopted to separate the whole dataset into a high-risk group ($n$ = 133) and a low-risk group ($n$ = 300). KM analysis also revealed that high-risk patients had a poorer prognosis than those in the low-risk group (log-rank $p$ value = 0e + 00, **Figure 4A**). Six autophagy-related expression profiles between low- and high-risk groups in the whole cohort were also showed in a heatmap (**Figure 4C**). Univariate and multivariate analysis still indicated that the risk signature was significantly associated with overall survival after adjustment for clinical parameters (**Table 3**). The ROC curves for 5 years overall survival also revealed that the risk score has the best predictive power of OS (AUC = 0.803) than the other traditional clinical parameters (**Figure 4B**). These results suggested the autophagy-related risk signature performed well in predicting clinical outcomes of LGG patients.

Last, we further compared the predictive capacity of our six autophagy-related genes signature with the two previous models based on autophagy-related genes, by performing ROC curves and Principal component analysis (PCA). The ROC curves for 5 years overall survival revealed that the AUC values of these two published signatures were 0.487 and 0.726 (**Supplementary Figure S2**), which are lower than our signature. The PCA analysis revealed that our six-autophagy-related genes signature could clearly split the LGG patients into a high- and low-risk group, and presents a best distinction effect compared with other risk models (**Supplementary Figure S3**). These results indicated that our risk model has greater predictive performance in predicting prognosis compared with other signatures.

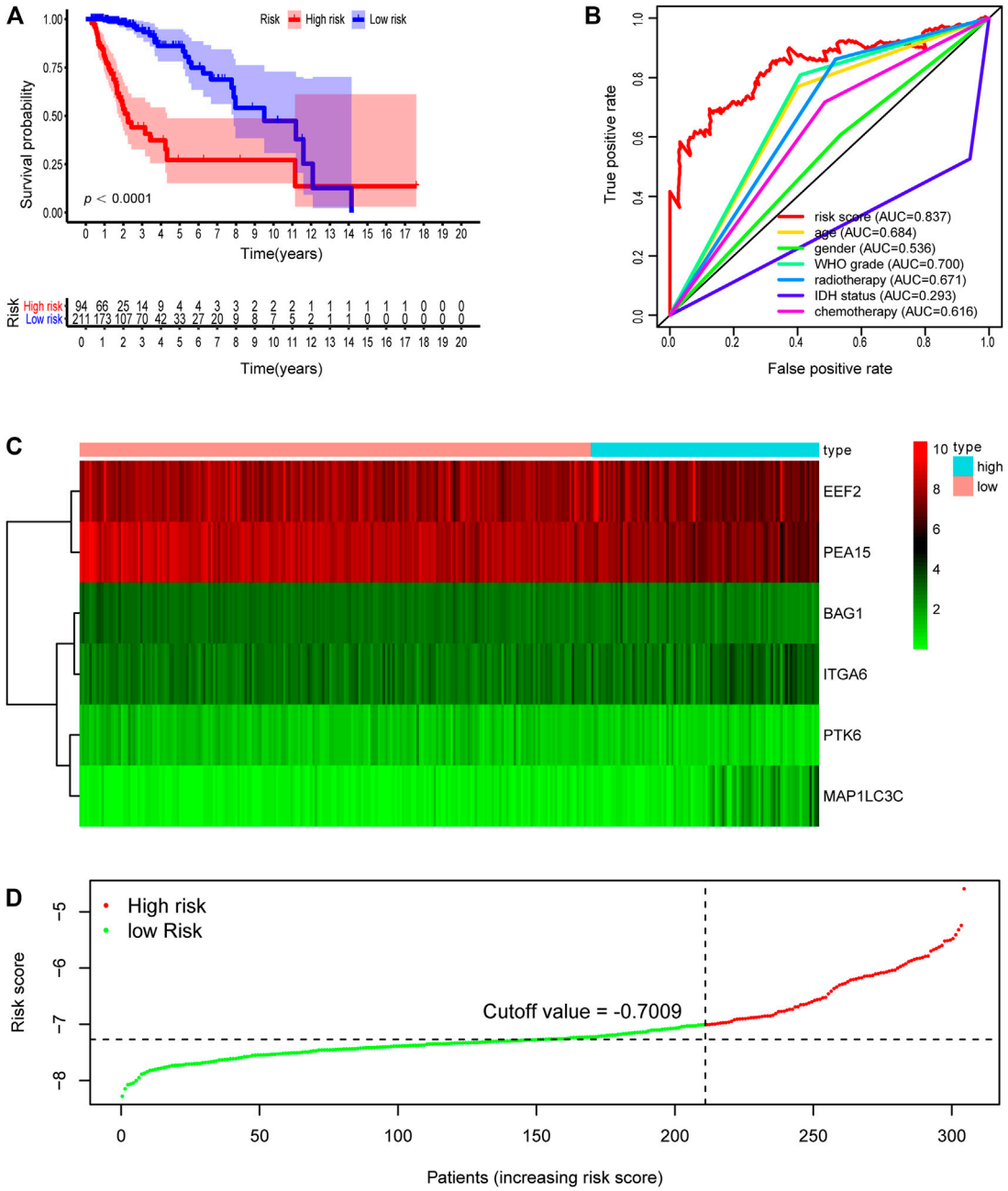


**FIGURE 2 |** Development of risk score based on the six autophagy-related gene signature of patients with TCGA-LGG training set. **(A)** Kaplan-Meier plot for overall survival (OS) based on risk score of the six gene based signature of patients with TCGA-LGG training cohort. **(B)** ROC curve for 5 years OS in training cohort. **(C)** Heatmap of the six autophagy-related gene expression in the training cohort. **(D)** Risk plot of each point sorted based on risk score. The black dotted line is the optimal cutoff (−7.009) classifying patients into low risk and high risk groups.

## The Association Between the Autophagy-Related Signature and Clinicopathological Factors

To probe the relationship between the risk model and clinical parameters, we firstly used a heatmap to show the distributions of age, gender, WHO grade, radiotherapy, chemotherapy, and IDH status between risk groups in the LGG whole cohort. **Figure 5A** showed that the risk groups were significantly associated with chemotherapy, radiotherapy, age, WHO grade, and survival status. And there were no significant differences between risk groups for gender. We next assessed the risk scores in various subgroups stratified by age, survival status, grade, chemotherapy, radiotherapy, and IDH status separately. Risk scores in patients

**TABLE 3 |** Univariate and multivariate Cox regression analysis in TCGA-LGG each cohorts.

| Variables | Univariate analysis | | Multivariate analysis | |
|---|---|---|---|---|
| | HR (95% CI) | *p* Value | HR (95% CI) | *p* Value |
| Training set (*n* = 305) | | | | |
| Age (<40/≥40) | 3.908 (2.214–6.898) | 2.5965E-06 | 2.750 (1.448–5.222) | 0.00198857 |
| Gender (female/male) | 1.250 (0.765–2.042) | 0.372437476 | 1.974 (1.160–3.360) | 0.01221692 |
| Grade (G2/G3) | 3.459 (1.972–6.066) | 1.49742E-05 | 1.774 (0.919–3.422) | 0.08750485 |
| Radiotherapy (no/yes) | 3.045 (1.583–5.854) | 0.000844437 | 1.507 (0.710–1.131) | 0.28553912 |
| IDH status (wild/mutation) | 0.143 (0.088–0.234) | 9.56649E-15 | 0.465 (0.191–1.131) | 0.09129914 |
| Chemotherapy (no/yes) | 1.628 (0.977–2.712) | 0.061242815 | 0.820 (0.470–1.432) | 0.4854889 |
| Risk score (low/high) | 4.645 (3.353–6.435) | 2.59641E-20 | 2.493 (1.336–4.651) | 0.0041002 |
| Validation set (*n* = 128) | | | | |
| Age (<40/≥40) | 3.425 (1.427–8.220) | 0.005861356 | 3.319 (1.097–10.05) | 0.03372453 |
| Gender (female/male) | 0.794 (0.377–1.673) | 0.544405373 | 1.059 (0.461–2.431) | 0.89283856 |
| Grade (G2/G3) | 3.572 (1.572–8.117) | 0.002367324 | 2.376 (0.817–6.911) | 0.11217943 |
| Radiotherapy (no/yes) | 1.775 (0.761–4.140) | 0.183865679 | 1.921 (0.669–5.517) | 0.22532202 |
| IDH status (wild/mutation) | 0.116 (0.047–0.288) | 3.63036E-06 | 0.776 (0.139–4.338) | 0.77242088 |
| Chemotherapy (no/yes) | 0.865 (0.421–1.778) | 0.693438967 | 0.218 (0.086–0.553) | 0.00131428 |
| Risk score (low/high) | 4.334 (2.546–7.381) | 6.64509E-08 | 3.583 (1.151–11.16) | 0.02762528 |
| Whole set (*n* = 433) | | | | |
| Age (<40/≥40) | 3.541 (2.243–5.590) | 5.70336E-08 | 2.918 (1.717–4.957) | 7.4951E-05 |
| Gender (female/male) | 1.060 (0.713–1.576) | 0.772843899 | 1.472 (0.964–2.248) | 0.07342518 |
| Grade (G2/G3) | 3.307 (2.213–5.151) | 1.22602E-07 | 1.880 (1.115–3.170) | 0.01789178 |
| Radiotherapy (no/yes) | 2.535 (1.516–4.239) | 0.000389848 | 1.484 (0.818–2.692) | 0.19380046 |
| IDH status (wild/mutation) | 0.147 (0.098–0.222) | 5.54714E-20 | 0.560 (0.272–1.154) | 0.11614564 |
| Chemotherapy (no/yes) | 1.333 (0.881–2.016) | 0.173180772 | 0.623 (0.394–0.985) | 0.04287472 |
| Risk score (low/high) | 4.593 (3.487–6.050) | 2.04139E-27 | 2.714 (1.644–4.482) | 9.5588E-05 |

above 40 years old were higher than those in the younger age group (**Figure 5B**). Patients in the alive subtype had obviously lower risk scores than those in the dead subtype (**Figure 5C**). For the WHO grade, the risk scores in the G3 subgroup were higher than those in the G2 subtype (**Figure 5D**). The risk scores of patients receiving chemotherapy and radiotherapy were separately higher than those without therapy (**Figures 5E,F**). With regard to IDH status subtypes, the risk scores significantly increased in the IDH-wild subtype than the IDH-mutation subtype (**Figure 5G**).

We also examined the predictive effects of the six autophagy-related risk model in different subgroups stratified by age, gender, WHO grade, IDH status, and history of radiotherapy or chemotherapy. In the two age subtypes, higher risk scores predicted decreased survival in both age subtypes (**Figures 6A,B**, $p < 0.001$). Risk scores could separate patients with or without chemotherapy (**Figures 6C,D**, $p < 0.001$) or radiotherapy (**Figure 6K,L**, $p < 0.001$) with distinct outcomes. Similar results were also found in the IDH wild- and mutation-type groups (**Figures 6I,J**, $p < 0.001$), WHO G2 and G3 groups (**Figures 6G,H**, $p < 0.0001$), and gender groups (**Figures 6E,F**, $p < 0.001$).

## Establishing a Nomogram as Prognostic Prediction Model

By integrating the six-autophagy-related signature and six traditional clinical parameters, we constructed a nomogram to predict the survival probability at 3 and 5 years of LGG patients in the whole cohort (**Figure 7B**). The C-index of the nomogram was 0.845. The AUCs of the nomogram for 3 and 5 years OS predictions were 0.884 and 0.855, respectively (**Figure 7A**). Meanwhile, the calibration plots also demonstrated a good agreement with predicted and observed values with respect to probabilities of 3 and 5 years survivals (**Figures 7C,D**). Together, those findings indicated that the nomogram predicts precisely the 3 and 5 years survivals for LGG patients.

## Functional Annotation and Pathway Enrichment Analysis Between the High-Risk Group and Low-Risk Group

To probe the potential biological function of risk groups, both the biological process (BPs) of gene ontology, KEGG, and GSEA were performed. By applying the limma package, the heatmap showed 1904 differentially expressed genes (**Figure 8A**) between risk groups. Significantly enriched BPs were mainly involved in extracellular matrix organization, T cell activation, and leukocyte cell-cell adhesion (**Figure 8B**). As for KEGG pathways enriched in these DEGs were cell adhesion molecules, phagosome, Th1 and Th2 cell differentiation, and antigen processing and presentation (**Figure 8D**). Functional enrichment analysis was then performed between risk groups. GSEA illustrated that the most significant pathways enriched in the high-risk group were Fc gamma receptor-mediated phagocytosis, leukocyte transendothelial migration, natural killer cell mediated cytotoxicity, regulation of actin cytoskeleton, and toll like receptor signaling pathway, while no significant pathways enriched in low-risk group (**Figure 8C**). A complete list of GSEA results can be found in **Supplementary Table S1**.

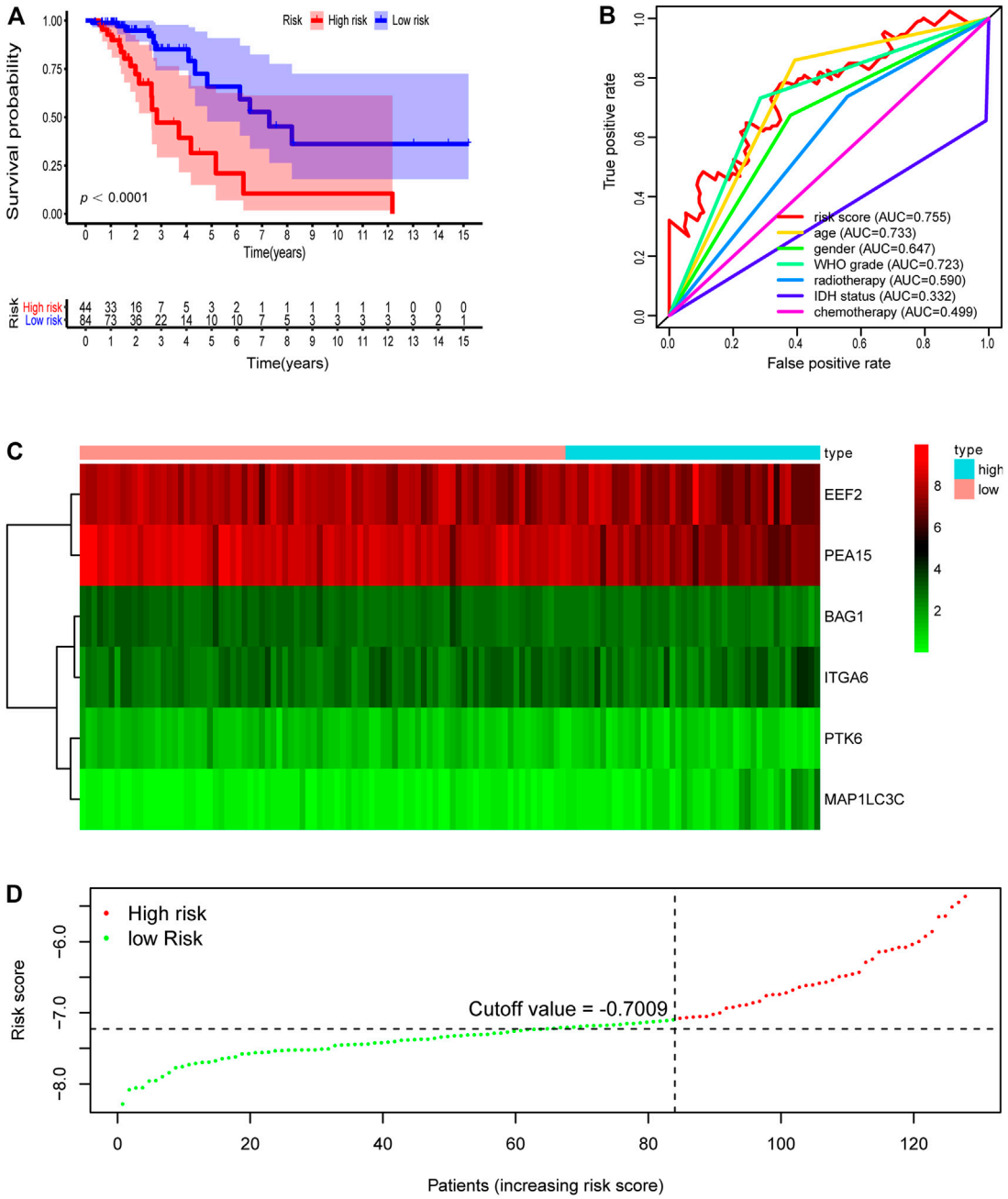


**FIGURE 3 |** Development of risk score based on the six autophagy-related gene signature of patients with TCGA-LGG validation set. **(A)** Kaplan-Meier plot for overall survival (OS) based on risk score of the six gene based signature of patients with TCGA-LGG validation cohort. **(B)** ROC curve for 5 years OS in validation cohort. **(C)** Heatmap of the six autophagy-related gene expression in the validation cohort. **(D)** Risk plot of each point sorted based on risk score. The black dotted line is the optimal cutoff (−7.009) classifying patients into low risk and high risk groups.

## Differential Expression of Potential Immunotherapy Targets and the Tumor-Infiltrating Immune Cells Between Two Groups

Pathway enrichment between risk groups suggested that autophagy-related genes signature was associated with some immune-related pathways. Thus, we investigated the abundances of the 22 immune cell types for each LGG patient from the whole cohort within the low-risk group and the high-risk group, according to the CIBERSORT algorithm. The comparison of 22 immune cells between risk groups displayed in a radar plot (**Figure 9A**). Macrophages M0, M1, and M2, and T cells CD8 were obviously increased in the high-risk group than the low-risk group; however, the

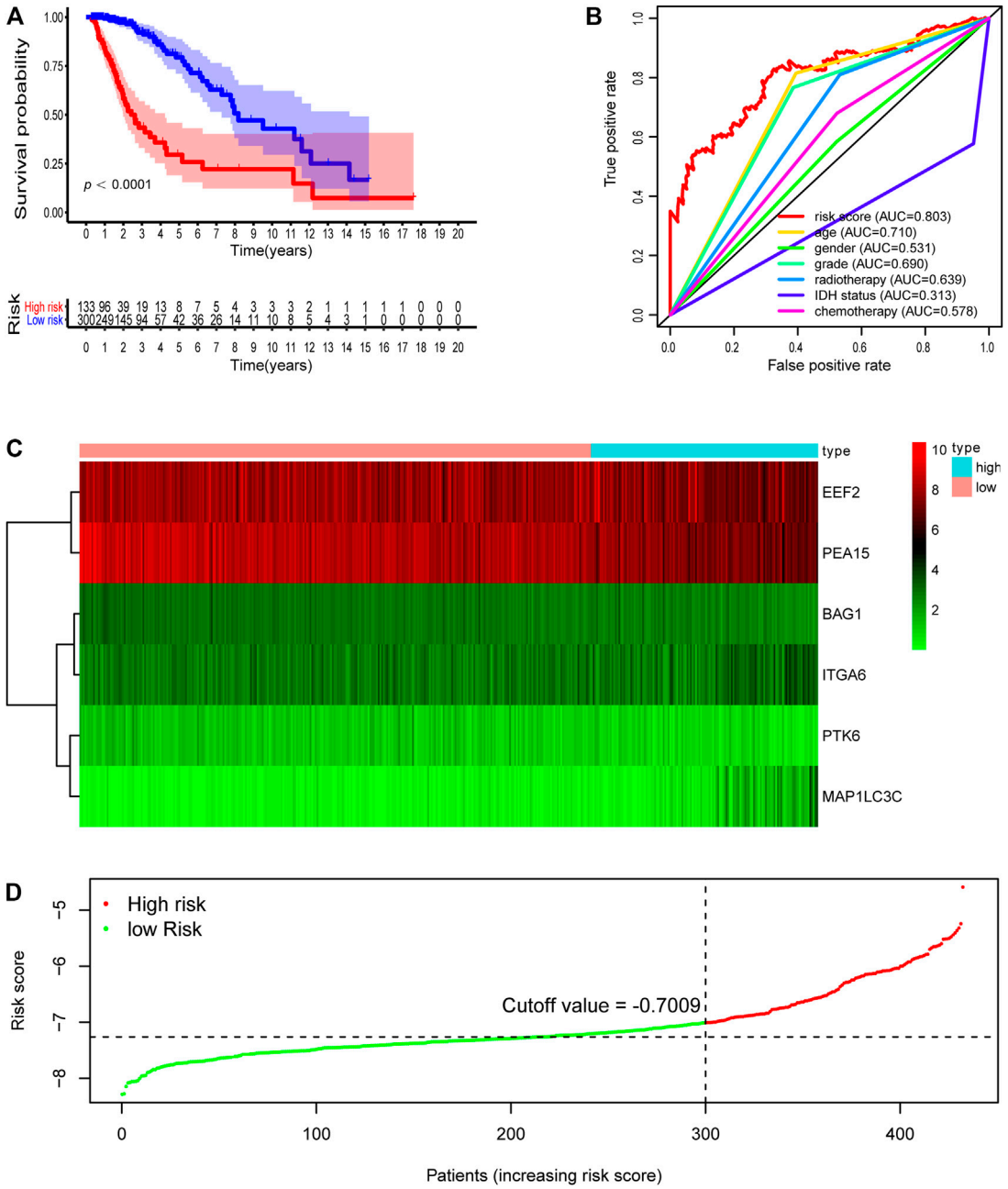


**FIGURE 4 |** Development of risk score based on the six autophagy-related gene signature of patients with TCGA-LGG whole set. **(A)** Kaplan-Meier plot for overall survival (OS) based on risk score of the six gene based signature of patients with TCGA-LGG whole cohort. **(B)** ROC curve for 5 years OS in whole cohort. **(C)** Heatmap of the six autophagy-related gene expression in the whole cohort. **(D)** Risk plot of each point sorted based on risk score. The black dotted line is the optimal cutoff (−7.009) classifying patients into low risk and high risk groups.

expression levels of Eosinophils, Mast cells activated, Monocytes, NK cells activated, and Plasma cells were obviously lower in the high-risk group (**Figure 10**). We also found the gene expressions of multiple promising immunotherapy targets, including CD47, CD276, CTLA-4, LAG3, PD-1/L1, and TIM3, and tumor mutation burden (TMB) were significantly increased in the high-risk group, while the expression levels of NKG2A was significantly upregulated in the low-risk group than in the high-risk group (**Figure 9B**).

## DISCUSSION

Autophagy has been reported involved in tumor formation and progression, and therapy resistance of multiple cancers, including glioma (Kondo et al., 2005; Mathew et al., 2007; White et al., 2010). Besides, autophagy can alter the tumor or stroma cell immunogenicity within the tumor microenvironment and the response to immunotherapy

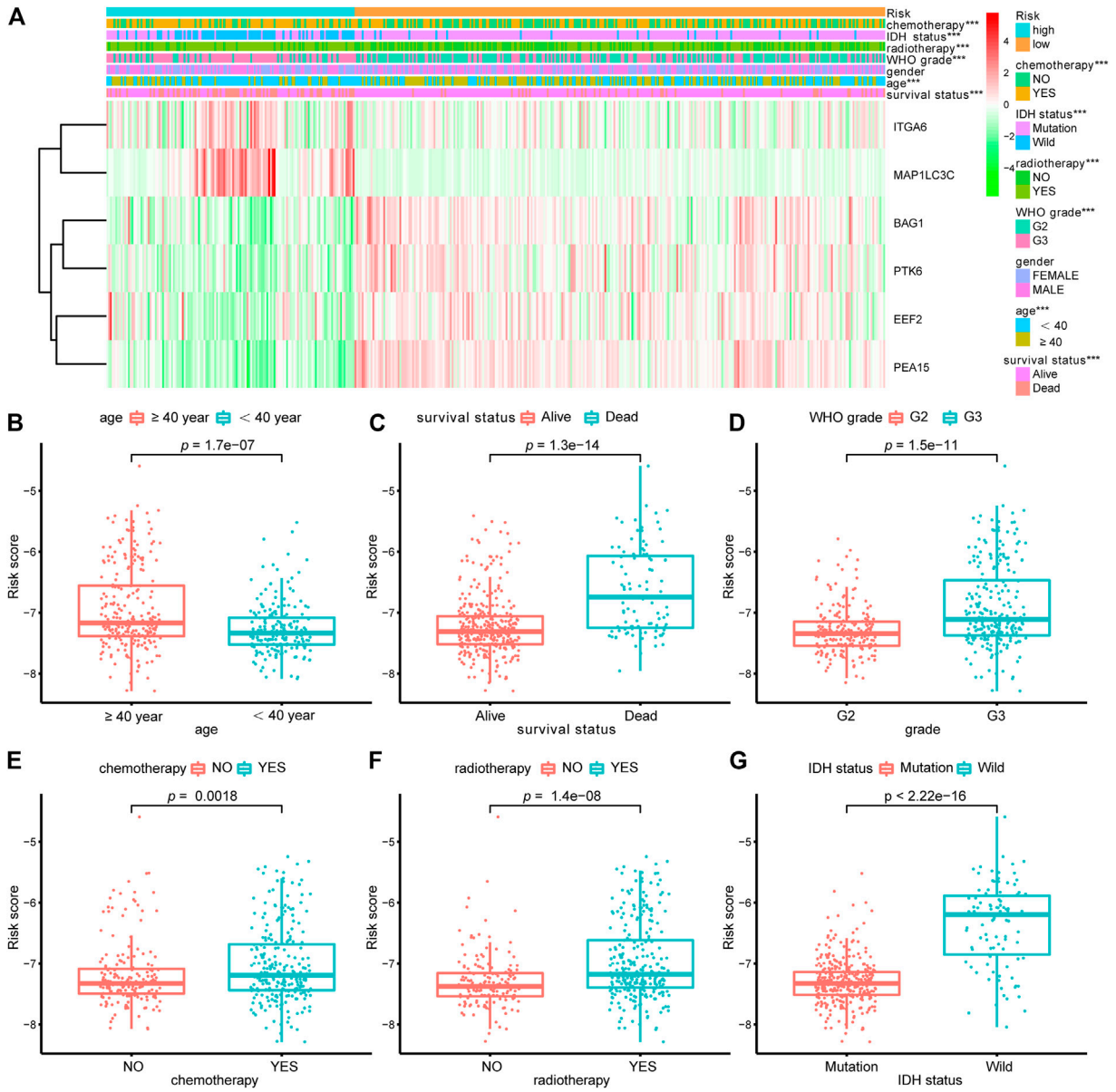


**FIGURE 5 |** Relationship between the signature risk scores and clinical factors. **(A)** The heatmap showed the relationship between the risk signature and the clinical features (chemotherapy, IDH status, radiotherapy, grade, gender, age and survival status) in the LGG-whole cohort. **(B–G)** The box plots revealed the association between risk score and clinical parameters. $^{*}p < 0.01$, $^{**}p < 0.001$, $^{***}p < 0.0001$.

(Gerada and Ryan, 2020). However, few studies have reported the impact on prognosis and the correlation with immune cells of autophagy in LGG. In this study, the whole samples of the TCGA-LGG project were randomly separated into a training set, and a validation set and the whole set were created for further verification. We established a novel prognosis signature of six autophagy-related genes of LGG in the training dataset, and the signature was verified in the validation and whole datasets. The risk score could well separate patients into a low-risk group and a high-risk group, with a significant difference in overall survival. The AUC of the risk score in predicting the 5 years survival rate in the training set, validation set, and the whole set was 0.837, 0.755, and 0.803, respectively, which suggested that the prognostic signature performed better in predicting clinical outcomes than other traditional clinical factors. The six autophagy-related genes signature could serve as the independent predictive factor of LGG patients, according to multivariate analysis and Kaplan-Meier method. Furthermore, our findings showed that significant differences in tumor immune microenvironment and promising immunotherapy targets between two risk groups in the whole cohort.

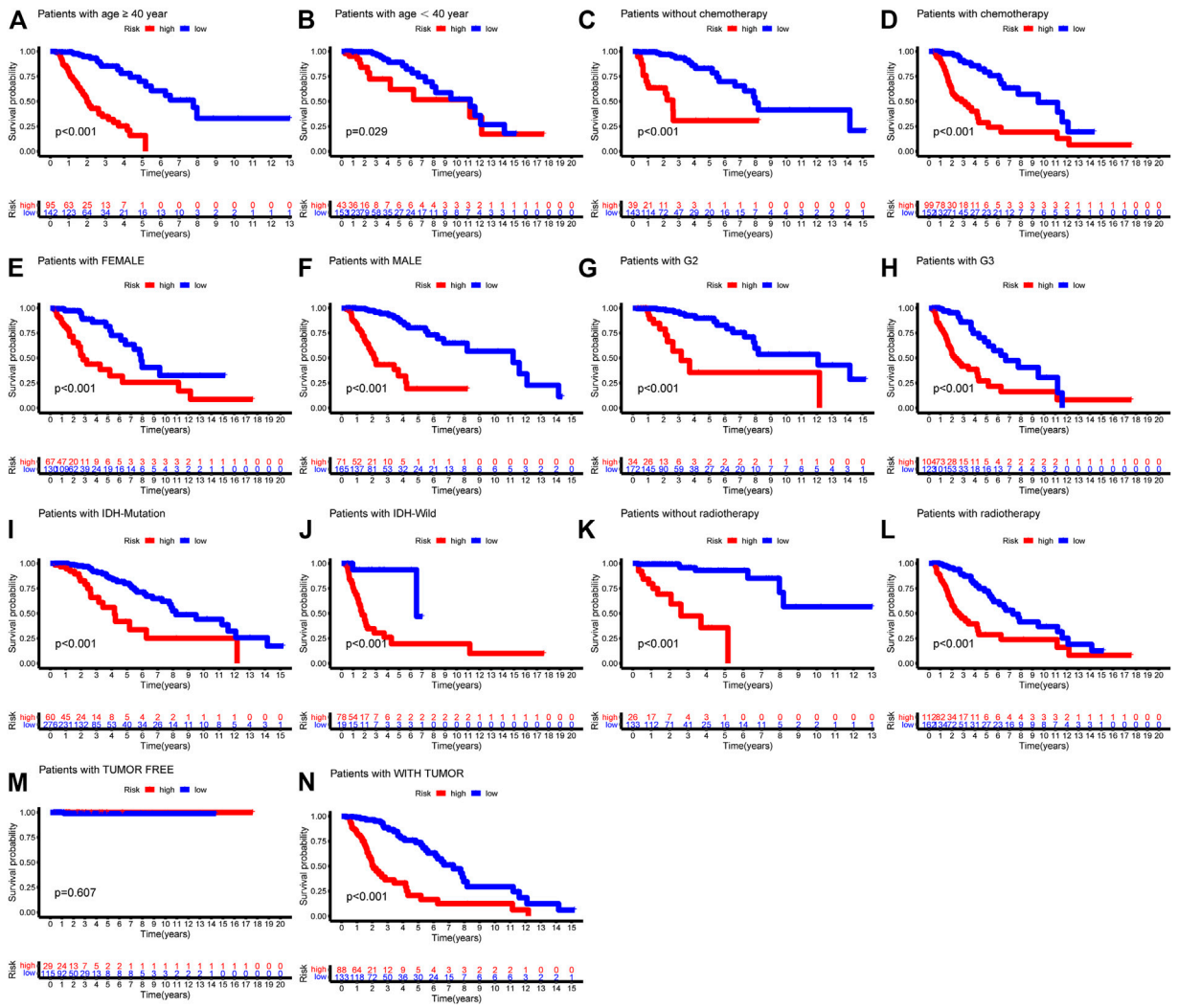


**FIGURE 6 |** Kaplan-Meier survival curves showed prognostic values of the risk signature in different subgroups of LGG-whole cohort. **(A)** age ≥ 40; **(B)** age < 40; **(C)** without chemotherapy; (**D**) chemotherapy; **(E)** Female; **(F)** Male; **(G)** G2; **(H)** G3; **(I)** IDH-mutation type; (**J**) IDH-wild type; **(K)** without radiotherapy; **(L)** radiotherapy.

Autophagy was involved in a broad range of cellular processes and human diseases, and it is responsible for both carcinogenesis and sensitivity to various therapies in recent years (Mathew et al., 2007; White et al., 2010; Gerada and Ryan, 2020). Hence, it was important to construct the prognostic model based on autophagy-related genes to predict overall survival of LGG patients. Our study first selected 53 DE-ARGs and then identified six genes significantly associated with prognosis. Among them, BAG1, PTK6, EEF2, and PEA15 were protected factors, but ITGA6 and MAP1LC3C were risk factors for LGG patients in univariate Cox regression. BAG1 is a multifunctional protein that associates with multiple cellular processes, such as apoptosis, proliferation, growth, and motility (Ostrom et al., 2013). Besides, BAG1 was reported to be a protective factor in breast cancer (Papadakis et al., 2017). Protein Tyrosine Kinase 6 (PTK6) encodes a cytoplasmic nonreceptor protein kinase, implicated in processes of proliferation, apoptosis, migration, and invasion in cancer cells (Harvey and Crompton, 2004; Shen et al., 2008; Xiang et al., 2008; Harvey et al., 2009; Locatelli et al., 2012; Park et al., 2015). PTK6 was found to be upregulated in many tumor tissues, including breast cancer (Barker et al., 1997), bladder cancer (Xu et al., 2017), non-small cell lung cancer (Zhao et al., 2013), and ovarian cancer (Schmandt et al., 2006), and is associated with adverse outcomes. However, another study showed that PTK6 expression was downregulated in laryngeal squamous cell carcinoma and esophageal squamous cell carcinoma tissues, and low expression levels of PTK6 predicted short survival (Liu et al., 2013; Chen et al., 2014). EEF2 plays an essential role in the translocation of peptidyl-tRNA during protein synthesis. Overexpression of EEF2 was associated with disease progression of lung adenocarcinoma cells (Chen et al., 2011). PEA15 is a 15-kDa phosphoprotein that impedes cell proliferation via inhibiting ERK-dependent proliferation and gene transcription (Formstecher et al., 2001;

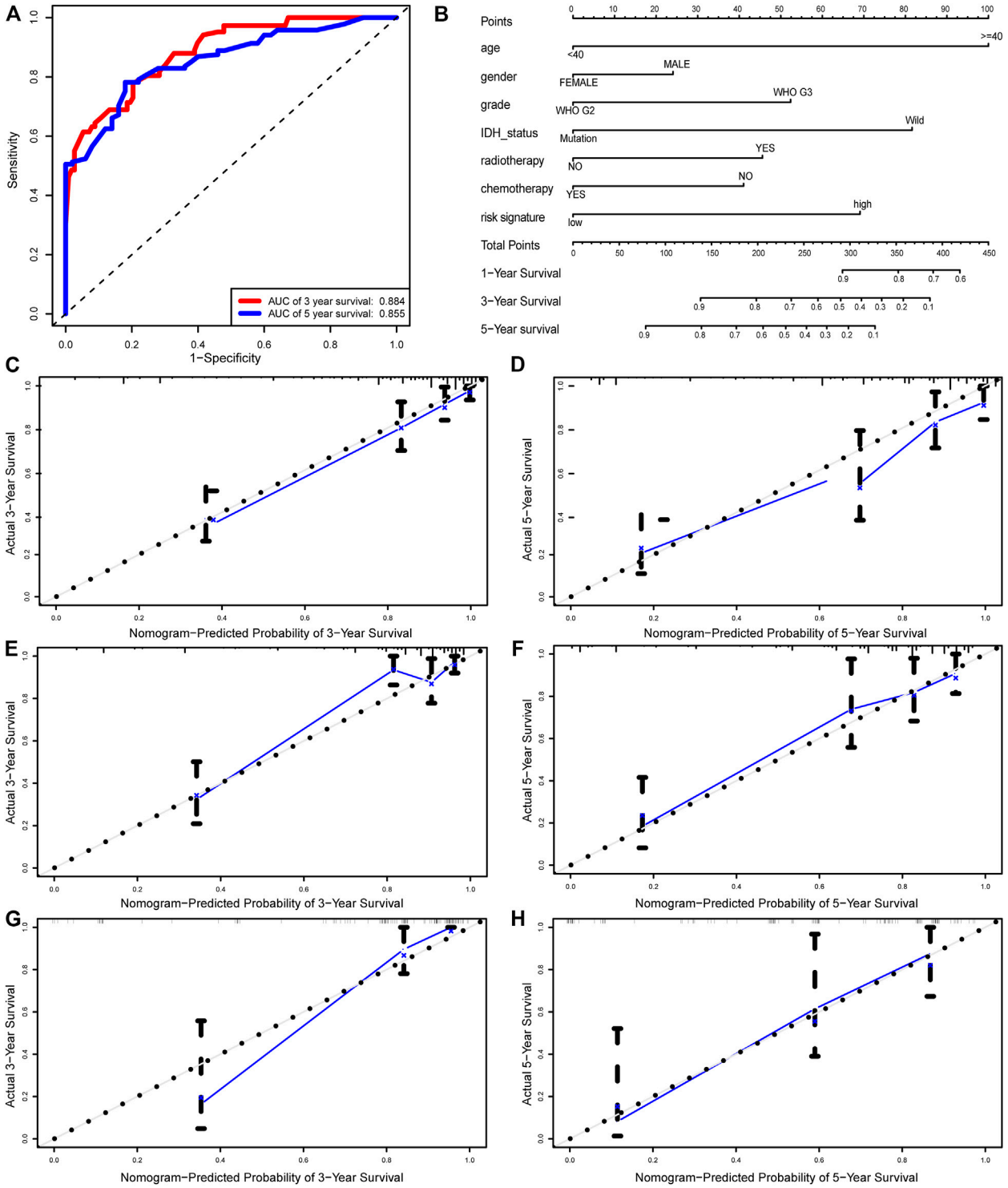


**FIGURE 7 |** Nomogram built to predict the prognosis of patients with LGG. **(A)** ROC analysis for 3 and 5 years OS predictions with the nomogram. **(B)** A nomogram based on risk score and other clinical parameters for predicting 3 and 5 years OS of LGG. Calibration curves of nomogram for predicting probabilities of 3 years **(C)**, and 5 years **(D)** overall survival of patients in the whole cohort. The calibration plots of for predicting probabilities of 3 years **(E)**, and 5 years **(F)** overall survival of patients in the training cohort. The calibration plots of for predicting probabilities of 3 years **(G)**, and 5 years **(H)** overall survival of patients in the validation cohort. The blue line indicates actual survival.

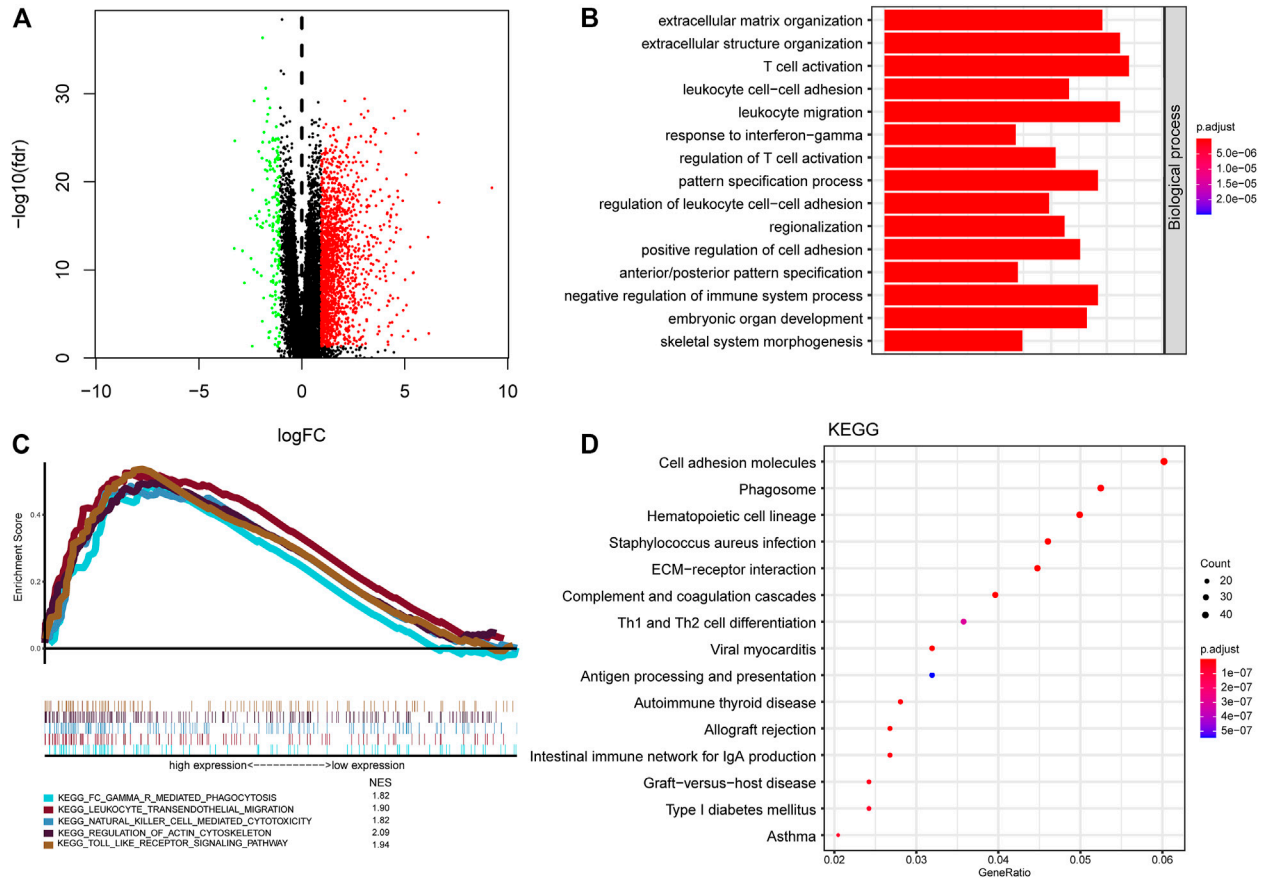


**FIGURE 8 |** Functional annotation and pathway enrichment analysis of risk groups. **(A)** Volcano plot of differential gene expression analysis between high-risk and low-risk groups. **(B)** Functional annotation for signature using GO biological process. **(C)** Gene set enrichment analysis of curated gene sets obtained from MSigDB Collections. Pathways of interest with significant enrichment in high-risk group was shown. **(D)** Pathway enrichment analysis by KEGG.

Bartholomeusz et al., 2006). In addition, PEA15 was found to induce autophagy via activation of the ERK1/2 pathway (Bartholomeusz et al., 2008). ITGA6 is a member of the integrin alpha chain family that conducts signals through interacting with extracellular matrix proteins, serving crucial roles in drug resistance of multiple cancers (Yamakawa et al., 2012; Brooks et al., 2016; Wei et al., 2019). Additionally, overexpression of ITGA6 is associated with shorter overall survival (Zhang et al., 2016; Wei et al., 2019). MAP1LC3A encodes a light chain subunit of the microtubule-associated protein 1-light chain three family, participating in the autophagy and cell mobility process. Giatromanolaki et al. (2014) reported that the overexpression of MAP1LC3A was correlated with impaired autophagic degradation activity, which may facilitate the carcinogenesis of glioblastoma. In addition, another study showed that the MAP1LC3A expression at the surgical margins could be a poor biomarker for clinical prognosis in oral squamous cell carcinoma (Terabe et al., 2018). In summary, BAG1, PTK6, EEF2, PEA15, ITGA6, and MAP1LC3C could serve as predictors for survival in multiple cancers, involving in various biological processes including autophagy. These ATGs may serve as promising prognostic biomarkers and therapeutic targets for guiding LGG therapy.

Then, we established and verified a novel six autophagy-related genes risk model that improves the survival prediction of LGG patients. According to the six autophagy-related signature, LGG patients were separated into a high-risk group and a low-risk group. Patients with high-risk scores predicted worse OS compared to patients with low-risk scores. Afterward, it was successfully validated in the validation and whole datasets, indicating the good reproducibility of this signature. Moreover, Cox regression analysis indicated that the risk score of autophagy-related genes signature is an independent prognostic factor of clinical outcome for LGG patients in multiple cohorts. Additionally, we observed that the risk scores were significantly associated with several clinical factors, including age, grade, IDH mutation status, chemotherapy and radiotherapy. As younger age, low grade glioma and IDH mutation were prognostic factors associated with better outcomes(Taillibert et al., 2004; Cancer Genome Atlas Research et al., 2015; Ostrom et al., 2020), we can speculated that these factors would associated with lower risk scores, which is consistent with our results. Chemotherapy is recommended as an

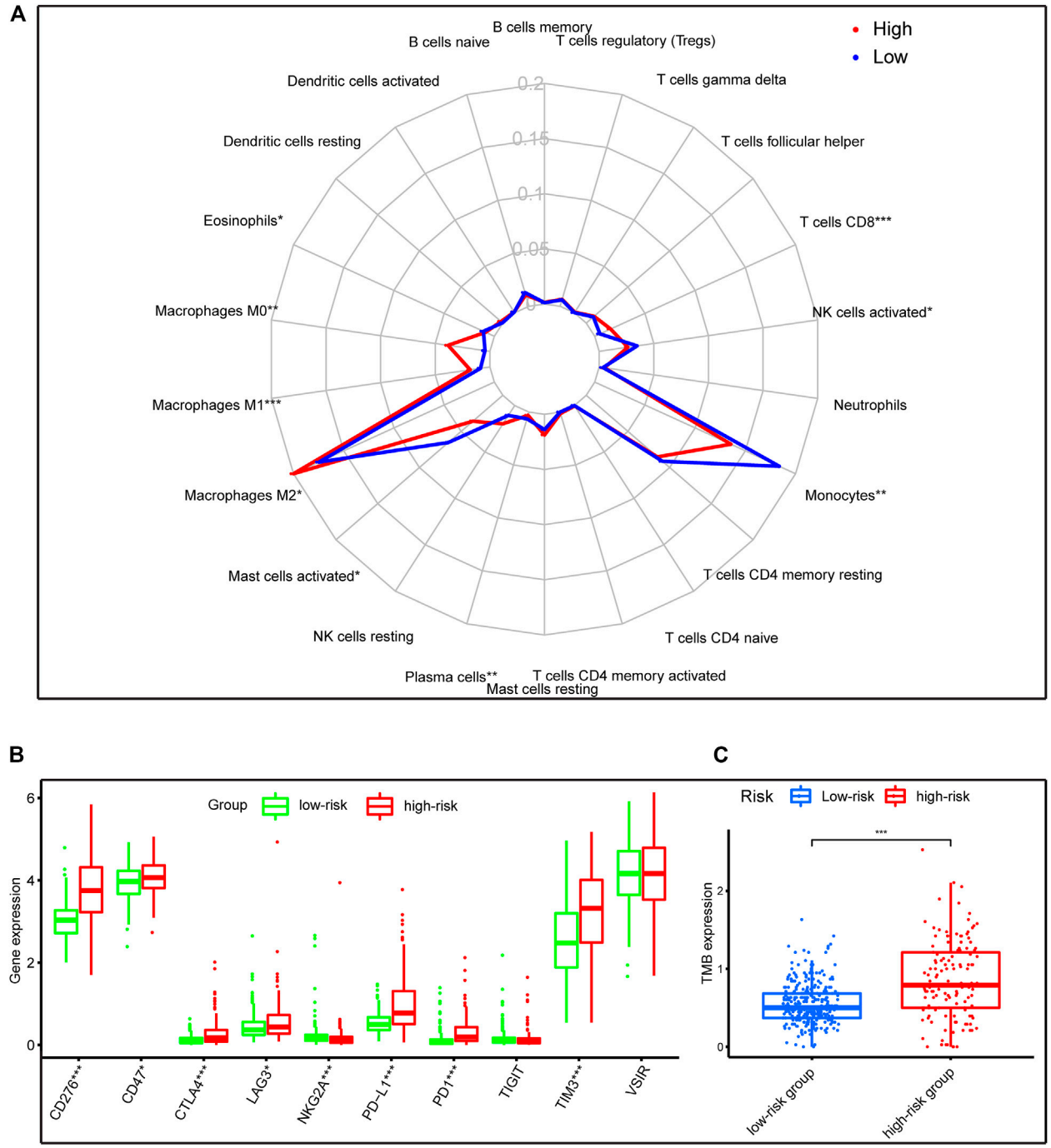


**FIGURE 9 |** Immune characteristics of risk groups in the whole cohort. **(A)** The radar plot showed the 22 different immune cell levels between high-risk and low-risk groups; **(B,C)** The levels of emerging immunotherapeutic targets and TMB between risk groups. *$p < 0.01$, **$p < 0.001$, ***$p < 0.0001$.

optional treatment alone or in combination with radiotherapy for newly diagnosed LGG patients who cannot undergo gross total resection (Ziu et al., 2015). The higher residual tumor volume (Wijnenga et al., 2018) was reported correlated with shorter OS after adjusting for other clinicopathological factors, suggesting that chemotherapy and radiotherapy might associated with unfavorable outcomes or higher risk scores, which is in accordance with our findings. Moreover, our risk model can classify LGG patients after clinicopathological parameters into high- and low-risk groups with a distinct prognosis, making the risk model can be used to guide individualize treatment. For example, the median age at time of diagnosis for LGG patients around 40 years and the older LGG patients more often associated with unfavorable prognostic factors, including focal

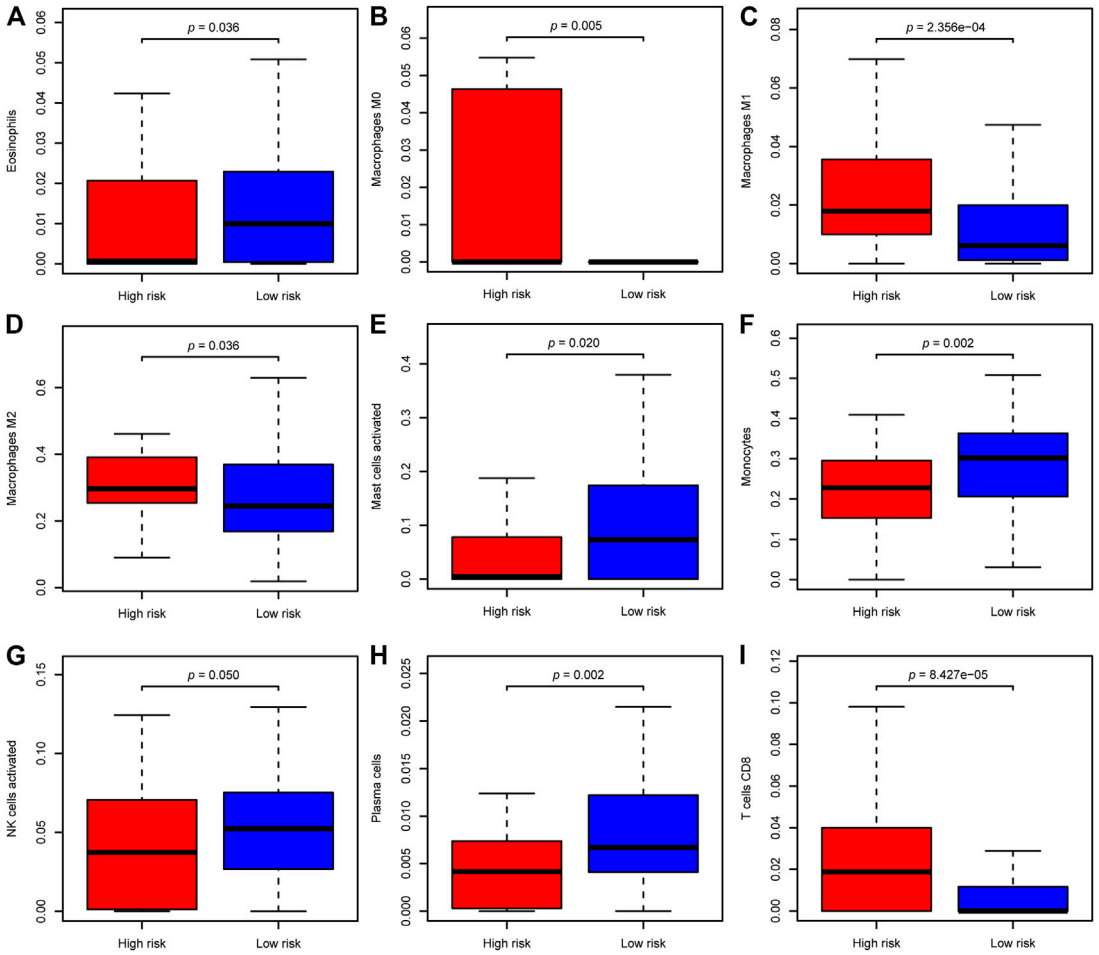


**FIGURE 10 |** The difference of significantly immune cells between risk groups. **(A)** Eosinophils; **(B)** Macrophages M0; **(C)** Macrophages M1; **(D)** Macrophages M2; **(E)** Mast cells activated; **(F)** Monocytes; **(G)** NK cells activated; **(H)** Plasma cells; **(I)** T cells CD8.

deficits, larger residual tumor volumes, compared with younger patients, which may be an explanation for advanced age patients in LGG usually with a poor prognosis (Corell et al., 2018). Additionally, previous study suggested undertreatment of the elderly patients could also contributed to their decreased survival (Kaloshi et al., 2009).Thus, it is crucial to predict the prognosis of the elderly LGG patients, to guide whether the older patients receive the active treatment or not. Fortunately, our autophagy-related genes signature can divide patients with more than 40 years into high- and low-risk groups with distinct outcomes, making the signature can be used to guide individualize treatment. Lastly, we constructed a nomogram comprising the risk score, age, gender, WHO grade, radiotherapy, chemotherapy, and IDH status, Calibration curves of the nomogram predicted the probabilities of 3 and 5 years survival, which corresponded closely with the actual survival rates, suggesting that the nomogram has an excellent predictive performance. Hence, our study identified a nomogram that could help identify LGG patients with a high risk of short survival and guide the selection of better treatment options, which is credible to both physicians and patients. To date, some autophagy-related prognostic classifiers of glioma were published. We further compared the predictive capacity of our risk model with two published signatures (Lin and Lin, 2021; Wang et al., 2021), by performing ROC curves and PCA analysis. These results proved that our six autophagy-related genes signature has the best predictive performance than another signatures, considering different selection criteria of autophagy-related genes yield different outcomes.

The tumor immune microenvironment plays a crucial role in cancer biology (Hanahan and Weinberg, 2011). Previous studies have evaluated the tumor-infiltrating immune cells were deeply involved in glioma development and progression (Perus and Walsh, 2019; Wang et al., 2020). And autophagy and immunity played a momentous role in the tumor microenvironment. Some studies have demonstrated that autophagy plays a critical role in innate immunity as well as the activation of lymphocytes and survival (Germic et al., 2019). Similar to previous findings, our functional analysis also indicated that the significant biological processes and pathways enriched in

the high-risk group were involved in some immune-related pathways, such as T cell activation, Th1 and Th2 cell differentiation, and NK cell-mediated cytotoxicity. We further evaluated the relationships of 22 types of immune cell between risk groups in LGG patients. There is a distinctive difference of the cellular component of innate immunity, such as eosinophils, monocytes, macrophages, mast cells, and natural killer (NK) cells between risk groups in the whole cohort. For the eosinophils, the role of autophagy for regulating eosinophil remains largely unknown, for less well studied. Mast cells activated were hypothesized to act as sentinel cells that respond with pathogens and trigger protective immune responses (Piliponsky and Romani, 2018). However, little is known about the mechanism of autophagy for regulating mast cell functions. As for macrophages, the level of macrophages (M0, M1, and M2 macrophages) were significantly increased in the high-risk group than those in the low-risk group, but eosinophils, mast cells activated, monocytes, and NK cells activated were higher in the low-risk group. M2 macrophages comprised the most considerable fraction of macrophages of the high-risk group in our results, which is consistent with the previous study that immunosuppressive M2 macrophages were the dominant type of tumor-associate macrophage (TAM) infiltrations in gliomas (Xu et al., 2020). M2 macrophages contributed to an immunosuppressive tumor microenvironment and promote glioma progression (Xu et al., 2020). Moreover, we found that the high-risk group have a lower abundance levels of NK cell, which have cytotoxic potential against tumor cells and its infiltration is associated with better clinical outcomes (Eckl et al., 2012). In addition, the high-risk group has higher fractions of $CD8^+$ T cells. Prior studies have demonstrated that increased $CD8^+$ T cells are related to prolonged survival in gliomas (Yang et al., 2010). However, increased expression of immune checkpoints (such as PD-1/L1, LAG3, TIM3) could contribute T cell to a dysfunctional exhausted status following activation (Woo et al., 2012). Our study found that the expression of immune checkpoints was significantly upregulated in the high-risk group compared to the low-risk group. Therefore, the immunosuppressive M2 macrophages, the lower level of NK cells, and the increased expression of immune checkpoints in patients with high risk may be an explanation for their decreased survival.

Cancer immunotherapy is now emerged as the fifth pillar of cancer treatment, with surgery, chemotherapy, targeted pathway inhibition, and radiation (Murciano-Goroff et al., 2020). Immune checkpoint inhibitors (ICIs) have now become the first-line therapies of choice in multiple cancers, such as advanced non-small cell lung cancer and melanoma (Larkin et al., 2015; Reck et al., 2016). However, upregulation of additional immune checkpoints conferring to ICIs resistance, there is a need to identify novel antitumor immune-activating agents. Emerging immunotherapy targets involved in adaptive immunity and innate immune processes, targeting these agents can greatly enhance antitumor immunity, thus eradicating cancer cells (Burugu et al., 2018). For example, LAG-3 has been reported positive expression on the surface of tumor-infiltrating lymphocytes (TILs) of multiple cancers (Deng et al., 2016; Shapiro et al., 2017; Tassi et al., 2017), correlating with aggressive clinical features. In preclinical mouse models, LAG-3 inhibition reenergizes $CD8^+$ T cell's cytotoxicity function and decreases Treg populations, combined with PD-1 inhibitor could improve the antitumor effect (Woo et al., 2012; Huang et al., 2015). Besides, TMB was a potential biomarker for PD-1 inhibitors and patients with high TMB receiving PD-1 inhibition have a higher objective response rate compared to patients with low TMB (Zhu et al., 2019). Our study investigated the immunotherapy target gene expression between different risk groups. The result showed that the gene levels of multiple potential immunotherapy targets, including CD276, CD47, CTLA-4, LAG3, PD-1/L1, and TIM3, and TMB were significantly increased in the high-risk group, while the expression levels of NKG2A was significantly upregulated in the low-risk group than in the high-risk group. Therefore, we speculated that the high-risk patients may benefit from the blockade of these immunotherapy targets in LGG.

The present study has some limitations. Firstly, we built the autophagy-related prognosis signature only with the RNA-seq expression profiles of LGG from TCGA. Although we have separated whole samples into two sets of training cohort and validation cohort, and then verified the performance of the risk signature constructed in the training cohort with the data in the validation and whole cohorts, our prognosis signature would be more powerful with verified in independent external cohorts. Secondly, more details about the molecular mechanisms of six autophagy-related genes and the cross-talk between the autophagy and immune cells in LGG patients required further assessment.

## CONCLUSION

In summary, we established a reliable autophagy-related six genes signature that can effectively assess the prognosis of LGG patients. Besides, we identified the immune microenvironments and immune targets were different between risk groups, which could be an explanation for poor prognosis in the high-risk group. Furthermore, the six autophagy-related genes risk model might guide the application of immunotherapy in LGG.

## DATA AVAILABILITY STATEMENT

The datasets presented in this study can be found in online repositories. The names of the repository/repositories and accession number(s) can be found in the article/**Supplementary Material**.

## ETHICS STATEMENT

The studies involving human participants were reviewed and approved by TCGA belongs to public databases. The patients involved in the database have obtained ethical approval. Users can download relevant data for free for research and publish relevant articles. Our study is based on open source data, so there

are no ethical issues and other conflicts of interest. Written informed consent to participate in this study was provided by the participants' legal guardian/next of kin.

## AUTHOR CONTRIBUTIONS

TL, HC, DL, JG, and XJ designed the study and wrote the original article. TL, LW, JK, LX, DL, CS, ZC, HL, ML, ZZ, WH, QH, SL, and CZ downloaded, analyzed, and validate the data. JG, and XJ supervised the study and edited the article.

## FUNDING

This work was supported by Natural Science Foundation of Guangdong Province (No. 2019A1515011943), China Postdoctoral Science Foundation (No. 2019M662974), Science and Technology Program of Guangzhou (No. 202002030445), and the Medical Research Foundation of Guangdong Province of China (No. A2020499, No. A2020505).

## ACKNOWLEDGMENTS

The authors would like to thank the TCGA project for sharing data.

## SUPPLEMENTARY MATERIAL

The Supplementary Material for this article can be found online at: https://www.frontiersin.org/articles/10.3389/fgene.2021.698284/full#supplementary-material

## REFERENCES

Alba, A. C., Agoritsas, T., Walsh, M., Hanna, S., Iorio, A., Devereaux, P. J., et al. (2017). Discrimination and Calibration of Clinical Prediction Models. *JAMA*. 318 (14), 1377–1384. doi:10.1001/jama.2017.12126

Barker, K. T., Jackson, L. E., and Crompton, M. R. (1997). BRK Tyrosine Kinase Expression in a High Proportion of Human Breast Carcinomas. *Oncogene*. 15 (7), 799–805. doi:10.1038/sj.onc.1201241

Bartholomeusz, C., Itamochi, H., Nitta, M., Saya, H., Ginsberg, M. H., and Ueno, N. T. (2006). Antitumor Effect of E1A in Ovarian Cancer by Cytoplasmic Sequestration of Activated ERK by PEA15. *Oncogene*. 25 (1), 79–90. doi:10.1038/sj.onc.1209014

Bartholomeusz, C., Rosen, D., Wei, C., Kazansky, A., Yamasaki, F., Takahashi, T., et al. (2008). PEA-15 Induces Autophagy in Human Ovarian Cancer Cells and Is Associated with Prolonged Overall Survival. *Cancer Res.* 68 (22), 9302–9310. doi:10.1158/0008-5472.CAN-08-2592

Brooks, D. L. P., Schwab, L. P., Krutilina, R., Parke, D. N., Sethuraman, A., Hoogewijs, D., et al. (2016). ITGA6 Is Directly Regulated by Hypoxia-Inducible Factors and Enriches for Cancer Stem Cell Activity and Invasion in Metastatic Breast Cancer Models. *Mol. Cancer*. 15, 26. doi:10.1186/s12943-016-0510-x

Burugu, S., Dancsok, A. R., and Nielsen, T. O. (2018). Emerging Targets in Cancer Immunotherapy. *Semin. Cancer Biol.* 52 (Pt 2), 39–52. doi:10.1016/j.semcancer.2017.10.001

Cancer Genome Atlas Research, N., Brat, D. J., and Verhaak, R. G. (2015). Comprehensive, Integrative Genomic Analysis of Diffuse Lower-Grade Gliomas. *N. Engl. J. Med.* 372 (26), 2481–2498. doi:10.1056/NEJMoa1402121

Chen, C.-Y., Fang, H.-Y., Chiou, S.-H., Yi, S.-E., Huang, C.-Y., Chiang, S.-F., et al. (2011). Sumoylation of Eukaryotic Elongation Factor 2 Is Vital for Protein Stability and Anti-apoptotic Activity in Lung Adenocarcinoma Cells. *Cancer Sci.* 102 (8), 1582–1589. doi:10.1111/j.1349-7006.2011.01975.x

Chen, Y.-F., Ma, G., Cao, X., Huang, Z.-L., Zeng, M.-S., and Wen, Z.-S. (2014). Downregulated Expression of PTK6 Is Correlated With Poor Survival in Esophageal Squamous Cell Carcinoma. *Med. Oncol.* 31 (12), 317. doi:10.1007/s12032-014-0317-9

Claus, E. B., Walsh, K. M., Wiencke, J. K., Molinaro, A. M., Wiemels, J. L., Schildkraut, J. M., et al. (2015). Survival and Low-Grade Glioma: the Emergence of Genetic Information. *Neurosurg. Focus.* 38 (1), E6. doi:10.3171/2014.10.FOCUS12367

Consortium, G. T. (2015). Human Genomics. The Genotype-Tissue Expression (GTEx) Pilot Analysis: Multitissue Gene Regulation in Humans. *Science*. 348 (6235), 648–660. doi:10.1126/science.1262110

Corell, A., Carstam, L., Smits, A., Henriksson, R., and Jakola, A. S. (2018). Age and Surgical Outcome of Low-Grade Glioma in Sweden. *Acta Neurol. Scand.* 138 (4), 359–368. doi:10.1111/ane.12973

Deng, W.-W., Mao, L., Yu, G.-T., Bu, L.-L., Ma, S.-R., Liu, B., et al. (2016). LAG-3 Confers Poor Prognosis and its Blockade Reshapes Antitumor Response in Head and Neck Squamous Cell Carcinoma. *Oncoimmunology*. 5 (11), e1239005. doi:10.1080/2162402X.2016.1239005

Eckl, J., Buchner, A., Prinz, P. U., Riesenberg, R., Siegert, S. I., Kammerer, R., et al. (2012). Transcript Signature Predicts Tissue NK Cell Content and Defines Renal Cell Carcinoma Subgroups Independent of TNM Staging. *J. Mol. Med.* 90 (1), 55–66. doi:10.1007/s00109-011-0806-7

Formstecher, E., Ramos, J. W., Fauquet, M., Calderwood, D. A., Hsieh, J.-C., Canton, B., et al. (2001). PEA-15 Mediates Cytoplasmic Sequestration of ERK MAP Kinase. *Developmental Cell.* 1 (2), 239–250. doi:10.1016/s1534-5807(01)00035-1

Friedman, J., Hastie, T., and Tibshirani, R. (2010). Regularization Paths for Generalized Linear Models via Coordinate Descent. *J. Stat. Softw.* 33 (1), 1–22. doi:10.18637/jss.v033.i01

Gerada, C., and Ryan, K. M. (2020). Autophagy, the Innate Immune Response and Cancer. *Mol. Oncol.* 14 (9), 1913–1929. doi:10.1002/1878-0261.12774

Germic, N., Frangez, Z., Yousefi, S., and Simon, H.-U. (2019). Regulation of the Innate Immune System by Autophagy: Neutrophils, Eosinophils, Mast Cells, NK Cells. *Cell Death Differ.* 26 (4), 703–714. doi:10.1038/s41418-019-0295-8

Giatromanolaki, A., Sivridis, E., Mitrakas, A., Kalamida, D., Zois, C. E., Haider, S., et al. (2014). Autophagy and Lysosomal Related Protein Expression Patterns in Human Glioblastoma. *Cancer Biol. Ther.* 15 (11), 1468–1478. doi:10.4161/15384047.2014.955719

Guo, J. Y., Chen, H.-Y., Mathew, R., Fan, J., Strohecker, A. M., Karsli-Uzunbas, G., et al. (2011). Activated Ras Requires Autophagy to Maintain Oxidative Metabolism and Tumorigenesis. *Genes Development* 25 (5), 460–470. doi:10.1101/gad.2016311

Hainfellner, J., Louis, D. N., and Perry, A. (2014). Letter in Response to David N. Louiset al, International Society of Neuropathology-Haarlem Consensus Guidelines for Nervous System Tumor Classification and Grading, Brain Pathology, doi:10.1111/bpa.12187). Letter in response to David N. Louis et Wesseling, P., International Society of Neuropathology-Haarlem Consensus Guidelines for Nervous System Tumor Classification and Grading. *Brain Pathol.* 24 (6), 671–672. doi:10.1111/bpa.12187

Hanahan, D., and Weinberg, R. A. (2011). Hallmarks of Cancer: the Next Generation. *Cell.* 144 (5), 646–674. doi:10.1016/j.cell.2011.02.013

Harrell, F. E., Jr., Lee, K. L., and Mark, D. B. (1996). Multivariable Prognostic Models: Issues in Developing Models, Evaluating Assumptions and Adequacy, and Measuring and Reducing Errors. *Statist. Med.* 15 (4), 361–387. doi:10.1002/(sici)1097-0258(19960229)15:4<361:aid-sim168>3.0.co;2-4

Hartmann, C., Hentschel, B., Wick, W., Capper, D., Felsberg, J., Simon, M., et al. (2010). Patients with IDH1 Wild Type Anaplastic Astrocytomas Exhibit Worse Prognosis Than IDH1-Mutated Glioblastomas, and IDH1 Mutation Status Accounts for the Unfavorable Prognostic Effect of Higher Age: Implications for

Classification of Gliomas. *Acta Neuropathol.* 120 (6), 707–718. doi:10.1007/s00401-010-0781-z

Harvey, A. J., and Crompton, M. R. (2004). The Brk Protein Tyrosine Kinase as a Therapeutic Target in Cancer: Opportunities and Challenges. *Anti-Cancer Drugs.* 15 (2), 107–111. doi:10.1097/00001813-200402000-00002

Harvey, A. J., Pennington, C. J., Porter, S., Burmi, R. S., Edwards, D. R., Court, W., et al. (2009). Brk Protects Breast Cancer Cells From Autophagic Cell Death Induced by Loss of anchorage. *Am. J. Pathol.* 175 (3), 1226–1234. doi:10.2353/ajpath.2009.080811

Huang, R.-Y., Eppolito, C., Lele, S., Shrikant, P., Matsuzaki, J., and Odunsi, K. (2015). LAG3 and PD1 Co-inhibitory Molecules Collaborate to Limit CD8+ T Cell Signaling and Dampen Antitumor Immunity in a Murine Ovarian Cancer Model. *Oncotarget.* 6 (29), 27359–27377. doi:10.18632/oncotarget.4751

Kaloshi, G., Psimaras, D., Mokhtari, K., Dehais, C., Houillier, C., Marie, Y., et al. (2009). Supratentorial Low-Grade Gliomas in Older Patients. *Neurology.* 73 (24), 2093–2098. doi:10.1212/wnl.0b013e3181c6781e

Kondo, Y., Kanzawa, T., Sawaya, R., and Kondo, S. (2005). The Role of Autophagy in Cancer Development and Response to Therapy. *Nat. Rev. Cancer.* 5 (9), 726–734. doi:10.1038/nrc1692

Larkin, J., Hodi, F. S., and Wolchok, J. D. (2015). Combined Nivolumab and Ipilimumab or Monotherapy in Untreated Melanoma. *N. Engl. J. Med.* 373 (13), 1270–1271. doi:10.1056/NEJMc1509660

Lin, J.-z., and Lin, N. (2021). A Risk Signature of Three Autophagy-Related Genes for Predicting Lower Grade Glioma Survival Is Associated with Tumor Immune Microenvironment. *Genomics.* 113 (1 Pt 2), 767–777. doi:10.1016/j.ygeno.2020.10.008

Linden, A., and Yarnold, P. R. (2017). Modeling Time-To-Event (Survival) Data Using Classification Tree Analysis. *J. Eval. Clin. Pract.* 23 (6), 1299–1308. doi:10.1111/jep.12779

Liu, X.-K., Zhang, X.-R., Zhong, Q., Li, M.-Z., Liu, Z.-M., Lin, Z.-R., et al. (2013). Low Expression of PTK6/Brk Predicts Poor Prognosis in Patients With Laryngeal Squamous Cell Carcinoma. *J. Transl Med.* 11, 59. doi:10.1186/1479-5876-11-59

Locatelli, A., Lofgren, K. A., Daniel, A. R., Castro, N. E., and Lange, C. A. (2012). Mechanisms of HGF/Met Signaling to Brk and Sam68 in Breast Cancer Progression. *Horm. Canc.* 3 (1-2), 14–25. doi:10.1007/s12672-011-0097-z

Louis, D. N., Perry, A., Reifenberger, G., von Deimling, A., Figarella-Branger, D., Cavenee, W. K., et al. (2016). The 2016 World Health Organization Classification of Tumors of the Central Nervous System: a Summary. *Acta Neuropathol.* 131 (6), 803–820. doi:10.1007/s00401-016-1545-1

Mächler, M., and Ligges, U. (2003). scatterplot3d - an R Package for Visualizing Multivariate Data. *J. Stat. Softw.* 08 (i11), 1–20. doi:10.18637/jss.v008.i11

Mathew, R., Kongara, S., Beaudoin, B., Karp, C. M., Bray, K., Degenhardt, K., et al. (2007). Autophagy Suppresses Tumor Progression by Limiting Chromosomal Instability. *Genes Development.* 21 (11), 1367–1381. doi:10.1101/gad.1545107

Moussay, E., Kaoma, T., Baginska, J., Muller, A., Van Moer, K., Nicot, N., et al. (2011). The Acquisition of Resistance to TNFα in Breast Cancer Cells Is Associated With Constitutive Activation of Autophagy as Revealed by a Transcriptome Analysis Using a Custom Microarray. *Autophagy.* 7 (7), 760–770. doi:10.4161/auto.7.7.15454

Murciano-Goroff, Y. R., Warner, A. B., and Wolchok, J. D. (2020). The Future of Cancer Immunotherapy: Microenvironment-Targeting Combinations. *Cell Res.* 30 (6), 507–519. doi:10.1038/s41422-020-0337-2

Newman, A. M., Liu, C. L., Green, M. R., Gentles, A. J., Feng, W., Xu, Y., et al. (2015). Robust Enumeration of Cell Subsets From Tissue Expression Profiles. *Nat. Methods.* 12 (5), 453–457. doi:10.1038/nmeth.3337

Ostrom, Q. T., Gittleman, H., Farah, P., Ondracek, A., Chen, Y., Wolinsky, Y., et al. (2013). CBTRUS Statistical Report: Primary Brain and Central Nervous System Tumors Diagnosed in the United States in 2006-2010. *Neuro Oncol.* 15 Suppl 2 (Suppl. 2), ii1–56. doi:10.1093/neuonc/not151

Ostrom, Q. T., Patil, N., Cioffi, G., Waite, K., Kruchko, C., and Barnholtz-Sloan, J. S. (2020). CBTRUS Statistical Report: Primary Brain and Other Central Nervous System Tumors Diagnosed in the United States in 2013-2017. *Neuro Oncol.* 22 (12 Suppl. 2), iv1–iv96. doi:10.1093/neuonc/noaa200

Papadakis, E. S., Reeves, T., Robson, N. H., Maishman, T., Packham, G., and Cutress, R. I. (2017). BAG-1 as a Biomarker in Early Breast Cancer Prognosis: a Systematic Review With Meta-Analyses. *Br. J. Cancer.* 116 (12), 1585–1594. doi:10.1038/bjc.2017.130

Park, S. H., Ito, K., Olcott, W., Katsyv, I., Halstead-Nussloch, G., and Irie, H. Y. (2015). PTK6 Inhibition Promotes Apoptosis of Lapatinib-Resistant Her2+ Breast Cancer Cells by Inducing Bim. *Breast Cancer Res.* 17, 86. doi:10.1186/s13058-015-0594-z

Perus, L. J. M., and Walsh, L. A. (2019). Microenvironmental Heterogeneity in Brain Malignancies. *Front. Immunol.* 10, 2294. doi:10.3389/fimmu.2019.02294

Piliponsky, A. M., and Romani, L. (2018). The Contribution of Mast Cells to Bacterial and Fungal Infection Immunity. *Immunol. Rev.* 282 (1), 188–197. doi:10.1111/imr.12623

Rabinowitz, J. D., and White, E. (2010). Autophagy and Metabolism. *Science.* 330, 1344–1348. doi:10.1126/science.1193497

Reck, M., Rodríguez-Abreu, D., Robinson, A. G., Hui, R., Csőszi, T., Fülöp, A., et al. (2016). Pembrolizumab versus Chemotherapy for PD-L1-Positive Non-Small-Cell Lung Cancer. *N. Engl. J. Med.* 375 (19), 1823–1833. doi:10.1056/NEJMoa1606774

Ritchie, M. E., Phipson, B., Wu, D., Hu, Y., Law, C. W., Shi, W., et al. (2015). Limma Powers Differential Expression Analyses for RNA-Sequencing and Microarray Studies. *Nucleic Acids Res.* 43 (7), e47. doi:10.1093/nar/gkv007

Schmandt, R. E., Bennett, M., Clifford, S., Thornton, A., Jiang, F., Broaddus, R. R., et al. (2006). The BRK Tyrosine Kinase Is Expressed in High-Grade Serous Carcinoma of the Ovary. *Cancer Biol. Ther.* 5 (9), 1136–1141. doi:10.4161/cbt.5.9.2953

Shapiro, M., Herishanu, Y., Katz, B.-Z., Dezorella, N., Sun, C., Kay, S., et al. (2017). Lymphocyte Activation Gene 3: a Novel Therapeutic Target in Chronic Lymphocytic Leukemia. *Haematologica.* 102 (5), 874–882. doi:10.3324/haematol.2016.148965

Shen, C.-H., Chen, H.-Y., Lin, M.-S., Li, F.-Y., Chang, C.-C., Kuo, M.-L., et al. (2008). Breast Tumor Kinase Phosphorylates p190RhoGAP to Regulate Rho and Ras and Promote Breast Carcinoma Growth, Migration, and Invasion. *Cancer Res.* 68 (19), 7779–7787. doi:10.1158/0008-5472.CAN-08-0997

Soffietti, R., Baumert, B. G., Bello, L., Von Deimling, A., Duffau, H., Frénay, M., et al. (2010). Guidelines on Management of Low-Grade Gliomas: Report of an EFNS-EANO* Task Force. *Eur. J. Neurol.* 17 (9), 1124–1133. doi:10.1111/j.1468-1331.2010.03151.x

Taillibert, S., Pedretti, M., and Sanson, M. (2004). Classification Actuelle des Gliomes. *La Presse Médicale.* 33 (18), 1274–1277. doi:10.1016/s0755-4982(04)98906-3

Tassi, E., Grazia, G., Vegetti, C., Bersani, I., Bertolini, G., Molla, A., et al. (2017). Early Effector T Lymphocytes Coexpress Multiple Inhibitory Receptors in Primary Non-Small Cell Lung Cancer. *Cancer Res.* 77 (4), 851–861. doi:10.1158/0008-5472.CAN-16-1387

Terabe, T., Uchida, F., Nagai, H., Omori, S., Ishibashi-Kanno, N., Hasegawa, S., et al. (2018). Expression of Autophagy-Related Markers at the Surgical Margin of Oral Squamous Cell Carcinoma Correlates With Poor Prognosis and Tumor Recurrence. *Hum. Pathol.* 73, 156–163. doi:10.1016/j.humpath.2017.11.019

Trejo-Solís, C., Serrano-Garcia, N., Escamilla-Ramírez, Á., Castillo-Rodríguez, R., Jimenez-Farfan, D., Palencia, G., et al. (2018). Autophagic and Apoptotic Pathways as Targets for Chemotherapy in Glioblastoma. *Int. J. Mol. Sci.* 19 (12), 3773. doi:10.3390/ijms19123773

Wang, C., Qiu, J., Chen, S., Li, Y., Hu, H., Cai, Y., et al. (2021). Prognostic Model and Nomogram Construction Based on Autophagy Signatures in Lower Grade Glioma. *J. Cell Physiol.* 236 (1), 235–248. doi:10.1002/jcp.29837

Wang, H., Xu, T., Huang, Q., Jin, W., and Chen, J. (2020). Immunotherapy for Malignant Glioma: Current Status and Future Directions. *Trends Pharmacol. Sci.* 41 (2), 123–138. doi:10.1016/j.tips.2019.12.003

Wei, L., Yin, F., Chen, C., and Li, L. (2019). Expression of Integrin α6 Is Associated With Multi Drug Resistance and Prognosis in Ovarian Cancer. *Oncol. Lett.* 17 (4), 3974–3980. doi:10.3892/ol.2019.10056

White, E., Karp, C., Strohecker, A. M., Guo, Y., and Mathew, R. (2010). Role of Autophagy in Suppression of Inflammation and Cancer. *Curr. Opin. Cell Biol.* 22 (2), 212–217. doi:10.1016/j.ceb.2009.12.008

Wick, W., Meisner, C., Hentschel, B., Platten, M., Schilling, A., Wiestler, B., et al. (2013). Prognostic or Predictive Value of MGMT Promoter Methylation in Gliomas Depends on IDH1 Mutation. *Neurology.* 81 (17), 1515–1522. doi:10.1212/WNL.0b013e3182a95680

Wijnenga, M. M. J., French, P. J., Dubbink, H. J., Dinjens, W. N. M., Atmodimedjo, P. N., Kros, J. M., et al. (2018). The Impact of Surgery in Molecularly Defined

Low-Grade Glioma: an Integrated Clinical, Radiological, and Molecular Analysis. *Neuro Oncol.* 20 (1), 103–112. doi:10.1093/neuonc/nox176

Woo, S.-R., Turnis, M. E., Goldberg, M. V., Bankoti, J., Selby, M., Nirschl, C. J., et al. (2012). Immune Inhibitory Molecules LAG-3 and PD-1 Synergistically Regulate T-Cell Function to Promote Tumoral Immune Escape. *Cancer Res.* 72 (4), 917–927. doi:10.1158/0008-5472.CAN-11-1620

Xiang, B., Chatti, K., Qiu, H., Lakshmi, B., Krasnitz, A., Hicks, J., et al. (2008). Brk Is Coamplified with ErbB2 to Promote Proliferation in Breast Cancer. *Proc. Natl. Acad. Sci.* 105 (34), 12463–12468. doi:10.1073/pnas.0805009105

Xu, S., Tang, L., Li, X., Fan, F., and Liu, Z. (2020). Immunotherapy for Glioma: Current Management and Future Application. *Cancer Lett.* 476, 1–12. doi:10.1016/j.canlet.2020.02.002

Xu, X.-l., Ye, Y.-L., Wu, Z.-M., He, Q.-M., Tan, L., Xiao, K.-H., et al. (2017). Overexpression of PTK6 Predicts Poor Prognosis in Bladder Cancer Patients. *J. Cancer.* 8 (17), 3464–3473. doi:10.7150/jca.21318

Yamakawa, N., Kaneda, K., Saito, Y., Ichihara, E., and Morishita, K. (2012). The Increased Expression of Integrin α6 (ITGA6) Enhances Drug Resistance in EVI1high Leukemia. *PLoS One.* 7 (1), e30706. doi:10.1371/journal.pone.0030706

Yang, I., Tihan, T., Han, S. J., Wrensch, M. R., Wiencke, J., Sughrue, M. E., et al. (2010). CD8+ T-Cell Infiltrate in Newly Diagnosed Glioblastoma Is Associated With Long-Term Survival. *J. Clin. Neurosci.* 17 (11), 1381–1385. doi:10.1016/j.jocn.2010.03.031

Yu, G., Wang, L.-G., Han, Y., and He, Q.-Y. (2012). ClusterProfiler: an R Package for Comparing Biological Themes Among Gene Clusters. *OMICS: A J. Integr. Biol.* 16 (5), 284–287. doi:10.1089/omi.2011.0118

Zeng, W.-J., Yang, Y.-L., Liu, Z.-Z., Wen, Z.-P., Chen, Y.-H., Hu, X.-L., et al. (2018). Integrative Analysis of DNA Methylation and Gene Expression Identify a Three-Gene Signature for Predicting Prognosis in Lower-Grade Gliomas. *Cell Physiol Biochem.* 47 (1), 428–439. doi:10.1159/000489954

Zhang, D.-H., Yang, Z.-L., Zhou, E.-X., Miao, X.-Y., Zou, Q., Li, J.-H., et al. (2016). Overexpression of Thy1 and ITGA6 Is Associated with Invasion, Metastasis and Poor Prognosis in Human Gallbladder Carcinoma. *Oncol. Lett.* 12 (6), 5136–5144. doi:10.3892/ol.2016.5341

Zhao, C., Chen, Y., Zhang, W., Zhang, J., Xu, Y., Li, W., et al. (2013). Expression of Protein Tyrosine Kinase 6 (PTK6) in Nonsmall Cell Lung Cancer and Their Clinical and Prognostic Significance. *Onco Targets Ther.* 6, 183–188. doi:10.2147/OTT.S41283

Zhu, J., Zhang, T., Li, J., Lin, J., Liang, W., Huang, W., et al. (2019). Association Between Tumor Mutation Burden (TMB) and Outcomes of Cancer Patients Treated With PD-1/PD-L1 Inhibitions: A Meta-Analysis. *Front. Pharmacol.* 10, 673. doi:10.3389/fphar.2019.00673

Ziu, M., Kalkanis, S. N., Gilbert, M., Ryken, T. C., and Olson, J. J. (2015). The Role of Initial Chemotherapy for the Treatment of Adults With Diffuse Low Grade Glioma. *J. Neurooncol.* 125 (3), 585–607. doi:10.1007/s11060-015-1931-x

**Conflict of Interest:** The authors declare that the research was conducted in the absence of any commercial or financial relationships that could be construed as a potential conflict of interest.

**Publisher's Note:** All claims expressed in this article are solely those of the authors and do not necessarily represent those of their affiliated organizations, or those of the publisher, the editors and the reviewers. Any product that may be evaluated in this article, or claim that may be made by its manufacturer, is not guaranteed or endorsed by the publisher.

frontiers | Frontiers in Genetics

ORIGINAL RESEARCH
published: 31 May 2022
doi: 10.3389/fgene.2022.851505

# ANXA1: An Important Independent Prognostic Factor and Molecular Target in Glioma

*Dongdong Zhang[1†], Wenyan Wang[1†], Huandi Zhou[1,2], Linlin Su[1], Xuetao Han[1], Xinyuan Zhang[1,3], Wei Han[1,4], Yu Wang[1] and Xiaoying Xue[1]**

[1]Department of Radiotherapy, The Second Hospital of Hebei Medical University, Shijiazhuang, China, [2]Department of Central Laboratory, The Second Hospital of Hebei Medical University, Shijiazhuang, China, [3]Department of Oncology, The First Hospital of Qinhuangdao, Qinhuangdao, China, [4]Department of Oncology, Hebei General Hospital, Shijiazhuang, China

**Objective:** The expression, prognosis, and related mechanisms of ANXA1 are investigated in glioma, with the objective to find potential therapeutic molecular targets for glioma.

**Methods:** We analyzed the gene expression of ANXA1 using glioma-related databases, including the Chinese Glioma Genome Atlas (CGGA) database, The Cancer Genome Atlas (TCGA) database, and the Gene Expression Omnibus (GEO) database. Moreover, we collected the sample tissues and corresponding paracancerous tissues of 23 glioma patients and then conducted a Western blot experiment to verify the expression and correlate survival of ANXA1. Moreover, we generated survival ROC curves, performing univariate and multivariate Cox analyses and the construction of the nomogram. Differential expression analysis was conducted by high and low grouping based on the median of the ANXA1 gene expression values. We conducted Kyoto Encyclopedia of Genes and Genomes (KEGG) enrichment analysis and Gene Set Enrichment Analysis (GSEA) to explore possible mechanisms, and gene co-expression analysis was also performed.

**Results:** The results showed that the ANXA1 expression level was higher in gliomas than in normal tissues, and a high expression level of ANXA1 in gliomas was associated with poorer prognosis. The independent prognosis analysis showed that the ANXA1 gene was an independent prognostic factor of glioma. In the analysis of KEGG and Gene Set Enrichment Analysis (GSEA), it is shown that ANXA1 may play an important role in glioma patients by affecting extracellular matrix (ECM)–receptor interaction and the focal adhesion signal pathway. The core genes, including COL1A1, COL1A2, FN1, ITGA1, and ITGB1, were screened for gene correlation and prognosis analysis. The expression level of the five genes was verified by qPCR in glioma. We concluded that these five core genes and ANXA1 could play a synergistic role in gliomas.

**Conclusion:** The results indicated that a high expression level of ANXA1 leads to worse prognosis and ANXA1 is an independent prognostic factor and a potentially important target for the treatment of gliomas.

**Keywords: ANXA1, glioma, prognosis, ECM, focal adhesion, molecular target**

OPEN ACCESS

***Edited by:***
*Pawel Buczkowicz, PhenoTips, Canada*

***Reviewed by:***
*David D. Eisenstat, Royal Children's Hospital, Australia*
*Sven R. Kantelhardt, Johannes Gutenberg University Mainz, Germany*

****Correspondence:***
*Xiaoying Xue*
*xxy0636@163.com*

*†These authors have contributed equally to this work*

***Specialty section:***
*This article was submitted to Cancer Genetics and Oncogenomics, a section of the journal Frontiers in Genetics*

***Received:*** *10 January 2022*
***Accepted:*** *20 April 2022*
***Published:*** *31 May 2022*

***Citation:***
*Zhang D, Wang W, Zhou H, Su L, Han X, Zhang X, Han W, Wang Y and Xue X (2022) ANXA1: An Important Independent Prognostic Factor and Molecular Target in Glioma. Front. Genet. 13:851505. doi: 10.3389/fgene.2022.851505*

## INTRODUCTION

Glioma is an intracranial tumor originating from glial cells, and it is the most common intracranial primary tumor, accounting for approximately 80% of intracranial malignant tumors (Ostrom et al., 2014). Glioma is often accompanied by local invasion, especially glioblastoma (GBM), which invades and destroys the surrounding normal brain tissue, and the degree of malignancy is high with a poor prognosis (Weller et al., 2015). High-grade gliomas (HGGs) are the most common primary brain malignancies, predicting a 5-year survival rate of less than 5% (Ostrom et al., 2014). These tumors may arise *de novo* as isocitrate dehydrogenase (IDH)–wildtype GBMs or develop from progressive lower-grade gliomas (LGGs; defined as World Health Organization (WHO) grades 2–3) (Aldape et al., 2015). According to the WHO, gliomas were divided into grades I–IV by pathological characteristics; grade II–IV gliomas are the largest entity in the group of intracranial brain tumors, with a survival rate of more than 10 years (grade II) to less than 1 year (grade IV) (Cordier et al., 2016). However, the therapeutic effect is limited with conventional treatment of gliomas, including complete surgical resection and postoperative radiotherapy and chemotherapy (Stupp et al., 2005; Bush et al., 2017). In recent years, molecular-targeted therapy and immunotherapy have achieved good results in many tumors, such as colorectal cancer, breast cancer, and lung cancer (Naylor et al., 2016; Esteva et al., 2019; Ganesh et al., 2019; Piawah and Venook, 2019). However, due to the existence of the blood–brain barrier in the brain and the unique tumor microenvironment in glioma, the therapeutic effect is poor (Quail and Joyce, 2017). However, at present, molecular-targeted therapy and immunotherapy have achieved some effective results. For example, vemurafenib has demonstrated long-lasting antitumor activity in some patients with *BRAFV600E* mutant glioma (Kaley et al., 2018). Neoadjuvant administration of PD-1 blockers enhances local and systemic antitumor immune responses (Cloughesy et al., 2019). With the advent of the molecular era, the classification of gliomas has changed. Combined with pathological and molecular characteristics, the classification of gliomas by the WHO in 2016 included molecular markers, such as IDH mutation and 1p19q (Louis et al., 2016). In 2021, the latest central nervous system tumor guidelines of the fifth edition of the WHO confirmed the importance of molecular typing. In the grading of gliomas, the importance of grading according to molecular characteristics is more prominent. For example, loss of CDKN2A/B homozygosity is closely related to poor prognosis, especially in WHO grade III glioma with loss of CDKN2A/B homozygosity, where the prognosis is similar to WHO grade IV glioma. Therefore, CDKN2A/B has been included in the molecular diagnosis of gliomas (Louis et al., 2021). However, molecular typing still needs to be further explored to identify more molecular targets for better diagnosis and treatment of clinical patients. Therefore, we explore new targets of glioma to provide new therapeutic targets.

Annexin is a well-known calcium-regulated and phospholipid-dependent membrane-binding protein (Lim and Pervaiz, 2007). ANXA1 is a member of the annexin family, which is involved in many important biological processes, such as inflammation, phagocytosis, proliferation, differentiation, and apoptosis (Monastyrskaya et al., 2009; Xia et al., 2020). Many studies have shown that ANXA1 is associated with the occurrence, invasion, and metastasis of cancer (Mussunoor and Murray, 2008; Guo et al., 2013). ANXA1 has been extensively studied in gastric cancer and breast cancer (Maschler et al., 2010; Cheng et al., 2012). Some studies in gliomas have shown that ANXA1 is a risk prognostic factor (Xu et al., 2017; Luo et al., 2021; Wei et al., 2021) Therefore, we investigated the expression, prognosis, and related mechanisms of ANXA1 using a public database to provide new markers and potential therapeutic targets for glioma patients.

## MATERIALS AND METHODS

### Data Acquisition and Download

The GSE4290, GSE7696, GSE29796, and GSE50161 expression sequences and clinical data were downloaded from the Gene Expression Omnibus (GEO, https://www.ncbi.nlm.nih.gov/geo/) database for gene expression analysis. The GSE4290 dataset included 23 normal samples, which were obtained from epilepsy patients and used as nontumor samples, and 153 tumor samples, which included 26 astrocytomas, 50 oligodendrogliomas, and 77 glioblastomas (Sun et al., 2006). The GSE7696 dataset included 80 glioblastoma specimens and four nontumor brain samples (Murat et al., 2008). The GSE29796 dataset included 20 normal samples and 52 tumor samples, and these samples were based on matching patients with disease and/or pathology, including 20 cases of epileptic pathology and 52 cases of glioma (Auvergne et al., 2013). The GSE50161 dataset collected samples from surgical brain tumors and normal brains, including 13 normal samples and 117 tumor samples (Griesinger et al., 2013). In addition, the expression sequences and clinical data of 1,018 samples were downloaded from the Chinese Glioma Genome Atlas (CGGA, http://www.cgga.org.cn/) database, and the expression sequences and clinical data of 592 samples were downloaded from The Cancer Genome Atlas (TCGA, https://portal.gdc.cancer.gov/) database (Jiang et al., 2016), which included 449 LGG samples and 143 glioblastoma (GBM) samples. Before further analysis, we performed a log2 transformation on RNA-sequencing data. All sample databases were screened to remove samples that had omitted clinical information.

### Acquisition of 23 Patient Tissues and Collection of Clinical Information

We collected sample tissues and corresponding paracancerous tissues (distance from tumor edge >2 cm) from 23 glioma patients, including eight GBM samples and their corresponding paracancerous tissues and 15 LGG samples and their corresponding paracancerous tissues. Under the guidance of neurosurgery experts, gliomas and corresponding paracancerous tissues were obtained from surgery. All samples were obtained with the informed consent of the patients and their families, and the present study was approved by the Ethics Committee of the

Second Hospital of Hebei Medical University. We followed up 23 glioma patients from January 2015 to December 2021, and we collected the following information: patient age, gender, grade, radiotherapy chemotherapy, and IDH mutation.

## Expression Analysis of the ANXA1 Gene

The GSE4290, GSE7696, GSE29796, and GSE50161 datasets were downloaded from the GEO database. The expression values of ANXA1 in glioma and normal brain tissues were imported into GraphPad Prism 8 software for analysis followed by verification with Gene Expression Profiling Interactive Analysis (GEPIA, http://gepia.cancer-pku.cn/) and Human Protein Atlas online analysis (https://www.proteinatlas.org/). Moreover, Western blot analysis was also performed to verify the expression level of ANXA1.

## Analysis of Clinical Prognosis and Clinicopathological Features of ANXA1

The clinical prognosis of ANXA1 was analyzed based on the transcriptome data and clinical information of 1,018 cases from the CGGA database. The expression level of ANXA1 was divided into high and low groups according to the median value. The survival curves of different expression levels of ANXA1 were drawn using the "survival" and "survivminer" software packages in R version 4.0.5. We used the "survival ROC" software package and the Kaplan–Meier method to calculate the receiver operator characteristic (ROC) curve of ANXA1 at 1, 3, and 5 years. The prognostic value of ANXA1 was further evaluated by univariate and multivariate Cox regression analyses, with a significance level of $p < 0.001$. To verify the accuracy of the ANXA1 prognosis, TCGA data were used to generate the survival and ROC curves and to perform univariate and multivariate analyses. Finally, based on the CGGA data, we used the "survival" and "RMS" software packages in R version 4.0.5 to construct a nomogram for 1-year, 2-year, and 3-year survival using the clinicopathological characteristics of ANXA1 expression. Subsequently, calibration curves were drawn to assess the accuracy of matching between predicted survival and actual survival. In addition, the correlation between the expression of ANXA1 and clinicopathological features was analyzed using the "beeswarm" package in R version 3.6.3.

## Analysis of Differentially Expressed Genes and Signal Pathway Mechanism

The mRNA sequencing data of the glioma database were normalized using the CGGA. The median expression value of ANXA1 was divided into high and low groups for differential expression analysis, and the Differentially Expressed Genes (DEGs), including significantly upregulated and downregulated genes, were screened by adjusted $p < 0.05$ and absolute log2 fold change (FC) > 1. The "limma" and "ggplot2" software packages (Ritchie et al., 2015) were used to generate a volcano plot to visualize the DEGs, and the 30 genes with the most significant upregulation and downregulation were selected to generate a heat map of the DEGs using the "pheatmap" software package in R version 4.0.5. Finally, mechanism analysis of the DEGs was performed using Metascape (https://metascape.org/). In addition, GSEA (https://www.gsea-msigdb.org/) was also utilized to indirectly explain the potential mechanism of ANXA1 function. When NES > 1, $p < 0.05$, and FDR < 0.05, the gene set was considered the enrichment group.

## Construction of the Protein–Protein Interaction Network of Differentially Expressed Genes

The median expression value of ANXA1 was divided into high and low groups using the cutoff of adjusted $p < 0.05$ and absolute log2 fold change (FC) > 1 to screen the DEGs, and a high threshold (0.7) binding degree was set for node screening through the STRING (https://string-db.org/) analysis to filter out the unconnected proteins. The remaining 1,034 proteins were imported into Cytoscape visualization software (version: 3.7.2). After installing the cytoHubba plug-in, the top 50 hub genes were screened by degree topology analysis.

## Coexpression Analysis of ANXA1 and Core Genes

We obtained the core genes of ECM–receptor interaction and focal adhesion pathways by GSEA. Through a protein–protein interaction (PPI) network analysis, the DEGs were imported into Cytoscape visualization software to screen the top 50 hub genes by using degree topology analysis. Five core genes were obtained through the intersection of the Venn diagram for gene correlation analysis and coexpression analysis. The relative expression levels of the five genes in glioma and their corresponding paracancerous tissues were further analyzed by qPCR.

## Chemical Reagents and Antibodies

The RIPA lysate (product number: p00138b) was purchased from Beyotime (Shanghai, China). Protein phosphatase inhibitors and BCA protein concentration determination kits were purchased from Solarbio (Beijing, China). ANXA1 antibody (catalog number: 21990-1-AP) and β-tubulin antibody (catalog number: 10094-1-ap) were obtained from Proteintech (Chicago, IL, United States). The anti-rabbit IgG HRP-conjugated antibody was purchased from Cell Signaling Technology. An ECL chromogenic solution (product number: BL520A) was obtained from Biosharp.

## Tissue Protein Extraction and Western Blot

Tissue samples were removed from the −80°C freezer and thawed on ice. An RIPA lysis buffer, containing protein phosphatase inhibitor, was added to each sample, and the samples were homogenized using a homogenizer. The samples were centrifuged at 4°C and 12,000 rpm for 10 min, and the supernatants were collected. The protein concentrations were determined using a commercially available BCA protein concentration kit. After denaturation, 10–20 μg of the protein

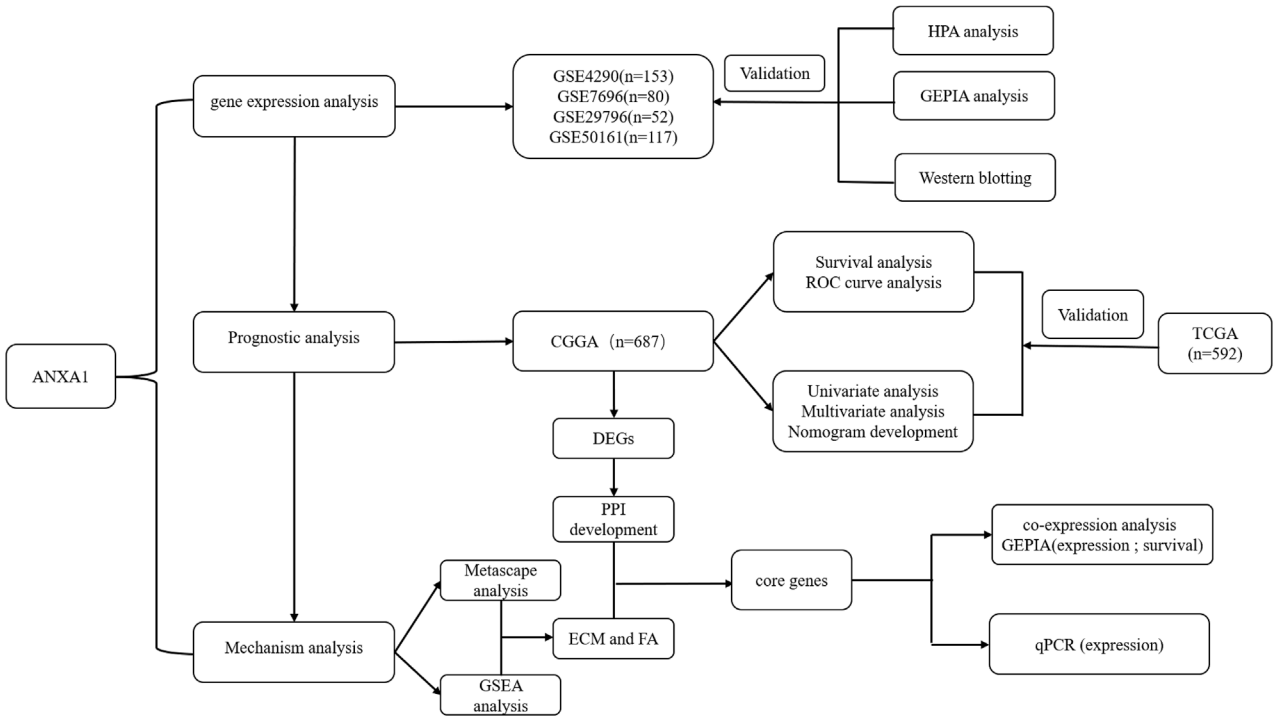


**FIGURE 1 |** Working diagram of the study. Abbreviations: GEO: Gene Expression Omnibus; CGGA: Chinese Glioma Genome Atlas; DEGs: differentially expressed genes; GSEA: Gene Set Enrichment Analysis; PPI: protein–protein interaction; ECM: extracellular matrix; FA: focal adhesion; HPA: Human Protein Atlas; GEPIA: Gene Expression Profiling Interactive Analysis; TCGA: The Cancer Genome Atlas.

was separated with 10% SDS-PAGE and then transferred onto PVDF membranes (Merck Millipore Ltd.). The membranes were then blocked with 5% nonfat milk powder for 1 h and incubated with primary antibodies (ANXA1 antibody, 1:2000; and β-tubulin antibody, 1:1000) at 4°C overnight. The membranes were then washed thrice with TBST (10 min each wash) followed by incubation with the appropriate secondary antibody (anti-rabbit IgG, 1:2000). The membranes were then washed thrice with TBST (10 min each wash) followed by development and imaging using a chemiluminescence photodocumentation system.

## RNA Isolation and qPCR

Total RNA was extracted from the remaining eight glioma samples and corresponding paracancerous tissues with TRIzol reagent (Invitrogen). The quality of the total RNA of these samples was evaluated by Nanodrop 2000c and agarose gel electrophoresis. Complementary DNA (cDNA) was synthesized using a revert aid first-strand cDNA synthesis kit (Thermo Fisher Scientific, Waltham, MA, United States). Quantitative PCR was performed with SYBR Green (Hieff qPCR SYBR Green Master Mix, YEASEN, Shanghai, China) on a qPCR system (Model No. CFX96$^{TM}$ Option Module, Bio-Rad, United States). The specific primers of each gene were used to analyze the expression of these extracted tissue samples. All samples were standardized according to the expression of the gene-encoding human glyceraldehyde 3-phosphate dehydrogenase (GAPDH) as a reference. Relative expression levels were calculated as $2^{-[(Ct\ of\ target\ gene)-(Ct\ of\ GAPDH)]}$. The sequences of the primers are listed in **Supplementary Table S1**.

## Statistical Analysis

Based on public databases, the following software programs and online tools were used for analysis: GraphPad Prism 8 software was used for gene expression analysis; R software (version: 4.0.1, http://www.r-project.org/) was used for survival prognosis analysis and gene correlation analysis; R software (version: 3.6.3, http://www.r-project.org/) was used for clinicopathological characteristics analysis; Metascape online website and GSEA software were used for mechanism analysis; and the GEPIA online website was used for core gene prognosis analysis. When the results met the requirements of $p < 0.05$ and FDR < 0.05, they were considered statistically significant. In addition, we used Western blot analysis to verify the expression levels of 23 gliomas and their corresponding paracancerous tissues. The protein gray values were measured by ImageJ software, and the results were imported into GraphPad Prism 8 software. qPCR was used to verify the expression of the five core genes in the remaining eight pairs of samples. $p < 0.05$ was considered statistically significant.

**TABLE 1 |** Clinical information materials of gliomas. CGGA: 686 glioma samples; TCGA: 592 glioma samples; clinical features: grade, gender, age, IDH mutation, 1p19q codeletion, MGMT, radiotherapy, and chemistry.

| | CGGA (*n* = 686) | | TCGA (*n* = 592) | |
|---|---|---|---|---|
| | Case | Proportion (%) | Case | Proportion (%) |
| WHO grade | | | | |
| II | 177 | 25.8 | 211 | 35.6 |
| III | 226 | 32.9 | 238 | 40.2 |
| IV | 283 | 41.3 | 143 | 24.2 |
| Gender | | | | |
| Male | 399 | 58.2 | 344 | 58.1 |
| Female | 287 | 41.8 | 248 | 41.9 |
| Age | | | | |
| ≥42 | 379 | 55.2 | 349 | 59.0 |
| <42 | 307 | 44.8 | 243 | 41.0 |
| IDH mutation | | | | |
| Yes | 371 | 54.1 | 372 | 62.8 |
| No | 315 | 45.9 | 220 | 37.2 |
| 1p19q codeletion | | | | |
| Yes | 141 | 20.6 | 149 | 25.2 |
| No | 545 | 79.4 | 443 | 74.8 |
| MGMT methylation | | | | |
| Yes | 386 | 56.3 | — | — |
| No | 300 | 43.7 | — | — |
| Radiotherapy | | | | |
| Yes | 544 | 79.3 | — | — |
| No | 142 | 20.7 | — | — |
| Chemotherapy | | | | |
| Yes | 501 | 73.0 | — | — |
| No | 185 | 27.0 | — | — |

# RESULTS

## Article Workflow and Sample Information

The workflow of the present study is shown in **Figure 1**. We downloaded the glioma sample information of the GSE4290, GSE7696, GSE29796, and GSE50161 datasets from the GEO database with 153, 80, 52, and 117 glioma samples and 23, 4, 20, and 52 normal samples, respectively. The clinicopathological information, including age, grade, category, 1p19q deletion status, and IDH mutation status, was obtained from the CGGA and TCGA databases. However, the TCGA database lacked clinical chemoradiotherapy and MGMT methylation data, which were only obtained from the CGGA database. The clinical information and categorical data of glioma patients from the CCGA and TGGA databases are shown in **Table 1**. The clinical information for the 23 glioma patients who provided samples for Western blot analysis is shown in **Supplementary Table S2**.

## ANXA1 is Overexpressed in Glioma

Based on the expression data for gliomas and normal tissues in the GSE4290, GSE7696, GSE29796, and GSE50161 datasets, the ANXA1 gene was significantly highly expressed in gliomas (**Figures 2A–D**), and the results were verified by GEPIA and Human Protein Atlas online analyses (**Figures 2E,F**). In addition, we evaluated 23 glioma sample tissues and their corresponding paracancerous tissues by Western blot analysis (**Figure 2G**), and the results showed that the ANXA1 expression levels were significantly higher in the 23 glioma sample tissues than their corresponding paracancerous tissues ($p < 0.05$, **Figure 2H**). A paired-sample *t*-test was performed separately in 15 LGG samples and their corresponding paracancerous tissues and in eight GBM samples and their corresponding paracancerous tissues. In addition, an independent-sample *t*-test was also performed in eight GBM samples and 15 LGG samples. The results demonstrated that ANXA1 was overexpressed in gliomas with higher expression in GBM samples than in LGG samples ($p < 0.05$, **Figure 2I**), supporting that ANXA1 is correlated with a higher grade of gliomas.

## High Expression of ANXA1 has a Poor Prognosis

The Kaplan–Meier survival method was performed to analyze the survival prognosis using the sample information from the CGGA database, which showed that high expression of ANXA1 had worse prognosis ($p < 0.001$, **Figure 3A**), and these results were verified by analysis of the TCGA database ($p < 0.001$, **Figure 3B**). Using the CGGA and TCGA databases, the ROC curve was generated. The ROC curve of ANXA1 for 1-, 3-, and 5-year outcomes had AUC values of 0.724, 0.800, and 0.821, respectively, in the CGGA database (**Figure 3C**). The ROC curve of the ANXA1 gene was verified in the TCGA database, with AUC values of 0.839, 0.858, and 0.776 for 1-, 3-, and 5-year outcomes, respectively (**Figure 3D**). Univariate Cox regression analyses showed that the expression of ANXA1 [HR = 1.370; 95% CI (1.313–1.431); $p < 0.001$], type, grade, age, IDH mutation, and 1p19q expression status were significantly correlated with survival prognosis (**Figure 3E**). Moreover, multivariate Cox regression analyses showed that the expression of ANXA1 [HR = 1.155; 95% CI (1.092–1.221); $p < 0.001$], type, grade, age, chemotherapy, and 1p19q expression status were also correlated with survival prognosis (**Figure 3F**). The univariate and multivariate regression analyses were verified in the TCGA database (**Figures 3G,H**). Therefore, these findings indicated that ANXA1 is an independent prognostic indicator of glioma. In addition, based on the clinical characteristics of the CGGA, including grade, IDH mutation, methylation level, 1p19q expression, and ANXA1 expression level, we constructed a nomogram for quantitative prediction (**Figure 3I**). Finally, we found that the actual and predicted survival times were better matched by the calibration curve in patients with 3-year survival (**Figures 3J–L**).

## Correlation Between ANXA1 Gene Expression and Clinicopathological Features

The correlation analysis of ANXA1 expression and clinicopathological features demonstrated that ANXA1 was overexpressed in patients older than 42 years ($p < 0.001$, **Figure 4A**). In addition, the expression of ANXA1 also

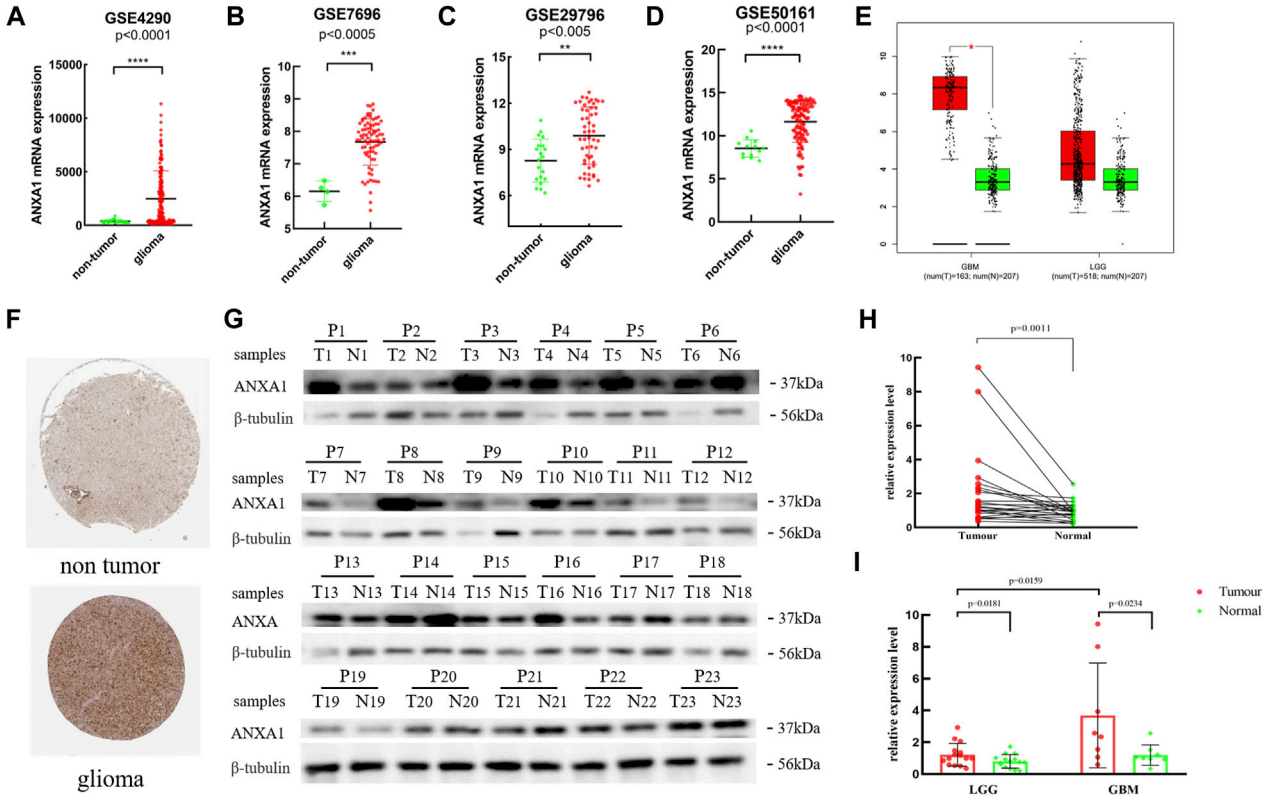


**FIGURE 2 |** Expression level of the ANXA1 gene in glioma and normal tissues. **(A)** GSE4290 data set. **(B)** GSE7696 data set. **(C)** GSE29796 data set. **(D)** GSE50161 data set. **(E)** Based on the GEPIA online website, the expression level of ANXA1 in glioma and normal samples. **(F)** Based on The Human Protein Atlas online website, the expression level of ANXA1 in the brain tissues of glioma (Intensity: strong; Quantity: 75%–25%) and normal controls (Intensity: weak; Quantity: 75%–25%). **(G)** Western blotting images of 23 glioma tissues and their corresponding paracancerous samples (P1–P8: GBM; P9–P23: LGGs). **(H)** Paired-sample *t*-test of 23 glioma tissues and their corresponding paracancerous tissues. **(I)** Paired-sample *t*-test of GBM and LGG tumor tissues and their corresponding paracancerous tissues, and independent-sample *t*-test of eight GBM and 15 LGG samples.

increased with the increase of tumor grade ($p < 0.001$, **Figure 4B**); among the type of pathological features, ANXA1 was more highly expressed in recurrent patients ($p < 0.001$, **Figure 4C**), and ANXA1 expression was low in patients with IDH mutation and combined 1p19q expression ($p < 0.001$, **Figures 4D,E**).

## Differentially Expressed Genes and Enrichment Analysis of the ANXA1 Gene

In the differential expression analysis of ANXA1, 1,256 upregulated genes and 227 downregulated genes were obtained and visualized by a volcano map (**Figure 5A**), and 30 genes with significant upregulation and downregulation were utilized to generate a heat map (**Figure 5B**). GSEA indicated that the ANXA1 gene was enriched in the ECM receiver interaction (NSE = 1.96, NOM *p*-val = 0.002, and FDR *q*-val = 0.023) and focal adhesion (NES = 1.99, NOM *p*-val = 0.004, and FDR *q*-val = 0.039) pathways (**Figures 5C, D**), and Metascape online analysis showed that the DEGs were enriched in the process of ECM and focal adhesion (**Figure 5E**).

## Construction of Protein–Protein Interaction of Differentially Expressed Genes, Filtration of Core Genes, Core Gene Correlation Analysis, and Prognostic Analysis

Based on the STRING online analysis, 1,034 proteins were screened and input into Cytoscape visualization software. The top 50 hub genes were obtained by a degree topology analysis using the cytoHubba plugin (**Figure 6A**). Univariate regression analysis was performed on the top 50 hub genes, which showed that these genes were risk factors for glioma ($p < 0.001$, **Figure 6B**). A Venn diagram was used to visualize the intersection of the top 50 hub genes with core genes enriched in the pathway, and five core genes were obtained, namely, COL1A1, COL1A2, FN1, ITGA1, and ITGB1 (**Figure 6C**). In addition, gene correlation analysis showed that ANXA1 was significantly correlated with COL1A1, COL1A2, FN1, ITGA1, and ITGB1 as indicated by the gene correlation circle diagram and scatter diagram (**Figures 6D–I**). In the remaining eight glioma samples (included four GBM and four LGG) and their corresponding paracancerous tissues, the relative expression levels of the five core genes were verified by qPCR (**Figures**

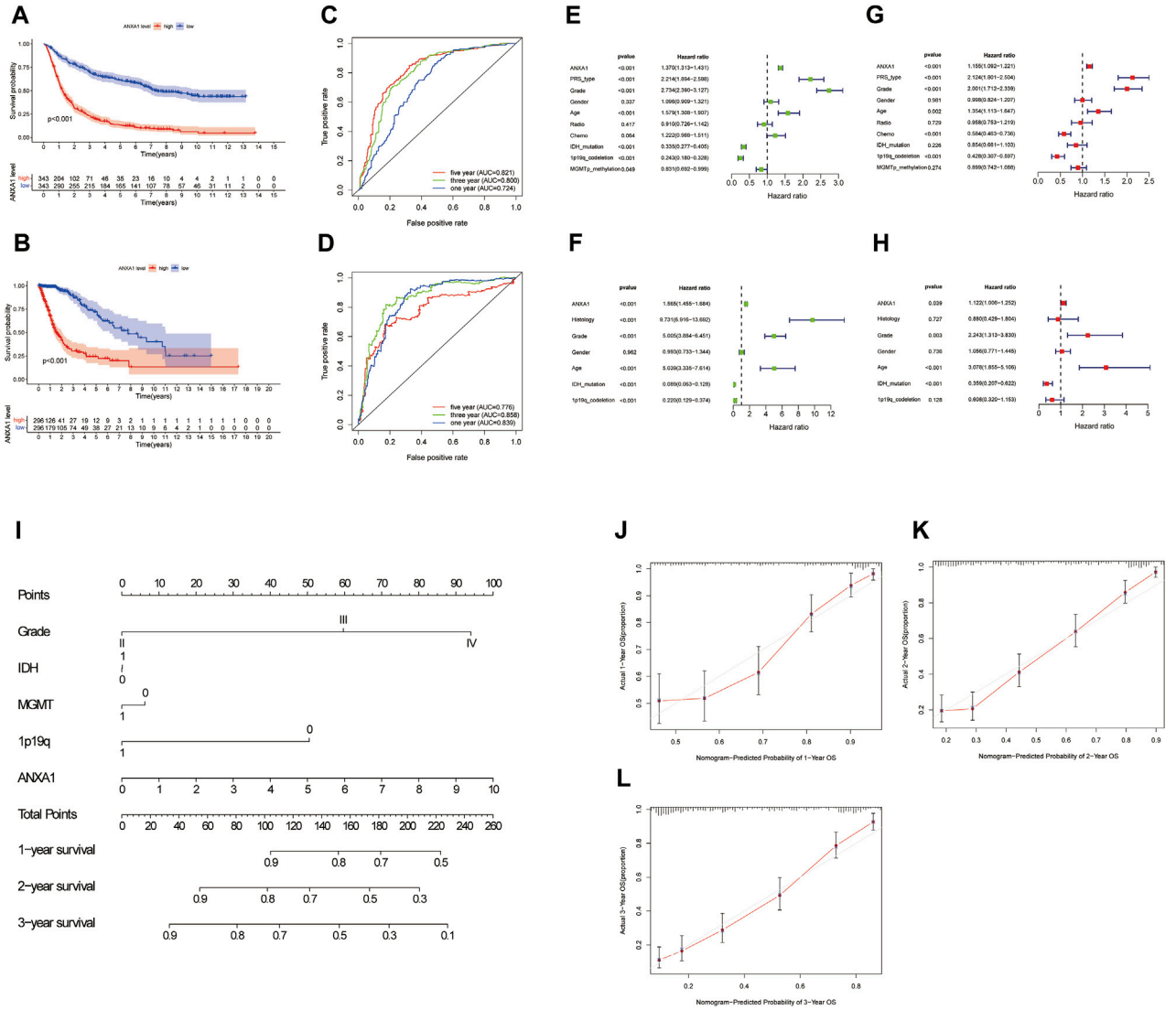


**FIGURE 3 |** Survival analysis and independent prognostic analysis of the ANXA1 gene in glioma. **(A,B)** Survival analysis of ANXA1. **(C,D)** Survival ROC curve of ANXA1 at 1, 3, and 5 years. **(E,F)** Univariate analysis of ANXA1. **(G,H)** Multivariate analysis of ANXA1. **(I)** Based on the clinical information of the CGGA database, a prognostic nomogram model was constructed. **(J–L)** Calibration curve was constructed according to the CGGA database information. The scores of ANXA1, grade, IDH, MGMT, and 1p19q factors were used to predict the calibration curve of the 1-year, 2-year, and 3-year prognostic nomogram.

**6J–N**). The relative expression level is described in the Method section. The statistics were carried out by the paired-sample *t*-test, and the *p* values were 0.0078, 0.0151, 0.0234, 0.0974, and 0.0234. The expression of these genes was higher in gliomas by GEPIA (**Figures 6O–S**). The higher expression of these genes in gliomas was often accompanied by worse survival prognosis (**Figures 6T–X**).

## DISCUSSION

Glioma is the most common brain malignant tumor, and its incidence rate has increased in recent years (Wen and Kesari, 2008). Radiotherapy and chemotherapy have become the standard of care in the treatment of gliomas (Nabors et al., 2017). Due to different molecular types and grades of gliomas, GBM, in particular, is often accompanied by high invasiveness and high recurrence. Even after routine surgery and concurrent chemoradiotherapy, the prognosis of glioma patients is still poor (Wang and Jiang, 2013). In recent years, targeted therapy and immunotherapy have improved the prognosis in other common tumors. Although some glioma patients have responded to targeted therapies or immunotherapies, there is still a lack of obvious effect in most patients with glioma (Chen et al., 2017; Xu et al., 2020). Therefore, new predictive targets and potential therapeutic targets for glioma need to be further explored and studied.

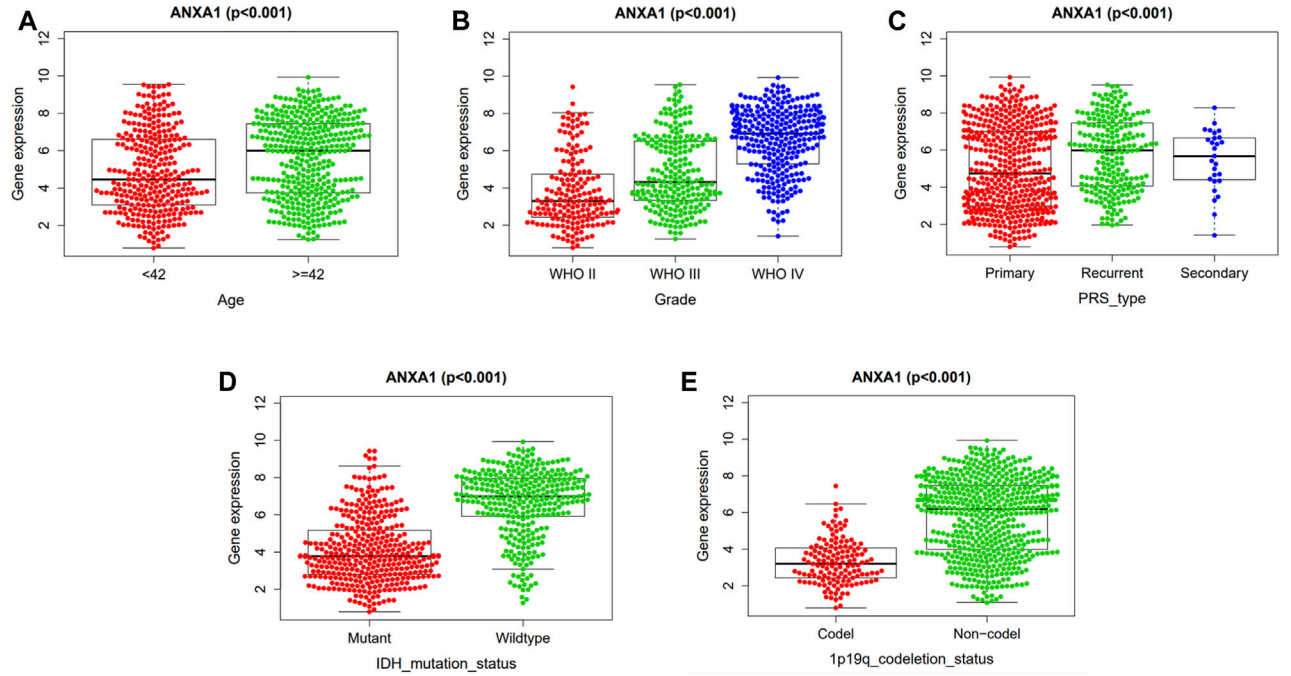


**FIGURE 4 |** Independent analysis of the ANXA1 gene and clinicopathological features. Based on 686 tumor samples in the CGGA database, the ANXA1 and clinical characteristics were analyzed independently: **(A)** Expression of ANXA1 in age (≥42 years, <42 years). **(B)** Expression of ANXA1 in glioma grade (WHO II, WHO III, and WHO IV). **(C)** Expression of ANXA1 in glioma types (primary, recurrent, and secondary). **(D)** Expression of ANXA1 in IDH mutation state (mutant and wild-type). **(E)** Expression of ANXA1 in 1p19q codeletion status (Codel and non-codel).

In our study, we analyzed the expression of ANXA1 in glioma through the GEO database, which demonstrated that ANXA1 was highly expressed in glioma patients. The GEPIA and Human Protein Atlas online analyses verified these results. Moreover, the overexpression of ANXA1 in glioma was verified by Western blotting analysis. Survival prognosis, ROC curve, and univariate and multivariate Cox regression analyses were performed using the CGGA and TCGA databases, which further showed that ANXA1 played an important role in the development of glioma and supported that ANXA1 was an independent prognostic index of glioma. In addition, the expression of ANXA1 was investigated according to the clinical case characteristics of glioma, and a clinical correlation nomogram was constructed using the CGGA database, which supported that ANXA1 was an important predictor of glioma. Finally, calibration curves were used to verify the matching of actual and predicted survival, and the matching degree of the 3-year survival is higher. Therefore, these findings suggested that ANXA1 warrants further study in glioma.

Previous studies have linked ANXA1 with thrombosis and inflammation (Parente and Solito, 2004; Senchenkova et al., 2019). In addition, it has been reported that ANXA1 is closely related to tumor development and invasion (Boudhraa et al., 2016; Foo et al., 2019). For example, the prognosis of lung cancer patients with a high ANXA1 expression is poor, and the growth of lung cancer cells is reduced by downregulating ANXA1 using small interference RNA (siRNA) (Chuang et al., 2021). Overexpression of ANXA1 promotes metastasis in breast cancer patients, resulting in poor prognosis (de Graauw et al., 2010). Therefore, ANXA1 plays an important role in tumors.

The tumor microenvironment is the internal and external environment for tumor survival. The components of the tumor microenvironment include not only tumor cells but also peripheral blood vessels, ECM, and some molecular signal factors (Hui and Chen, 2015). In the tumor microenvironment, tumor cells change and maintain their own development needs through autocrine and paracrine factors. There is a two-way driving effect between the tumor microenvironment and tumor cell progression, invasion, and metastasis (Meurette and Mehlen, 2018), in which the molecular mechanism is complex. Moreover, due to the complex process of the occurrence, development, invasion, and infiltration of tumor cells (Parker et al., 2020) and the resourcefulness of tumor cells themselves (Dunn et al., 2002), it is difficult to effectively control tumors. GBM, a malignant brain tumor with rapid progression and recurrence, is more difficult to clinically control (Weller et al., 2015). After an analysis of the potential molecular targets of glioma, we found that ANXA1 may play an important role in glioma through ECM–receptor interaction and focal adhesion signal pathways. As an important part of the tumor microenvironment, the ECM has a critical role in tumor occurrence, development, and invasion (Mohan et al., 2020). Focal adhesion is a subcellular structure, which not only has strong adhesion to the ECM but also promotes intracellular reorganization, resulting in a series of

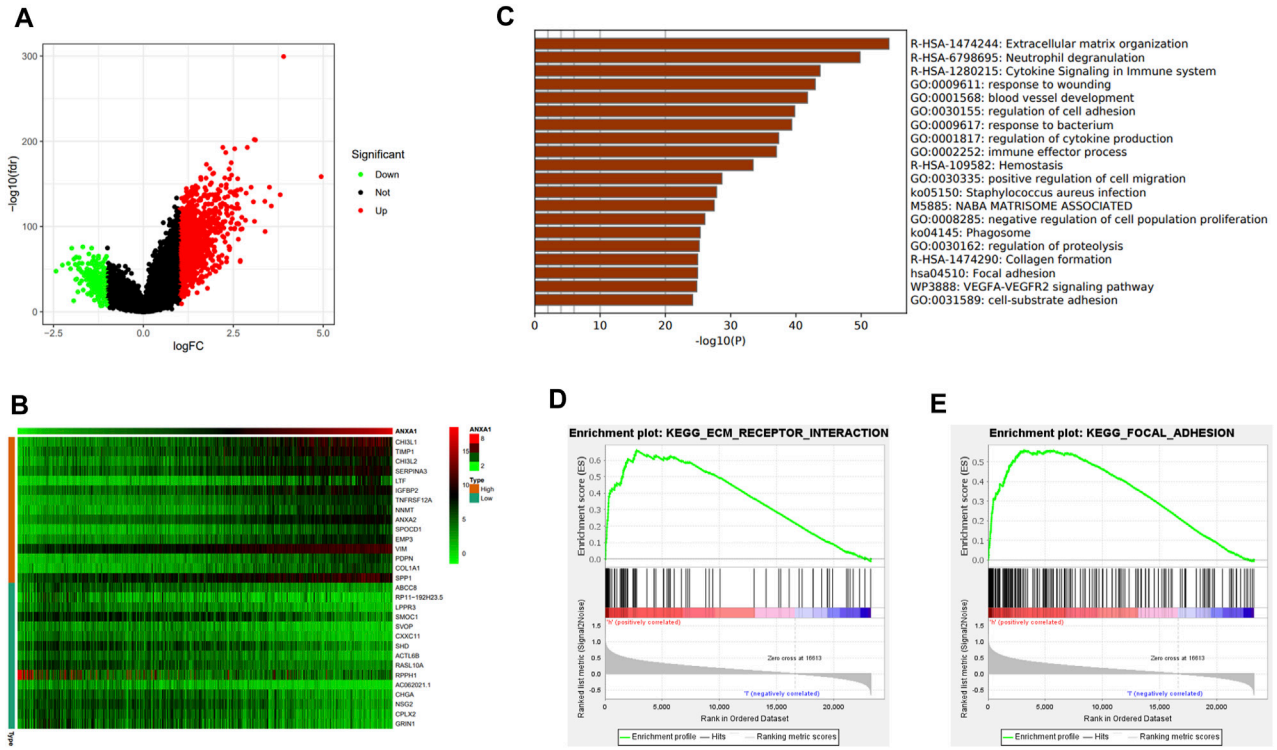


**FIGURE 5 |** DEG analysis and ANXA1 gene mechanism analysis. **(A)** Visual volcano plot of differentially expressed genes. **(B)** Heat map of DEGs was drawn, showing DEGs that were significantly upregulated and significantly downregulated. **(C)** Visual heat map for the mechanism analysis of DEGs on the Metascape online website. **(D,E)** Enriched ECM–receptor interaction and focal adhesion signal pathway by GSEA.

dynamic changes in cell function and morphology. Focal adhesion also plays an important role in the process of tumorigenesis, development, and infiltration (Legate et al., 2009). Multifunctional and multiprotein focal adhesion complexes play a key role in the underlying mechanism, which not only promote contact with the ECM but also promote the close conjunction between the ECM and actin cytoskeleton. Therefore, these complexes control the external morphology and internal signals of cells in terms of structure and function to promote cell growth and development, proliferation, differentiation, and motility (Legate and Fässler, 2009; Eke and Cordes, 2015). The main component of the ECM is collagen (Nissen et al., 2019). Type I collagen exists in most connective and embryonic tissues. In general, type I collagen consists of two chains of the alpha 1 chain (COL1A1) and one chain of the alpha 2 chain (COL1A2) (Gelse et al., 2003; Exposito et al., 2010). The alpha 1 chain of type I collagen is encoded by the COL1A1 gene and has been reported to be expressed in a variety of cancers, such as gastric cancer (Wang and Yu, 2018) and glioma (Balbous et al., 2014). COL1A1 is considered to be a marker of mesenchymal osteoblasts (Mori-Akiyama et al., 2003) and is also defined as a glioma endothelial marker selectively expressed in microvessels (Liu et al., 2010). COL1A2 is one of the most abundant collagen types in the human body, and it is involved in the process of angiogenesis. It has been reported that COL1A2 is upregulated in cancer (Greco et al., 2010) and that it promotes the proliferation and invasion of various cancers, such as gastric cancer and pancreatic cancer (Wu et al., 2019; Pan et al., 2021). FN1 is a type of adhesion glycoprotein involved in the ECM function of tumor cells, including cell adhesion, proliferation, and migration (Ko et al., 2020). Integrins play an important role in tumorigenesis, progression, and metastasis because they mediate the adhesion, migration, proliferation, invasion, and tumorigenicity of cancer cells (Pinon and Wehrle-Haller, 2011; Boudjadi et al., 2017). Among them, integrin α1 (ITGA1) and integrin β1 (ITGB1) are important members of the integrin family (Humphries et al., 2006; Hu et al., 2017).

Finally, through the intersection of the enriched core genes of the two pathways and the hub genes, we found that COL1A1, COL1A2, FN1, ITGA1, and ITGB1 were highly correlated with the ANXA1 gene, and these genes were overexpressed in glioma compared to normal brain tissues, which was verified in small samples of gliomas by the qPCR experiment. Through GEPIA, we found that the overexpression of these five core genes had poor prognosis in gliomas. Overall, the present study indicated that these five core genes and the ANXA1 gene participated in the occurrence and development of gliomas and suggested that they may play a synergistic role in the prognosis of gliomas. Therefore, the impact of these genes on gliomas should be further studied to seek the outcomes for glioma patients.

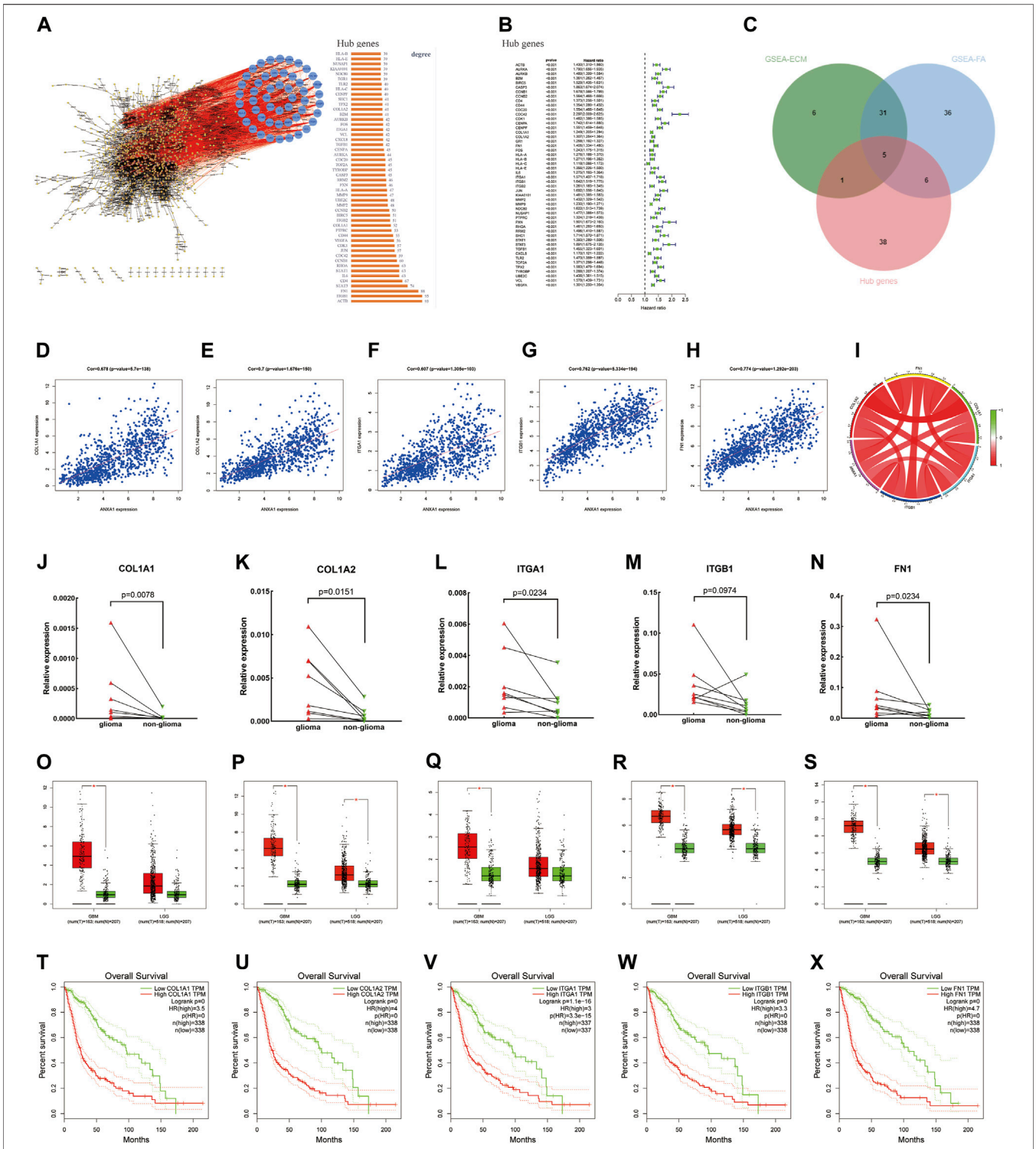


**FIGURE 6 |** Screening of core genes, gene correlation analysis, and prognostic analysis. **(A)** PPI was constructed by the STRING online website and Cytoscape visualization software, and the top 50 Hub proteins with degree values were screened. **(B)** Univariate regression analysis of the top 50 Hub genes. **(C)** Intersection between ECM–receptor interaction and focal adhesion pathway genes and 50 Hub genes and displayed by the Venn diagram. **(D–I)** Gene correlation circle diagram and scatter diagram. **(J–N)** Relative expression levels of the five core genes were detected by qPCR. **(O–S)** Expression level of core genes in glioma and normal tissues according to the analysis of the GEPIA online website. **(T–X)** High expression level of the core genes has poor prognosis in gliomas.

## CONCLUSION

Glioma is a common primary tumor in the brain. The high recurrence and invasion of gliomas endanger the survival of patients and pose a serious challenge to human health. Therefore, we investigated the expression of the ANXA1 gene in glioma and found that ANXA1 was overexpressed in gliomas. Moreover, we found that the prognosis of glioma patients with a high ANXA1 expression was worse and that ANXA1 was an independent prognostic index of gliomas. The present findings also indicated that ANXA1 may play an important role in the occurrence, development, invasion, and infiltration by affecting the ECM–receptor interaction and the focal adhesion signal pathways. Finally, by using gene correlation analysis, we found that the COL1A1, COL1A2, FN1, ITGA1, ITGB1, and ANXA1 genes may play a synergistic role in glioma patients. Therefore, the present study using public data recommends that ANXA1 may be an important molecular target for glioma. Blocking the overexpression of the ANXA1 gene is likely to improve the prognosis of glioma patients. Because the present study was based on online databases and glioma tissue samples, there were several limitations, indicating that additional clinical experimental studies are needed to improve the reliability of ANXA1 in glioma research.

## DATA AVAILABILITY STATEMENT

The original contributions presented in the study are included in the article/**Supplementary Materials**, further inquiries can be directed to the corresponding author.

## ETHICS STATEMENT

The studies involving human participants were reviewed and approved by the Second Hospital of Hebei Medical University. The patients/participants provided their written informed consent to participate in this study. The animal study was reviewed and approved by the Second Hospital of Hebei Medical University. Written informed consent was obtained from the individual(s) for the publication of any potentially identifiable images or data included in this article.

## AUTHOR CONTRIBUTIONS

DZ and WW conceived and/or designed experiments, conducted experiments, analyzed data, prepared charts, wrote and/or reviewed drafts of manuscripts, and approved final drafts. HZ conceived and/or designed the experiment, wrote and/or reviewed drafts of manuscripts, and approved the final draft. LS, XH, XZ, WH, and YW conducted data analysis and/or prepared charts, participated in the writing of the article, and reviewed the draft manuscript. XX conceived and designed the experiment, guided the writing and review of the draft manuscript, and approved the final draft.

## FUNDING

This work was supported by The Key Research and Development Project of Hebei Province- Special Project of Biomedicine (Grant Number 19277737D).

## ACKNOWLEDGMENTS

We thank all participating members in the Central Laboratory of the Second Hospital of Hebei Medical University and the Radiotherapy Department of the Second Hospital of Hebei Medical University.

## SUPPLEMENTARY MATERIAL

The Supplementary Material for this article can be found online at: https://www.frontiersin.org/articles/10.3389/fgene.2022.851505/full#supplementary-material

## REFERENCES

Aldape, K., Zadeh, G., Mansouri, S., Reifenberger, G., and von Deimling, A. (2015). Glioblastoma: Pathology, Molecular Mechanisms and Markers. *Acta Neuropathol.* 129, 829–848. doi:10.1007/s00401-015-1432-1

Auvergne, R. M., Sim, F. J., Wang, S., Chandler-Militello, D., Burch, J., Al Fanek, Y., et al. (2013). Transcriptional Differences between Normal and Glioma-Derived Glial Progenitor Cells Identify a Core Set of Dysregulated Genes. *Cell Rep.* 3, 2127–2141. doi:10.1016/j.celrep.2013.04.035

Balbous, A., Cortes, U., Guilloteau, K., Villalva, C., Flamant, S., Gaillard, A., et al. (2014). A Mesenchymal Glioma Stem Cell Profile is Related to Clinical Outcome. *Oncogenesis* 3, e91. doi:10.1038/oncsis.2014.5

Boudhraa, Z., Bouchon, B., Viallard, C., D' Incan, M., and Degoul, F. (2016). Annexin A1 Localization and its Relevance to Cancer. *Clin. Sci. Lond.* 130, 205–220. doi:10.1042/CS20150415

Boudjadi, S., Bernatchez, G., Sénicourt, B., Beauséjour, M., Vachon, P., Carrier, J., et al. (2017). Involvement of the Integrin α1β1 in the Progression of Colorectal Cancer. *Cancers* 9, 96. doi:10.3390/cancers9080096

Bush, N. A. O., Chang, S. M., and Berger, M. S. (2017). Current and Future Strategies for Treatment of Glioma. *Neurosurg. Rev.* 40, 1–14. doi:10.1007/s10143-016-0709-8

Chen, R., Smith-Cohn, M., Cohen, A. L., and Colman, H. (2017). Glioma Subclassifications and Their Clinical Significance. *Neurotherapeutics* 14, 284–297. doi:10.1007/s13311-017-0519-x

Cheng, T.-Y., Wu, M.-S., Lin, J.-T., Lin, M.-T., Shun, C.-T., Huang, H.-Y., et al. (2012). Annexin A1 is Associated with Gastric Cancer Survival and Promotes Gastric Cancer Cell Invasiveness through the Formyl Peptide Receptor/extracellular Signal-Regulated Kinase/integrin Beta-1-Binding Protein 1 Pathway. *Cancer* 118, 5757–5767. doi:10.1002/cncr.27565

Chuang, M.-C., Lung, J.-H., Chen, Y.-C., Lin, Y.-C., Li, Y.-C., and Hung, M.-S. (2021). The Association of Annexin A1 and Chemosensitivity to Osimertinib in Lung Cancer Cells. *Cancers* 13, 4106. doi:10.3390/cancers13164106

Cloughesy, T. F., Mochizuki, A. Y., Orpilla, J. R., Hugo, W., Lee, A. H., Davidson, T. B., et al. (2019). Neoadjuvant Anti-PD-1 Immunotherapy Promotes a Survival

Benefit with Intratumoral and Systemic Immune Responses in Recurrent Glioblastoma. *Nat. Med.* 25, 477–486. doi:10.1038/s41591-018-0337-7

Cordier, D., Krolicki, L., Morgenstern, A., and Merlo, A. (2016). Targeted Radiolabeled Compounds in Glioma Therapy. *Seminars Nucl. Med.* 46, 243–249. doi:10.1053/j.semnuclmed.2016.01.009

de Graauw, M., van Miltenburg, M. H., Schmidt, M. K., Pont, C., Lalai, R., Kartopawiro, J., et al. (2010). Annexin A1 Regulates TGF-β Signaling and Promotes Metastasis Formation of Basal-like Breast Cancer Cells. *Proc. Natl. Acad. Sci. U.S.A.* 107, 6340–6345. doi:10.1073/pnas.0913360107

Dunn, G. P., Bruce, A. T., Ikeda, H., Old, L. J., and Schreiber, R. D. (2002). Cancer Immunoediting: From Immunosurveillance to Tumor Escape. *Nat. Immunol.* 3, 991–998. doi:10.1038/ni1102-991

Eke, I., and Cordes, N. (2015). Focal Adhesion Signaling and Therapy Resistance in Cancer. *Seminars Cancer Biol.* 31, 65–75. doi:10.1016/j.semcancer.2014.07.009

Esteva, F. J., Hubbard-Lucey, V. M., Tang, J., and Pusztai, L. (2019). Immunotherapy and Targeted Therapy Combinations in Metastatic Breast Cancer. *Lancet Oncol.* 20, e175–e186. doi:10.1016/S1470-2045(19)30026-9

Exposito, J.-Y., Valcourt, U., Cluzel, C., and Lethias, C. (2010). The Fibrillar Collagen Family. *Int. J. Mol. Sci.* 11, 407–426. doi:10.3390/ijms11020407

Foo, S. L., Yap, G., Cui, J., and Lim, L. H. K. (2019). Annexin-A1 - A Blessing or a Curse in Cancer? *Trends Mol. Med.* 25, 315–327. doi:10.1016/j.molmed.2019.02.004

Ganesh, K., Stadler, Z. K., Cercek, A., Mendelsohn, R. B., Shia, J., Segal, N. H., et al. (2019). Immunotherapy in Colorectal Cancer: Rationale, Challenges and Potential. *Nat. Rev. Gastroenterol. Hepatol.* 16, 361–375. doi:10.1038/s41575-019-0126-x

Gelse, K., Pöschl, E., and Aigner, T. (2003). Collagens-structure, Function, and Biosynthesis. *Adv. Drug Deliv. Rev.* 55, 1531–1546. doi:10.1016/j.addr.2003.08.002

Greco, C., Bralet, M.-P., Ailane, N., Dubart-Kupperschmitt, A., Rubinstein, E., Le Naour, F., et al. (2010). E-cadherin/p120-catenin and Tetraspanin Co-029 Cooperate for Cell Motility Control in Human Colon Carcinoma. *Cancer Res.* 70, 7674–7683. doi:10.1158/0008-5472.CAN-09-4482

Griesinger, A. M., Birks, D. K., Donson, A. M., Amani, V., Hoffman, L. M., Waziri, A., et al. (2013). Characterization of Distinct Immunophenotypes across Pediatric Brain Tumor Types. *J. Immunol.* 191, 4880–4888. doi:10.4049/jimmunol.1301966

Guo, C., Liu, S., and Sun, M.-Z. (2013). Potential Role of Anxa1 in Cancer. *Future Oncol.* 9, 1773–1793. doi:10.2217/fon.13.114

Hu, C., Ni, Z., Li, B.-s., Yong, X., Yang, X., Zhang, J.-w., et al. (2017). hTERT Promotes the Invasion of Gastric Cancer Cells by Enhancing FOXO3a Ubiquitination and Subsequent ITGB1 Upregulation. *Gut* 66, 31–42. doi:10.1136/gutjnl-2015-309322

Hui, L., and Chen, Y. (2015). Tumor Microenvironment: Sanctuary of the Devil. *Cancer Lett.* 368, 7–13. doi:10.1016/j.canlet.2015.07.039

Humphries, J. D., Byron, A., and Humphries, M. J. (2006). Integrin Ligands at a Glance. *J. Cell. Sci.* 119, 3901–3903. doi:10.1242/jcs.03098

Jiang, T., Mao, Y., Ma, W., Mao, Q., You, Y., Yang, X., et al. (2016). CGCG Clinical Practice Guidelines for the Management of Adult Diffuse Gliomas. *Cancer Lett.* 375, 263–273. doi:10.1016/j.canlet.2016.01.024

Kaley, T., Touat, M., Subbiah, V., Hollebecque, A., Rodon, J., Lockhart, A. C., et al. (2018). BRAF Inhibition in BRAFV600-Mutant Gliomas: Results from the VE-BASKET Study. *J. Clin. Oncol.* 36, 3477–3484. doi:10.1200/JCO.2018.78.9990

Ko, Y.-C., Lai, T.-Y., Hsu, S.-C., Wang, F.-H., Su, S.-Y., Chen, Y.-L., et al. (2020). Index of Cancer-Associated Fibroblasts Is Superior to the Epithelial-Mesenchymal Transition Score in Prognosis Prediction. *Cancers* 12, 1718. doi:10.3390/cancers12071718

Legate, K. R., and Fässler, R. (2009). Mechanisms that Regulate Adaptor Binding to β-integrin Cytoplasmic Tails. *J. Cell. Sci.* 122, 187–198. doi:10.1242/jcs.041624

Legate, K. R., Wickström, S. A., and Fässler, R. (2009). Genetic and Cell Biological Analysis of Integrin Outside-In Signaling. *Genes Dev.* 23, 397–418. doi:10.1101/gad.1758709

Lim, L. H. K., and Pervaiz, S. (2007). Annexin 1: The New Face of an Old Molecule. *FASEB J.* 21, 968–975. doi:10.1096/fj.06-7464rev

Liu, Y., Carson-Walter, E. B., Cooper, A., Winans, B. N., Johnson, M. D., and Walter, K. A. (2010). Vascular Gene Expression Patterns are Conserved in Primary and Metastatic Brain Tumors. *J. Neurooncol.* 99, 13–24. doi:10.1007/s11060-009-0105-0

Louis, D. N., Perry, A., Reifenberger, G., von Deimling, A., Figarella-Branger, D., Cavenee, W. K., et al. (2016). The 2016 World Health Organization Classification of Tumors of the Central Nervous System: a Summary. *Acta Neuropathol.* 131, 803–820. doi:10.1007/s00401-016-1545-1

Louis, D. N., Perry, A., Wesseling, P., Brat, D. J., Cree, I. A., Figarella-Branger, D., et al. (2021). The 2021 WHO Classification of Tumors of the Central Nervous System: a Summary. *Neuro Oncol.* 23, 1231–1251. doi:10.1093/neuonc/noab106

Luo, Z., Liu, L., Li, X., Chen, W., and Lu, Z. (2021). Tat-NTS Suppresses the Proliferation, Migration and Invasion of Glioblastoma Cells by Inhibiting Annexin-A1 Nuclear Translocation. *Cell. Mol. Neurobiol.* doi:10.1007/s10571-021-01134-y

Maschler, S., Gebeshuber, C. A., Wiedemann, E. M., Alacakaptan, M., Schreiber, M., Custic, I., et al. (2010). Annexin A1 Attenuates EMT and Metastatic Potential in Breast Cancer. *EMBO Mol. Med.* 2, 401–414. doi:10.1002/emmm.201000095

Meurette, O., and Mehlen, P. (2018). Notch Signaling in the Tumor Microenvironment. *Cancer Cell* 34, 536–548. doi:10.1016/j.ccell.2018.07.009

Mohan, V., Das, A., and Sagi, I. (2020). Emerging Roles of ECM Remodeling Processes in Cancer. *Seminars Cancer Biol.* 62, 192–200. doi:10.1016/j.semcancer.2019.09.004

Monastyrskaya, K., Babiychuk, E. B., and Draeger, A. (2009). The Annexins: Spatial and Temporal Coordination of Signaling Events during Cellular Stress. *Cell. Mol. Life Sci.* 66, 2623–2642. doi:10.1007/s00018-009-0027-1

Mori-Akiyama, Y., Akiyama, H., Rowitch, D. H., and de Crombrugghe, B. (2003). Sox9 is Required for Determination of the Chondrogenic Cell Lineage in the Cranial Neural Crest. *Proc. Natl. Acad. Sci. U.S.A.* 100, 9360–9365. doi:10.1073/pnas.1631288100

Murat, A., Migliavacca, E., Gorlia, T., Lambiv, W. L., Shay, T., Hamou, M.-F., et al. (2008). Stem Cell-Related "Self-Renewal" Signature and High Epidermal Growth Factor Receptor Expression Associated with Resistance to Concomitant Chemoradiotherapy in Glioblastoma. *J. Clin. Oncol.* 26, 3015–3024. doi:10.1200/JCO.2007.15.7164

Mussunoor, S., and Murray, G. (2008). The Role of Annexins in Tumour Development and Progression. *J. Pathol.* 216, 131–140. doi:10.1002/path.2400

Nabors, L. B., Portnow, J., Ammirati, M., Baehring, J., Brem, H., Butowski, N., et al. (2017). NCCN Guidelines Insights: Central Nervous System Cancers, Version 1.2017. *J. Natl. Compr. Canc Netw.* 15, 1331–1345. doi:10.6004/jnccn.2017.0166

Naylor, E. C., Desani, J. K., and Chung, P. K. (2016). Targeted Therapy and Immunotherapy for Lung Cancer. *Surg. Oncol. Clin. N. Am.* 25, 601–609. doi:10.1016/j.soc.2016.02.011

Nissen, N. I., Karsdal, M., and Willumsen, N. (2019). Collagens and Cancer Associated Fibroblasts in the Reactive Stroma and its Relation to Cancer Biology. *J. Exp. Clin. Cancer Res.* 38, 115. doi:10.1186/s13046-019-1110-6

Ostrom, Q. T., Bauchet, L., Davis, F. G., Deltour, I., Fisher, J. L., Langer, C. E., et al. (2014). The Epidemiology of Glioma in Adults: A "state of the Science" Review. *Neuro Oncol.* 16, 896–913. doi:10.1093/neuonc/nou087

Pan, H., Ding, Y., Jiang, Y., Wang, X., Rao, J., Zhang, X., et al. (2021). LncRNA LIFR-AS1 Promotes Proliferation and Invasion of Gastric Cancer Cell via miR-29a-3p/COL1A2 axis. *Cancer Cell Int.* 21, 7. doi:10.1186/s12935-020-01644-7

Parente, L., and Solito, E. (2004). Annexin 1: More Than an Anti-phospholipase Protein. *Inflamm. Res.* 53, 125–132. doi:10.1007/s00011-003-1235-z

Parker, T. M., Henriques, V., Beltran, A., Nakshatri, H., and Gogna, R. (2020). Cell Competition and Tumor Heterogeneity. *Seminars Cancer Biol.* 63, 1–10. doi:10.1016/j.semcancer.2019.09.003

Piawah, S., and Venook, A. P. (2019). Targeted Therapy for Colorectal Cancer Metastases: A Review of Current Methods of Molecularly Targeted Therapy and the Use of Tumor Biomarkers in the Treatment of Metastatic Colorectal Cancer. *Cancer* 125, 4139–4147. doi:10.1002/cncr.32163

Pinon, P., and Wehrle-Haller, B. (2011). Integrins: Versatile Receptors Controlling Melanocyte Adhesion, Migration and Proliferation. *Pigment. Cell Melanoma Res.* 24, 282–294. doi:10.1111/j.1755-148X.2010.00806.x

Quail, D. F., and Joyce, J. A. (2017). The Microenvironmental Landscape of Brain Tumors. *Cancer Cell* 31, 326–341. doi:10.1016/j.ccell.2017.02.009

Ritchie, M. E., Phipson, B., Wu, D., Hu, Y., Law, C. W., Shi, W., et al. (2015). Limma Powers Differential Expression Analyses for RNA-Sequencing and Microarray Studies. *Nucleic Acids Res.* 43, e47. doi:10.1093/nar/gkv007

Senchenkova, E. Y., Ansari, J., Becker, F., Vital, S. A., Al-Yafeai, Z., Sparkenbaugh, E. M., et al. (2019). Novel Role for the AnxA1-Fpr2/ALX Signaling Axis as a Key Regulator of Platelet Function to Promote Resolution of Inflammation. *Circulation* 140, 319–335. doi:10.1161/CIRCULATIONAHA.118.039345

Stupp, R., Mason, W. P., van den Bent, M. J., Weller, M., Fisher, B., Taphoorn, M. J. B., et al. (2005). Radiotherapy Plus Concomitant and Adjuvant Temozolomide for Glioblastoma. *N. Engl. J. Med.* 352, 987–996. doi:10.1056/NEJMoa043330

Sun, L., Hui, A.-M., Su, Q., Vortmeyer, A., Kotliarov, Y., Pastorino, S., et al. (2006). Neuronal and Glioma-Derived Stem Cell Factor Induces Angiogenesis within the Brain. *Cancer Cell* 9, 287–300. doi:10.1016/j.ccr.2006.03.003

Wang, Y., and Jiang, T. (2013). Understanding High Grade Glioma: Molecular Mechanism, Therapy and Comprehensive Management. *Cancer Lett.* 331, 139–146. doi:10.1016/j.canlet.2012.12.024

Wang, Q., and Yu, J. (2018). MiR-129-5p Suppresses Gastric Cancer Cell Invasion and Proliferation by Inhibiting COL1A1. *Biochem. Cell Biol.* 96, 19–25. doi:10.1139/bcb-2016-0254

Wei, L., Li, L., Liu, L., Yu, R., Li, X., and Luo, Z. (2021). Knockdown of Annexin-A1 Inhibits Growth, Migration and Invasion of Glioma Cells by Suppressing the PI3K/Akt Signaling Pathway. *ASN Neuro* 13, 175909142110012. doi:10.1177/17590914211001218

Weller, M., Wick, W., Aldape, K., Brada, M., Berger, M., Pfister, S. M., et al. (2015). Glioma. *Nat. Rev. Dis. Prim.* 1, 15017. doi:10.1038/nrdp.2015.17

Wen, P. Y., and Kesari, S. (2008). Malignant Gliomas in Adults. *N. Engl. J. Med.* 359, 492–507. doi:10.1056/NEJMra0708126

Wu, J., Liu, J., Wei, X., Yu, Q., Niu, X., Tang, S., et al. (2019). A Feature-Based Analysis Identifies COL1A2 as a Regulator in Pancreatic Cancer. *J. Enzyme Inhibition Med. Chem.* 34, 420–428. doi:10.1080/14756366.2018.1484734

Xia, W., Zhu, J., Wang, X., Tang, Y., Zhou, P., Hou, M., et al. (2020). ANXA1 Directs Schwann Cells Proliferation and Migration to Accelerate Nerve Regeneration through the FPR2/AMPK Pathway. *FASEB J.* 34, 13993–14005. doi:10.1096/fj.202000726RRR

Xu, Y., Wang, J., Xu, Y., Xiao, H., Li, J., and Wang, Z. (2017). Screening Critical Genes Associated with Malignant Glioma Using Bioinformatics Analysis. *Mol. Med. Rep.* 16, 6580–6589. doi:10.3892/mmr.2017.7471

Xu, S., Tang, L., Li, X., Fan, F., and Liu, Z. (2020). Immunotherapy for Glioma: Current Management and Future Application. *Cancer Lett.* 476, 1–12. doi:10.1016/j.canlet.2020.02.002

**Conflict of Interest:** The authors declare that the research was conducted in the absence of any commercial or financial relationships that could be construed as a potential conflict of interest.

**Publisher's Note:** All claims expressed in this article are solely those of the authors and do not necessarily represent those of their affiliated organizations, or those of the publisher, the editors, and the reviewers. Any product that may be evaluated in this article, or claim that may be made by its manufacturer, is not guaranteed or endorsed by the publisher.

frontiers | Frontiers in Genetics

ORIGINAL RESEARCH
published: 27 June 2022
doi: 10.3389/fgene.2022.905047

# Comprehensive Characterization of a Novel E3-Related Gene Signature With Implications in Prognosis and Immunotherapy of Low-Grade Gliomas

*Shichuan Tan*[1,2,3], *Ryan Spear*[4], *Juan Zhao*[1,5], *Xiulian Sun*[1,3,6]* *and Pin Wang*[1,5]*

[1]NHC Key Laboratory of Otorhinolaryngology, Qilu Hospital of Shandong University, Jinan, China, [2]Department of Neurology, Qilu Hospital of Shandong University, Jinan, China, [3]Brain Research Institute, Qilu Hospital of Shandong University, Jinan, China, [4]Department of Medicine, Rush University Medical Center, Chicago, IL, United States, [5]Department of Otorhinolaryngology, Qilu Hospital of Shandong University, Jinan, China, [6]The Key Laboratory of Cardiovascular Remodeling and Function Research, Chinese Ministry of Education, Chinese National Health Commission, Qilu Hospital of Shandong University, Jinan, China

OPEN ACCESS

**Edited by:**
Quan Cheng,
Central South University, China

**Reviewed by:**
Xinwei Han,
Zhengzhou University, China
Jiahang Song,
The First Affiliated Hospital of Nanjing Medical University, China

***Correspondence:**
Xiulian Sun
xiulians@gmail.com
Pin Wang
wangpin@sdu.edu.cn

**Specialty section:**
This article was submitted to Cancer Genetics and Oncogenomics, a section of the journal Frontiers in Genetics

**Received:** 26 March 2022
**Accepted:** 13 May 2022
**Published:** 27 June 2022

**Citation:**
Tan S, Spear R, Zhao J, Sun X and Wang P (2022) Comprehensive Characterization of a Novel E3-Related Gene Signature With Implications in Prognosis and Immunotherapy of Low-Grade Gliomas. Front. Genet. 13:905047. doi: 10.3389/fgene.2022.905047

Gliomas, a type of primary brain tumor, have emerged as a threat to global mortality due to their high heterogeneity and mortality. A low-grade glioma (LGG), although less aggressive compared with glioblastoma, still exhibits high recurrence and malignant progression. Ubiquitination is one of the most important posttranslational modifications that contribute to carcinogenesis and cancer recurrence. E3-related genes (E3RGs) play essential roles in the process of ubiquitination. Yet, the biological function and clinical significance of E3RGs in LGGs need further exploration. In this study, differentially expressed genes (DEGs) were screened by three differential expression analyses of LGG samples from The Cancer Genome Atlas (TCGA) database. DEGs with prognostic significance were selected by the univariate Cox regression analysis and log-rank statistical test. The LASSO-COX method was performed to identify an E3-related prognostic signature consisting of seven genes AURKA, PCGF2, MAP3K1, TRIM34, PRKN, TLE3, and TRIM17. The Chinese Glioma Genome Atlas (CGGA) dataset was used as the validation cohort. Kaplan–Meier survival analysis showed that LGG patients in the low-risk group had significantly higher overall survival time than those in the high-risk group in both TCGA and CGGA cohorts. Furthermore, multivariate Cox regression analysis revealed that the E3RG signature could be used as an independent prognostic factor. A nomogram based on the E3RG signature was then established and provided the prediction of the 1-, 3-, and 5-year survival probability of patients with LGGs. Moreover, DEGs were analyzed based on the

**Abbreviations:** WHO, World Health Organization; LGG, low-grade glioma; GBM, glioblastoma multiforme; PTMs, post-translational modifications; UPS, ubiquitin-proteasome system; DUBs, deubiquitinating enzymes; E3RGs, E3-related genes; PROTAC, proteolysis targeting chimeric; TCGA, The Cancer Genome Atlas; CPM, counts per million reads mapped; FPKM, Fragments Per Kilobase of transcript per Million mapped reads; DEGs, differentially expressed genes; LASSO, least absolute shrinkage and selection operator; HRs, hazard ratios; CIs, confidence intervals; ROC, receiver operating characteristic; GO, Gene Ontology; KEGG, Kyoto Encyclopedia of Genes and Genomes; BP, biological process; CC, cellular component; MF, molecular function; GSEA, gene set enrichment analysis; ssGSEA, single-sample gene set enrichment analysis; PPI, protein–protein interaction network; AUC, area under the curve; TIME, tumor immune microenvironment; GSCs, glioma stem cells; TMZ, temozolomide; MHC, major histocompatibility complex; ECM, extracellular matrix.

risk signature, on which function analyses were performed. GO and KEGG analyses uncovered gene enrichment in extracellular matrix–related functions and immune-related biological processes in the high-risk group. GSEA revealed high enrichment in pathways that promote tumorigenesis and progression in the high-risk group. Furthermore, ESTIMATE algorithm analysis showed a significant difference in immune and stroma activity between high- and low-risk groups. Positive correlations between the risk signature and the tumor microenvironment immune cell infiltration and immune checkpoint molecules were also observed, implying that patients with the high-risk score may have better responses to immunotherapy. Overall, our findings might provide potential diagnostic and prognostic markers for LGG patients and offer meaningful insight for individualized treatment.

**Keywords: E3-related genes, prognosis, tumor immune microenvironment, risk signature, low-grade gliomas**

## INTRODUCTION

Glioma is a primary type of tumor that occurs in the brain and spinal cord. The World Health Organization (WHO) classification system categorizes gliomas from grade I (lowest grade) through grade IV (highest grade) according to the malignant histological features (Wesseling and Capper, 2018). Low-grade gliomas (LGGs), which are less aggressive than glioblastoma multiforme (GBM), mainly originate from astrocytes and oligodendrocytes. Patients with LGGs are categorized as WHO grade II–III gliomas. The standard management of patients with LGG primarily involves surgical resection followed by adjuvant radiotherapy and chemotherapy (Lombardi et al., 2020). Even after patients receive these standard clinical interventions, the highly invasive nature and heterogeneity of LGGs can still lead to high rates of tumor recurrence and noteworthy malignant progression (Brat et al., 2015; Xia et al., 2018; Gittleman et al., 2020). Furthermore, the prognosis of LGGs varies diversely due to tumor heterogeneity. LGG patients (mean age 41 years) are proposed to have survival averaging approximately 7 years, which is a significant sign of poor prognosis (Claus et al., 2015). Therefore, it is imperative to gain a more comprehensive understanding of the pathogenesis of LGG, identify effective and reliable biomarkers that could predict clinical outcomes, and formulate optimum therapeutic strategies.

Posttranslational modifications (PTMs) refer to covalent processing events of proteins which occur after synthesis and are normally mediated by diverse enzymes. Ubiquitination is a crucial posttranslational modification of a protein. It is an ATP-dependent reversible process mediated by the ubiquitin-proteasome system (UPS), including E1 ubiquitin–activating enzymes, E2 ubiquitin–conjugating enzymes, E3 ubiquitin-protein ligases, and deubiquitinating enzymes (DUBs) (Reyes-Turcu et al., 2009; Schulman and Harper, 2009; Buetow and Huang, 2016; Stewart et al., 2016). The dysregulation of UPS is largely involved in numerous biological functions, including cell cycle progression, cell proliferation, apoptosis, gene transcription, metastasis, transcriptional regulation, signaling, and inflammation (Deng et al., 2020). Accordingly, abnormal ubiquitination may contribute to various human pathologies such as neurodegeneration (Stieren et al., 2011; Popovic et al., 2014), autoimmune responses (Zangiabadi and Abdul-Sater, 2022), and oncogenic processes (Rape, 2018). In the UPS, E3 ubiquitin ligase serves as the essential part of the ubiquitination process owing to its substrate specificity (Zheng and Shabek, 2017). UPS is stringently regulated by E3 ligases that convey the specificity of ubiquitination. In particular, ubiquitin molecules are transferred from ubiquitin-conjugating enzymes to specific substrates by E3 ubiquitin–protein ligases. The misregulation of UPS led by mutations in E3-related genes (E3RGs) is highly correlated with poor prognosis of cancers (Seeler and Dejean, 2017). Accumulating studies have demonstrated the tremendous contribution of E3-related proteins in glioma pathogenesis. For instance, MYH9-mediated ubiquitination of GSK-3β promotes malignant progression and chemoresistance in glioma (Que et al., 2022). The degradation of TUSC2 induced by NEDD4 facilitates glioblastoma progression (Rimkus et al., 2022). PARK2, frequently mutated in glioma, acts as a tumor suppressor by boosting ubiquitination-dependent degradation of β-catenin, which results in attenuation of Wnt signaling (Veeriah et al., 2010; Lin et al., 2015). Tripartite motif-containing protein 11 (TRIM11), overexpressed in glioma, promotes proliferation, invasion, migration, and glial tumor growth *via* the induction of EGFR (Di et al., 2013). In addition, many E3 ligases have been reported to play vital roles in glioma carcinogenesis *via* the regulating PI3K/Akt pathway, such as $SCF^{\beta-TrCP}$ (Warfel et al., 2011), TRAF6 (Feng et al., 2014), and TRIM21 (Lee et al., 2017). Based on the significant function of E3 ligases in cancer pathogenesis, therapeutics targeting UPS have shown promising effects in clinical trials against cancers, such as PROTAC (proteolysis-targeting chimeric) (Qi et al., 2021). Two PROTAC strategies targeting CDK4 and/or CDK6 have been tested in glioma cells and are expected in clinical trials soon (Zhao and Burgess, 2019). Given the crucial roles of E3-related genes in glioma, the mechanism underlying the relationship between E3-related genes and the prognosis of LGG needs to be further addressed.

In the present study, a comprehensive analysis of E3RGs in LGG was conducted. Transcriptome data and clinical data of LGG samples were downloaded from The Cancer Genome Atlas (TCGA) database. Differentially expressed genes (DEGs) with

prognostic significance were screened and identified. Subsequently, an E3-related prognostic signature was constructed, and the nomogram based on the risk signature was established to predict the prognosis of LGG. Meanwhile, enrichment analyses of risk-related differentially expressed genes and substrates of the risk signature genes were performed to disclose the underlying mechanism of LGG progression. Finally, the correlation between the risk signature and tumor immunity was analyzed. Our work provided an effective clinical tool for LGG prognosis prediction and preliminarily explored the biological functions and immune processes involved in the signature and the relative regulatory networks.

# MATERIALS AND METHODS

## Datasets and E3-Related Gene Acquisition

The transcriptome sequencing data and corresponding clinical data of primary LGG were obtained from the TCGA database (https://portal.gdc.cancer.gov/) and the Chinese Glioma Genome Atlas (CGGA) database, respectively, (http://www.cgga.org.cn/). The TCGA LGG cohort was selected as the training set, which included 451 tumor samples and five normal brain samples. The CGGA cohort (DataSet ID: mRNAseq_693) was chosen as the validation set, containing 240 primary LGG patients. The samples with incomplete clinical information and overall survival < 30 days had been excluded. Count data from TCGA and FPKM data from CGGA were applied for further analysis. The GSE68848 and GSE4290 datasets procured from the Gene Expression Omnibus database (GEO; https://www.ncbi.nlm.nih.gov/geo/) were utilized to validate the expression of the signature genes. The 630 E3RGs utilized in this study were collected from the ESBL database (https://esbl.nhlbi.nih.gov/Databases/KSBP2/Targets/Lists/E3-ligases/) and iUUCD2.0 database (http://iuucd.biocuckoo.org/) (**Supplementary Table S1**).

## Identification of Differentially Expressed E3-Related Genes

E3-related DEGs between LGG tissues and normal brain tissues were analyzed using the "limma," "edgeR," and "DESeq2" R packages with the cut-off criteria of $|\log_2 FC| \geq 1$ and $p < 0.05$ (Robinson et al., 2010; Love et al., 2014; Ritchie et al., 2015). The raw count data of the TCGA LGG cohort were used as the input for limma, edgeR, and DESeq. Volcano plots were generated to display DEG distribution from three algorithms mentioned earlier with the "tinyarray" R package. Venn diagrams were intersected to obtain the overlapping enriched terms also with the "tinyarray" R package.

## Identification of E3-Related Differentially Expressed Genes With the Prognostic Value

The CPM of genes and clinical information were used for the subsequent analyses. The univariate Cox regression analysis and log-rank statistical test with the cut-off criteria of $p < 0.05$ for E3-related DEGs were applied to select the genes with prognostic significance, using "survival" and "survminer" packages in R software. Venn diagrams were used to present the intersection of the enriched genes from Cox regression analysis and log-rank analysis.

## Construction and Validation of the Prognostic Signature

To minimize the overfitting high-dimensional prognostic E3-related DEGs, least absolute shrinkage and selection operator (LASSO) regression analysis was performed with the "glmnet" R package (Friedman et al., 2010). Multivariate Cox regression analysis was conducted to construct prognostic models with the R package "My.stepwise". Hazard ratios (HRs) and 95% confidence intervals (CIs) were reported where applicable. The median risk score was calculated to categorize the LGG patients into high-risk and low-risk groups, based on the following formula:

$$\text{Risk score} = \sum_{i=1}^{n} \text{Coef}_i \times \text{Exp}r_i,$$

(where $\text{Coe}f_i$ is the coefficient and $\text{Exp}r_i$ is the expression level of each intersected gene).

A Kaplan–Meier survival curve was used to determine the differences in overall survival using the R package "survival". Time-dependent receiver operating characteristic (ROC) analysis was executed to evaluate the prognostic accuracy of the seven-E3RG risk signature using R package "timeROC" (Blanche et al., 2013). The survival analysis result was presented by the R package "tinyarray" and "patchwork."

## Development and Evaluation of the Nomogram

To assess whether the seven-E3RG prognostic risk signature can be utilized as an independent prognostic factor, univariate and multivariate Cox regression analyses were performed using R package "survival" and "My.stepwise." The nomogram was constructed with independent prognostic parameters using the "rms" R package, and the calibration curves were utilized to reflect the accuracy of the nomogram.

## Risk-Related Differentially Expressed Gene Analysis

LGG patients were divided into high-risk and low-risk groups according to the median risk score. The raw count data of the TCGA LGG cohort were used as the input data for limma, edgeR, and DESeq. "limma," "edgeR," and "DESeq2" R packages with the cut-off criteria of $|\log_2 FC| \geq 1$ and $p < 0.05$ were applied to two groups for DEG screening. Volcano plots were generated to display DEG distribution from three algorithms. Venn diagrams were intersected to obtain the overlapping enriched terms.

## Functional Enrichment and GSEA

Gene Ontology (GO) and Kyoto Encyclopedia of Genes and Genomes (KEGG) analyses were performed utilizing the "clusterProfiler" package to predict the biological function and related pathways (Yu et al., 2012). The top five enriched terms in

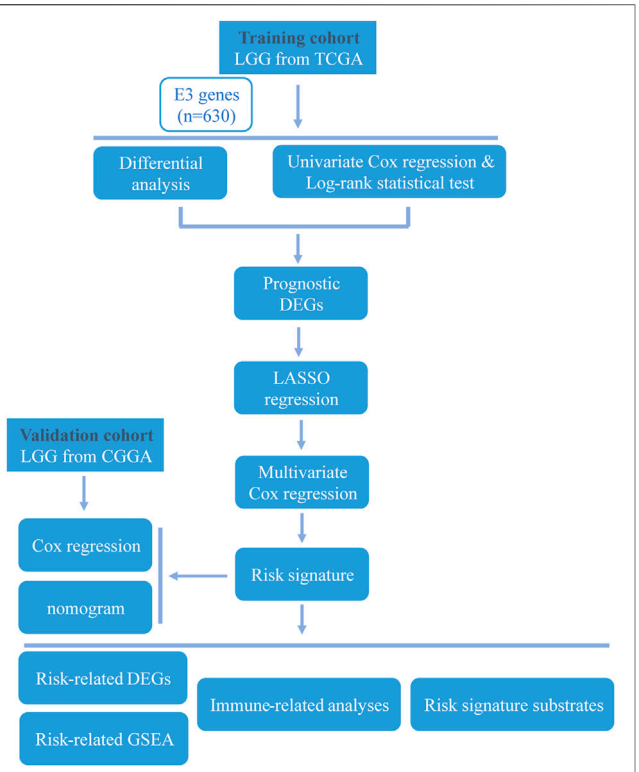


**FIGURE 1 |** Workflow of the study.

the biological process (BP), cellular component (CC), and molecular function (MF) were visualized using "ggplot2" and "enrichplot" R packages. KEGG pathways with P. adjust<0.01 were chosen for presentation. Gene set enrichment analysis (GSEA) was conducted using GSEA v4.2.3 software with hallmark gene sets.

## Immune Microenvironment Analysis

The tumor immune microenvironment (TIME) cell infiltration characterization was evaluated by the single-sample gene set enrichment analysis (ssGSEA) with the "GSVA" R package (Hänzelmann et al., 2013). An ESTIMATE algorithm was used to evaluate the immune and stromal activity in the LGG microenvironment with the "estimate" R package (Yoshihara et al., 2013). The correlation analysis was performed based on Pearson's correlation coefficient and presented using R packages "corrplot" and "circlize" (Gu et al., 2014).

## Protein–Protein Interaction Network Analysis

A PPI network was constructed based on the substrates of E3RG signature with required interaction score > 0.4 using the STRING database (https://cn.string-db.org/) and visualized using Cytoscape (version 3.9.1) (Shannon et al., 2003; Szklarczyk et al., 2019). The top 10 hub genes in the PPI network were identified using the MCC algorithm with the CytoHubba plugin in Cytoscape.

# RESULTS

## Identification of Differentially Expressed E3-Related Genes With the Prognostic Value in Low-Grade Gliomas

The overall study workflow is presented in **Figure 1**. The TCGA cohort was used as the training set. The transcriptome and clinical data from TCGA included 451 tumor samples and five normal brain samples. The 630 E3RGs were selected and applied in this study (**Supplementary Table S1**). Three differential expression analyses were performed. According to the $|\log_2 FC| > 1.0$ and $p < 0.05$, DEGs were displayed in volcano plots (**Figure 2A**). The overlapping of DEGs from three differential expression analyses indicated that 44 genes were upregulated and 47 genes were downregulated in tumor samples (**Figure 2B**). Subsequently, DEGs were further analyzed by univariate Cox regression analysis and log-rank statistical test to evaluate the prognostic significance. In total, 38 E3RGs with a significant prognostic value were obtained by the intersection of results from both analyses (**Figure 2C**).

## Construction of E3-Related Gene Prognostic Risk Signature in Low-Grade Gliomas

To further explore the prognostic value of E3RGs in LGGs, 38 overall survival–associated E3RGs were incorporated into the LASSO regression (Liu et al., 2021; 2022a; 2022b; 2022c), 20 of which were selected for further multivariate Cox regression analysis (**Figures 3A,B**). Following this, a seven-E3RG prognostic signature significantly correlated with LGG prognosis was developed by performing multivariate Cox regression analysis and shown in the forest plot (**Figure 3C**). The risk score was calculated for each LGG patient by the following formula:

Riskscore=(0.4121493)* AURKA+ (-0.8124184)*PCGF2+ (0.6318466)*MAP3K1+ (0.2558092)*TRIM34+(-0.5951688)* PRKN+(-0.5669701)*TLE3+(0.1586579)*TRIM17.

The expression of the signature genes was validated in both GSE4290 and GSE68848 datasets and proved consistent with that in the TCGA cohort (**Figures 3D,E**). Univariate Cox regression analysis revealed that seven signature genes were all strongly correlated with the prognosis (**Figure 4A**). As shown in the Kaplan–Meier curves, four genes of the E3RG signature were considered to have favorable prognostic effects, while three were considered to have poor prognostic effects (**Figure 4B**).

Based on the seven-E3RG risk signature, patients were divided into the high-risk and low-risk subgroups according to the median risk score in TCGA cohorts. The resulting Kaplan–Meier curve displayed a significant difference in overall survival between the LGG patients in the high-risk and the low-risk group, suggesting the established signature effectively predicts survival (**Figure 5A**; $p < 0.0001$). The overall survival of patients with low-risk scores was significantly higher than that of patients with high-risk scores. The genes referred to in the signature were remarkably differentially expressed in the high-risk group and the low-risk group. The

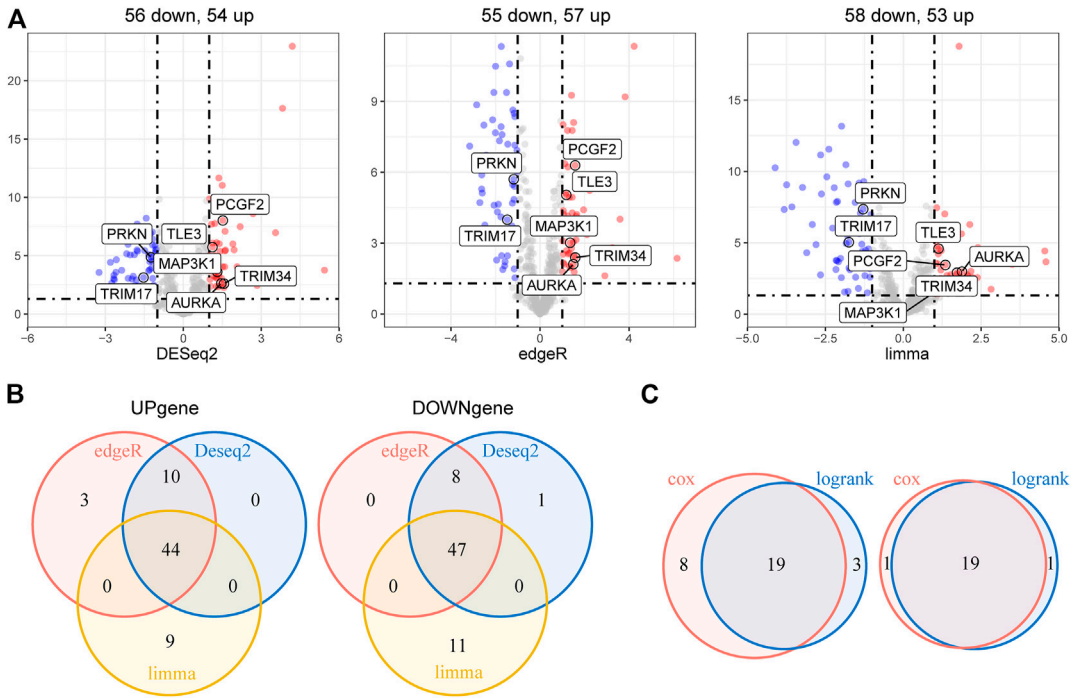


**FIGURE 2 |** Identification of E3-related DEGs with prognostic value in LGG. **(A)** Volcano plot of E3-related DEGs between 451 LGG samples and five normal brain samples identified using edgeR, limma, and DESeq2 algorithms, with the cut-off criterion $p < 0.05$ and $|\log_2 FC| \geq 1$. Blue dots: significantly downregulated genes; red dots: significantly upregulated genes. **(B)** Venn diagram of the overlapping E3-related DEGs screened by the three differential expression analyses. **(C)** Venn diagram of the intersection for overall survival–correlated E3-related DEGs identified using univariate Cox regression analysis and log-rank statistical test with the cut-off criteria of $p < 0.05$. Left, predicted favorable prognosis; right, predicted poor prognosis.

expression of AURKA, MAP3K1, and TRIM34 was lower in low-risk patients than in high-risk patients, while PCGF2, PRKN, TLE3, and TRIM17 expressions were higher in patients with low-risk scores than in those with high-risk scores. The distribution of risk score, survival status, and the expression of the signature genes is shown in **Figures 5B–D**. To evaluate the predictive effect of the prognostic model, 1-year, 3-year, and 5-year time-dependent ROC curves were plotted, and the concordance index was calculated. The area under the curve (AUC) values were 0.9 (1-year ROC), 0.89 (3-year ROC), and 0.85 (5-year ROC) (**Figure 5E**). Given the results earlier, the risk signature presented a superior predictive capacity for LGGs.

## Validation of the Risk Signature in the Chinese Glioma Genome Atlas Cohort

To test whether the prognostic gene signature has similar predictive performance and accuracy in other LGG cohorts, the CGGA cohort was used as a validation set. In the CGGA cohort, the patients were divided into low-risk and high-risk groups by the median risk score with the same formula calculated from the TCGA cohort (**Figure 6B**). Consistent with the results obtained from the training set, survival analysis using the Kaplan–Meier method exhibited a better prognosis for patients in the low-risk group (**Figure 6A**, $p < 0.0001$). The distribution of risk score and survival status is shown in **Figures 6B,C**. A heatmap of gene expression in the CGGA cohort is presented in **Figure 6D**, based on the risk score. The predicted AUCs of 1 year, 3 year, and 5 year are 0.80, 0.79, and 0.71, respectively (**Figure 6E**). Prognostic analyses showed similar results. These results demonstrated that the E3RG risk signature was positively correlated with LGG prognosis.

## Independent Prognostic Value of the E3-Related Gene Risk Signature in the Cancer Genome Atlas and the Chinese Glioma Genome Atlas Low-Grade Glioma Cohorts and Construction of a Nomogram

We first evaluated the prognostic value of age, gender, and risk score in patients with LGG from the TCGA cohort through univariate Cox regression analysis. The result revealed that both age (HR = 1.07, 95% CI = 1.05–1.09, $p < 0.001$) and risk score (HR = 2.72, 95% CI = 2.26–3.27, $p < 0.001$) of LGG patients were significantly correlated with overall survival (**Figure 7A**). Moreover, multivariate Cox regression analysis showed that age (HR = 1.05, 95% CI = 1.03–1.07, $p < 0.001$) and risk score (HR = 2.28, 95% CI = 1.87–2.76, $p < 0.001$) affected overall survival as independent prognostic factors (**Figure 7B**). Similar results were obtained when univariate and multivariate Cox regression analyses were applied in LGG patients from the CGGA cohort. Of note, gender (HR = 1.56, 95% CI = 1–2.44, $p = 0.049$) and risk score (HR = 1.97, 95% CI = 1.62–2.38, $p < 0.001$) were correlated with overall survival, but only risk score (HR = 1.97, 95% CI = 1.62–2.39, $p < 0.001$) became an

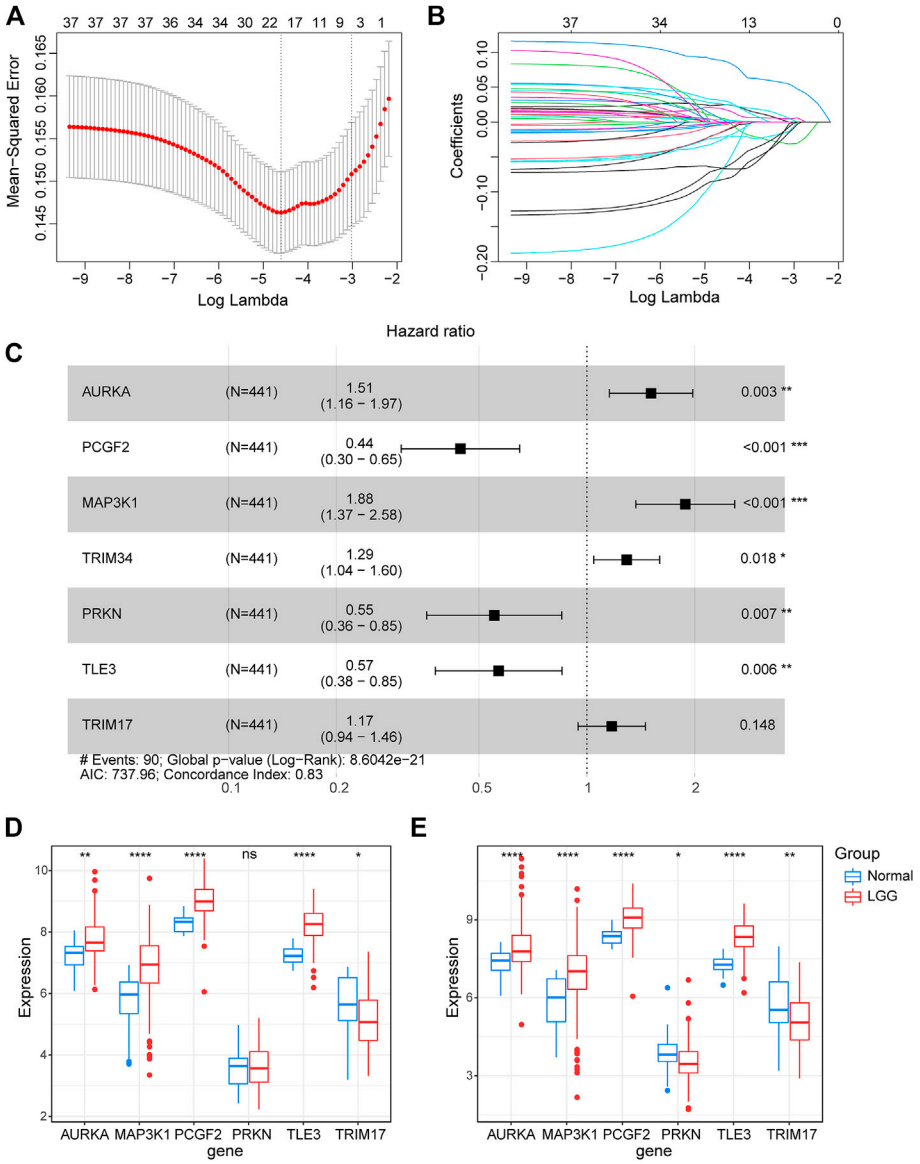


**FIGURE 3 |** Construction of the prognostic E3-related signature. **(A)** LASSO regression cross-validation for tuning parameter lambda selection. **(B)** Coefficient profiles of the LASSO regression analysis. **(C)** Seven optimal prognostic E3-related DEGs selected by multivariate Cox regression analysis are shown in the forest plot. **(D)** Expression of the signature genes in the GSE4290 dataset. **(E)** Expression of the signature genes in the GSE68848 dataset. (*$p < 0.05$; **$p < 0.01$; ***$p < 0.001$; ****$p < 0.0001$; ns, not significant).

independent prognostic factor in the CGGA cohort (**Figures 7C,D**). The subtle difference may be attributed to the ethnicity difference.

On the basis of the seven-E3RG risk signature, we established a nomogram that could predict the prognosis of LGG in the TCGA cohort (**Figure 7E**). Briefly, the points of different variables were mapped to the corresponding lines, while the total points of the patients were calculated and normalized to a distribution of 0–100. By performing this, the 1-, 3-, and 5-year survival status for LGG patients could be approximately estimated based on the prognosis axis and total point axis. In addition, the calibration curves for the probability of 1-, 3-, and 5-year overall survival showed a strong consistency between the predicted value of the nomogram and the actual value in both the TCGA and CGGA cohorts (**Figures 7F,G**). Thus, the nomogram could serve as a favorable reference for clinical decision-making.

## Identification and Function Analysis of Risk-Related Differentially Expressed Genes

To further investigate the potential biological functions and pathways of the risk signature, we screened the DEGs by three

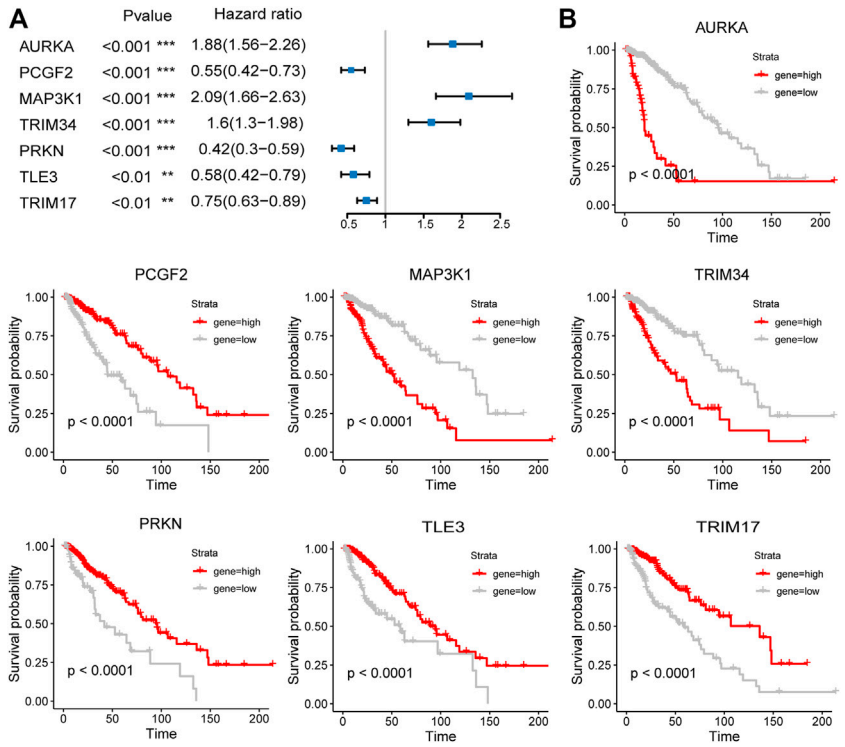


**FIGURE 4 |** Prognostic analysis of the seven-E3RG risk signature. Univariate Cox regression analysis **(A)** and Kaplan–Meier curves **(B)** of the seven-E3RG prognostic signature (**$p < 0.01$; ***$p < 0.001$).

differential expression analyses between the high-risk group and the low-risk group in the TCGA LGG cohort. These results were displayed in volcano plots (**Figure 8A**). As shown by the Venn diagrams in **Figure 8B**, 528 upregulated genes and 134 downregulated genes in the high-risk group were identified and applied for GO and KEGG pathway analyses (**Figure 8B**). From the GO analysis, the risk-related DEGs were enriched in extracellular matrix–related functions, which suggested stronger migration and invasion potentials of tumors for LGG patients in the high-risk group, such as collagen-containing extracellular matrix and extracellular matrix structural constituent. Meanwhile, the risk-related DEG high enrichment was observed in several immune-related biological processes, such as MHC class II protein complex, MHC protein complex, MHC class II receptor activity, and immune receptor activity (**Figure 8C**). Moreover, the KEGG pathway enrichment analysis showed that risk-related DEGs were principally intensified in immune-related pathways and cell adhesion molecules, which reflected the malignant characteristics of LGG in the high-risk group (**Figure 8D**). This was also consistent with the results of GO analysis.

## GSEA Enrichment Analysis

To elucidate the potential functional differences between the high-risk and low-risk groups, GSEA was performed with the TCGA LGG cohort. GSEA revealed that pathways related to inflammatory response, such as complement, IL-2/STAT5 signaling, IL-6/JAK/STAT3 signaling, and inflammatory response, were enriched in the high-risk group. Pathways that promote tumorigenesis and progression were also enriched in the high-risk group, such as PI3K/AKT/MTOR signaling, mTORC1 signaling, epithelial–mesenchymal transition, glycolysis, and KRAS signaling up. The enrichment of genes related to E2F targets, G2M checkpoint, and mitotic spindle suggested the correlation of cell cycle dysregulation with the risk score (**Figure 9**).

## The Role of the E3-Related Gene Risk Signature in the Tumor Immune Microenvironment

In order to further investigate the roles of the risk signature in TIME cell infiltration, we evaluated the landscape of 28 TIME-infiltrating cell types in the low-risk and high-risk groups by ssGSEA (Charoentong et al., 2017). In total, 25 TIME cell types presented significant differences in infiltration between low-risk and high-risk groups (**Figure 10A**). Although eosinophils, monocytes, and CD56 dim natural killer cells were not highly enriched in the high-risk group, a mild increase was still noted in eosinophils and monocytes. The expression of immune cell markers was displayed in a heatmap (**Figure 10B**). Next, the ESTIMATE algorithm was applied to evaluate the immune and stromal activity in the LGG tumor microenvironment. The results disclosed that the immune and stromal activities were

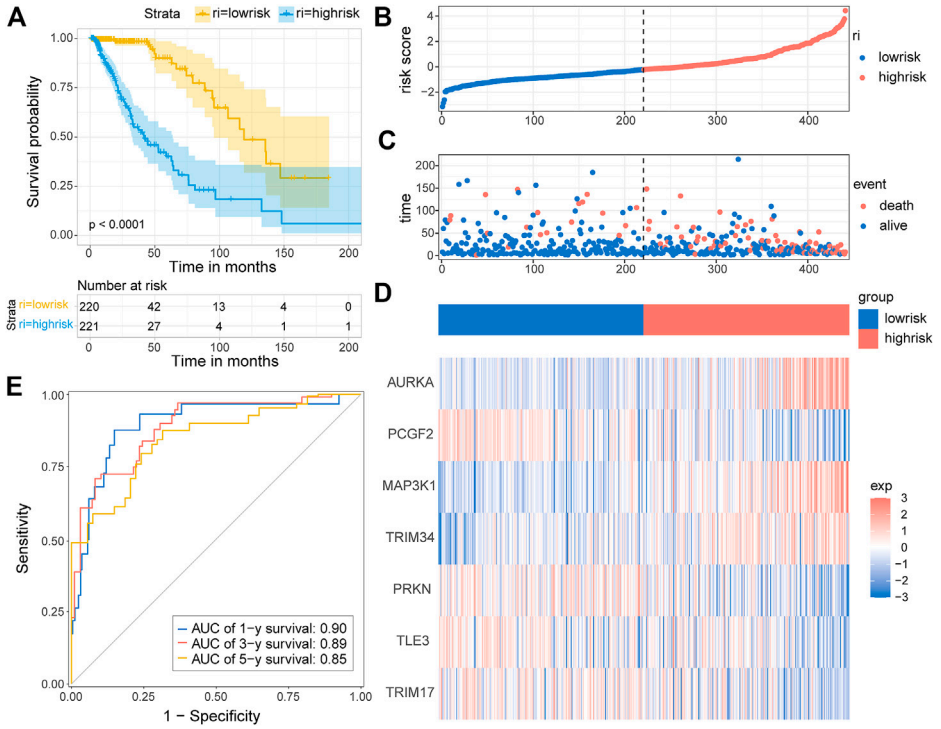


**FIGURE 5 |** Distribution and prognostic analysis of the E3RG prognostic signature in the TCGA cohort. **(A)** Kaplan–Meier curves of overall survival for the patients in the high-risk group and the low-risk group of the TCGA cohort. The distribution plots **(B)**, corresponding survival status **(C)**, and the expression of the seven signature genes **(D)** in the TCGA cohort. **(E)** Time-dependent ROC curve validation of the predictive capacity of the risk signature in the TCGA cohort.

significantly elevated in the high-risk group, which might provide evidence for the contribution of an inflammatory environment of LGG as well (**Figures 10C,D**). Correlation analysis was performed, and potential relations between the risk score signature and each TIME cell type are shown in **Figure 10E**. A significant positive correlation between the risk score and TIME cell infiltration was observed, except for eosinophils, monocytes, and CD56 dim natural killer cells. The risk score was proven to be positively correlated with the expression of immune checkpoint molecules (**Figure 10F**), implying the meaningful roles of risk score signature in predicting the possible response of LGG patients to clinical immunotherapy.

## Function Analysis of Substrates of E3-Related Gene Risk Signature in Low-Grade Gliomas

To acquire a better understanding of the potential biological function of the risk signature, the potential substrates of E3-related gene signature were searched on Ubibrowser 2.0 (http://ubibrowser.bio-it.cn/ubibrowser_v3/). The known substrates were applied for protein–protein interaction network analysis using the STRING database (https://cn.string-db.org/). A PPI network of 76 substrates of the risk signature, including 69 nodes and 772 edges, was constructed using the STRING database (**Figure 11A**). The top 10 hub genes with the highest linkage degrees were obtained using the MCC algorithm of the cytoHubba plugin in Cytoscape3.9.1. These genes included PARK2, VDAC1, DNM1L, MFN2, MFN1, PINK1, TOMM20, PARK7, BCL2L1, and SNCA (**Figure 11B**). To disclose the potential biological functions of the substrates that were involved, GO and KEGG pathway analyses were performed. GO analysis presented high enrichment in neuron death (regulation of neuron death, neuron death, negative regulation of neuron death, apoptotic mitochondrial changes, and death domain binding) and ubiquitin-related functions (ubiquitin-like protein ligase binding and ubiquitin–protein ligase binding) (**Figure 11C**). KEGG pathway analysis results demonstrated that the substrates were mostly correlated with neurodegeneration (pathways of neurodegeneration, Parkinson's disease, and amyotrophic lateral sclerosis), cell death (mitophagy, apoptosis, and autophagy), and immune response (NOD-like receptor signaling pathway, PD-L1 expression, and PD-1 checkpoint pathway in cancer) (**Figure 11D**).

## DISCUSSION

In the past few decades, overwhelming evidence indicates that E3 ubiquitin ligases play pivotal roles in tumorigenesis, cancer progression, and treatment responses. Since E3 ligases determine the targets of the UPS, they play an essential role in cellular functions. They take part in biological processes,

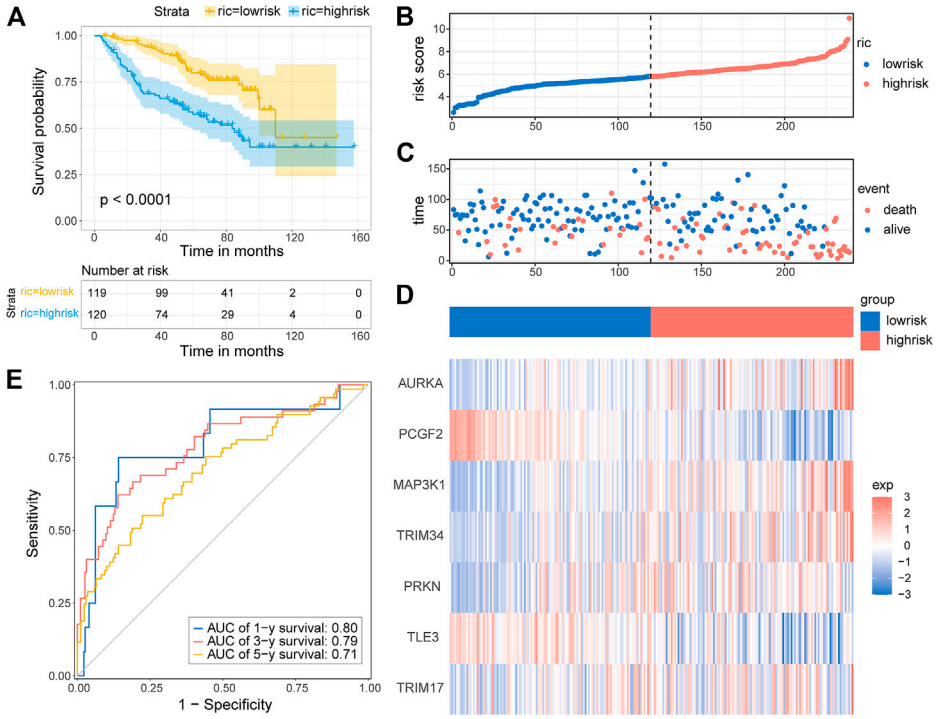


**FIGURE 6 |** Validation of the E3RG prognostic signature in the CGGA cohort. **(A)** Kaplan–Meier curves of the overall survival in the high-risk group and low-risk group of the CGGA cohort. The distribution plots **(B)**, survival status **(C)**, and the expression of seven signature genes **(D)** in the CGGA cohort. **(E)** Time-dependent ROC curve validation of the predictive capacity of the risk signature in the CGGA cohort.

including but not limited to apoptosis, cell growth, senescence, proliferation, immune system evasion, metabolism, DNA repair, inflammation, invasion, metastasis, and angiogenesis. In GBM, alterations in EGFR are commonly seen (Brennan et al., 2013). EGFR could be downregulated by PARK2 but increased by TRIM11; both are E3 ligases possessing opposite effects on EGFR (Di et al., 2013; Lin et al., 2015). The PI3K/Akt pathway is altered in approximately 90% of GBM cases (Brennan et al., 2013). The PI3K/Akt signaling could be modulated by the $SCF^{\beta-TrCP}$ complex and $SCF^{Skp2}$ complex and regulate the proliferation of primary GBM cell lines, glioma stem cells (GSCs), and established GBM cell line models (Winston et al., 1999; Li et al., 2009; Yang et al., 2009; Chan et al., 2012; Feng et al., 2014). Hence, more and more E3 ubiquitin ligases emerge as potential targets of drug designs for cancer therapies as they own better specificity for the recognition of substrates.

In this study, we first identified 38 DEGs with survival significance, in which seven DEGs showed strong prognostic performance and constituted a risk signature. The signature consists of AURKA, MAP3K1, TRIM34, PCGF2, PRKN, TLE3, and TRIM17. Patients in the high-risk group were more likely to have a worse prognosis compared with the ones in the low-risk group. Among the seven genes of the risk signature, many have been reported in glioma pathogenesis. Aurora kinase A (AURKA) has emerged as a drug target for glioblastoma for being highly involved in cell proliferation, migration, and invasion (Wang et al., 2018; Nguyen et al., 2021). MAP3K1 might promote glioma stem cell progression and be positively associated with resistance to temozolomide (TMZ) and radiotherapy (Bi et al., 2020; Wang et al., 2020). PRKN, first found to be mutated in patients with early-onset Parkinson's disease, has also been confirmed to carry mutations and deletions in human malignancies including glioblastoma, colon cancer, and lung cancers (Veeriah et al., 2010). In addition, PRKN inhibits glioma cell growth *in vitro* and *in vivo* by downregulating the intracellular levels of β-catenin and EGFR, leading to decreased activation of both Wnt- and EGF-stimulated pathways (Lin et al., 2015). Although having not been reported in glioma-related research, TRIM34, PCGF2, TLE3, and TRIM17 have been revealed to contribute to the carcinogenesis of other cancers. TRIM34 appears to attenuate colon inflammation and tumorigenesis by sustaining barrier integrity, highlighting its role in immune responses (Lian et al., 2021). PCGF2 serves as a tumor suppressor in breast cancer, gastric cancer, and colon cancer probably for the negative regulation of Akt activation (Wang et al., 2009; Guo et al., 2010; Zhang et al., 2010). TLE3 expression is positively correlated with taxane sensitivity in patients with ovarian carcinoma but not breast cancer (Samimi et al., 2012; Bartlett et al., 2015). TRIM17 augments BRAF-targeted therapy sensitivity of melanoma cells by preventing BCL2A1 from being ubiquitinated and degraded by TRIM28 (Lionnard et al., 2019). The studies mentioned earlier once again

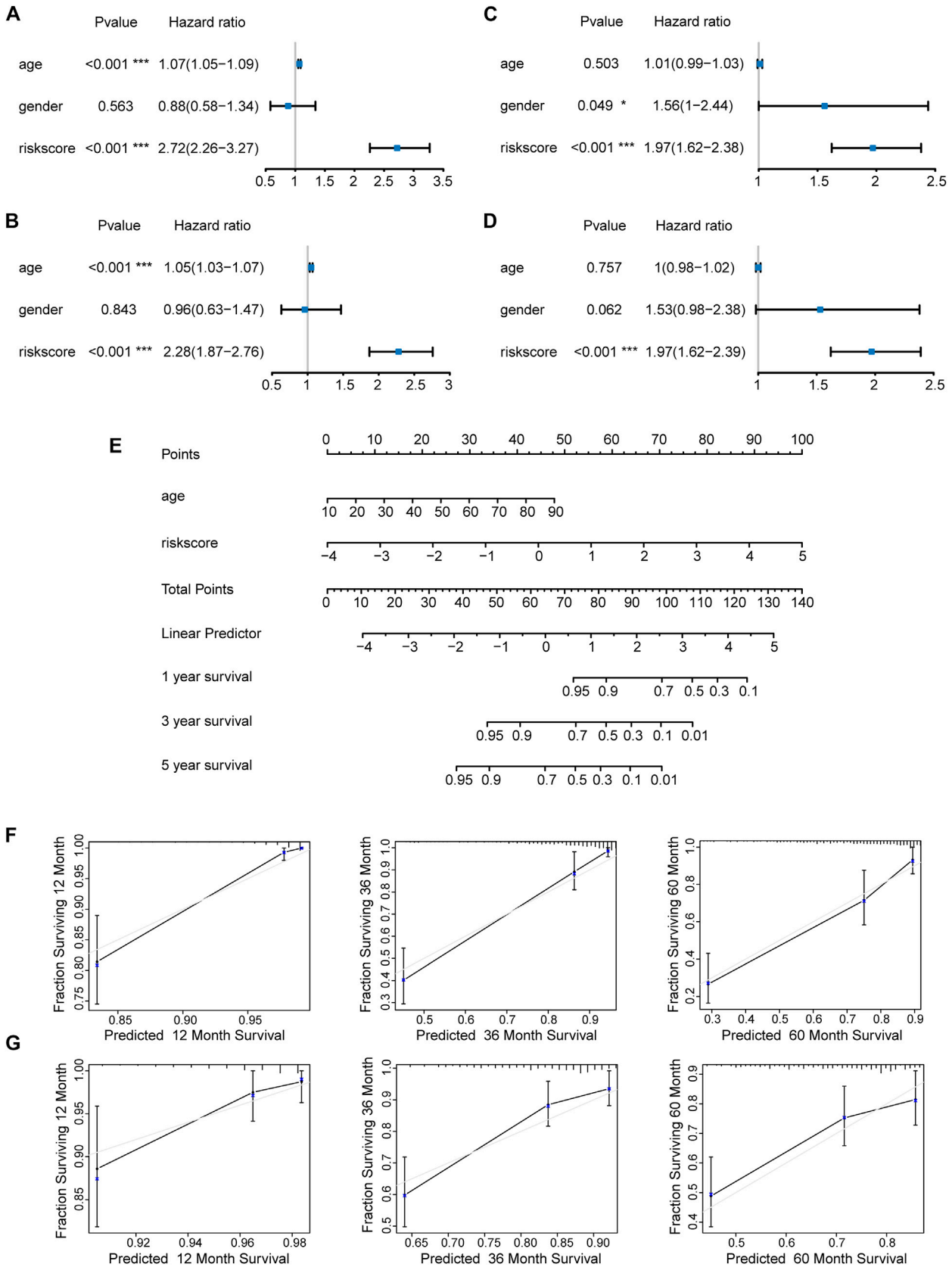


**FIGURE 7 |** Construction and evaluation of a nomogram. Independent prognostic factors were identified by univariate and multivariate Cox regression analyses

(*Continued*)

**FIGURE 7 |** regarding overall survival in the TCGA cohort **(A,B)** and the CGGA cohort **(C,D)** (*$p < 0.05$; ***$p < 0.001$). **(E)** Construction of a nomogram based on the independent prognostic values in the TCGA cohort. The calibration curves between predicted and observed 1-year, 3-year, and 5-year outcomes of nomograms in the TCGA cohort **(F)** and the CGGA cohort **(G)**. Gray diagonal line represented ideal prediction.

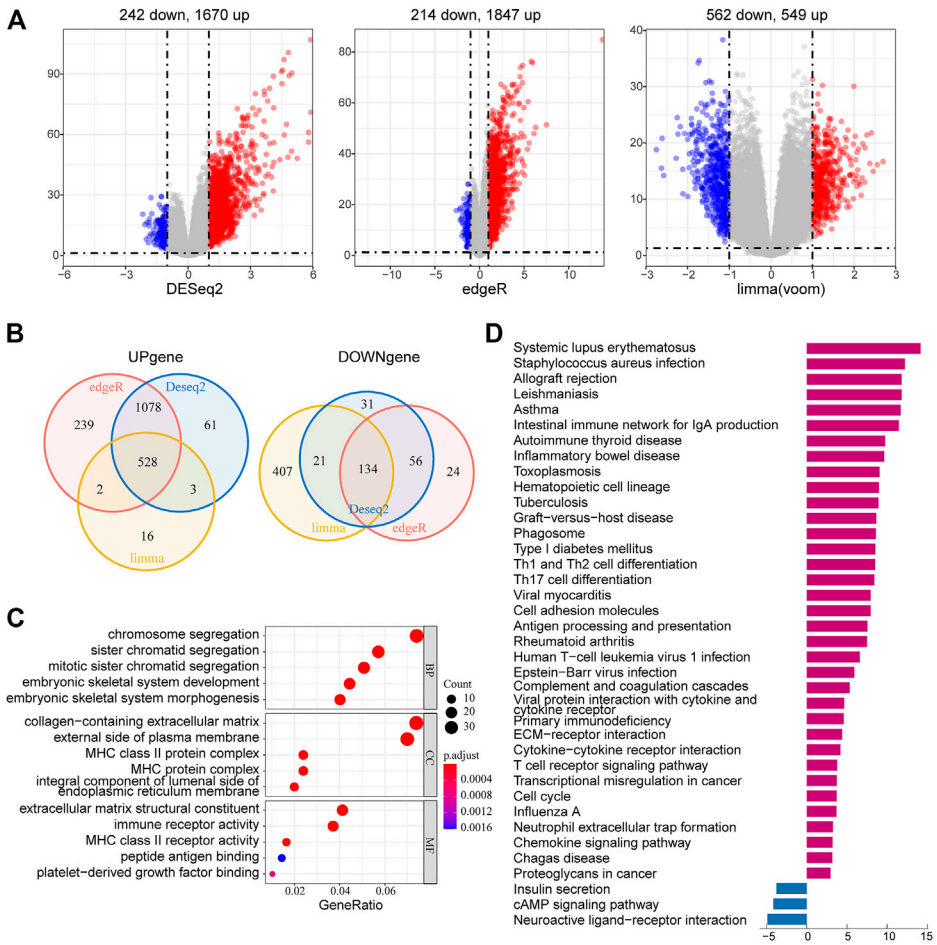


**FIGURE 8 |** Identification and functional enrichment analyses of risk-related DEGs. **(A)** Volcano plot of risk-related DEGs between the high-risk group and low-risk group identified using edgeR, limma, and DESeq2 algorithms, with the cut-off criterion $p < 0.05$ and $|\log_2 FC| \geq 1$. Blue dots: significantly downregulated genes; red dots: significantly upregulated genes. **(B)** Venn diagram of the overlapping risk-related DEGs screened by the three differential expression analyses. **(C)** GO analysis of risk-related DEGs with three terms biological processes, cellular components, and molecular functions (P.adjust < 0.05). **(D)** KEGG pathways enriched in the upregulated and downregulated risk-related DEGs (P.adjust < 0.01).

address the potent roles of our risk genes in modulating cancer biological functions.

We screened the DEGs between high-risk and low-risk groups and performed the GO and KEGG pathway analyses. GO analysis revealed that the DEGs were enriched in extracellular matrix–related (ECM-related) functions in the high-risk group. The glioma ECM has several unique characteristics that make it distinct from the ECM of normal brain tissue. Glioma cells express components such as tenascin-C, fibronectin, and thrombospondin, which support the adhesion and migration of glioma cells. Furthermore, signals driven by the ECM also help shape tumor phenotypes (Sood et al., 2019). Our result corroborated that glioma ECM is tightly related to tumor cell proliferation and differentiation and poor prognosis. In addition, DEG high enrichment was observed in several immune-related biological processes such as MHC-related complex and immune receptor activity. The glioma TIME has diverse cell types and immune cell infiltration which consequently create a field of dynamic cytokine and chemokine communication. MHCII is expressed in different types of gliomas and is associated with increased infiltration of

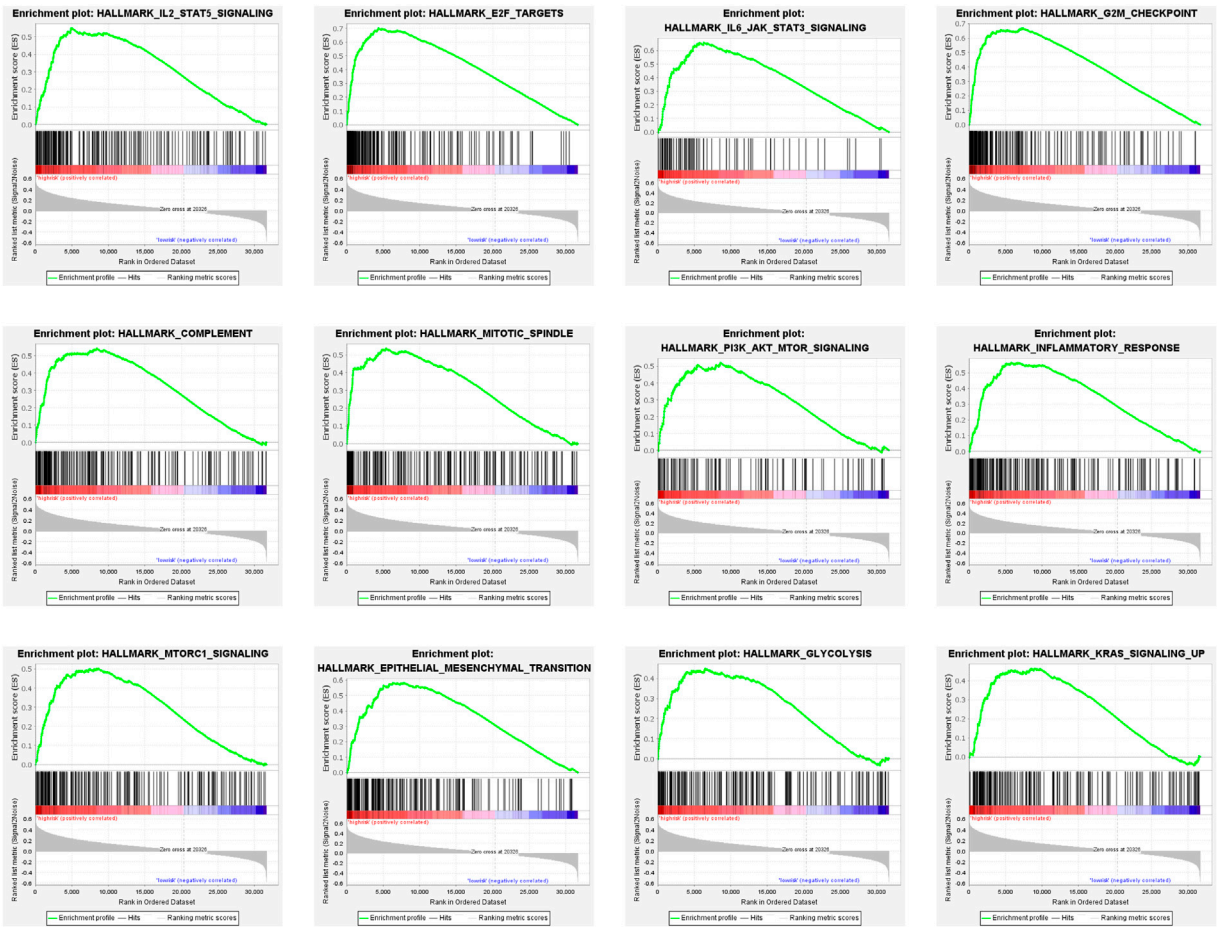


**FIGURE 9 |** Gene set enrichment analysis (GSEA) of DEGs in the high-risk group.

T cells. Both clinical and transcriptomic data have uncovered that tumoral MHCII is tightly correlated with poor prognosis and immune responses (Chih et al., 2021, 01). The KEGG pathway enrichment analysis showed that risk-related DEGs were primarily intensified in immune-related pathways and cell adhesion molecules. Accordingly, both pathways contribute to the invasion and metastasis of glioma.

GSEA results showed that pathways related to inflammatory responses were enriched in the high-risk group. Previous research indicates that about 15–20% of cancer cases suffer infection, chronic inflammation, or autoimmunity in the same tissue before solid tumor formation (Grivennikov et al., 2010). Meanwhile, the inflammatory nature of the tumor microenvironment promotes the development and survival of tumors (Mantovani et al., 2008). IL-2/STAT5 signaling is crucial for the regulation of regulatory T cells and immune tolerance (Shi et al., 2018). Similarly, the IL6-JAK-STAT3 signaling pathway may promote tumor cell proliferation, invasion, and metastasis and suppress immune response (Johnson et al., 2018). In addition, inflammatory responses and complement-related pathways could affect the tumorigenesis, immune surveillance, and immunotherapy response (Greten and Grivennikov, 2019). Our study showed the enrichment of the immune-related pathways in the high-risk group, which emphasized their significant roles in glioma prognosis. Furthermore, pathways that facilitate tumorigenesis and progression were also enriched in the high-risk group. The PI3K/AKT/mTOR pathway is widely dysregulated almost in all human cancers and is pivotal to cancer cell proliferation, survival, and therapy resistance (Cirone, 2021; Pungsrinont et al., 2021). Mutations within genes of this signaling pathway are the most common events occurring in solid malignancies including glioma (Baghery Saghchy Khorasani et al., 2021). mTORC1, one of the mTOR forms, comprises mTOR, raptor, GβL, and deptor. In particular, mTORC1 signaling is mainly involved in cell growth and metabolism (Unni and Arteaga, 2019). Furthermore, AKT/PI3K signaling could indirectly activate mTORC1 by the phosphorylation of PRAS40, a known mTORC1 inhibitor (Sancak et al., 2007; Thedieck et al., 2007; Vander Haar et al., 2007; Wang et al., 2007). Activated mTORC1 signaling may trigger recurrent reprograming that helps escape from glycolytic addiction in cancer cell lines from various solid tumor types (Pusapati et al.,

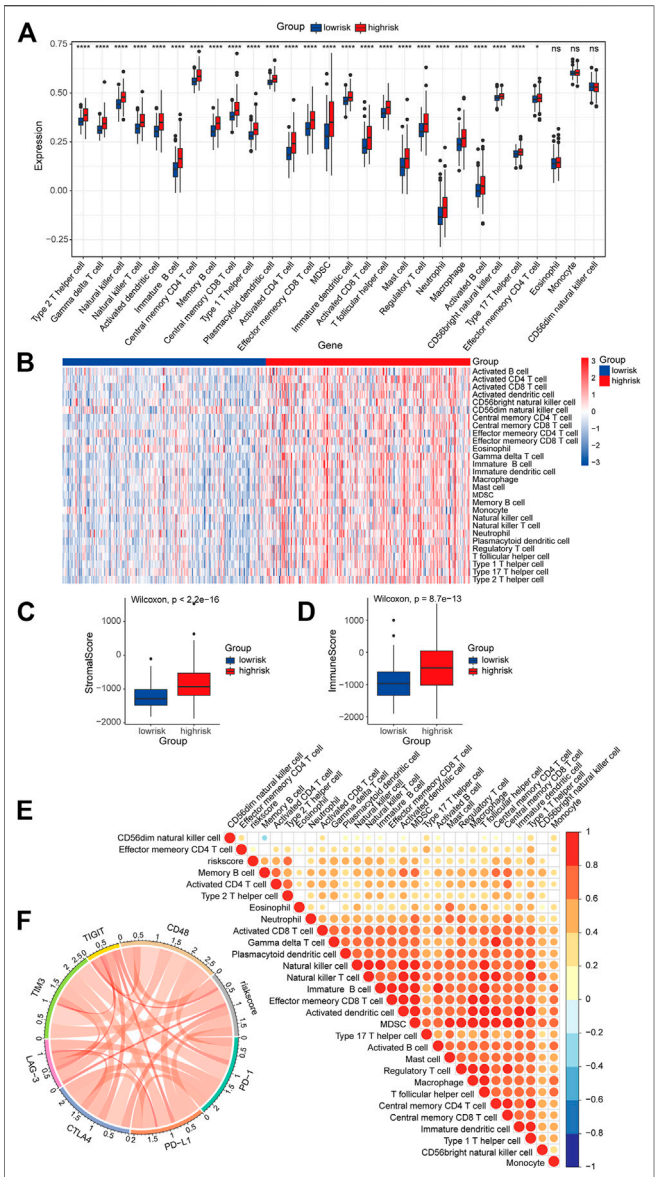


**FIGURE 10 |** Role of the risk signature in the TIME. **(A)** ssGSEA scores of the 28 immune cells in the high-risk group and the low-risk group (*$p < 0.05$; ****$p < 0.0001$; ns, not significant). **(B)** Heatmap of the expression of the immune cell markers in the low-risk and the high-risk groups. **(C,D)** Differences in overall immune and stromal activity between the high-risk group and the low-risk group using the ESTIMATE algorithm. **(E)** Correlation between the risk signature and 28 TIME cell infiltration. **(F)** Correlation between the risk signature and immune checkpoints.

2016). Recently, treatments targeting PI3K/AKT/mTOR and mTORC1 pathways have emerged as promising strategies in cancer therapeutics (Yang et al., 2019; Peng et al., 2022). Epithelial–mesenchymal transition (EMT) is a process that the majority of tumors have gone through during tumor progression. The role of EMT in tumorigenesis has been extensively investigated in different cancers including glioma (Lee et al., 2006; Phillips et al., 2006; Hugo et al., 2007; Thiery et al., 2009; Zarkoob et al., 2013). Activated EMT has also been found to be associated with the generation of cancer stem cells (Ye and Weinberg, 2015). KRAS gene polymorphisms are associated with the risk of glioma (Guan et al., 2021). Collectively, GSEA results suggested that LGG patients with high-risk scores tend to develop a faster deterioration than patients with the low-risk scores.

Recently, a growing body of studies has demonstrated how E3 ligases function in the tumor microenvironment (Do et al., 2022; Hosein et al., 2022; Iwamoto et al., 2022). The tumor microenvironment consists of different cells, including tumor cells, tumor stem cells, and stromal cells. These cells form a complex network and interact with one another to regulate tumor malignant behaviors and treatment resistance. Growth factors, chemokines, and cytokines released by immune cells are widely involved in tumor progression and therapy responses (Bindea et al., 2013). Here, we assessed the infiltration level of 28 TIME immune cells in the high- and low-risk groups to explore the roles of identified signature genes. By ssGSEA, our results showed that 25 out of 28 immune cells are more abundant in the high-risk group than in the low-risk group. In line with other studies, macrophages seem to constitute a majority of infiltration in low-grade gliomas (Rossi et al., 1988; Mieczkowski et al., 2015). These could be important findings since it has been shown that the infiltration of macrophages is highly associated with shorter overall survival in low-grade glioma (Müller et al., 2017). Our study observed the increase of most immune cells infiltrated in the high-risk group, which might be correlated with poor prognosis. The immune activity and stromal activity were remarkably elevated in the high-risk group, which once again reiterated the heterogeneity of the glioma TIME between the two groups. Determining the roles of the signature genes in TIME cell infiltration heterogeneity will be beneficial to better understand the mechanisms of the TIME antitumor immune response and developing novel immunotherapy strategies (Kim et al., 2022; Ogino et al., 2022; Tian et al., 2022).

Previous studies have identified different immune checkpoint molecules in gliomas, such as CTLA-4, TIM-3, PD-1, CD48, and LAG3 (Chouaib, 2020). Immunotherapy-targeting immune checkpoint proteins have been found to trigger an antitumor immune response (Zeng et al., 2013; Reardon et al., 2016; Boussiotis and Charest, 2018). Therefore, we evaluated the correlation between the risk score and the expression of immune checkpoint molecules. It is worth noting that the risk scores were positively correlated with the expression of immune checkpoint molecules. These results implied the involvement of the signature genes in the pathogenesis of the gliomas *via* regulating immune-related pathways. Accordingly, a preliminary function analysis for the predicted substrates of the risk signature was used. The results suggested that the substrates might regulate the pathways of cell death and immune responses. This partially explained better responses of individuals with high-risk scores to immunotherapies. Yet,

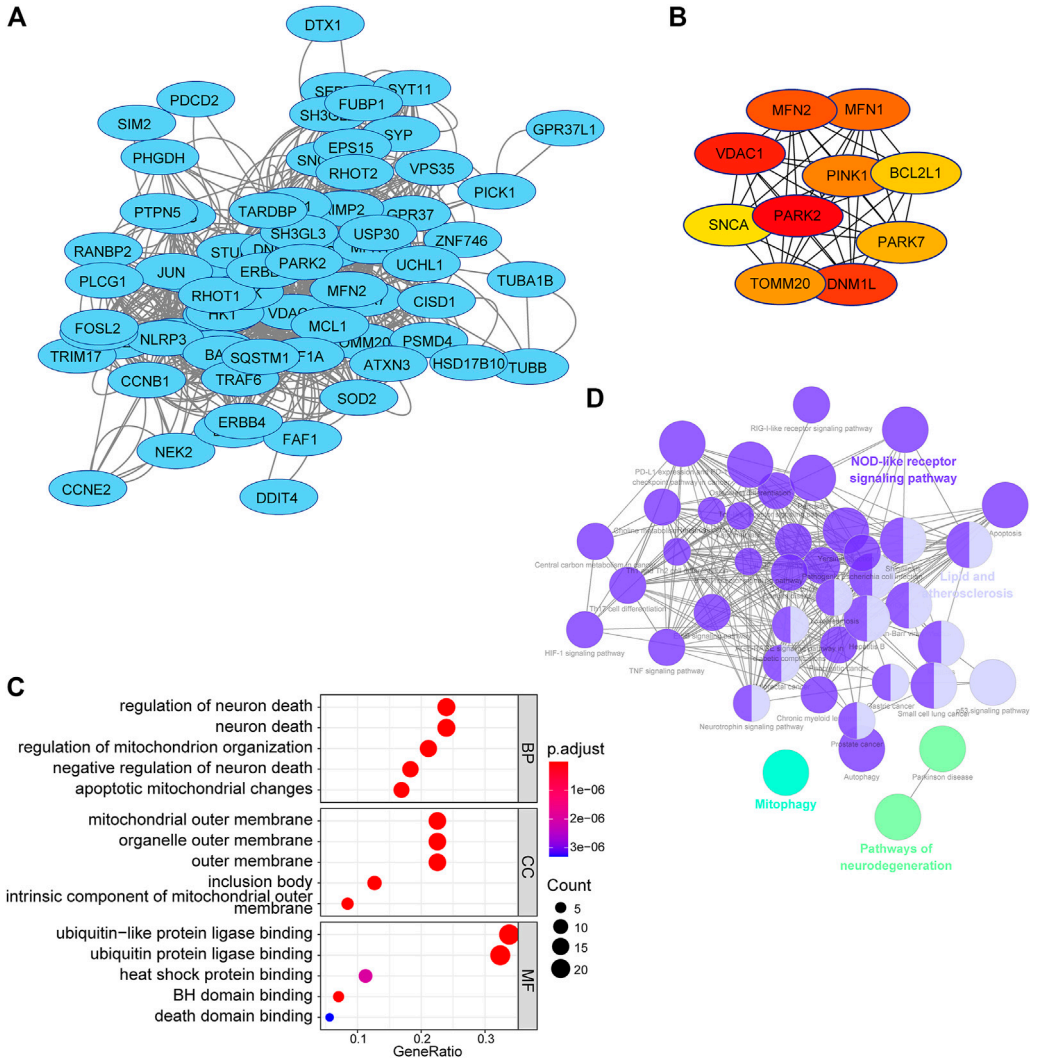


**FIGURE 11 |** PPI network and functional analysis of substrates of the E3RG signature in LGG. **(A)** PPI network of substrates of the E3RG signature obtained with interaction scores > 0.4 based on the STRING online database and visualized using Cytoscape. **(B)** Top 10 hub genes identified using the MCC algorithm of the cytoHubba plugin in Cytoscape. **(C)** GO analysis of substrates of the E3RG signature with three terms biological processes, cellular components, and molecular functions (P.adjust < 0.05). **(D)** KEGG pathways enriched in the substrates of the E3RG signature analyzed using ClueGO plugin in Cytoscape ($p$ < 0.01).

these results further verified the reliability of the risk model in predicting LGG prognosis.

Here, we constructed a prognostic model based on E3RGs and a relevant nomogram in LGG. Of note, we identified a risk signature in the TCGA dataset, which consisted predominately of Caucasian and African American cases. Then, we validated the effect of the risk signature in the CGGA dataset which consisted of Chinese patients. The similar survival analysis results observed in both training and validation sets proved that our model could predict LGG prognosis in varying ethnicities. Therefore, the predictive capability of this model could be beneficial to clinical decision-making with LGG patients. Nevertheless, the construction and validation of the risk model were accomplished by retrospective analysis. Prospective clinical research needs to be rendered for further validation of this model. Moreover, the molecular mechanism of the genes in the risk model requires in-depth investigation in the future.

## CONCLUSION

In summary, by differential expression analyses following univariate Cox regression analysis and log-rank statistical test, E3-related DEGs with a prognostic value were identified. A seven-gene risk signature was constructed using the LASSO-Cox regression model. The risk signature achieved good performance in predicting the prognosis of LGG. Patients with

high-risk scores were more likely to have a poor prognosis compared with the ones with low-risk scores. Functional analyses of the risk signature were performed. This study is expected to benefit the diagnosis and the potential therapeutics of low-grade glioma.

## DATA AVAILABILITY STATEMENT

The datasets presented in this study can be found in online repositories. The names of the repository/repositories and accession number(s) can be found in the article/**Supplementary Material**.

## AUTHOR CONTRIBUTIONS

ST and PW conceived and designed the study. ST and JZ performed the literature review and conceptualization. ST and PW performed the statistical analyses and wrote the original draft. XS and RS revised the manuscript. All authors read and approved the final manuscript.

## FUNDING

This study was supported by grants from the National Natural Science Foundation of China (Grant Number: 81771155). This study was approved by the Ethics Committee of Qilu Hospital of Shandong University.

## SUPPLEMENTARY MATERIAL

The Supplementary Material for this article can be found online at: https://www.frontiersin.org/articles/10.3389/fgene.2022.905047/full#supplementary-material

## REFERENCES

Baghery Saghchy Khorasani, A., Pourbagheri-Sigaroodi, A., Pirsalehi, A., Safaroghli-Azar, A., Zali, M. R., and Bashash, D. (2021). The PI3K/Akt/mTOR Signaling Pathway in Gastric Cancer; from Oncogenic Variations to the Possibilities for Pharmacologic Interventions. *Eur. J. Pharmacol.* 898, 173983. doi:10.1016/j.ejphar.2021.173983

Bartlett, J. M. S., Nielsen, T. O., Nielsen, T. O., Gao, D., Gelmon, K. A., Quintayo, M. A., et al. (2015). TLE3 Is Not a Predictive Biomarker for Taxane Sensitivity in the NCIC CTG MA.21 Clinical Trial. *Br. J. Cancer* 113, 722–728. doi:10.1038/bjc.2015.271

Bi, C.-L., Liu, J.-F., Zhang, M.-Y., Lan, S., Yang, Z.-Y., and Fang, J.-S. (2020). LncRNA NEAT1 Promotes Malignant Phenotypes and TMZ Resistance in Glioblastoma Stem Cells by Regulating let-7g-5p/MAP3K1 axis. *Biosci. Rep.* 40, BSR20201111. doi:10.1042/BSR20201111

Bindea, G., Mlecnik, B., Tosolini, M., Kirilovsky, A., Waldner, M., Obenauf, A. C., et al. (2013). Spatiotemporal Dynamics of Intratumoral Immune Cells Reveal the Immune Landscape in Human Cancer. *Immunity* 39, 782–795. doi:10.1016/j.immuni.2013.10.003

Blanche, P., Dartigues, J.-F., and Jacqmin-Gadda, H. (2013). Estimating and Comparing Time-dependent Areas under Receiver Operating Characteristic Curves for Censored Event Times with Competing Risks. *Stat. Med.* 32, 5381–5397. doi:10.1002/sim.5958

Boussiotis, V. A., and Charest, A. (2018). Immunotherapies for Malignant Glioma. *Oncogene* 37, 1121–1141. doi:10.1038/s41388-017-0024-z

Brat, D. J., Verhaak, R. G. W., Aldape, K. D., Yung, W. K. A., Salama, S. R., Cooper, L. A. D., et al. (2015). Comprehensive, Integrative Genomic Analysis of Diffuse Lower-Grade Gliomas. *N. Engl. J. Med.* 372, 2481–2498. doi:10.1056/NEJMoa1402121

Brennan, C. W., Verhaak, R. G., McKenna, A., Campos, B., Noushmehr, H., Salama, S. R., et al. (2013). The Somatic Genomic Landscape of Glioblastoma. *Cell* 155, 462–477. doi:10.1016/j.cell.2013.09.034

Buetow, L., and Huang, D. T. (2016). Structural Insights into the Catalysis and Regulation of E3 Ubiquitin Ligases. *Nat. Rev. Mol. Cell Biol.* 17, 626–642. doi:10.1038/nrm.2016.91

Chan, C.-H., Li, C.-F., Yang, W.-L., Gao, Y., Lee, S.-W., Feng, Z., et al. (2012). The Skp2-SCF E3 Ligase Regulates Akt Ubiquitination, Glycolysis, Herceptin Sensitivity, and Tumorigenesis. *Cell* 151, 913–914. doi:10.1016/j.cell.2012.10.025

Charoentong, P., Finotello, F., Angelova, M., Mayer, C., Efremova, M., Rieder, D., et al. (2017). Pan-cancer Immunogenomic Analyses Reveal Genotype-Immunophenotype Relationships and Predictors of Response to Checkpoint Blockade. *Cell Rep.* 18, 248–262. doi:10.1016/j.celrep.2016.12.019

Chih, Y., Sahm, K., Sadik, A., Bunse, T., Trautwein, N., Pusch, S., et al. (2021). KS01.3.A Tumoral MHC Class II Expression in Gliomas Drives T Cell Exhaustion. *Neuro-Oncology* 23, ii3. ii3–ii3. doi:10.1093/neuonc/noab180.007

Chouaib, S. (Editor) (2020). *Autophagy in Immune Response: Impact on Cancer Immunotherapy* (London ; San Diego, CA: Academic Press).

Cirone, M. (2021). Cancer Cells Dysregulate PI3K/AKT/mTOR Pathway Activation to Ensure Their Survival and Proliferation: Mimicking Them Is a Smart Strategy of Gammaherpesviruses. *Crit. Rev. Biochem. Mol. Biol.* 56, 500–509. doi:10.1080/10409238.2021.1934811

Claus, E. B., Walsh, K. M., Wiencke, J. K., Molinaro, A. M., Wiemels, J. L., Schildkraut, J. M., et al. (2015). Survival and Low-Grade Glioma: the Emergence of Genetic Information. *Foc* 38, E6. doi:10.3171/2014.10.FOCUS12367

Deng, L., Meng, T., Chen, L., Wei, W., and Wang, P. (2020). The Role of Ubiquitination in Tumorigenesis and Targeted Drug Discovery. *Sig Transduct. Target Ther.* 5, 11. doi:10.1038/s41392-020-0107-0

Di, K., Linskey, M. E., and Bota, D. A. (2013). TRIM11 Is Overexpressed in High-Grade Gliomas and Promotes Proliferation, Invasion, Migration and Glial Tumor Growth. *Oncogene* 32, 5038–5047. doi:10.1038/onc.2012.531

Do, T. T., Yeh, C.-C., Wu, G.-W., Hsu, C.-C., Chang, H.-C., and Chen, H.-C. (2022). TRIM37 Promotes Pancreatic Cancer Progression through Modulation of Cell Growth, Migration, Invasion, and Tumor Immune Microenvironment. *Ijms* 23, 1176. doi:10.3390/ijms23031176

Feng, H., Lopez, G. Y., Kim, C. K., Alvarez, A., Duncan, C. G., Nishikawa, R., et al. (2014). EGFR Phosphorylation of DCBLD2 Recruits TRAF6 and Stimulates AKT-Promoted Tumorigenesis. *J. Clin. Invest.* 124, 3741–3756. doi:10.1172/JCI73093

Friedman, J., Hastie, T., and Tibshirani, R. (2010). Regularization Paths for Generalized Linear Models via Coordinate Descent. *J. Stat. Softw.* 33, 1–22. doi:10.18637/jss.v033.i01

Gittleman, H., Sloan, A. E., and Barnholtz-Sloan, J. S. (2020). An Independently Validated Survival Nomogram for Lower-Grade Glioma. *Neuro Oncol.* 22, 665–674. doi:10.1093/neuonc/noz191

Greten, F. R., and Grivennikov, S. I. (2019). Inflammation and Cancer: Triggers, Mechanisms, and Consequences. *Immunity* 51, 27–41. doi:10.1016/j.immuni.2019.06.025

Grivennikov, S. I., Greten, F. R., and Karin, M. (2010). Immunity, Inflammation, and Cancer. *Cell* 140, 883–899. doi:10.1016/j.cell.2010.01.025

Gu, Z., Gu, L., Eils, R., Schlesner, M., and Brors, B. (2014). Circlize Implements and Enhances Circular Visualization in R. *Bioinformatics* 30, 2811–2812. doi:10.1093/bioinformatics/btu393

Guan, Q., Yuan, L., Lin, A., Lin, H., Huang, X., Ruan, J., et al. (2021). KRAS Gene Polymorphisms Are Associated with the Risk of Glioma: a Two-Center Case-Control Study. *Transl. Pediatr.* 10, 579–586. doi:10.21037/tp-20-359

Guo, B.-H., Zhang, X., Zhang, H.-Z., Lin, H.-L., Feng, Y., Shao, J.-Y., et al. (2010). Low Expression of Mel-18 Predicts Poor Prognosis in Patients with Breast Cancer. *Ann. Oncol.* 21, 2361–2369. doi:10.1093/annonc/mdq241

Haar, E. V., Lee, S.-I., Bandhakavi, S., Griffin, T. J., and Kim, D.-H. (2007). Insulin Signalling to mTOR Mediated by the Akt/PKB Substrate PRAS40. *Nat. Cell Biol.* 9, 316–323. doi:10.1038/ncb1547

Hänzelmann, S., Castelo, R., and Guinney, J. (2013). GSVA: Gene Set Variation Analysis for Microarray and RNA-Seq Data. *BMC Bioinforma.* 14, 7. doi:10.1186/1471-2105-14-7

Hosein, A. N., Dangol, G., Okumura, T., Roszik, J., Rajapakshe, K., Siemann, M., et al. (2022). Loss of Rnf43 Accelerates Kras-Mediated Neoplasia and Remodels the Tumor Immune Microenvironment in Pancreatic Adenocarcinoma. *Gastroenterology* 162, 1303–1318. e18. doi:10.1053/j.gastro.2021.12.273

Hugo, H., Ackland, M. L., Blick, T., Lawrence, M. G., Clements, J. A., Williams, E. D., et al. (2007). Epithelial-mesenchymal and Mesenchymal-Epithelial Transitions in Carcinoma Progression. *J. Cell. Physiol.* 213, 374–383. doi:10.1002/jcp.21223

Iwamoto, A., Tsukamoto, H., Nakayama, H., and Oshiumi, H. (2022). E3 Ubiquitin Ligase Riplet Is Expressed in T Cells and Suppresses T Cell-Mediated Antitumor Immune Responses. *J. I.* 208, 2067–2076. doi:10.4049/jimmunol.2100096

Johnson, D. E., O'Keefe, R. A., and Grandis, J. R. (2018). Targeting the IL-6/JAK/STAT3 Signalling axis in Cancer. *Nat. Rev. Clin. Oncol.* 15, 234–248. doi:10.1038/nrclinonc.2018.8

Kim, A.-R., Choi, S. J., Park, J., Kwon, M., Chowdhury, T., Yu, H. J., et al. (2022). Spatial Immune Heterogeneity of Hypoxia-Induced Exhausted Features in High-Grade Glioma. *Oncoimmunology* 11, 2026019. doi:10.1080/2162402X.2022.2026019

Lee, J.-H., Liu, R., Li, J., Zhang, C., Wang, Y., Cai, Q., et al. (2017). Stabilization of Phosphofructokinase 1 Platelet Isoform by AKT Promotes Tumorigenesis. *Nat. Commun.* 8, 949. doi:10.1038/s41467-017-00906-9

Lee, T. K., Poon, R. T. P., Yuen, A. P., Ling, M. T., Kwok, W. K., Wang, X. H., et al. (2006). Twist Overexpression Correlates with Hepatocellular Carcinoma Metastasis through Induction of Epithelial-Mesenchymal Transition. *Clin. Cancer Res.* 12, 5369–5376. doi:10.1158/1078-0432.CCR-05-2722

Li, X., Liu, J., and Gao, T. (2009). β-TrCP-Mediated Ubiquitination and Degradation of PHLPP1 Are Negatively Regulated by Akt. *Mol. Cell Biol.* 29, 6192–6205. doi:10.1128/MCB.00681-09

Lian, Q., Yan, S., Yin, Q., Yan, C., Zheng, W., Gu, W., et al. (2021). TRIM34 Attenuates Colon Inflammation and Tumorigenesis by Sustaining Barrier Integrity. *Cell Mol. Immunol.* 18, 350–362. doi:10.1038/s41423-020-0366-2

Lin, D.-C., Xu, L., Chen, Y., Yan, H., Hazawa, M., Doan, N., et al. (2015). Genomic and Functional Analysis of the E3 Ligase PARK2 in Glioma. *Cancer Res.* 75, 1815–1827. doi:10.1158/0008-5472.CAN-14-1433

Lionnard, L., Duc, P., Brennan, M. S., Kueh, A. J., Pal, M., Guardia, F., et al. (2019). TRIM17 and TRIM28 Antagonistically Regulate the Ubiquitination and Anti-apoptotic Activity of BCL2A1. *Cell Death Differ.* 26, 902–917. doi:10.1038/s41418-018-0169-5

Liu, Z., Guo, C., Dang, Q., Wang, L., Liu, L., Weng, S., et al. (2022a). Integrative Analysis from Multi-Center Studies Identities a Consensus Machine Learning-Derived lncRNA Signature for Stage II/III Colorectal Cancer. *EBioMedicine* 75, 103750. doi:10.1016/j.ebiom.2021.103750

Liu, Z., Liu, L., Weng, S., Guo, C., Dang, Q., Xu, H., et al. (2022b). Machine Learning-Based Integration Develops an Immune-Derived lncRNA Signature for Improving Outcomes in Colorectal Cancer. *Nat. Commun.* 13, 816. doi:10.1038/s41467-022-28421-6

Liu, Z., Weng, S., Xu, H., Wang, L., Liu, L., Zhang, Y., et al. (2021). Computational Recognition and Clinical Verification of TGF-β-Derived miRNA Signature with Potential Implications in Prognosis and Immunotherapy of Intrahepatic Cholangiocarcinoma. *Front. Oncol.* 11, 757919. doi:10.3389/fonc.2021.757919

Liu, Z., Xu, H., Ge, X., Weng, S., Dang, Q., and Han, X. (2022c). Gene Expression Profile Reveals a Prognostic Signature of Non-MSI-H/pMMR Colorectal Cancer. *Front. Cell Dev. Biol.* 10, 790214. doi:10.3389/fcell.2022.790214

Lombardi, G., Barresi, V., Castellano, A., Tabouret, E., Pasqualetti, F., Salvalaggio, A., et al. (2020). Clinical Management of Diffuse Low-Grade Gliomas. *Cancers* 12, 3008. doi:10.3390/cancers12103008

Love, M. I., Huber, W., and Anders, S. (2014). Moderated Estimation of Fold Change and Dispersion for RNA-Seq Data with DESeq2. *Genome Biol.* 15, 550. doi:10.1186/s13059-014-0550-8

Mantovani, A., Allavena, P., Sica, A., and Balkwill, F. (2008). Cancer-related Inflammation. *Nature* 454, 436–444. doi:10.1038/nature07205

Mieczkowski, J., Kocyk, M., Nauman, P., Gabrusiewicz, K., Sielska, M., Przanowski, P., et al. (2015). Down-regulation of IKKβ Expression in Glioma-Infiltrating Microglia/macrophages Is Associated with Defective Inflammatory/immune Gene Responses in Glioblastoma. *Oncotarget* 6, 33077–33090. doi:10.18632/oncotarget.5310

Müller, S., Kohanbash, G., Liu, S. J., Alvarado, B., Carrera, D., Bhaduri, A., et al. (2017). Single-cell Profiling of Human Gliomas Reveals Macrophage Ontogeny as a Basis for Regional Differences in Macrophage Activation in the Tumor Microenvironment. *Genome Biol.* 18, 234. doi:10.1186/s13059-017-1362-4

Nguyen, T. T. T., Shang, E., Shu, C., Kim, S., Mela, A., Humala, N., et al. (2021). Aurora Kinase A Inhibition Reverses the Warburg Effect and Elicits Unique Metabolic Vulnerabilities in Glioblastoma. *Nat. Commun.* 12, 5203. doi:10.1038/s41467-021-25501-x

Ogino, H., Taylor, J. W., Nejo, T., Gibson, D., Watchmaker, P. B., Okada, K., et al. (2022). Randomized Trial of Neoadjuvant Vaccination with Tumor-Cell Lysate Induces T Cell Response in Low-Grade Gliomas. *J. Clin. Invest.* 132, e151239. doi:10.1172/JCI151239

Peng, Y., Wang, Y., Zhou, C., Mei, W., and Zeng, C. (2022). PI3K/Akt/mTOR Pathway and its Role in Cancer Therapeutics: Are We Making Headway? *Front. Oncol.* 12, 819128. doi:10.3389/fonc.2022.819128

Phillips, H. S., Kharbanda, S., Chen, R., Forrest, W. F., Soriano, R. H., Wu, T. D., et al. (2006). Molecular Subclasses of High-Grade Glioma Predict Prognosis, Delineate a Pattern of Disease Progression, and Resemble Stages in Neurogenesis. *Cancer Cell* 9, 157–173. doi:10.1016/j.ccr.2006.02.019

Popovic, D., Vucic, D., and Dikic, I. (2014). Ubiquitination in Disease Pathogenesis and Treatment. *Nat. Med.* 20, 1242–1253. doi:10.1038/nm.3739

Pungsrinont, T., Kallenbach, J., and Baniahmad, A. (2021). Role of PI3K-AKT-mTOR Pathway as a Pro-survival Signaling and Resistance-Mediating Mechanism to Therapy of Prostate Cancer. *Ijms* 22, 11088. doi:10.3390/ijms222011088

Pusapati, R. V., Daemen, A., Wilson, C., Sandoval, W., Gao, M., Haley, B., et al. (2016). mTORC1-Dependent Metabolic Reprogramming Underlies Escape from Glycolysis Addiction in Cancer Cells. *Cancer Cell* 29, 548–562. doi:10.1016/j.ccell.2016.02.018

Qi, S.-M., Dong, J., Xu, Z.-Y., Cheng, X.-D., Zhang, W.-D., and Qin, J.-J. (2021). PROTAC: An Effective Targeted Protein Degradation Strategy for Cancer Therapy. *Front. Pharmacol.* 12, 692574. doi:10.3389/fphar.2021.692574

Que, T., Zheng, H., Zeng, Y., Liu, X., Qi, G., La, Q., et al. (2022). Correction to: HMGA1 Stimulates MYH9-dependent Ubiquitination of GSK-3β via PI3K/Akt/c-Jun Signaling to Promote Malignant Progression and Chemoresistance in Gliomas. *Cell Death Dis.* 13, 164. doi:10.1038/s41419-022-04547-9

Rape, M. (2018). Ubiquitylation at the Crossroads of Development and Disease. *Nat. Rev. Mol. Cell Biol.* 19, 59–70. doi:10.1038/nrm.2017.83

Reardon, D. A., Gokhale, P. C., Klein, S. R., Ligon, K. L., Rodig, S. J., Ramkissoon, S. H., et al. (2016). Glioblastoma Eradication Following Immune Checkpoint Blockade in an Orthotopic, Immunocompetent Model. *Cancer Immunol. Res.* 4, 124–135. doi:10.1158/2326-6066.CIR-15-0151

Reyes-Turcu, F. E., Ventii, K. H., and Wilkinson, K. D. (2009). Regulation and Cellular Roles of Ubiquitin-specific Deubiquitinating Enzymes. *Annu. Rev. Biochem.* 78, 363–397. doi:10.1146/annurev.biochem.78.082307.091526

Rimkus, T. K., Arrigo, A. B., Zhu, D., Carpenter, R. L., Sirkisoon, S., Doheny, D., et al. (2022). NEDD4 Degrades TUSC2 to Promote Glioblastoma Progression. *Cancer Lett.* 531, 124–135. doi:10.1016/j.canlet.2022.01.029

Ritchie, M. E., Phipson, B., Wu, D., Hu, Y., Law, C. W., Shi, W., et al. (2015). Limma Powers Differential Expression Analyses for RNA-Sequencing and Microarray Studies. *Nucleic Acids Res.* 43, e47. doi:10.1093/nar/gkv007

Robinson, M. D., McCarthy, D. J., and Smyth, G. K. (2010). edgeR: a Bioconductor Package for Differential Expression Analysis of Digital Gene Expression Data. *Bioinformatics* 26, 139–140. doi:10.1093/bioinformatics/btp616

Rossi, M. L., Cruz-Sanchez, F., Hughes, J. T., Esiri, M. M., Coakham, H. B., and Moss, T. H. (1988). Mononuclear Cell Infiltrate and HLA-DR Expression in Low Grade Astrocytomas. *Acta Neuropathol.* 76, 281–286. doi:10.1007/BF00687776

Samimi, G., Ring, B. Z., Ross, D. T., Seitz, R. S., Sutherland, R. L., O'Brien, P. M., et al. (2012). TLE3 Expression Is Associated with Sensitivity to Taxane Treatment in Ovarian Carcinoma. *Cancer Epidemiol. Biomarkers Prev.* 21, 273–279. doi:10.1158/1055-9965.EPI-11-0917

Sancak, Y., Thoreen, C. C., Peterson, T. R., Lindquist, R. A., Kang, S. A., Spooner, E., et al. (2007). PRAS40 Is an Insulin-Regulated Inhibitor of the mTORC1 Protein Kinase. *Mol. Cell* 25, 903–915. doi:10.1016/j.molcel.2007.03.003

Schulman, B. A., and Wade Harper, J. (2009). Ubiquitin-like Protein Activation by E1 Enzymes: the Apex for Downstream Signalling Pathways. *Nat. Rev. Mol. Cell Biol.* 10, 319–331. doi:10.1038/nrm2673

Seeler, J.-S., and Dejean, A. (2017). SUMO and the Robustness of Cancer. *Nat. Rev. Cancer* 17, 184–197. doi:10.1038/nrc.2016.143

Shannon, P., Markiel, A., Ozier, O., Baliga, N. S., Wang, J. T., Ramage, D., et al. (2003). Cytoscape: a Software Environment for Integrated Models of Biomolecular Interaction Networks. *Genome Res.* 13, 2498–2504. doi:10.1101/gr.1239303

Shi, H., Liu, C., Tan, H., Li, Y., Nguyen, T.-L. M., Dhungana, Y., et al. (2018). Hippo Kinases Mst1 and Mst2 Sense and Amplify IL-2R-STAT5 Signaling in Regulatory T Cells to Establish Stable Regulatory Activity. *Immunity* 49, 899–914. e6. doi:10.1016/j.immuni.2018.10.010

Sood, D., Tang-Schomer, M., Pouli, D., Mizzoni, C., Raia, N., Tai, A., et al. (2019). 3D Extracellular Matrix Microenvironment in Bioengineered Tissue Models of Primary Pediatric and Adult Brain Tumors. *Nat. Commun.* 10, 4529. doi:10.1038/s41467-019-12420-1

Stewart, M. D., Ritterhoff, T., Klevit, R. E., and Brzovic, P. S. (2016). E2 Enzymes: More Than Just Middle Men. *Cell Res.* 26, 423–440. doi:10.1038/cr.2016.35

Stieren, E. S., El Ayadi, A., Xiao, Y., Siller, E., Landsverk, M. L., Oberhauser, A. F., et al. (2011). Ubiquilin-1 Is a Molecular Chaperone for the Amyloid Precursor Protein. *J. Biol. Chem.* 286, 35689–35698. doi:10.1074/jbc.M111.243147

Szklarczyk, D., Gable, A. L., Lyon, D., Junge, A., Wyder, S., Huerta-Cepas, J., et al. (2019). STRING V11: Protein-Protein Association Networks with Increased Coverage, Supporting Functional Discovery in Genome-wide Experimental Datasets. *Nucleic Acids Res.* 47, D607–D613. doi:10.1093/nar/gky1131

Thedieck, K., Polak, P., Kim, M. L., Molle, K. D., Cohen, A., Jenö, P., et al. (2007). PRAS40 and PRR5-like Protein Are New mTOR Interactors that Regulate Apoptosis. *PLoS One* 2, e1217. doi:10.1371/journal.pone.0001217

Thiery, J. P., Acloque, H., Huang, R. Y. J., and Nieto, M. A. (2009). Epithelial-mesenchymal Transitions in Development and Disease. *Cell* 139, 871–890. doi:10.1016/j.cell.2009.11.007

Tian, T., Liang, R., Erel-Akbaba, G., Saad, L., Obeid, P. J., Gao, J., et al. (2022). Immune Checkpoint Inhibition in GBM Primed with Radiation by Engineered Extracellular Vesicles. *ACS Nano* 16, 1940–1953. doi:10.1021/acsnano.1c05505

Unni, N., and Arteaga, C. L. (2019). Is Dual mTORC1 and mTORC2 Therapeutic Blockade Clinically Feasible in Cancer? *JAMA Oncol.* 5, 1564–1565. doi:10.1001/jamaoncol.2019.2525

Veeriah, S., Taylor, B. S., Meng, S., Fang, F., Yilmaz, E., Vivanco, I., et al. (2010). Somatic Mutations of the Parkinson's Disease-Associated Gene PARK2 in Glioblastoma and Other Human Malignancies. *Nat. Genet.* 42, 77–82. doi:10.1038/ng.491

Wang, J., Zuo, J., Wahafu, A., Wang, M. d., Li, R. c., and Xie, W. f. (2020). Combined Elevation of TRIB2 and MAP3K1 Indicates Poor Prognosis and Chemoresistance to Temozolomide in Glioblastoma. *CNS Neurosci. Ther.* 26, 297–308. doi:10.1111/cns.13197

Wang, L., Harris, T. E., Roth, R. A., and Lawrence, J. C. (2007). PRAS40 Regulates mTORC1 Kinase Activity by Functioning as a Direct Inhibitor of Substrate Binding. *J. Biol. Chem.* 282, 20036–20044. doi:10.1074/jbc.M702376200

Wang, R., Zhang, S., Chen, X., Li, N., Li, J., Jia, R., et al. (2018). EIF4A3-induced Circular RNA MMP9 (circMMP9) Acts as a Sponge of miR-124 and Promotes Glioblastoma Multiforme Cell Tumorigenesis. *Mol. Cancer* 17, 166. doi:10.1186/s12943-018-0911-0

Wang, W., Yuasa, T., Tsuchiya, N., Ma, Z., Maita, S., Narita, S., et al. (2009). The Novel Tumor-Suppressor Mel-18 in Prostate Cancer: its Functional Polymorphism, Expression and Clinical Significance. *Int. J. Cancer* 125, 2836–2843. doi:10.1002/ijc.24721

Warfel, N. A., Niederst, M., Stevens, M. W., Brennan, P. M., Frame, M. C., and Newton, A. C. (2011). Mislocalization of the E3 Ligase, β-Transducin Repeat-Containing Protein 1 (β-TrCP1), in Glioblastoma Uncouples Negative Feedback between the Pleckstrin Homology Domain Leucine-Rich Repeat Protein Phosphatase 1 (PHLPP1) and Akt. *J. Biol. Chem.* 286, 19777–19788. doi:10.1074/jbc.M111.237081

Wesseling, P., and Capper, D. (2018). WHO 2016 Classification of Gliomas. *Neuropathol. Appl. Neurobiol.* 44, 139–150. doi:10.1111/nan.12432

Winston, J. T., Strack, P., Beer-Romero, P., Chu, C. Y., Elledge, S. J., and Harper, J. W. (1999). The SCFbeta -TRCP-Ubiquitin Ligase Complex Associates Specifically with Phosphorylated Destruction Motifs in Ikappa Balpha and Beta -catenin and Stimulates Ikappa Balpha Ubiquitination *In Vitro*. *Genes & Dev.* 13, 270–283. doi:10.1101/gad.13.3.270

Xia, L., Fang, C., Chen, G., and Sun, C. (2018). Relationship between the Extent of Resection and the Survival of Patients with Low-Grade Gliomas: a Systematic Review and Meta-Analysis. *BMC Cancer* 18, 48. doi:10.1186/s12885-017-3909-x

Yang, J., Nie, J., Ma, X., Wei, Y., Peng, Y., and Wei, X. (2019). Targeting PI3K in Cancer: Mechanisms and Advances in Clinical Trials. *Mol. Cancer* 18, 26. doi:10.1186/s12943-019-0954-x

Yang, W.-L., Wang, J., Chan, C.-H., Lee, S.-W., Campos, A. D., Lamothe, B., et al. (2009). The E3 Ligase TRAF6 Regulates Akt Ubiquitination and Activation. *Science* 325, 1134–1138. doi:10.1126/science.1175065

Ye, X., and Weinberg, R. A. (2015). Epithelial-Mesenchymal Plasticity: A Central Regulator of Cancer Progression. *Trends Cell Biol.* 25, 675–686. doi:10.1016/j.tcb.2015.07.012

Yoshihara, K., Shahmoradgoli, M., Martínez, E., Vegesna, R., Kim, H., Torres-Garcia, W., et al. (2013). Inferring Tumour Purity and Stromal and Immune Cell Admixture from Expression Data. *Nat. Commun.* 4, 2612. doi:10.1038/ncomms3612

Yu, G., Wang, L.-G., Han, Y., and He, Q.-Y. (2012). clusterProfiler: an R Package for Comparing Biological Themes Among Gene Clusters. *OMICS A J. Integr. Biol.* 16, 284–287. doi:10.1089/omi.2011.0118

Zangiabadi, S., and Abdul-Sater, A. A. (2022). Regulation of the NLRP3 Inflammasome by Posttranslational Modifications. *J. I.* 208, 286–292. doi:10.4049/jimmunol.2100734

Zarkoob, H., Taube, J. H., Singh, S. K., Mani, S. A., and Kohandel, M. (2013). Investigating the Link between Molecular Subtypes of Glioblastoma, Epithelial-Mesenchymal Transition, and CD133 Cell Surface Protein. *PLoS One* 8, e64169. doi:10.1371/journal.pone.0064169

Zeng, J., See, A. P., Phallen, J., Jackson, C. M., Belcaid, Z., Ruzevick, J., et al. (2013). Anti-PD-1 Blockade and Stereotactic Radiation Produce Long-Term Survival in Mice with Intracranial Gliomas. *Int. J. Radiat. Oncology*Biology*Physics* 86, 343–349. doi:10.1016/j.ijrobp.2012.12.025

Zhang, X.-W., Sheng, Y.-P., Li, Q., Qin, W., Lu, Y.-W., Cheng, Y.-F., et al. (2010). BMI1 and Mel-18 Oppositely Regulate Carcinogenesis and Progression of Gastric Cancer. *Mol. Cancer* 9, 40. doi:10.1186/1476-4598-9-40

Zhao, B., and Burgess, K. (2019). PROTACs Suppression of CDK4/6, Crucial Kinases for Cell Cycle Regulation in Cancer. *Chem. Commun.* 55, 2704–2707. doi:10.1039/c9cc00163h

Zheng, N., and Shabek, N. (2017). Ubiquitin Ligases: Structure, Function, and Regulation. *Annu. Rev. Biochem.* 86, 129–157. doi:10.1146/annurev-biochem-060815-014922

**Conflict of Interest:** The authors declare that the research was conducted in the absence of any commercial or financial relationships that could be construed as a potential conflict of interest.

**Publisher's Note:** All claims expressed in this article are solely those of the authors and do not necessarily represent those of their affiliated organizations, or those of the publisher, the editors, and the reviewers. Any product that may be evaluated in this article, or claim that may be made by its manufacturer, is not guaranteed or endorsed by the publisher.

frontiers | Frontiers in Genetics

TYPE Original Research
PUBLISHED 29 August 2022
DOI 10.3389/fgene.2022.931222



OPEN ACCESS

EDITED BY
Juilee Thakar,
University of Rochester, United States

REVIEWED BY
Xiangqi Meng,
Harbin Medical University, China
Xuejun Li,
Xiangya Hospital, Central South University, China

*CORRESPONDENCE
Yunfei Zha,
zhayunfei999@126.com
Zijun Wu,
963512631@qq.com

SPECIALTY SECTION
This article was submitted to Cancer Genetics and Oncogenomics, a section of the journal Frontiers in Genetics

RECEIVED 28 April 2022
ACCEPTED 05 August 2022
PUBLISHED 29 August 2022

CITATION
Yang Y, Duan M, Zha Y and Wu Z (2022), CENP-A is a potential prognostic biomarker and correlated with immune infiltration levels in glioma patients. *Front. Genet.* 13:931222. doi: 10.3389/fgene.2022.931222



# CENP-A is a potential prognostic biomarker and correlated with immune infiltration levels in glioma patients

Yuan Yang[1], Mengyun Duan[2], Yunfei Zha[1]* and Zijun Wu[1]*

[1]Department of Radiology, Renmin Hospital of Wuhan University, Wuhan, China, [2]Health Science Center, Department of Medical Imaging, Yangtze University, Jingzhou, China

**Background:** Centromeric protein A (*CENP-A*), an essential protein involved in chromosomal segregation during cell division, is associated with several cancer types. However, its role in gliomas remains unclear. This study examined the clinical and prognostic significance of *CENP-A* in gliomas.

**Methods:** Data of patients with glioma were collected from the Cancer Genome Atlas. Logistic regression, the Kruskal–Wallis test, and the Wilcoxon signed-rank test were performed to assess the relationship between *CENP-A* expression and clinicopathological parameters. The Cox regression model and Kaplan–Meier curve were used to analyze the association between *CENP-A* and survival outcomes. A prognostic nomogram was constructed based on Cox multivariate analysis. Gene set enrichment analysis (GSEA) was conducted to identify key *CENP-A*-related pathways and biological processes.

**Results:** *CENP-A* was upregulated in glioma samples. Increased *CENP-A* levels were significantly associated with the world health organization (WHO) grade [Odds ratio (OR) = 49.88 (23.52–129.06) for grade 4 vs. grades 2 and 3], primary therapy outcome [OR = 2.44 (1.64–3.68) for progressive disease (PD) and stable disease (SD) vs. partial response (PR) and complete response (CR)], isocitrate dehydrogenase (IDH) status [OR = 13.76 (9.25–20.96) for wild-type vs. mutant], 1p/19q co-deletion [OR = 5.91 (3.95–9.06) for no codeletion vs. co-deletion], and age [OR = 4.02 (2.68–6.18) for > 60 vs. ≤ 60]. Elevated *CENP-A* expression was correlated with shorter overall survival in both univariate [hazard ratio (HR): 5.422; 95% confidence interval (CI): 4.044–7.271; $p < 0.001$] and multivariate analyses (HR: 1.967; 95% CI: 1.280–3.025; $p < 0.002$). GSEA showed enrichment of numerous cell cycle-and tumor-related pathways in the *CENP-A* high expression phenotype. The calibration plot and C-index indicated the favorable performance of our nomogram for prognostic prediction in patients with glioma.

**Conclusion:** We propose a role for *CENP-A* in glioma progression and its potential as a biomarker for glioma diagnosis and prognosis.

KEYWORDS

**CENP-A, glioma, prognosis, biomarker, microenvironment**

## Introduction

Gliomas are among the most lethal cancers and are characterized by invasive growth within the central nervous system. The intratumoral heterogeneity of gliomas and the intrinsic structure of contribute to tumor progression and treatment resistance (Jackson et al., 2019). Despite current multimodal therapies, including surgical resection and postoperative chemoradiotherapy, the prognosis of gliomas, especially high-grade gliomas, remains low with a median overall survival (OS) of 15 months (Weller et al., 2015). Owing to advances in the molecular genetics of gliomas in the past decade, the diagnostic classification, treatment development, and prognosis monitoring of gliomas have improved (Reifenberger et al., 2017). The novel glioma classification system integrates molecular biomarkers with classic histological features to define glioma entities (Wesseling and Capper, 2018). Additionally, preclinical and clinical studies have explored emerging pharmacological and immunotherapeutic strategies. Predictive molecular profiling has been proposed to guide individualized therapy in patients with glioma (Bi et al., 2020). However, further studies are required to investigate glioma biomarkers and therapeutic targets.

Centromeric factors are increasingly shown to be involved in tumor pathogenesis and have been proposed as potential therapeutic targets or prognostic markers (Filipescu et al., 2017). Centromeric protein A (CENP-A) is a histone H3-like protein that is enriched at active centromeres and serves as an epigenetic mark of centromere identity (Hoffmann et al., 2020). *CENP-A* regulates centromere integrity and chromosome segregation during cell division, and its overexpression leads to ectopic *CENP-A* deposition causing consequent defects in chromosome segregation (Lacoste et al., 2014). Accordingly, mislocalization of *CENP-A* resulting from its overexpression contributes to chromosomal instability and aneuploidy (Shrestha et al., 2021), which have long been recognized as hallmarks of tumor growth, malignant progression, and treatment resistance (Zhang et al., 2016; Sansregret et al., 2018). Recent studies have indicated that *CENP-A* overexpression induces chromosomal instability in cancer cells (Amato et al., 2009; Quevedo et al., 2020). Additionally, increased *CENP-A* expression is implicated in malignant progression (Sun et al., 2016) and correlates with poor prognosis in cancers (Zhang et al., 2020a; Saha et al., 2020; Xu et al., 2020), including breast (Rajput et al., 2011), lung (Wu et al., 2012; Liu et al., 2018), and hepatic carcinoma (Zhang et al., 2020b). *CENP-A* downregulation induces cell cycle arrest and cell death in hepatoma and lung carcinoma (Li et al., 2011; Wu et al., 2014). In patients with high-grade glioblastoma (GBM), increased *CENP-A* expression is associated with short OS(Stangeland et al., 2015; Chen et al., 2020). However, although *CENP-A* overexpression was proposed as a common feature of numerous cancer types (Li et al., 2019; Qi et al., 2019), its role in gliomas is unclear. The prognostic value of *CENP-A* in gliomas including GBM and low-grade gliomas remains to be investigated. In particular, the association between *CENP-A* expression and clinicopathological features of patients with glioma, as well as the detailed molecular mechanism of CENP-A in gliomas, have not been reported yet.

In the present study, we explored The Cancer Genome Atlas (TCGA) database to obtain glioma RNA-sequencing data and performed a series of bioinformatic analyses to comprehensively investigate *CENP-A* expression patterns and its prognostic significance in gliomas. We compared *CENP-A* expression among patients with glioma and healthy individuals, and analyzed the association of *CENP-A* mRNA expression with parameters in clinical data. To determine the effects of *CENP-A* on glioma prognosis, we performed survival analyses using *CENP-A* expression and clinicopathological features in the Cox regression model and developed a nomogram to predict glioma prognosis. We also verified the expression pattern and role of *CENP-A* at the mRNA level in The Chinese Glioma Genome Atlas (CGGA) cohort. To highlight the genes and functional pathways closely correlated with *CENP-A* expression, enrichment analysis was performed, including gene ontology (GO), Kyoto Encyclopedia of Genes and Genomes (KEGG), and gene set enrichment analysis (GSEA). Our study investigated the role of *CENP-A* in gliomas and discussed the possible *CENP-A*-related immune mechanisms involved in the pathogenesis of glioma.

## Materials and methods

### Data sources and pre-processing

We obtained publicly available RNA-seq and clinicopathological data of 696 glioma patient samples from TCGA and data of normal brain samples from the GTEx database. For subsequent analyses, all gene expression profiles were processed using Toil software (Vivian et al., 2017) and normalized as values in transcripts per million reads (TPM). The relevant clinical information of patients included age, gender, world health organization (WHO) grade, histological diagnosis, status of molecular markers, and follow-up outcomes. Our study conforms to the publication requirements of TCGA. For further validation, glioma data from the Chinese cohorts were obtained from CGGA datasets.

### Differentially expressed genes analysis

*CENP-A* expression in patients across TCGA was statistically ranked by median value and defined as high and low expression groups. Differentially expressed genes (DEGs) between the high- and low-*CENP-A* expression groups were identified *via* entry of

expression profiles (HTseq-Counts) into the DESeq2 R package (Love et al., 2014). Genes with | log2 fold change (FC) | > 2.0 and an adjusted $p < 0.01$ were included to obtain statistically significant differences.

## Metascape enrichment analysis

Metascape is a well-maintained online portal for comprehensive gene list analyses and interpretations. Herein, enrichment analysis of pathways and biological processes was performed for *CENP-A*-specific DEGs using Metascape (Zhou et al., 2019). Only conditions with an enrichment factor > 1.5, minimum count of 3, and $p < 0.01$ were considered significant. To further explore DEGs, protein-protein interaction (PPI) networks were modeled by importing the data from three databases, BioGrid, OminiPath, and InWeb_IM, into Metascape along with the Molecular Complex Detection (MCODE) algorithm, in which the tightly connected PPI network components were identified.

## Gene set enrichment analysis

To explore the underlying functional or pathway differences between high- and low-*CENP-A* groups, GSEA was conducted using the R package clusterProfiler (3.14.3) (Yu et al., 2012). For each analysis, gene cluster random permutations were performed 1,000 times. The terms with |NES| > 1, adjusted $p < 0.05$, and FDR $q$ value < 0.25 were interpreted as statistically significant differences between the groups.

## Analysis of immune infiltration and its correlation with centromeric protein A expression

By adopting the single-sample GSEA (ssGSEA) approach in the R package GSVA, we analyzed immune infiltration in glioma and the correlation between infiltration level and *CENP-A* expression. To analyze the relative invasion levels of 24 immune cell types, the enrichment of published immunocyte signature genes (Bindea et al., 2013) was qualified using the expression profiling of each tumor sample. The Wilcoxon rank-sum test was employed to investigate the enrichment differences in immune cells between the *CENP-A* high and low expression groups. The association between *CENP-A* and immune cell infiltration was determined using Spearman's correlation coefficient.

## Statistical analyses

All statistical analyses were performed using the R software (v3.6.2). Wilcoxon signed-rank and Wilcoxon rank-sum tests were performed to compare *CENP-A* expression levels in glioma and normal samples. The receiver operating characteristic (ROC) curve obtained using the pROC package was used to evaluate the effectiveness of *CENP-A* expression in discriminating between glioma and healthy samples (Robin et al., 2011). We used the Wilcoxon test, Kruskal–Wallis test, and Spearman's correlation to evaluate the association between *CENP-A* and clinicopathological characteristics. Fisher's exact test, Pearson's $\chi^2$ test, and univariate logistic regression analyses were conducted to evaluate the correlation between *CENP-A* expression level and clinicopathological variables. Significant variables ($p < 0.01$) based on the univariate Cox regression analysis were included in the multivariate Cox regression model to identify independent prognostic parameters. Accordingly, survival curves were generated using the Kaplan–Meier method and compared using the log-rank test for each subgroup. Based on the optimal model determined by the above multivariate analysis, a nomogram was established using the R package rms to individualize the prediction of patient survival probability. The hazard ratio (HR) with a 95% confidence interval (95% CI) was used to measure the risk of individual clinical characteristics. Statistical significance was set at $p < 0.05$.

# Results

## Clinical characteristics of patients

The clinicopathological characteristics of patients with glioma collected from TCGA included age, WHO grade, isocitrate dehydrogenase (IDH) status, 1p/19q co-deletion, primary therapy outcome, gender, and histological type. A cohort of 298 females and 398 males was studied. Analysis of clinical data indicated that *CENP-A* expression was significantly associated with age ($p < 0.001$), WHO grade ($p < 0.001$), IDH status ($p < 0.001$), 1p/19q co-deletion ($p < 0.001$), primary therapy outcome ($p < 0.001$), and histological type ($p < 0.001$). No statistical association was detected between *CENP-A* expression and gender (Table 1).

## Centromeric protein A expression and clinical correlation in the cancer genome atlas and validation in Chinese glioma genome atlas

To compare *CENP-A* expression levels in glioma and normal samples, Wilcoxon signed-rank tests were used. *CENP-A* expression was significantly higher in glioma tissues than in healthy tissues (Figure 1A). As shown in Figure 1B, *CENP-A* expression showed excellent ability in distinguishing tumors from healthy tissues with an area under the ROC curve (AUC) of 0.960. Pan-cancer analysis consistently showed upregulated *CENP-A* expression in numerous tumor types (Figure 1C).

TABLE 1 Clinical characteristics of patients with glioma from TCGA.

| Characteristic | Low *CENP-A* expression | High *CENP-A* expression | *p*-value |
|---|---|---|---|
| Number of cases | 348 | 348 | |
| WHO grade, n (%) | | | <0.001 |
| G2 | 188 (29.6%) | 36 (5.7%) | |
| G3 | 115 (18.1%) | 128 (20.2%) | |
| G4 | 6 (0.9%) | 162 (25.5%) | |
| IDH status, n (%) | | | <0.001 |
| WT | 36 (5.2%) | 210 (30.6%) | |
| Mut | 309 (45%) | 131 (19.1%) | |
| 1p/19q co-deletion, n (%) | | | <0.001 |
| Co-deletion | 137 (19.9%) | 34 (4.9%) | |
| No co-deletion | 210 (30.5%) | 308 (44.7%) | |
| Primary therapy outcome, n (%) | | | <0.001 |
| PD | 52 (11.3%) | 60 (13%) | |
| SD | 92 (19.9%) | 55 (11.9%) | |
| PR | 51 (11%) | 13 (2.8%) | |
| CR | 102 (22.1%) | 37 (8%) | |
| Gender, n (%) | | | 0.592 |
| Female | 153 (22%) | 145 (20.8%) | |
| Male | 195 (28%) | 203 (29.2%) | |
| Age, n (%) | | | <0.001 |
| ≤60 | 313 (45%) | 240 (34.5%) | |
| >60 | 35 (5%) | 108 (15.5%) | |
| Histological type, n (%) | | | <0.001 |
| Astrocytoma | 112 (16.1%) | 83 (11.9%) | |
| Glioblastoma | 6 (0.9%) | 162 (23.3%) | |
| Oligoastrocytoma | 90 (12.9%) | 44 (6.3%) | |
| Oligodendroglioma | 140 (20.1%) | 59 (8.5%) | |
| Age, median (IQR) | 39 (32, 51) | 53 (39, 63) | <0.001 |

WHO, world health organization; IDH, isocitrate dehydrogenase; WT, wild-type; MUT, mutated; PD, progressive disease; SD, stable disease; PR, partial response; CR, complete response.

Moreover, results based on clinical information and expression data (Figure 2) showed that, the expression level of *CENP-A* was associated with age ($p < 0.001$), WHO grade ($p < 0.001$), IDH status ($p < 0.001$), 1p/19q co-deletion ($p < 0.001$), and primary therapy outcome ($p < 0.001$). The analysis stratified by WHO grade indicated consistent results in low-grade glioma (Supplementary Figure S1). In CGGA dataset, results (Supplementary Figure S2) showed consistent association between *CENP-A* expression and WHO grade ($p < 0.001$), age ($p < 0.001$), IDH mutation ($p < 0.001$), 1p/19q co-deletion ($p < 0.001$), as well as IDH mutation & 1p/19q co-deletion status ($p < 0.001$).

To determine the correlation between *CENP-A* expression levels and clinicopathological variables, univariate logistic regression was performed. Elevated *CENP-A* expression was significantly associated with poor prognostic characteristics, including age > 60 years [OR = 4.024 (2.678–6.175) for >60 vs. ≤ 60 years], high WHO grade [OR = 49.884 (23.515–129.060) for G4 vs. G2 and G3], poor primary therapy outcome [OR = 2.444 (1.641–3.675) for progressive disease (PD) and stable disease (SD) vs. partial response (PR) and complete response (CR)], wild-type (WT) IDH [OR = 13.760 (9.247–20.963) for WT vs. mutated], and absence of 1p/19q co-deletion [OR = 5.910 (3.947–9.061) for no co-deletion vs. co-deletion], with $p < 0.001$. These results were validated using Chi-square analysis (Table 2). Our observations suggest that gliomas with upregulated *CENP-A* expression are prone to poor clinicopathological factors and a high degree of malignancy.

## Centromeric protein A was an independent prognostic factor for glioma patients

To determine the correlation between *CENP-A* expression and survival of patients with gliomas, univariate and multivariate

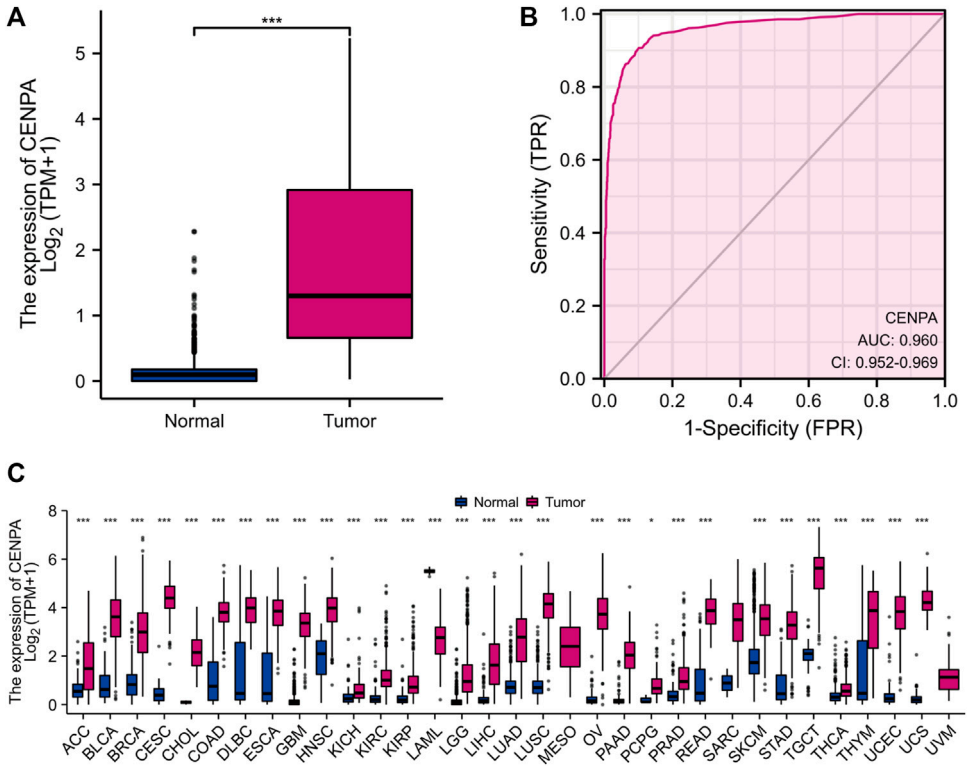


FIGURE 1
High *CENP-A* expression in tumor tissues. **(A)** *CENP-A* expression levels in glioma tissues compared with normal tissues (control). **(B)** ROC analysis of *CENP-A* expression showing its excellent ability in distinguishing tumors from normal tissues. **(C)** Pan-cancer analysis of CENP-A expression across different cancers based on TCGA data. ns, no significance, $p > 0.05$; *$p < 0.05$; **$p < 0.01$; ***$p < 0.001$.

analyses were performed. As shown in Figures 3A–C, Kaplan–Meier survival analysis indicated that glioma cases with elevated *CENP-A* expression had a worse prognosis than those with low *CENP-A* levels ($p < 0.001$). Univariate assessment revealed that high *CENP-A* expression was markedly correlated with shorter OS (HR: 5.42; 95% CI: 4.04–7.27; $p < 0.001$), poor disease-specific survival (HR: 5.81; 95% CI: 4.25–7.95; $p < 0.001$), and poor progression-free interval (HR: 3.34; 95% CI: 2.66–4.19; $p < 0.001$). Additionally, multivariate analysis supported an independent correlation between *CENP-A* and OS (HR: 1.967; 95% CI: 1.280–3.025; $p < 0.002$) as well as between OS and age, WHO grade, primary therapy outcome, and IDH status (Table 3). Therefore, elevated *CENP-A* expression was of prognostic significance in glioma.

## Development and validation of a centromeric protein A based prognostic prediction nomogram

To predict the survival of glioma individuals using a visualized approach, a nomogram was created by integrating *CENP-A* expression and other independent prognostic factors including age, WHO grade, primary therapy outcome, IDH status, and 1p/19q co-deletion (Figure 3D), which were determined by the above multivariate Cox analysis. A lower survival probability was represented by a higher value of total points accumulated from the points of all variables on the nomogram. A calibration plot for survival probabilities showed that nomogram prediction well agrees with observed fraction (Figure 3E). Our prognostic nomogram achieved promising predicting efficacy for the 1-, 3-, and 5-years survival probabilities. Moreover, Harrell's concordance index (C-index) for the nomogram was 0.859, with 1,000 bootstrap resamples. These findings indicate that the nomogram performs better than clinical prognostic factors in predicting the survival probability of patients with glioma.

## Effect of centromeric protein A expression on glioma prognosis in patient subgroups

To better assess the prognostic ability of *CENP-A*, the relationship between *CENP-A* expression and patient survival

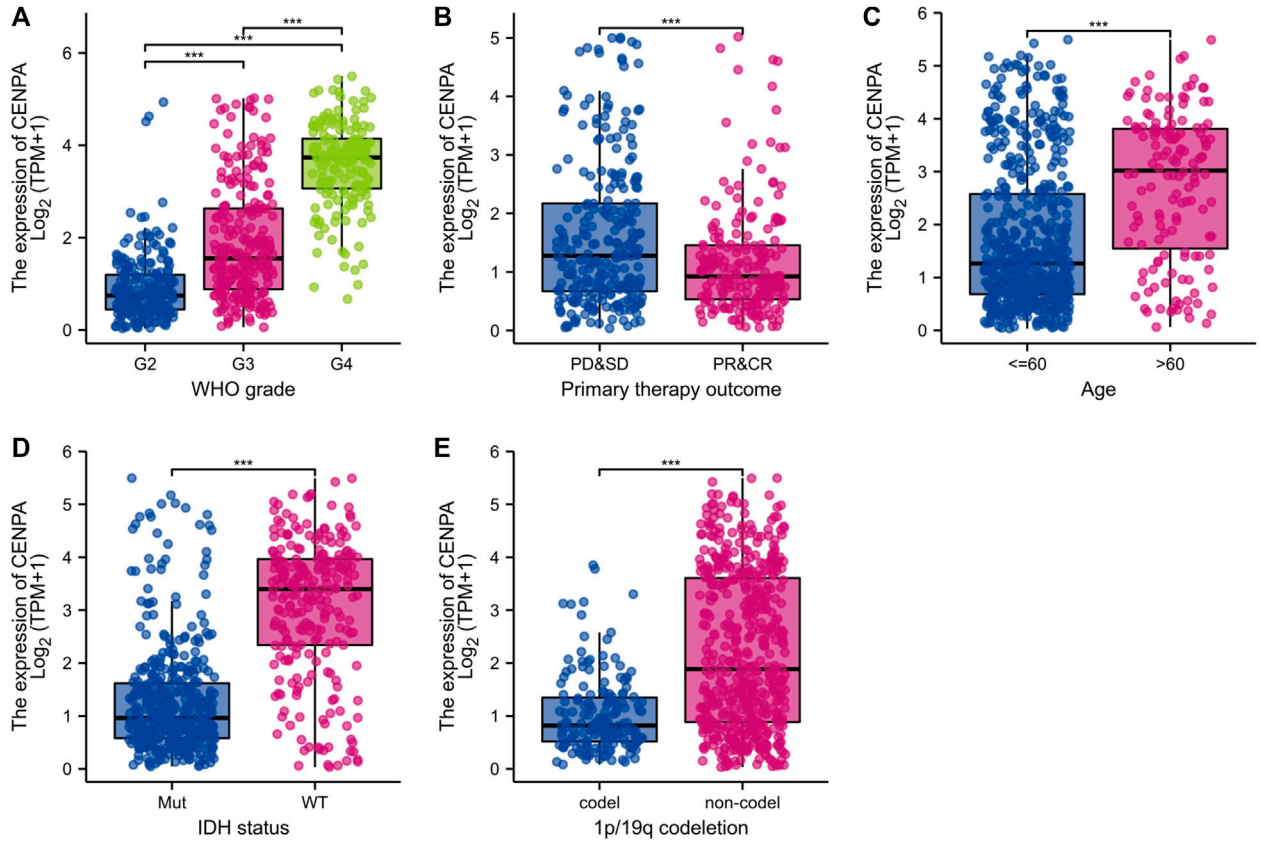


FIGURE 2
Clinical correlation analysis of *CENP-A* expression with clinicopathologic features. **(A)** WHO grade, **(B)** Primary therapy outcome, **(C)** Age, **(D)** IDH status, and **(E)** 1p/19q co-deletion. WHO, World health organization; IDH, isocitrate dehydrogenase; WT, wild type; MUT, mutated.

TABLE 2 Association of *CENP-A* expression with the clinicopathological characteristics of patients with glioma (logistic regression).

| Characteristics | Total (n) | Odds ratio (OR) | *p*-value |
|---|---|---|---|
| WHO grade (G4 vs. G2 and G3) | 635 | 49.884 (23.515–129.060) | <0.001 |
| Primary therapy outcome (PD and SD vs. PR and CR) | 462 | 2.444 (1.641–3.675) | <0.001 |
| IDH status (WT vs. Mut) | 686 | 13.760 (9.247–20.963) | <0.001 |
| 1p/19q co-deletion (no co-deletion vs. co-deletion) | 689 | 5.910 (3.947–9.061) | <0.001 |
| Age (>60 vs. ≤60) | 696 | 4.024 (2.678–6.175) | <0.001 |
| Gender (Male vs. Female) | 696 | 1.098 (0.813–1.484) | 0.540 |

WHO, world health organization; IDH, isocitrate dehydrogenase; WT, wild-type; MUT, mutated; PD, progressive disease; SD, stable disease; PR, partial response; CR, complete response.

in subgroups stratified by clinicopathological characteristics was investigated using univariate Cox analysis (Figure 4). High *CENP-A* expression was associated with shorter OS among patients with different 1p/19q co-deletion statuses and age (Figures 4B–E). Additionally, elevated *CENP-A* expression was specifically associated with decreased OS in patients with mutated IDH [HR = 2.41 (1.55–3.76), $p < 0.001$] and in patients with WHO grades G2 and G3 [HR = 3.25 (2.14–4.92), $p < 0.001$], but not in other subgroups (Figures 4F–I). Glioma patients in CGGA showed similar results, especially within WHO grade G2 and G3 cohort ($p < 0.05$, Supplementary Figure S3). The results confirmed that CENP-A retained its ability to predict survival among subgroups with various clinicopathological factors.

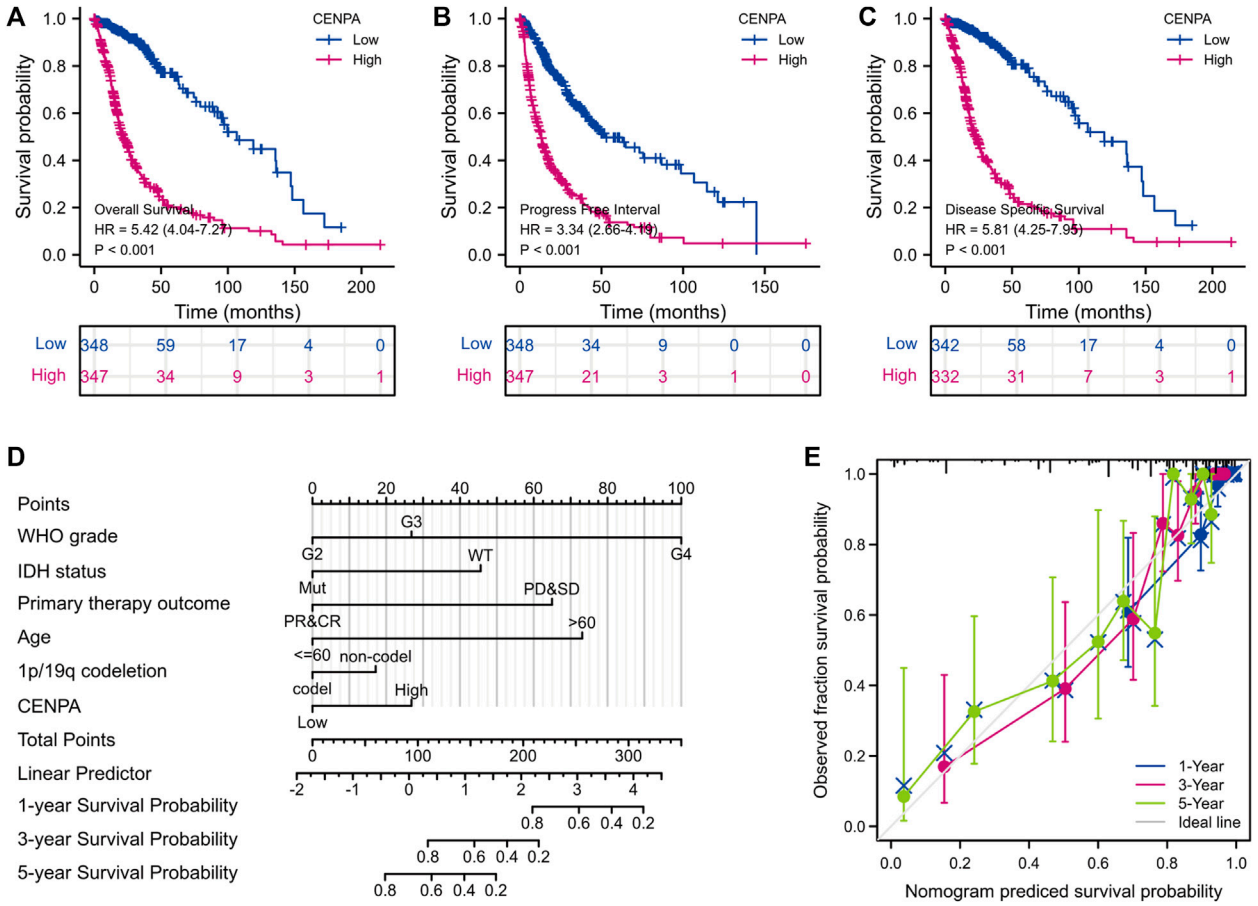


FIGURE 3
Survival analyses and prognostic nomogram. **(A–C)** Impact of *CENP-A* on the overall, progression-free, and disease-specific survival rates in glioma according to TCGA. **(D,E)** Development and verification of a glioma predictive nomogram based on *CENP-A* expression levels and independent prognostic factors.

## Identification of differentially expressed genes between high- and -low centromeric protein A in patients with glioma

Based on threshold values (|log2 FC| > 2 and adjusted $p < 0.01$) (Love et al., 2014), DEGs between high- and -low *CENP-A* were identified after an analysis of HTSeq-Counts data from TCGA using the R package DESeq2. DEGs are presented in a heatmap and volcano plot (Figure 5). A total of 521 DEGs (460 upregulated and 61 downregulated) that correlated with *CENP-A* are included in the volcano plot (Figure 5A). The top and bottom five genes in the heatmap showed significantly positive and negative correlations with *CENP-A* expression, respectively (Figure 5B). Among the DEGs, *CENP-A* was positively correlated with UBE2C (Spearman's $r = 0.969$, $p < 0.001$), BIRC5 (Spearman's $r = 0.966$, $p < 0.001$), and CCNB2 (Spearman's $r = 0.964$, $p < 0.001$) (Figures 5C–E). UBE2C, BIRC5, and CCNB2 were reported to be oncogenic and are associated with several cancers including glioma (Renner et al., 2016; Dastsooz et al., 2019; Wang et al., 2021b). These results suggest the involvement of *CENP-A* in a wide array of pathways and processes through gene regulation.

## Gene ontology and kyoto encyclopedia of genes and genomes functional enrichment and protein-protein interaction network analyses of differentially expressed genes

For an in-depth understanding of the identified DEGs, we proceeded to GO and KEGG functional enrichment analyses using Metascape tools and found that 521 DEGs were involved in diverse biological processes (BP), cellular components (CC), and molecular functions. Those associated with *CENP-A*-related DEGs included cell cycle, skeletal system development,

TABLE 3 The correlation of *CENP-A* and clinicopathologic characteristics with overall survival in patients with glioma in TCGA, and the multivariate survival model based on univariate selection (Cox regression).

| Characteristics | Total (n) | Univariate analysis | | Multivariate analysis | |
|---|---|---|---|---|---|
| | | Hazard ratio (95% CI) | *p*-value | Hazard ratio (95% CI) | *p*-value |
| WHO grade | 634 | | | | |
| G2 and G3 | 466 | Reference | | | |
| G4 | 168 | 9.496 (7.212–12.503) | <0.001 | 4.106 (1.429–11.794) | 0.009 |
| IDH status | 685 | | | | |
| Mut | 439 | Reference | | | |
| WT | 246 | 8.551 (6.558–11.150) | <0.001 | 2.708 (1.712–4.282) | <0.001 |
| 1p/19q co-deletion | 688 | | | | |
| No co-deletion | 518 | Reference | | | |
| Co-deletion | 170 | 0.226 (0.147–0.347) | <0.001 | 0.736 (0.422–1.285) | 0.281 |
| Primary therapy outcome | 461 | | | | |
| PD&SD | 259 | Reference | | | |
| PR&CR | 202 | 0.209 (0.120–0.366) | <0.001 | 0.302 (0.164–0.559) | <0.001 |
| Age | 695 | | | | |
| ≤60 | 552 | Reference | | | |
| >60 | 143 | 4.668 (3.598–6.056) | <0.001 | 4.116 (2.548–6.647) | <0.001 |
| CENP-A | 695 | | | | |
| Low | 348 | Reference | | | |
| High | 347 | 5.422 (4.044–7.271) | <0.001 | 1.967 (1.280–3.025) | 0.002 |

WHO, world health organization; IDH, isocitrate dehydrogenase; WT, wild-type; MUT, mutated; PD, progressive disease; SD, stable disease; PR, partial response; CR, complete response.

embryonic morphogenesis, Naba matrisome associated, mitotic cell cycle phase transition, extracellular matrix organization, assembly of collagen fibrils and other multimeric structures, Naba core matrisome, and PID aurora b pathway (Figure 6). Accordingly, *CENP-A*-specific DEGs were closely associated with cell cycle progression. Furthermore, PPI networks were constructed in Metascape to identify protein interactions between DEGs and better illuminate the biological significance (Figure 6D). To derive more biologically interpretable results, the most significant MCODE sub-networks that are highly interlinked were extracted from PPI, and each complex was assigned a unique color (Figure 6E). These pathways or processes may provide clues for exploring the potential functions of *CENP-A* in glioma.

## Identification of centromeric protein A-related signaling pathways

GSEA of high and low *CENP-A* expression datasets was conducted to identify the critical signaling pathways or phenotypes involved in gliomas. There was a significant differential enrichment of numerous pathways within the MSigDB collection (c2.cp.v7.2.symbols, h. all.v7.2.symbols, and c5.all.v7.2.symbols) with a threshold of FDR < 0.25 and adjusted $p < 0.05$. As shown in Figure 7, the signaling cascades, including cell cycle, DNA conformation change, chromosome condensation, chromosome segregation, G2M checkpoint, IL6-JAK-STAT3 signaling, apoptosis, nucleosome assembly, and histone modifications, were enriched in the high-*CENP-A* group, thereby highlighting the potential functions of *CENP-A* in gliomagenesis.

## Correlation of centromeric protein A with immune infiltration

Brain tumor immunity has gained increased attention for its vital role in affecting therapeutic response and prognosis (Sampson et al., 2020). We further explored the correlation between *CENP-A* expression and immunocyte enrichment levels quantified by ssGSEA in the glioma tumor microenvironment *via* Spearman correlation. The results showed that Th2 cells had a remarkable positive correlation with *CENP-A* expression (Spearman's $r = 0.85$, $p < 0.001$; Figure 8). Moreover, as illustrated by the Wilcoxon rank-sum test, the enrichment score of Th2 cells was significantly higher in high-*CENP-A* samples than in low-CENP-A samples. The relative abundance of other immune cell populations, including plasmacytoid dendritic cells

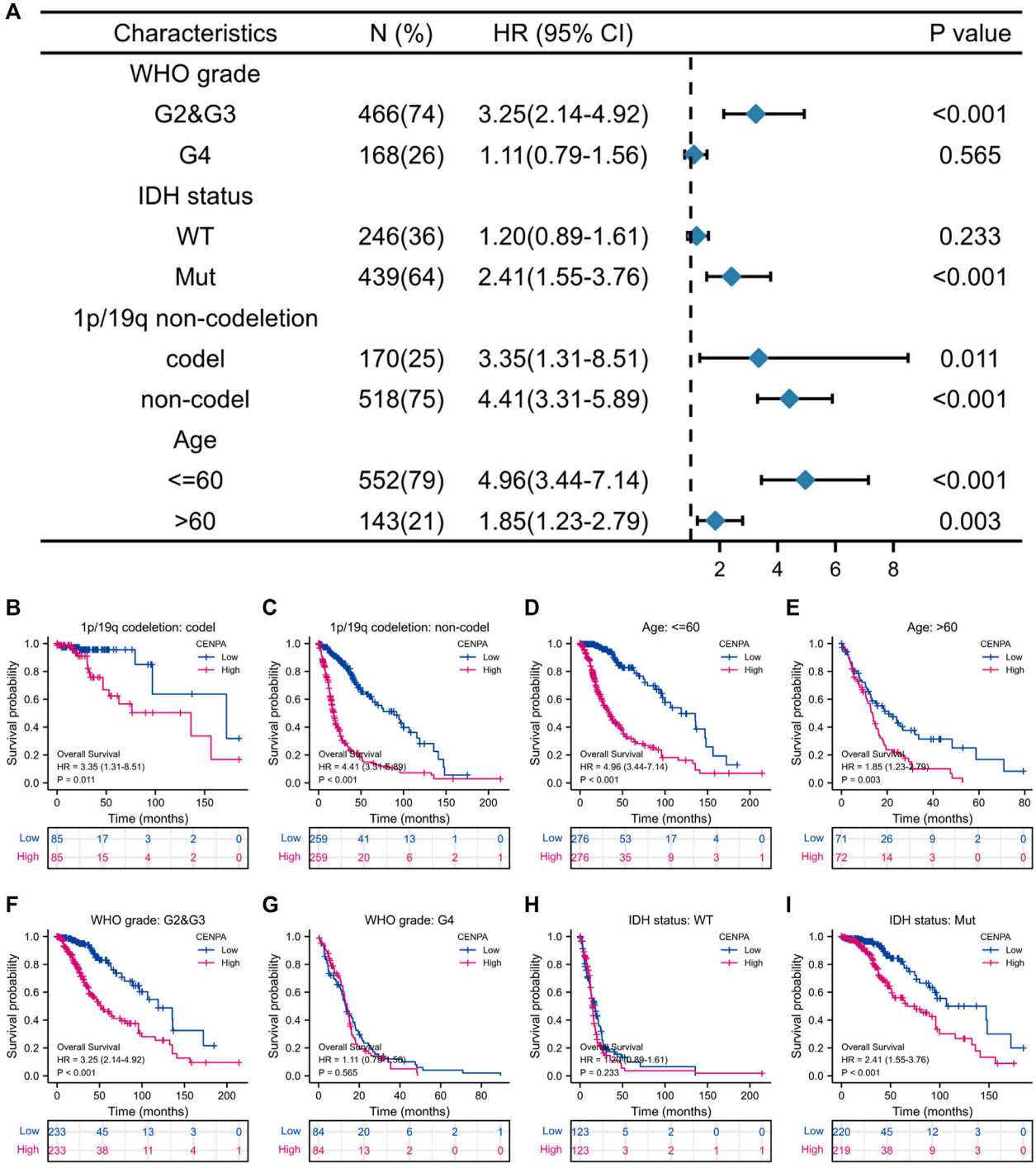


FIGURE 4
The correlation of *CENP-A* expression with glioma prognosis among patients with various clinicopathological characteristics. **(A)** Forest plots showing the subgroup analysis of overall survival. **(B–I)** Kaplan–Meier survival curves of each patient subgroup.

(pDCs), macrophages, eosinophils, and activated dendritic cells (aDCs), was moderately correlated with *CENP-A* expression. Glioma data from CGGA showed similar correlation trend between *CENP-A* expression and infiltration of Th2 cells and pDCs (Supplementary Figure S4).

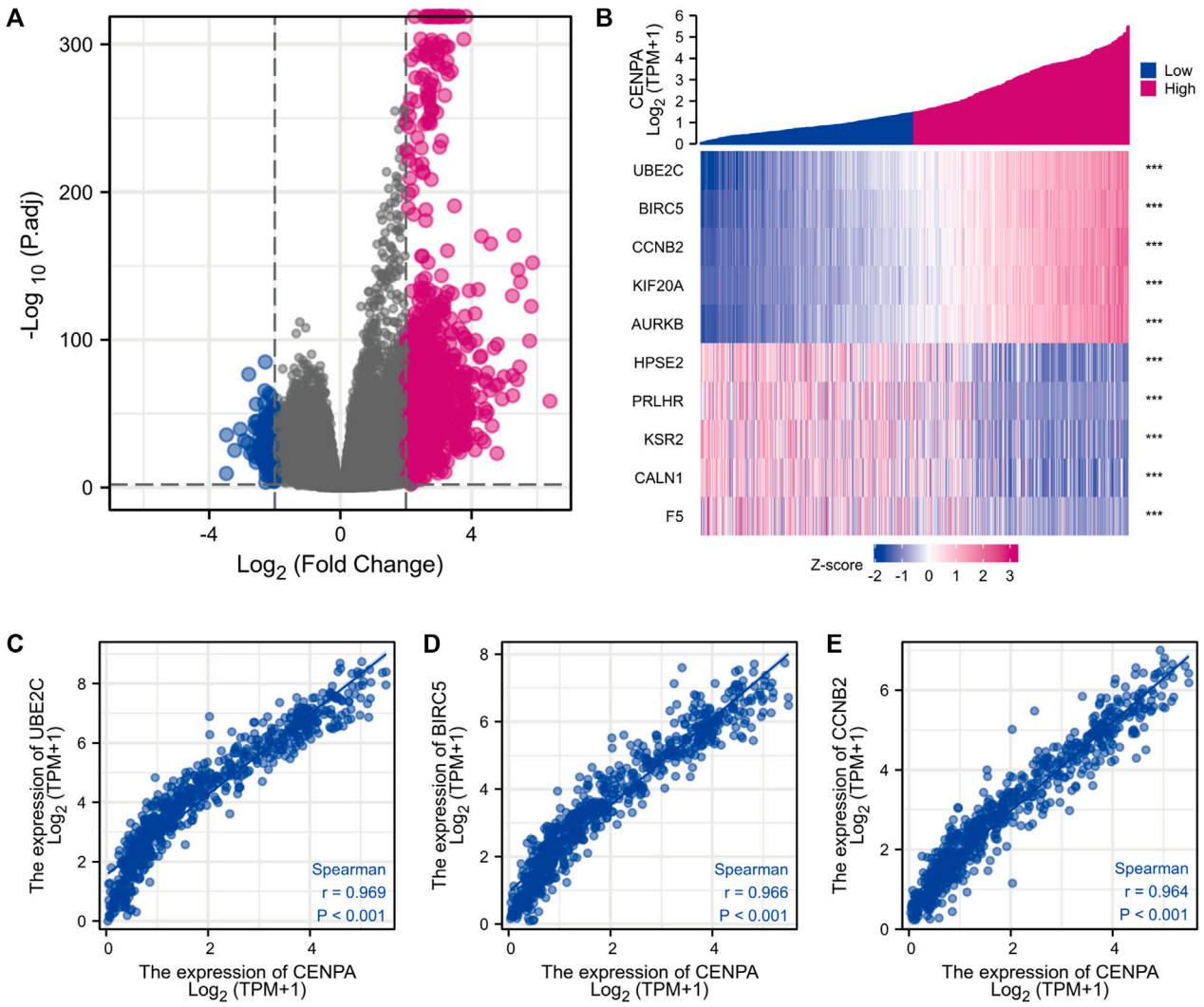


FIGURE 5
Differentially expressed genes (DEGs) between high and low *CENP-A* expression glioma groups in TCGA dataset. **(A)** Heatmap of the top five upregulated and downregulated DEGs. **(B)** Volcano plot of DEGs expression profiles. **(C–E)** Scatter plot showing the correlation between *CENP-A* expression and *UBE2C* **(C),** *BIRC5* **(D),** and *CCNB2* **(E)** expression.

## Discussion

At present, the study of gene expression profiles in glioma has been widely applied to explore glioma pathogenesis and management. Identifying molecular markers is a promising way to guide decision-making and improve prognosis for clinical glioma. *CENP-A* regulates centromere protein assembly and is essential for progression through chromosome segregation, mitosis, and cell division. Experiments have demonstrated that excess *CENP-A* accumulates ectopically in the human cancer genome (Athwal et al., 2015). Accumulating evidences have verified that the overexpression of *CENP-A* becomes a common result in a growing body of research on cancers (Renaud-Pageot et al., 2022). *CENP-A* overexpression plays a pivotal role in chromosomal instability and pathogenesis of malignancies through chromosome segregation defects (Shrestha et al., 2017), a mechanism involved *CENP-A* in cancers (Sun et al., 2016; Sharma et al., 2019). In addition, elevated *CENP-A* levels promote the proliferation of cancer cells in hepatoma (Li et al., 2011), prostate (Saha et al., 2020) and renal cell carcinoma (Wang et al., 2021a). The observations support an association of *CENP-A* function with cell proliferation. Besides a role in cell proliferation following malignant transformation, in the cellular context of defective p53 (Filipescu et al., 2017; Jeffery et al., 2021), *CENP-A* overexpression stimulates epithelial-mesenchymal transition, a major contributing factor in the metastasis of cancer cells (Jeffery et al., 2021). *CENP-A* expression was

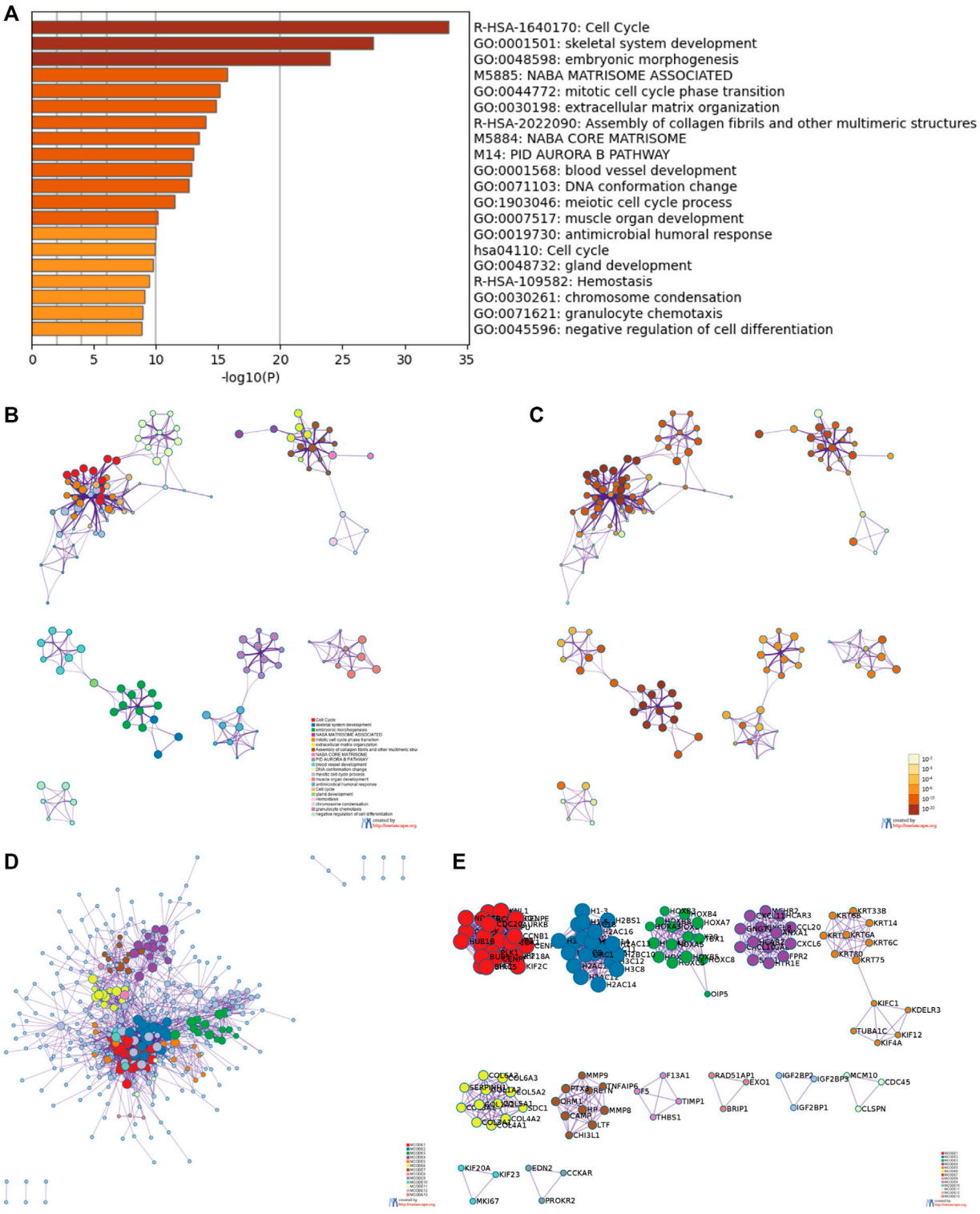


FIGURE 6
Functional enrichment and protein-protein interaction (PPI) enrichment analyses of *CENP-A*-related DEGs. **(A)** Heatmap showing Gene Ontology (GO) functional enrichment analysis. **(B,C)** Visualized network of top 20 GO enriched terms. **(D,E)** PPI networks and the most significant Molecular Complex Detection (MCODE) sub-networks.

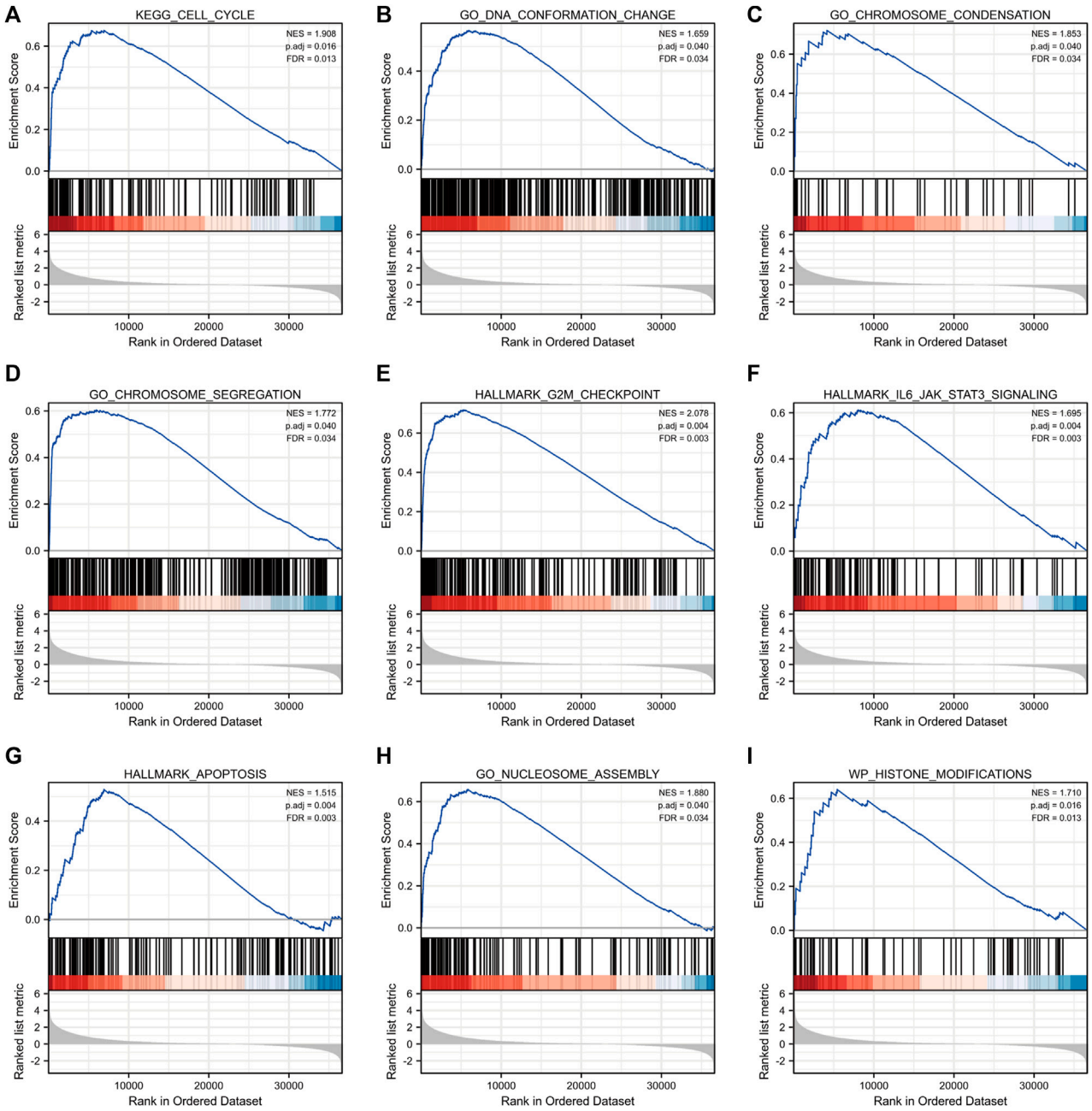


FIGURE 7
Gene set enrichment analysis (GSEA) enrichment plots including **(A)** cell cycle, **(B)** DNA conformation change, **(C)** chromosome condensation, **(D)** chromosome segregation, **(E)** G2M checkpoint, **(F)** IL6-JAK-STAT3 signaling, **(G)** apoptosis, **(H)** nucleosome assembly and **(I)** histone modifications.

positively associated with cancer metastasis in gastric (Xu et al., 2020) and renal (Wang et al., 2021a) cancers. Taking the evidence together, we believe that *CENP-A* overexpression is related to malignant transformation, tumor invasiveness and metastasis in specific cancer contexts. In reports with patient data, elevated *CENP-A* levels prognosticate poor patient survival for cancers (Zhang et al., 2016; Saha et al., 2020) and patient outcome after chemotherapy (Zhang et al., 2016). However, the clinical significance of *CENP-A* in glioma, especially its expression pattern and prognostic role, has not yet been systematically explored. In our study, bioinformatic analyses of TCGA RNA-sequencing data combining GBM and low-grade glioma

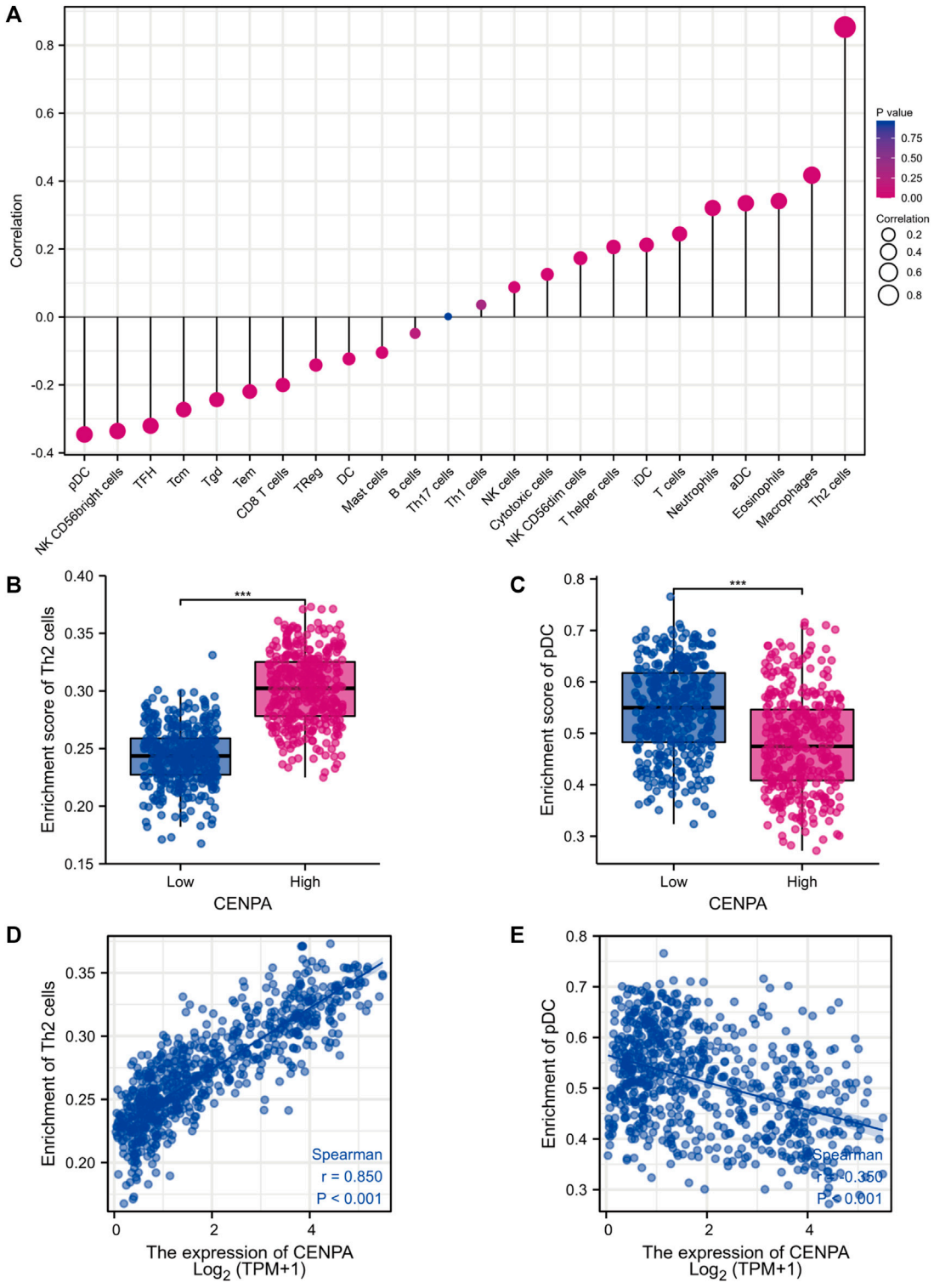


FIGURE 8
The role of CENP-A in tumor immune responses. **(A)** A forest plot showing the association between *CENP-A* expression and immune infiltration level. **(B,C)** The abundances of Th2 cells and pDC cells among low- and high-*CENP-A* expression groups. **(D,E)** The correlation between *CENP-A* expression levels and the relative enrichment levels of Th2 and pDC cells.

confirmed increased *CENP-A* expression which was associated with malignant clinicopathological status (high WHO grade, primary therapy outcome of PD&SD, age > 60, WT IDH status, and absence of 1p/19q co-deletion), short survival time, and poor prognosis. The results were further validated in CGGA dataset. Furthermore, GSEA revealed that the high-*CENP-A* phenotype showed differential enrichment of pathways including cell cycle, DNA conformation change, chromosome condensation, chromosome segregation, G2M checkpoint, IL6-JAK-STAT3 signaling, apoptosis, nucleosome assembly, and histone modifications. Immune filtration analysis suggested that the expression of *CENP-A* correlated with immune infiltration status. Our results support *CENP-A* as a potential prognostic biomarker for gliomas.

In subgroup analysis, *CENP-A* expression remained correlated with poor prognosis in subsets grouped by WHO grade, IDH, 1p/19q co-deletion, and age statuses, which strongly suggests that *CENP-A* is a glioma grading biomarker within these subsets. We found a marked association between expression levels of *CENP-A* and OS in all 1p/19q co-deletion and age subgroups. Notably, there was a significant association between *CENP-A* expression levels and OS in grades 2 and 3 and mutated IDH status, but not in grade 4 and wild-type IDH status. The results from CGGA dataset validated this association in glioma, as well as grade 2 and 3 subgroups. These findings indicate that the association between *CENP-A* expression levels and survival varies by WHO grade and IDH status, and high *CENP-A* expression is more likely to negatively impact the survival of patients with low-grade gliomas.

The Cox model showed that *CENP-A* was an independent prognostic predictor of glioma. Subsequently, a nomogram was developed for the accurate prediction of prognosis with a personalized score for individual patients, and the model combined *CENP-A* with other predictors, including WHO grade, primary therapy outcome, age, IDH status, and 1p/19q co-deletion. Glioma with high WHO grade, IDH-wild-type, 1p/19q-non-codeleted and primary therapy outcome of PD are inclined to adverse survival (Eckel-Passow et al., 2015; Weller et al., 2015). IDH and 1p/19q co-deletion statuses were determined as classifying factors in the 2016 WHO diagnostic criteria for gliomas. IDH-mutant and 1p/19q-codeleted have been regarded as clinically relevant biomarkers in lower-grade gliomas with a favorable prognosis (Brat et al., 2015). 1p/19q co-deletion status is especially associated with patient outcomes in response to adjuvant chemotherapy (van den Bent et al., 2013). Age at diagnosis affects incidence rates of glioma remarkably. Older Age is associated with worse glioma survival and the effect on survival differs in glioma subtypes (Ostrom et al., 2019). The C-index and calibration plot confirmed that the nomogram performed well in predicting the 1-, 3-, and 5-year survival of patients with glioma. Therefore, our nomogram is a valuable clinical prognostic model.

To further investigate *CENP-A* function, GSEA was performed which showed that *CENP-A* was associated with cell cycle regulation, chromosome segregation, and nucleosome assembly in glioma. Previous studies have revealed that defects in chromosome segregation can lead to the phenotypes observed in tumor cells. Additionally, chromosomal instability induced by abnormal nucleosome assembly and chromosome segregation in the cell cycle may contribute to the progression of glioma (Milinkovic et al., 2012; Ferguson et al., 2015). Our results revealed an association between *CENP-A* and apoptosis, which is consistent with a previous study showing that nucleosome assembly failure is correlated with radiation-induced GBM cell death (Serafim et al., 2020). Moreover, HJURP is recognized as a *CENP-A*-specific chaperone, and its overexpression often accompanies the overexpression of *CENP-A* (Foltz et al., 2009). HJURP knockdown increases radiation-induced apoptosis in glioblastoma cells (Serafim et al., 2020). The functional enrichment analysis with Metascape (Zhou et al., 2019) showed consistent results that found an enrichment in cell cycle. Therefore, *CENP-A* may play a role in the cell cycle regulation to promote the survival and proliferation of glioma cells. However, it remains unclear whether elevated *CENP-A* levels contribute to glioma progression by inducing chromosomal instability.

Additionally, we revealed that high *CENP-A* expression phenotype was strongly associated with the inflammation-related IL6-JAK-STAT3 signaling pathway, which is associated with poor prognosis in patients with glioma (Yao et al., 2016). In the tumor immune microenvironment, the IL6-JAK-STAT3 pathway is hyperactivated in a multitude of cancers, which suppresses the anti-tumor immune response and promotes tumor progression (Yao et al., 2016). Preclinical and clinical investigations showed that IL6-JAK-STAT3 pathway inhibition has therapeutic benefits in cancer and that STAT3 inhibition inhibits the growth of glioma cells (Shen et al., 2009; Johnson et al., 2018). Nevertheless, the regulatory mechanisms underlying these associated functions and pathways remain poorly characterized and require further research.

Tumor immunosuppressive microenvironment represents an important factor of cancer progression and poor prognosis in glioma (Jackson et al., 2019). Since the prognostic role of infiltrating immune cells have been proposed across many human cancers (Gentles et al., 2015), we pay attention to the link between glioma immunity and *CENP-A* in this research. Several research models regarding centromeric factor in cancer proposed the association with immune infiltration (Shi et al., 2021; Zeng et al., 2021; Zhou et al., 2021). We also showed that *CENP-A* expression level was associated with the level of infiltrating immune cells in gliomas and presented the strongest correlation with Th2 cells and pDCs. Tumor-specific Th2 cell responses are associated with tumor immune evasion, and Th2 cytokines such as IL-4 and IL-13 are implicated in the suppression of host immune effector responses to tumors (Gordon and Martinez, 2010; Tosolini et al., 2011). Th2 cytokines are strongly expressed in glioma cell lines and GBM samples (Hao et al., 2002). Moreover, a strong Th2-bias

response was reported in patients with gliomas, especially those with recurrent GBM(Shimato et al., 2012; Harshyne et al., 2016), and the Th2 phenotype is associated with a poor prognosis in patients with glioma (Piperi et al., 2011; Shimato et al., 2012). This is consistent with our results that found an increased enrichment of Th2 cell in high *CENP-A* expression, which predicted poor prognosis. Additionally, pDCs play a suppressive role in tumors and impaired pDC activity is implicated in reduced immune responses in tumors (Reizis, 2019). Diffuse low-grade glioma with a better outcome showed elevated pDC level (Wu et al., 2020). pDCs induce anti-tumor therapeutic efficacy in GBM by producing IFN-α (Candolfi et al., 2012). Therefore, elevated *CENP-A* expression may induce Th2 cell infiltration and pDC deficiency in the tumor microenvironment, which contributes to immunotherapy resistance and poor treatment response in glioma. Collectively, our results indicate the potential role of *CENP-A* in modulating glioma-related immune responses; however, the underlying regulatory mechanisms require further investigation.

The present study has several limitations. First, it was based on open tumor databases and bioinformatics analysis and was not validated *in vitro* or *in vivo*. Second, the analysis was conducted only on the expression profiles at the mRNA level, not protein expression levels. Therefore, our results need to be validated using CENP-A protein expression levels and subsequent laboratory experiments.

In summary, our findings highlight the prognostic value and immune relevance of *CENP-A* in glioma, supporting its exploration as a potential biomarker for prognosis or a target for molecular targeted therapy. Furthermore, *CENP-A* may contribute to glioma progression through the regulation of pathways, including the cell cycle, nucleosome assembly, IL6-JAK-STAT3 signaling, and DNA repair. Further studies are required to elucidate the clinicopathological and biological significance of *CENP-A* expression. This study provides new insights into the molecular pathogenesis and individualized treatment of gliomas.

## Data availability statement

The datasets presented in this study can be found in online repositories. The names of the repository/repositories and accession number(s) can be found in the article/Supplementary Material.

## Ethics statement

Written informed consent was obtained from the individual(s) for the publication of any potentially identifiable images or data included in this article.

## Author contributions

ZW conceived and designed the study; YY, MD, and ZW collected the data; YY and ZW performed the data analyses and wrote the manuscript. YZ directed the research group in all aspects. The submission of final paper was reviewed and approved by all contributors.

## Acknowledgments

The authors appreciate the cooperation of the TCGA and CGGA databases for the original data, as well as Editage (www.Editage.com) for the language enhancement.

## Conflict of interest

The authors declare that the research was conducted in the absence of any commercial or financial relationships that could be construed as a potential conflict of interest.

## Publisher's note



## Supplementary material

The Supplementary Material for this article can be found online at: https://www.frontiersin.org/articles/10.3389/fgene.2022.931222/full#supplementary-material

## References

Amato, A., Schillaci, T., Lentini, L., and Di Leonardo, A. (2009). CENPA overexpression promotes genome instability in pRb-depleted human cells. *Mol. Cancer* 8, 119. doi:10.1186/1476-4598-8-119

Athwal, R. K., Walkiewicz, M. P., Baek, S., Fu, S., Bui, M., Camps, J., et al. (2015). CENP-A nucleosomes localize to transcription factor hotspots and subtelomeric sites in human cancer cells. *Epigenetics Chromatin* 8, 2. doi:10.1186/1756-8935-8-2

Bi, J., Chowdhry, S., Wu, S., Zhang, W., Masui, K., and Mischel, P. S. (2020). Altered cellular metabolism in gliomas - an emerging landscape of actionable co-dependency targets. *Nat. Rev. Cancer* 20 (1), 57–70. doi:10.1038/s41568-019-0226-5

Bindea, G., Mlecnik, B., Tosolini, M., Kirilovsky, A., Waldner, M., Obenauf, A. C., et al. (2013). Spatiotemporal dynamics of intratumoral immune cells reveal the immune landscape in human cancer. *Immunity* 39 (4), 782–795. doi:10.1016/j.immuni.2013.10.003

Brat, D. J., Verhaak, R. G., Aldape, K. D., Yung, W. K., Salama, S. R., Cooper, L. A., et al. (2015). Comprehensive, integrative genomic analysis of diffuse lower-grade gliomas. *N. Engl. J. Med.* 372 (26), 2481–2498. doi:10.1056/NEJMoa1402121

Candolfi, M., King, G. D., Yagiz, K., Curtin, J. F., Mineharu, Y., Muhammad, A. K., et al. (2012). Plasmacytoid dendritic cells in the tumor microenvironment: Immune targets for glioma therapeutics. *Neoplasia* 14 (8), 757–770. doi:10.1593/neo.12794

Chen, X., Pan, Y., Yan, M., Bao, G., and Sun, X. (2020). Identification of potential crucial genes and molecular mechanisms in glioblastoma multiforme by bioinformatics analysis. *Mol. Med. Rep.* 22 (2), 859–869. doi:10.3892/mmr.2020.11160

Dastsooz, H., Cereda, M., Donna, D., and Oliviero, S. (2019). A comprehensive bioinformatics analysis of UBE2C in cancers. *Int. J. Mol. Sci.* 20 (9), E2228. doi:10.3390/ijms20092228

Eckel-Passow, J. E., Lachance, D. H., Molinaro, A. M., Walsh, K. M., Decker, P. A., Sicotte, H., et al. (2015). Glioma groups based on 1p/19q, IDH, and TERT promoter mutations in tumors. *N. Engl. J. Med.* 372 (26), 2499–2508. doi:10.1056/NEJMoa1407279

Ferguson, L. R., Chen, H., Collins, A. R., Connell, M., Damia, G., Dasgupta, S., et al. (2015). Genomic instability in human cancer: Molecular insights and opportunities for therapeutic attack and prevention through diet and nutrition. *Semin. Cancer Biol.* 35, S5-S24–S24. doi:10.1016/j.semcancer.2015.03.005

Filipescu, D., Naughtin, M., Podsypanina, K., Lejour, V., Wilson, L., Gurard-Levin, Z. A., et al. (2017). Essential role for centromeric factors following p53 loss and oncogenic transformation. *Genes. Dev.* 31 (5), 463–480. doi:10.1101/gad.290924.116

Foltz, D. R., Jansen, L. E., Bailey, A. O., Yates, J. R., 3rd, Bassett, E. A., Wood, S., et al. (2009). Centromere-specific assembly of CENP-a nucleosomes is mediated by HJURP. *Cell* 137 (3), 472–484. doi:10.1016/j.cell.2009.02.039

Gentles, A. J., Newman, A. M., Liu, C. L., Bratman, S. V., Feng, W., Kim, D., et al. (2015). The prognostic landscape of genes and infiltrating immune cells across human cancers. *Nat. Med.* 21 (8), 938–945. doi:10.1038/nm.3909

Gordon, S., and Martinez, F. O. (2010). Alternative activation of macrophages: Mechanism and functions. *Immunity* 32 (5), 593–604. doi:10.1016/j.immuni.2010.05.007

Hao, C., Parney, I. F., Roa, W. H., Turner, J., Petruk, K. C., and Ramsay, D. A. (2002). Cytokine and cytokine receptor mRNA expression in human glioblastomas: Evidence of Th1, Th2 and Th3 cytokine dysregulation. *Acta Neuropathol.* 103 (2), 171–178. doi:10.1007/s004010100448

Harshyne, L. A., Nasca, B. J., Kenyon, L. C., Andrews, D. W., and Hooper, D. C. (2016). Serum exosomes and cytokines promote a T-helper cell type 2 environment in the peripheral blood of glioblastoma patients. *Neuro. Oncol.* 18 (2), 206–215. doi:10.1093/neuonc/nov107

Hoffmann, S., Izquierdo, H. M., Gamba, R., Chardon, F., Dumont, M., Keizer, V., et al. (2020). A genetic memory initiates the epigenetic loop necessary to preserve centromere position. *EMBO J.* 39 (20), e105505. doi:10.15252/embj.2020105505

Jackson, C. M., Choi, J., and Lim, M. (2019). Mechanisms of immunotherapy resistance: lessons from glioblastoma. *Nat. Immunol.* 20 (9), 1100–1109. doi:10.1038/s41590-019-0433-y

Jeffery, D., Gatto, A., Podsypanina, K., Renaud-Pageot, C., Ponce Landete, R., Bonneville, L., et al. (2021). CENP-A overexpression promotes distinct fates in human cells, depending on p53 status. *Commun. Biol.* 4 (1), 417. doi:10.1038/s42003-021-01941-5

Johnson, D. E., O'Keefe, R. A., and Grandis, J. R. (2018). Targeting the IL-6/JAK/STAT3 signalling axis in cancer. *Nat. Rev. Clin. Oncol.* 15 (4), 234–248. doi:10.1038/nrclinonc.2018.8

Lacoste, N., Woolfe, A., Tachiwana, H., Garea, A. V., Barth, T., Cantaloube, S., et al. (2014). Mislocalization of the centromeric histone variant CenH3/CENP-A in human cells depends on the chaperone DAXX. *Mol. Cell* 53 (4), 631–644. doi:10.1016/j.molcel.2014.01.018

Li, B., Pu, K., and Wu, X. (2019). Identifying novel biomarkers in hepatocellular carcinoma by weighted gene co-expression network analysis. *J. Cell. Biochem.* 120, 11418–11431. doi:10.1002/jcb.28420

Li, Y., Zhu, Z., Zhang, S., Yu, D., Yu, H., Liu, L., et al. (2011). ShRNA-targeted centromere protein A inhibits hepatocellular carcinoma growth. *PLoS One* 6 (3), e17794. doi:10.1371/journal.pone.0017794

Liu, W. T., Wang, Y., Zhang, J., Ye, F., Huang, X. H., Li, B., et al. (2018). A novel strategy of integrated microarray analysis identifies CENPA, CDK1 and CDC20 as a cluster of diagnostic biomarkers in lung adenocarcinoma. *Cancer Lett.* 425, 43–53. doi:10.1016/j.canlet.2018.03.043

Love, M. I., Huber, W., and Anders, S. (2014). Moderated estimation of fold change and dispersion for RNA-seq data with DESeq2. *Genome Biol.* 15 (12), 550. doi:10.1186/s13059-014-0550-8

Milinkovic, V., Bankovic, J., Rakic, M., Milosevic, N., Stankovic, T., Jokovic, M., et al. (2012). Genomic instability and p53 alterations in patients with malignant glioma. *Exp. Mol. Pathol.* 93 (2), 200–206. doi:10.1016/j.yexmp.2012.05.010

Ostrom, Q. T., Cioffi, G., Gittleman, H., Patil, N., Waite, K., Kruchko, C., et al. (2019). CBTRUS statistical report: Primary brain and other central nervous system tumors diagnosed in the United States in 2012-2016. *Neuro. Oncol.* 21, v1–v100. doi:10.1093/neuonc/noz150

Piperi, C., Samaras, V., Levidou, G., Kavantzas, N., Boviatsis, E., Petraki, K., et al. (2011). Prognostic significance of IL-8-STAT-3 pathway in astrocytomas: correlation with IL-6, VEGF and microvessel morphometry. *Cytokine* 55 (3), 387–395. doi:10.1016/j.cyto.2011.05.012

Qi, L., Gao, C., Feng, F., Zhang, T., Yao, Y., Wang, X., et al. (2019). MicroRNAs associated with lung squamous cell carcinoma: New prognostic biomarkers and therapeutic targets. *J. Cell. Biochem.* 120 (11), 18956–18966. doi:10.1002/jcb.29216

Quevedo, R., Spreafico, A., Bruce, J., Danesh, A., El Ghamrasni, S., Giesler, A., et al. (2020). Centromeric cohesion failure invokes a conserved choreography of chromosomal mis-segregations in pancreatic neuroendocrine tumor. *Genome Med.* 12 (1), 38. doi:10.1186/s13073-020-00730-9

Rajput, A. B., Hu, N., Varma, S., Chen, C. H., Ding, K., Park, P. C., et al. (2011). Immunohistochemical assessment of expression of centromere protein-A (CENPA) in human invasive breast cancer. *Cancers (Basel)* 3 (4), 4212–4227. doi:10.3390/cancers3044212

Reifenberger, G., Wirsching, H. G., Knobbe-Thomsen, C. B., and Weller, M. (2017). Advances in the molecular genetics of gliomas - implications for classification and therapy. *Nat. Rev. Clin. Oncol.* 14 (7), 434–452. doi:10.1038/nrclinonc.2016.204

Reizis, B. (2019). Plasmacytoid dendritic cells: Development, regulation, and function. *Immunity* 50 (1), 37–50. doi:10.1016/j.immuni.2018.12.027

Renaud-Pageot, C., Quivy, J. P., Lochhead, M., and Almouzni, G. (2022). CENP-A regulation and cancer. *Front. Cell Dev. Biol.* 10, 907120. doi:10.3389/fcell.2022.907120

Renner, G., Janouskova, H., Noulet, F., Koenig, V., Guerin, E., Bär, S., et al. (2016). Integrin α5β1 and p53 convergent pathways in the control of anti-apoptotic proteins PEA-15 and survivin in high-grade glioma. *Cell Death Differ.* 23 (4), 640–653. doi:10.1038/cdd.2015.131

Robin, X., Turck, N., Hainard, A., Tiberti, N., Lisacek, F., Sanchez, J. C., et al. (2011). pROC: an open-source package for R and S+ to analyze and compare ROC curves. *BMC Bioinforma.* 12, 77. doi:10.1186/1471-2105-12-77

Saha, A. K., Contreras-Galindo, R., Niknafs, Y. S., Iyer, M., Qin, T., Padmanabhan, K., et al. (2020). The role of the histone H3 variant CENPA in prostate cancer. *J. Biol. Chem.* 295 (25), 8537–8549. doi:10.1074/jbc.RA119.010080

Sampson, J. H., Gunn, M. D., Fecci, P. E., and Ashley, D. M. (2020). Brain immunology and immunotherapy in brain tumours. *Nat. Rev. Cancer* 20 (1), 12–25. doi:10.1038/s41568-019-0224-7

Sansregret, L., Vanhaesebroeck, B., and Swanton, C. (2018). Determinants and clinical implications of chromosomal instability in cancer. *Nat. Rev. Clin. Oncol.* 15 (3), 139–150. doi:10.1038/nrclinonc.2017.198

Serafim, R. B., Cardoso, C., Di Cristofaro, L. F. M., Pienna Soares, C., Araújo Silva, W., Jr., Espreafico, E. M., et al. (2020). HJURP knockdown disrupts clonogenic capacity and increases radiation-induced cell death of glioblastoma cells. *Cancer Gene Ther.* 27 (5), 319–329. doi:10.1038/s41417-019-0103-0

Sharma, A. B., Dimitrov, S., Hamiche, A., and Van Dyck, E. (2019). Centromeric and ectopic assembly of CENP-A chromatin in health and cancer: Old marks and new tracks. *Nucleic Acids Res.* 47 (3), 1051–1069. doi:10.1093/nar/gky1298

Shen, J., Li, R., and Li, G. (2009). Inhibitory effects of decoy-ODN targeting activated STAT3 on human glioma growth *in vivo*. *Vivo* 23 (2), 237–243.

Shi, K., Zhu, X., Wu, J., Chen, Y., Zhang, J., and Sun, X. (2021). Centromere protein E as a novel biomarker and potential therapeutic target for retinoblastoma. *Bioengineered* 12 (1), 5950–5970. doi:10.1080/21655979.2021.1972080

Shimato, S., Maier, L. M., Maier, R., Bruce, J. N., Anderson, R. C., and Anderson, D. E. (2012). Profound tumor-specific Th2 bias in patients with malignant glioma. *BMC Cancer* 12, 561. doi:10.1186/1471-2407-12-561

Shrestha, R. L., Ahn, G. S., Staples, M. I., Sathyan, K. M., Karpova, T. S., Foltz, D. R., et al. (2017). Mislocalization of centromeric histone H3 variant CENP-A

contributes to chromosomal instability (CIN) in human cells. *Oncotarget* 8 (29), 46781–46800. doi:10.18632/oncotarget.18108

Shrestha, R. L., Rossi, A., Wangsa, D., Hogan, A. K., Zaldana, K. S., Suva, E., et al. (2021). CENP-A overexpression promotes aneuploidy with karyotypic heterogeneity. *J. Cell Biol.* 220 (4), e202007195. doi:10.1083/jcb.202007195

Stangeland, B., Mughal, A. A., Grieg, Z., Sandberg, C. J., Joel, M., Nygard, S., et al. (2015). Combined expressional analysis, bioinformatics and targeted proteomics identify new potential therapeutic targets in glioblastoma stem cells. *Oncotarget* 6 (28), 26192–26215. doi:10.18632/oncotarget.4613

Sun, X., Clermont, P. L., Jiao, W., Helgason, C. D., Gout, P. W., Wang, Y., et al. (2016). Elevated expression of the centromere protein-A(CENP-A)-encoding gene as a prognostic and predictive biomarker in human cancers. *Int. J. Cancer* 139 (4), 899–907. doi:10.1002/ijc.30133

Tosolini, M., Kirilovsky, A., Mlecnik, B., Fredriksen, T., Mauger, S., Bindea, G., et al. (2011). Clinical impact of different classes of infiltrating T cytotoxic and helper cells (Th1, th2, treg, th17) in patients with colorectal cancer. *Cancer Res.* 71 (4), 1263–1271. doi:10.1158/0008-5472.can-10-2907

van den Bent, M. J., Brandes, A. A., Taphoorn, M. J., Kros, J. M., Kouwenhoven, M. C., Delattre, J. Y., et al. (2013). Adjuvant procarbazine, lomustine, and vincristine chemotherapy in newly diagnosed anaplastic oligodendroglioma: long-term follow-up of EORTC brain tumor group study 26951. *J. Clin. Oncol.* 31 (3), 344–350. doi:10.1200/jco.2012.43.2229

Vivian, J., Rao, A. A., Nothaft, F. A., Ketchum, C., Armstrong, J., Novak, A., et al. (2017). Toil enables reproducible, open source, big biomedical data analyses. *Nat. Biotechnol.* 35 (4), 314–316. doi:10.1038/nbt.3772

Wang, Q., Xu, J., Xiong, Z., Xu, T., Liu, J., Liu, Y., et al. (2021a). CENPA promotes clear cell renal cell carcinoma progression and metastasis via Wnt/β-catenin signaling pathway. *J. Transl. Med.* 19 (1), 417. doi:10.1186/s12967-021-03087-8

Wang, Y., Zhang, H., Wang, M., He, J., Guo, H., Li, L., et al. (2021b). CCNB2/SASP/Cathepsin B & PGE2 Axis induce cell senescence mediated malignant transformation. *Int. J. Biol. Sci.* 17 (13), 3538–3553. doi:10.7150/ijbs.63430

Weller, M., Wick, W., Aldape, K., Brada, M., Berger, M., Pfister, S. M., et al. (2015). Glioma. *Nat. Rev. Dis. Prim.* 1, 15017. doi:10.1038/nrdp.2015.17

Wesseling, P., and Capper, D. (2018). WHO 2016 Classification of gliomas. *Neuropathol. Appl. Neurobiol.* 44 (2), 139–150. doi:10.1111/nan.12432

Wu, F., Wang, Z. L., Wang, K. Y., Li, G. Z., Chai, R. C., Liu, Y. Q., et al. (2020). Classification of diffuse lower-grade glioma based on immunological profiling. *Mol. Oncol.* 14 (9), 2081–2095. doi:10.1002/1878-0261.12707

Wu, Q., Chen, Y. F., Fu, J., You, Q. H., Wang, S. M., Huang, X., et al. (2014). Short hairpin RNA-mediated down-regulation of CENP-A attenuates the aggressive phenotype of lung adenocarcinoma cells. *Cell. Oncol.* 37 (6), 399–407. doi:10.1007/s13402-014-0199-z

Wu, Q., Qian, Y. M., Zhao, X. L., Wang, S. M., Feng, X. J., Chen, X. F., et al. (2012). Expression and prognostic significance of centromere protein A in human lung adenocarcinoma. *Lung Cancer* 77 (2), 407–414. doi:10.1016/j.lungcan.2012.04.007

Xu, Y., Liang, C., Cai, X., Zhang, M., Yu, W., and Shao, Q. (2020). High centromere protein-A (CENP-A) expression correlates with progression and prognosis in gastric cancer. *Onco. Targets. Ther.* 13, 13237–13246. doi:10.2147/OTT.S263512

Yao, Y., Ye, H., Qi, Z., Mo, L., Yue, Q., Baral, A., et al. (2016). B7-H4(B7x)-Mediated cross-talk between glioma-initiating cells and macrophages via the IL6/JAK/STAT3 pathway lead to poor prognosis in glioma patients. *Clin. Cancer Res.* 22 (11), 2778–2790. doi:10.1158/1078-0432.ccr-15-0858

Yu, G., Wang, L. G., Han, Y., and He, Q. Y. (2012). clusterProfiler: an R package for comparing biological themes among gene clusters. *OMICS* 16 (5), 284–287. doi:10.1089/omi.2011.0118

Zeng, Z., Jiang, X., Pan, Z., Zhou, R., Lin, Z., Tang, Y., et al. (2021). Highly expressed centromere protein L indicates adverse survival and associates with immune infiltration in hepatocellular carcinoma. *Aging (Albany NY)* 13 (19), 22802–22829. doi:10.18632/aging.203574

Zhang, W., Mao, J. H., Zhu, W., Jain, A. K., Liu, K., Brown, J. B., et al. (2016). Centromere and kinetochore gene misexpression predicts cancer patient survival and response to radiotherapy and chemotherapy. *Nat. Commun.* 7, 12619. doi:10.1038/ncomms12619

Zhang, W., Xu, Y., Zhang, J., and Wu, J. (2020a). Identification and analysis of novel biomarkers involved in chromophobe renal cell carcinoma by integrated bioinformatics analyses. *Biomed. Res. Int.* 2020, 2671281. doi:10.1155/2020/2671281

Zhang, Y., Yang, L., Shi, J., Lu, Y., Chen, X., and Yang, Z. (2020b). The oncogenic role of CENPA in hepatocellular carcinoma development: Evidence from bioinformatic analysis. *Biomed. Res. Int.* 2020, 3040839. doi:10.1155/2020/3040839

Zhou, H., Bian, T., Qian, L., Zhao, C., Zhang, W., Zheng, M., et al. (2021). Prognostic model of lung adenocarcinoma constructed by the CENPA complex genes is closely related to immune infiltration. *Pathol. Res. Pract.* 228, 153680. doi:10.1016/j.prp.2021.153680

Zhou, Y., Zhou, B., Pache, L., Chang, M., Khodabakhshi, A. H., Tanaseichuk, O., et al. (2019). Metascape provides a biologist-oriented resource for the analysis of systems-level datasets. *Nat. Commun.* 10 (1), 1523. doi:10.1038/s41467-019-09234-6

frontiers | Frontiers in Immunology

TYPE Original Research
PUBLISHED 13 November 2023
DOI 10.3389/fimmu.2023.1247288



OPEN ACCESS

EDITED BY
Caroline Chung,
University of Texas MD Anderson Cancer Center, United States

REVIEWED BY
Aimin Jiang,
The First Affiliated Hospital of Xi'an Jiaotong University, China
João Pessoa,
University of Aveiro, Portugal

*CORRESPONDENCE
Haibo Sun
frenksun@126.com
Weibing Dong
weibing.dong@lnnu.edu.cn

†These authors have contributed equally to this work

RECEIVED 25 June 2023
ACCEPTED 30 October 2023
PUBLISHED 13 November 2023

CITATION
Shi B, Ge F, Cai L, Yang Y, Guo X, Wu R, Fan Z, Cao B, Wang N, Si Y, Lin X, Dong W and Sun H (2023) Significance of NotchScore and JAG1 in predicting prognosis and immune response of low-grade glioma.
*Front. Immunol.* 14:1247288.
doi: 10.3389/fimmu.2023.1247288



# Significance of NotchScore and JAG1 in predicting prognosis and immune response of low-grade glioma

Bo Shi[1,2,3†], Fei Ge[4†], Liangliang Cai[1,3†], Yi Yang[1,3†], Xiaohui Guo[2], Rui Wu[2], Zhehao Fan[1,3], Binjie Cao[1,3], Ning Wang[1,3], Yue Si[1,3], Xinyue Lin[1,3], Weibing Dong[2*] and Haibo Sun[1,3*]

[1]Institute of Translational Medicine, Medical College, Yangzhou University, Yangzhou, China, [2]School of Life Science, Liaoning Normal University, Dalian, Liaoning, China, [3]Jiangsu Key Laboratory of Experimental & Translational Non-Coding RNA Research, Yangzhou, Jiangsu, China, [4]Department of Gastroenterology, Haian Hospital of Traditional Chinese Medicine Affiliated to Nanjing University of Chinese Medicine, Nantong, Jiangsu, China

**Introduction:** Low-grade glioma (LGG) is a prevalent malignant tumor in the intracranial region. Despite the advancements in treatment methods for this malignancy over the past decade, significant challenges still persist in the form of drug resistance and tumor recurrence. The Notch signaling pathway plays essential roles in many physiological processes as well as in cancer development. However, the significance of the pathway and family genes in LGG are poorly understood.

**Methods:** We conducted gene expression profiling analysis using the TCGA dataset to investigate the gene set associated with the Notch signaling pathway. we have proposed a metric called "NotchScore" that quantifies the strength of the Notch signaling pathway and enables us to assess its significance in predicting prognosis and immune response in LGG. We downregulated JAG1 in low-grade gliomas to assess its influence on the proliferation and migration of these tumors. Ultimately, we determined the impact of the transcription factor VDR on the transcription of PDL1 through chip-seq data analysis.

**Results:** Our findings indicate that tumors with a higher NotchScore, exhibit poorer prognosis, potentially due to their ability to evade the anti-tumor effects of immune cells by expressing immune checkpoints. Among the genes involved in the Notch signaling pathway, JAG1 has emerged as the most representative in terms of capturing the characteristics of both NotchScore and Notch pathways. The experimental results demonstrate that silencing JAG1 yielded a significant decrease in tumor cell proliferation in LGG cell lines. Our study revealed mechanisms by which tumors evade the immune system through the modulation of PDL1 transcription levels via the PI3K-Akt signaling pathway. Additionally, JAG1 potentially influences PDL1 in LGG by regulating the PI3K-Akt signaling pathway and the expression of the transcription factor VDR.

**Discussion:** These findings contribute to our understanding of immune evasion by tumors in LGG. The insights gained from this research may have implications for the development of therapeutic interventions for LGG.

KEYWORDS

notch, low-grade glioma, prognosis, tumor immune microenvironment, JAG1, PDL1

# Introduction

Glioma is a type of tumor that commonly develops within the central nervous system and has been extensively researched. The World Health Organization (WHO) has established a classification system for gliomas, which categorizes them into four grades according to their histopathological and molecular features (1, 2). Low-grade gliomas (LGG) are normally considered to have a low malignancy. However, LGG can still proliferate and progress in various ways, and the survival rate for patients with LGG is not ideal. According to a recent study, the median overall survival for grade II glioma patients with LGG is 78.1 months (2). Therefore, early diagnosis and treatment of LGG are crucial, and regular follow-up of LGG patients is necessary to detect any deterioration in their condition and to adjust treatment plans in a timely manner.

The Notch signaling pathway is a highly conserved pathway across evolution that contributes in regulating a number of cellular behaviors. These processes encompass cell proliferation, apoptosis, differentiation, tissue homeostasis maintenance, immune regulation, and disease progression (3, 4). Importantly, reports have discovered that blockade of the Notch pathway disrupts tumor blood vessel structure and promotes tumor metastasis (5). In osteosarcoma tissues and cells, there is a high expression of different molecules involved in the Notch signaling pathway (6). Specifically, the protein JAG1, belonging to the Notch family, exhibits significantly increased levels in highly metastatic osteosarcoma cells compared to low metastatic ones. Recent studies have demonstrated that suppressing JAG1 expression results in decreased proliferation, migration, and invasion capabilities of osteosarcoma cells (7).

As research on the tumor microenvironment (TME) continues, immunotherapy based on TME has been increasingly applied in clinical practice with promising results (8, 9). Recent studies have highlighted the close relationship between the biological characteristics of gliomas and their immune microenvironment (TME) (10). Glioma cells secrete diverse chemokines, cytokines, and growth factors that contribute in promoting immune cell infiltration into the tumor microenvironment. These cell types comprise most of the white blood cells including circulating progenitor cells, astrocytes, pericytes, endothelial cells, as well as various immune cells, including peripheral macrophages, microglia, effector T cells, and regulatory T cells (Treg cells) (11). Identifying these factors may aid in enhancing the immune modulation utilized by glioma cells, thereby serving as a basis for glioma immunotherapy (11, 12). In previous studies, mice with glioblastoma (GBM) were subjected to treatment using anti-PD-1 antibody or combinational therapies using anti-PD-1 and anti-CTLA-4 antibodies. Notably, both wild-type (WT) mice and CD73-/- mice receiving the combination therapy, which included anti-PD-L1, exhibited significantly improved survival rates compared to the control group (13). Hence, exploring the benefits of immune checkpoint inhibitors in LGG might be a viable approach.

Here, we studied the role of the Notch signaling pathway in low-grade gliomas (LGG). By analyzing the gene expression profiles of Notch signaling pathway-related genes in the TCGA dataset, we developed a metric called "NotchScore" to distinguish two distinct subtypes of LGG (CS1-CS2). Subsequently, we assessed the prognostic relevance of these two subtypes and investigated their disparities concerning the TME. Lastly, we conducted experimental validation to establish the critical role of the Notch family protein JAG1 in this process. These findings may provide a solid foundation for future research on targeted therapy for LGG.

# Results

## NotchScore clustering

In this study, we collected Notch signaling pathway-related genes from the HALLMARK database and previous studies. Utilizing the STRING database, we performed a protein-protein interaction (PPI) network analysis for identification of the crucial genes within the selected gene set and elucidate their interactions. We aimed to identify the core genes of the Notch signaling pathway within the selected gene set and gain a comprehensive understanding of their interactions. (Figure 1A). To explore the prognosis of LGG patients with different expression levels of Notch gene sets, unsupervised clustering analysis was performed on 483 LGG samples to determine the expression patterns of different groups of Notch gene sets. Cluster-consensus analysis and inter-group principal component analysis indicated that K=2 was the optimal cluster number, and thus the LGG samples were divided into two groups for further analysis (Figures 1B–E). The study established a NotchScore scoring method using the Genomic Grade Index to evaluate the expression of Notch-associated genes from each group of patients. These findings indicated that the CS2 group exhibited a higher NotchScore in comparison to the CS1 group

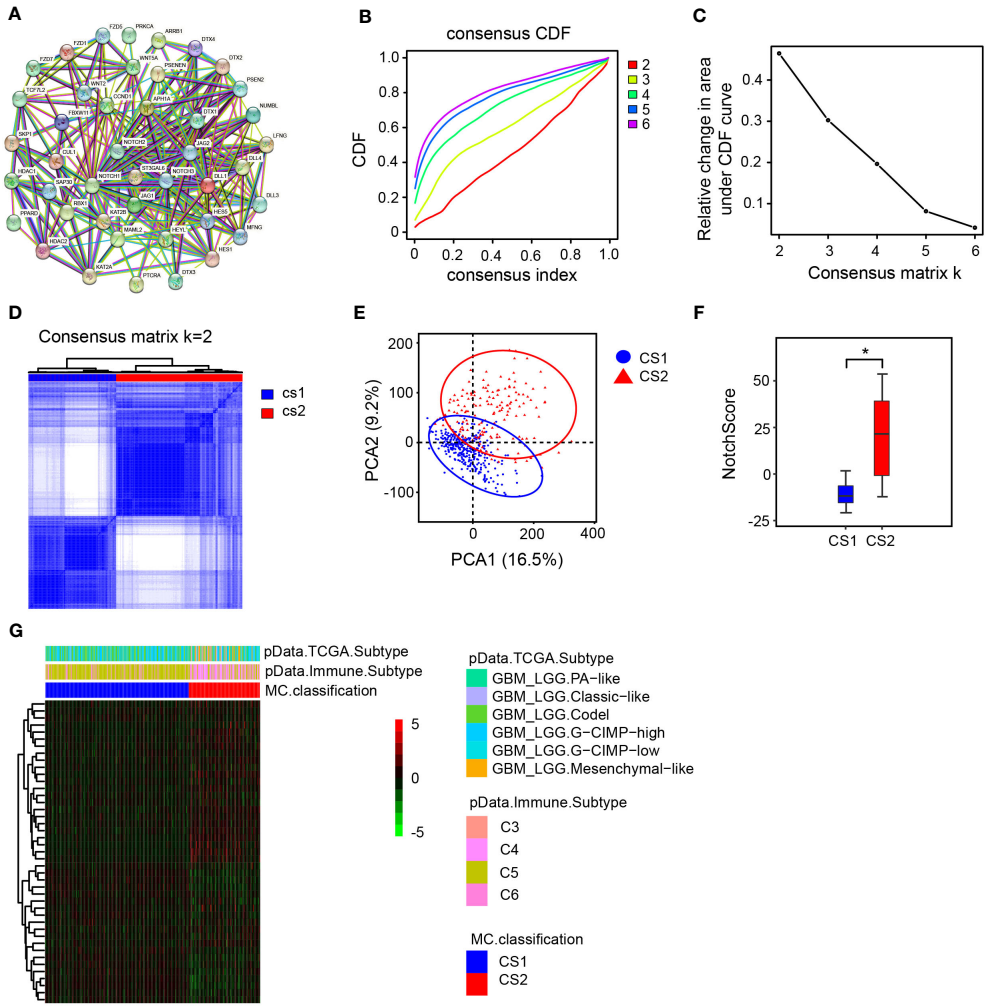


FIGURE 1
Cluster analysis and NotchScore. **(A)** Protein-protein interaction network diagram of Notch-related genes. **(B)** consensus matrix CDFs from K=2 to 6. The cumulative distribution functions are shown for varying values of k. CDF: cumulative distribution function. **(C)** Delta Area Plot, this graph illustrates the relative change in the area under the cumulative distribution function (CDF) curve when compared to k-1., **(D)** Heatmap of the matrix for k = 2. **(E)** Principal Component Analysis (PCA) based on mRNA expression patterns in LGG. PCA quantifies the differences between two groups of sample data by extracting two principal components, PC1 (Principal Component 1) and PC2 (Principal Component 2), which capture the largest and second-largest variations in the data, respectively. **(F)** Establishment of NotchScore to compare the differences between the two groups. **(G)** Heatmap illustrating the expression patterns of Notch-related genes in the two groups. PA-like: Based on the molecular similarity with pilocytic-astrocytomas. Classic-like: tumors belonging to the classical gene expression signature. Codel: consisting of IDH-mutant-codel LGGs. CIMP-high: IDH-mutant-non-codel glioma (LGG, GBM) manifesting relatively low genome wide DNA methylation. CIMP-low: IDH-mutant-non-codel glioma (LGG, GBM) with higher global levels of DNA methylation. Mesenchymal-like: enriched with mesenchymal subtype tumors.

(Figure 1F), and the heat map shows that samples in the CS2 group exhibit a diverse opposite patten of Notch gene expressions compared to CS1 group (Figure 1G).

## The NotchScore is related to LGG prognosis and specific signaling pathways

To examine the correlation between NotchScore and prognosis of LGG patients, survival analysis was performed using TCGA dataset. The results showed that patients in the CS2 group, characterized by high NotchScore, had a poorer prognosis compared to those in the CS1 group, characterized by low NotchScore (Figure 2A).To further explore the association between the mRNA levels of Notch-associated genes and prognosis, we conducted differential gene analysis. This analysis involved applying specific criteria, including a fold change (FC) threshold of >2 or<-2, $|\log_2 FC|>1$, and significant p-values (p.val)< 0.05, $-\log_{10}$ (p.val) >$-\log_{10}$ 0.05. As a result, we identified 738 upregulated differentially expressed genes (DEGs) and 909 downregulated DEGs (Figure 2B).We performed enrichment analysis on the DEGs to identify relevant biological functions and signaling pathways. The gene ontology (GO) analysis revealed enrichment in channel activity, positive regulation of cell adhesion, and actin cytoskeleton. Additionally, the Kyoto Encyclopedia of Genes and Genomes (KEGG) analysis identified several important signaling pathways, including the p53, cAMP, MAPK, cell cycle, and PI3K-Akt signaling pathways (Figures 2C, D).

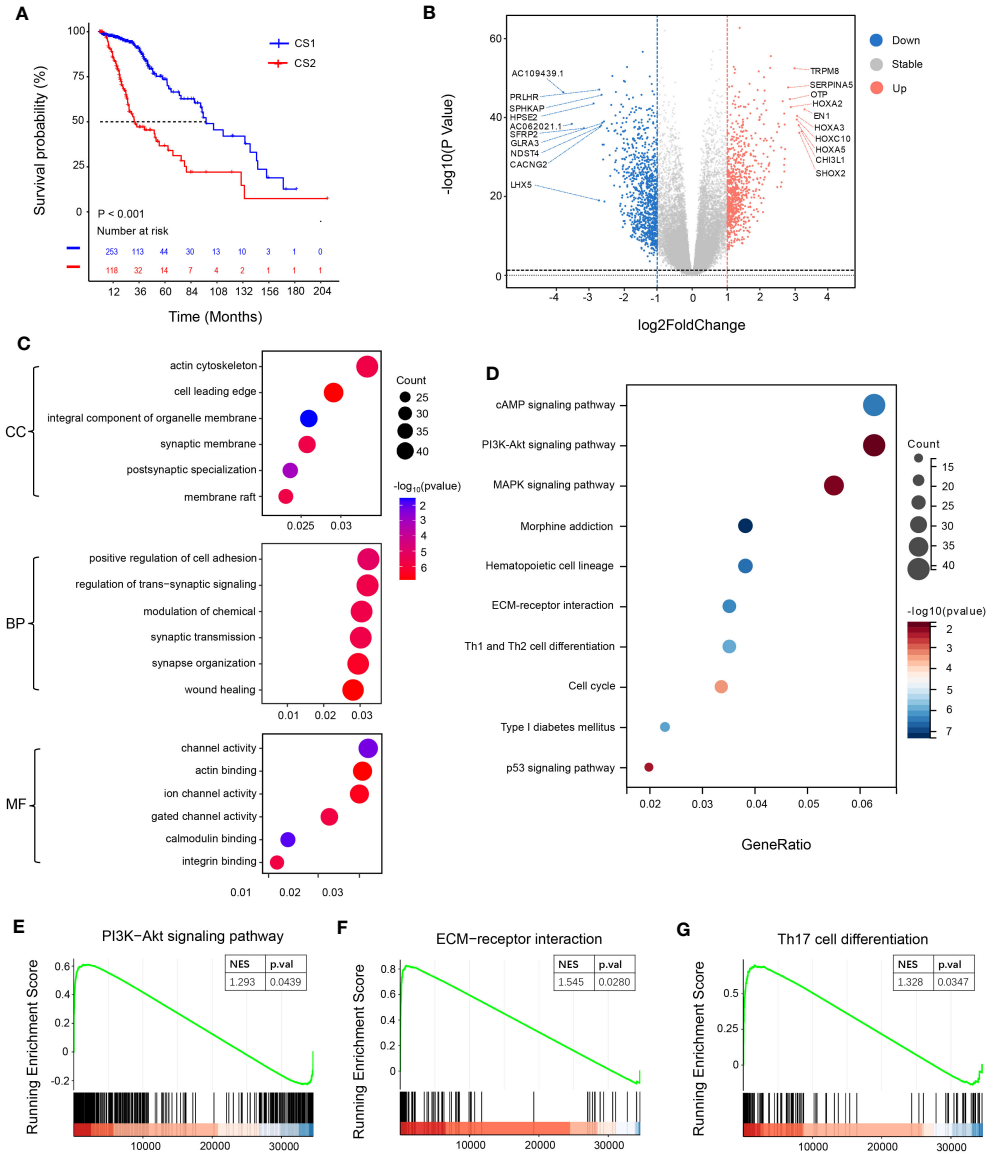


FIGURE 2
Survival analysis and functional specificity analysis of subgroups. **(A)** Kaplan-Meier curves of overall survival (OS) for the two groups after clustering analysis. **(B)** Volcano plot illustrating the distribution of differentially expressed genes. Genes with a P-value< 0.05 and |log2FoldChange| > 1 are considered differentially expressed, with 738 genes upregulated and 909 genes downregulated. **(C)** Gene Ontology (GO) enrichment pathway analysis. The x-axis of the bubble plot represents the proportion of differentially expressed genes in each pathway, while the y-axis represents the enriched pathways. "Count" indicates the number of differentially expressed genes enriched in each pathway. The color of the circles represents the -log10(P-value) of pathway enrichment. **(D)** Kyoto Encyclopedia of Genes and Genomes (KEGG) enrichment pathway analysis. **(E–G)** Pathway analysis using the gene set enrichment analysis (GSEA) method (CSEA).

Moreover, we conducted gene set enrichment analysis (GSEA) and observed that the CS2 group exhibited upregulation of the ECM-receptor interaction, PI3K-Akt signaling pathway, and Th17 cell differentiation (Figures 2E–G).

## NotchScore and Notch-related genes are correlated with TME

Recent studies have demonstrated that T cell antigen receptor (TCR), CD28, and interleukin-2 receptor activate PI3K through the phosphorylation and deactivation of PI3K inhibitory molecules. PI3K converts PIP2 into PIP3, which in turn recruits downstream signaling molecules such as PDK1 and Akt to the membrane and activates them (14). mTORC2 further activates Akt and promotes metabolic expansion and T cell effector function (14, 15). The enrichment pathway analysis showed significant enrichments of the PI3K-Akt and Th1 and Th2 cell differentiation signaling pathways, indicating notable differences in immune function between the two groups. Using GSVA gene set variation analysis, the study found that compared to the CS1 group, the CS2 group had an upregulation trend in antigen presentation, white blood cell function, lymphocyte functions (B cell, T cell, and NK cell), and cell cycle (Figure 3A). These findings imply potential variations in the tumor immune

10.3389/fimmu.2023.1247288

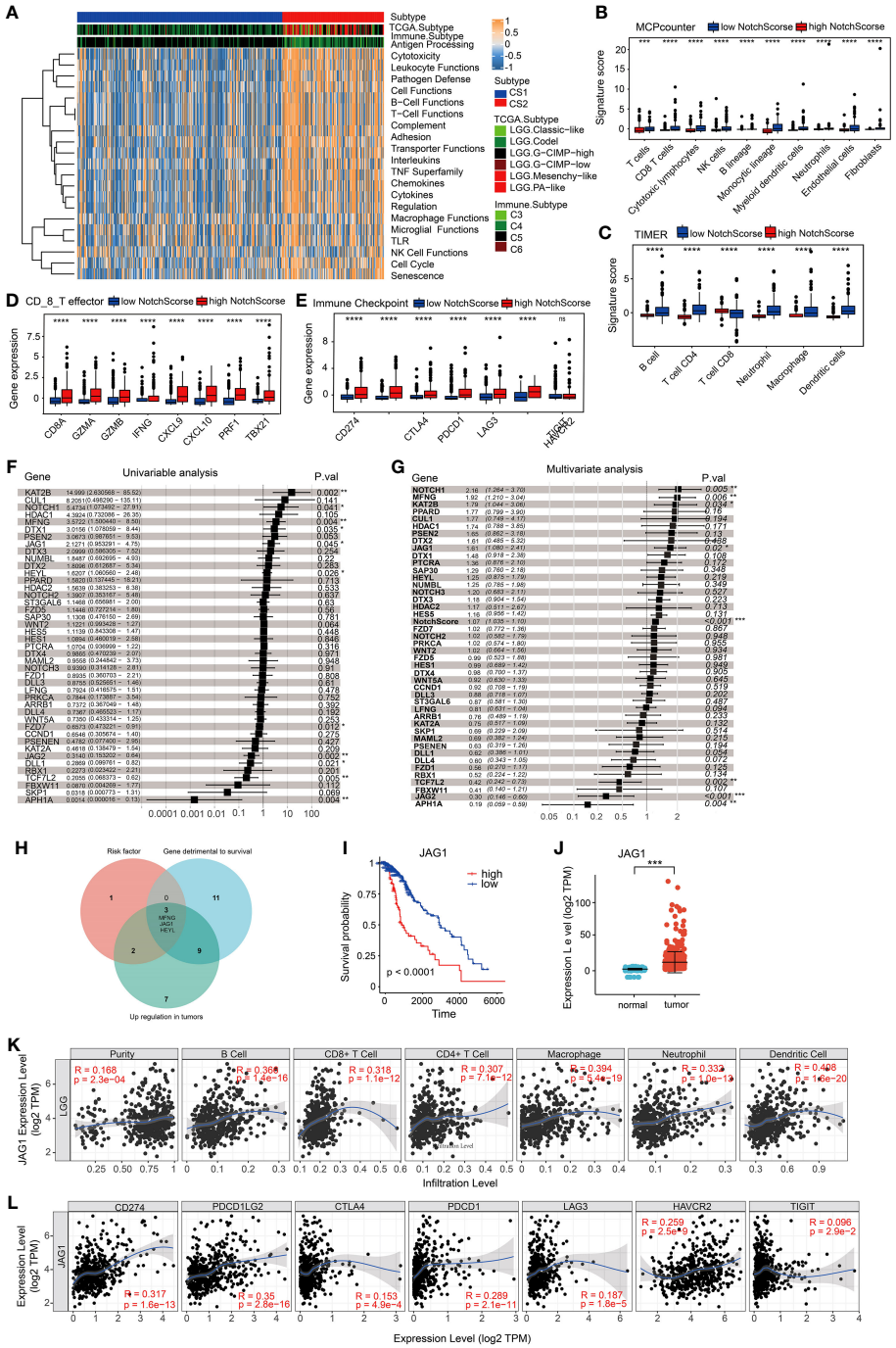

FIGURE 3
Immune characteristics of two subclasses in the metadata set. **(A)** Evaluation of pathway/function activity changes using Gene Set Variation Analysis (GSVA). **(B, C)** Analysis of differences in immune cell abundance between different groups using two methods: MCPcounter and TIMER. **(D, E)** Expression levels of CD8_T effector factors and immune checkpoints. The x-axis represents different genes, while the y-axis represents gene expression levels. **(F)** Univariable cox analysis. **(G)** Univariable cox analysis. **(H)** Venn diagram illustrating three genes that meet the criteria for risk factors, with higher gene expression levels in tumors. High expression of these genes in patient samples is associated with poor prognosis. **(I)** Kaplan-Meier curve demonstrating the expression of JAG1 and overall survival (OS) in LGG patients. **(J)** Differential expression of JAG1 between normal brain tissue and LGG. **(K, L)** Correlation between JAG1 expression and immune infiltration levels, as well as the expression of immune checkpoints. *:P<0.05, **:P<0.01, ***P<0.001.

microenvironment between the CS1 and CS2 groups. Therefore, the study analyzed related immune factors such as immune infiltration and immune checkpoints. MCPcounter and TIMER were utilized to assess the immunoheterogeneity between these subtypes and provide a comprehensive overview of distinct immune cell infiltrations. Specifically, compared to samples with low NotchScore, samples with high NotchScore showed low levels of immune cell infiltration, including T cells, cytotoxic lymphocytes,

macrophages, NK cells, and B cells (Figures 3B, C). Furthermore, immune checkpoint and CD8 T cell effectors were significantly upregulated in the group with higher NotchScore (Figures 3D, E). The TIDE Score Calculation, utilized for evaluating the potential clinical effectiveness of immunotherapy in various risk groups, mirrors the potential tumor immune evasion capability (Figure S1-B). The analysis results suggest an elevated probability of immune evasion in patients with a high NotchScore. Univariable analysis and multivariate analysis of the Notch gene set showed that genes were identified as risk factors for the CS2 group (Figures 3F, G). The NotchScore value exhibits statistical significance in its impact on survival time(HR=1.07, 95%CI 1.035-1.10, P<0.001) (Figure 3G). We then set the criteria for gene selection, focusing on genes that were not only risk factors for the CS2 group but also exhibited higher expression levels in tumors and their high expression in patient was associated with poor prognosis. Venn diagram analysis revealed that three genes, namely JAG1, MFNG, and HEYL, met these criteria (Figure 3H). The data analysis revealed a significant correlation between high JAG1 expression and poor prognosis in patients. Additionally, the expression of JAG1 in tumor tissues is elevated compared to normal brain tissues (Figures 3I, J). Specifically, JAG1 expression showed a positive correlation with the immune cell infiltrations of various cell types, including B cells, T cells, neutrophils, macrophages and dendritic cells. Additionally, There is a positive correlation between mRNA levels of JAG1 and various immune checkpoint markers, including CD274, PDCD1, PDCD1-LG2, and HAVCR2 (Figures 3K, L). These findings show that JAG1 may be a new target for detecting sensitivity to tumor and immune therapy, as well as for tumor treatment.

## JAG1 silencing reduces Notch signaling transduction

To evaluate the effects of JAG1 silencing on the cell proliferation and migration capabilities in low-grade glioma (LGG) cells, we employed small interfering RNA (siRNA) specifically designed for JAG1 and transfected it into SW1088 and HS683 cell lines. Subsequently, we examined the expression of JAG1 after siRNA interference and confirmed that JAG1 expression was effectively suppressed both at the mRNA and protein levels (Figures 4A, B). The downstream factors of Notch signaling pathway including Hes1, Hey1, and VEGF of the were also examined, and qPCR results showed that their transcription levels were decreased after JAG1 silencing, indicating that Notch signal transduction was inhibited (Figure 4C). MTT assays were further conducted in order to evaluate the impact of JAG1 silencing on cell proliferation. The results demonstrated a notable reduction in the proliferation capacity of HS683 and SW1088 cells compared to the control group. (Figure 4D). Scratch assays were thereafter conducted to test JAG1 silencing on the migration ability and results revealed a decrease in the migration ability of HS683 and SW1088 cells following JAG1 silencing. (Figures 4E–H). Furthermore, changes in the cell cycle of HS683 and SW1088 cells after JAG1 silencing were examined. The results indicated a rise in the population of cells in the G1 phase, together with a reduction in cells in the S and G2 phases. These findings suggest a potential cell cycle arrest effect. (Figures 4I–L). Additionally, immunoblot results showed that core cell cycle regulating factors such as MCM2, cyclin D1 and cyclin E1 were downregulated at the protein level after JAG1 silencing (Figure 4M).

## JAG1 expression regulates immune checkpoint-related genes

To examine the association between JAG1 and immune checkpoints, this research assessed the mRNA levels of immune checkpoints. The findings revealed a noteworthy reduction in the expression of PDL1 and PDCD1 upon JAG1 knockdown. However, the expression levels of other immune checkpoints remained unaltered. (Figures 5A, B). Previous research has indicated that the AKT-mTOR pathway promotes immune evasion in lung adenocarcinoma by driving PD-L1 expression (16). Furthermore, the Notch signaling pathway interacts with the PI3K-AKT pathway to some extent. In this study, we indeed found a strong significance of the PI3K-AKT signaling pathway in differential gene enrichment pathways and P-AKT levels were decreased after JAG1 knockdown (Figure 5C). To investigate the transcriptional regulatory relationship between JAG1 and PDL1, this study predicted the transcription factors of PDL1 through cistrome DB (Figure 5D), and then selected the top 10 ranked transcription factors for mRNA-level detection. The qPCR results showed that among the 10 transcription factors, C-JUN, NFKB2, and VDR were downregulated at the mRNA level in HS683 and SW1088 cells when JAG1 was silenced (Figure 5E). Additionally, we reanalyzed previous reported CHIP-seq data of C-JUN (GSM1208639), NFKB2 (GSM1208776), and VDR (GSM791404), and discovered that VDR may exhibit a higher binding peak by binding to the promoter region of PDL1 (Figures 5F, G). Simultaneously, we observed distinct binding peaks of VDR in the PDL1 promoter region across various tissues (Figures S1-C). Since VDR has been shown to regulate PDL1 transcription (17, 18), our preliminary results indicate that JAG1 may activate PDL1 transcription through up-regulation of VDR.

# Discussion

The Notch signaling pathway is a conserved signaling pathway that depends on direct cell-to-cell contact between cells of the same type or different types for signal transmission (7). The Notch receptor and ligand can be expressed on the same cell or on different cells (3). Due to its robust intercellular communication, the Notch signaling pathway plays an important role in regulating and controlling cell fate. The Notch pathway has been associated with various types of cancer including brain cancer, breast cancer, and lung cancer, among others (3). This provides a solid theoretical basis for further investigating the Notch signaling pathway in low-grade glioma (LGG). Our analysis revealed that high expression levels of Notch-related genes are linked to poor survival and

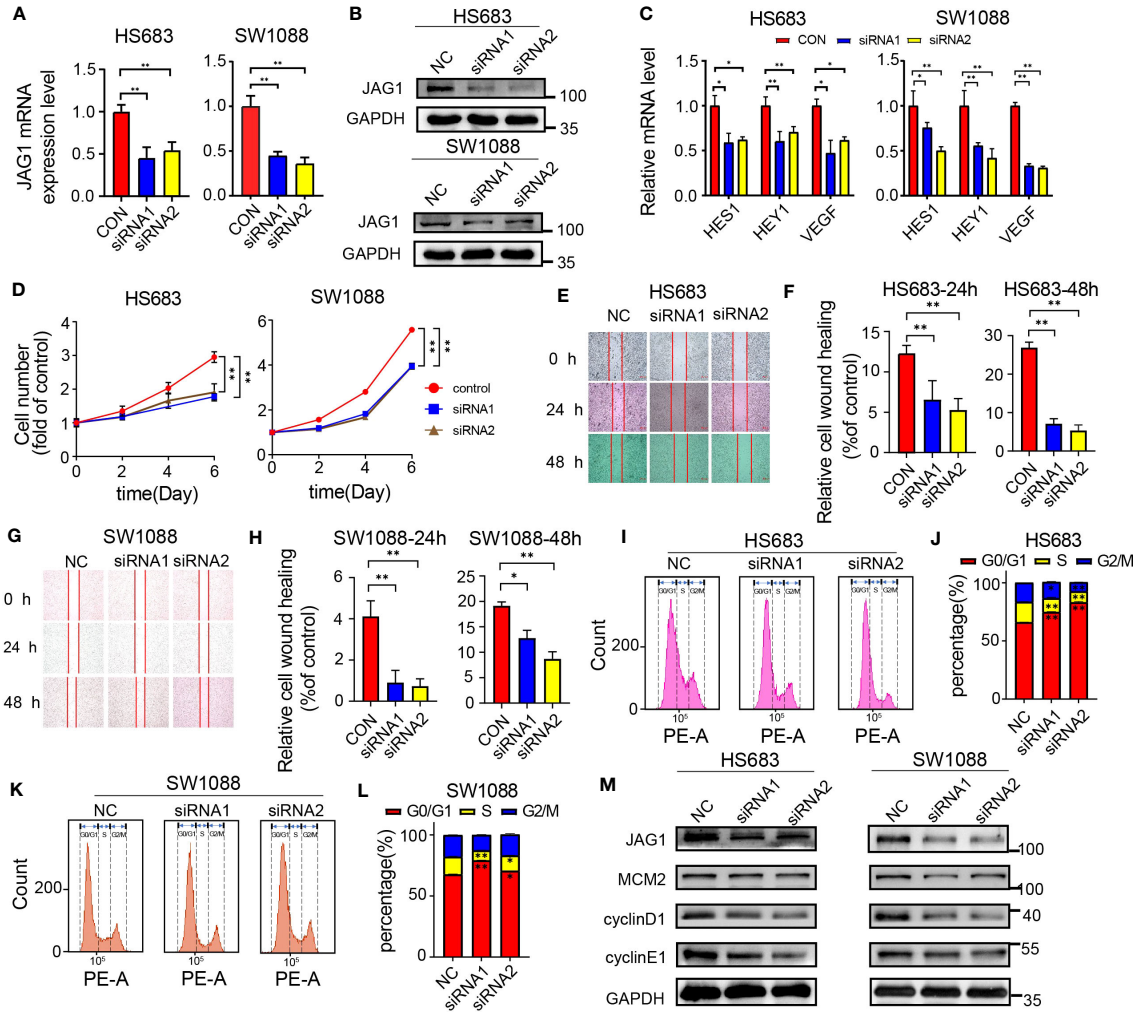


FIGURE 4
JAG1 regulates the proliferation and migration of LGG cells. **(A)** qPCR results confirm the effective downregulation of JAG1 in HS683 and SW1088 cells. **(B)** Western blot results validate the successful silencing of JAG1 in HS683 and SW1088 cells. **(C)** qPCR analysis reveals the expression levels of downstream factors (HES1, hey1, VEGF) in the Notch signaling pathway at the RNA level. **(D)** Impact of JAG1 silencing on the proliferation of HS683 and SW1088 cells. **(E, G)** Effect of JAG1 silencing on the migration capability of SW1088 and HS683 cells. **(F, H)** Bar graphs depicting cell migration rates at 24 hours and 48 hours. **(I, K)** Flow cytometry analysis investigating the influence of JAG1 silencing on the cell cycle of HS683 and SW1088 cells. **(J, L)** Bar graphs illustrating the distribution of cells in the G0/G1, S, and G2/M phases. **(M)** Western blot analysis of key cell cycle regulators. *:P<0.05, **:P<0.01, ***P<0.001.

reduced immune infiltration. These findings suggest that the Notch signaling pathway is vital for immune cell differentiation, tumor microenvironment formation, and tumor development. Analysis using COX regression and a comparison of Notch gene expression between normal tissues and tumors revealed that JAG1 expression is elevated in tumors and is positively associated with a poorer prognosis. Moreover, JAG1 exhibits a strong correlation with the immune response. These results suggest the importance of JAG1 in LGG.

In brain and ovarian cancer, JAG1 is strongly expressed in tumor-associated blood vessels, suggesting its involvement in angiogenesis (19). Previous studies have demonstrated that increased JAG1 expression activates the Notch signaling pathway, promoting the proliferation of invasive cancer cells in adrenocortical carcinoma (20). Interestingly, a previous immunohistochemical assay showed an increase in JAG1 expression with higher WHO grades of gliomas (levels from II to IV) (21), which indicates JAG1 protein expression maybe associated with progression of the disease. In the context of LGG, experimental results indicate that silencing JAG1 reduces the mRNA expression level of VEGF, a key regulator of angiogenesis, and weakens the migration ability of HS683 and SW1088 cells (3). Cell cycle analysis revealed that JAG1 knockdown led to an increased proportion of cells in the G0/G1 phase. Moreover, the protein levels of cell cycle regulatory proteins, such as cyclin D1 and cyclin E1, were reduced. These proteins has been recognized to regulate the transition of G1 to S phase of the cell cycle. These findings suggest that JAG1 potentially influences the proliferation and migration of LGG cells by modulating downstream activity of the Notch pathway and cell cycle regulatory proteins, thereby promoting tumor progression.

In addition, the researchers found that soluble monomeric JAG1 signaling significantly reduced the immunosuppressive

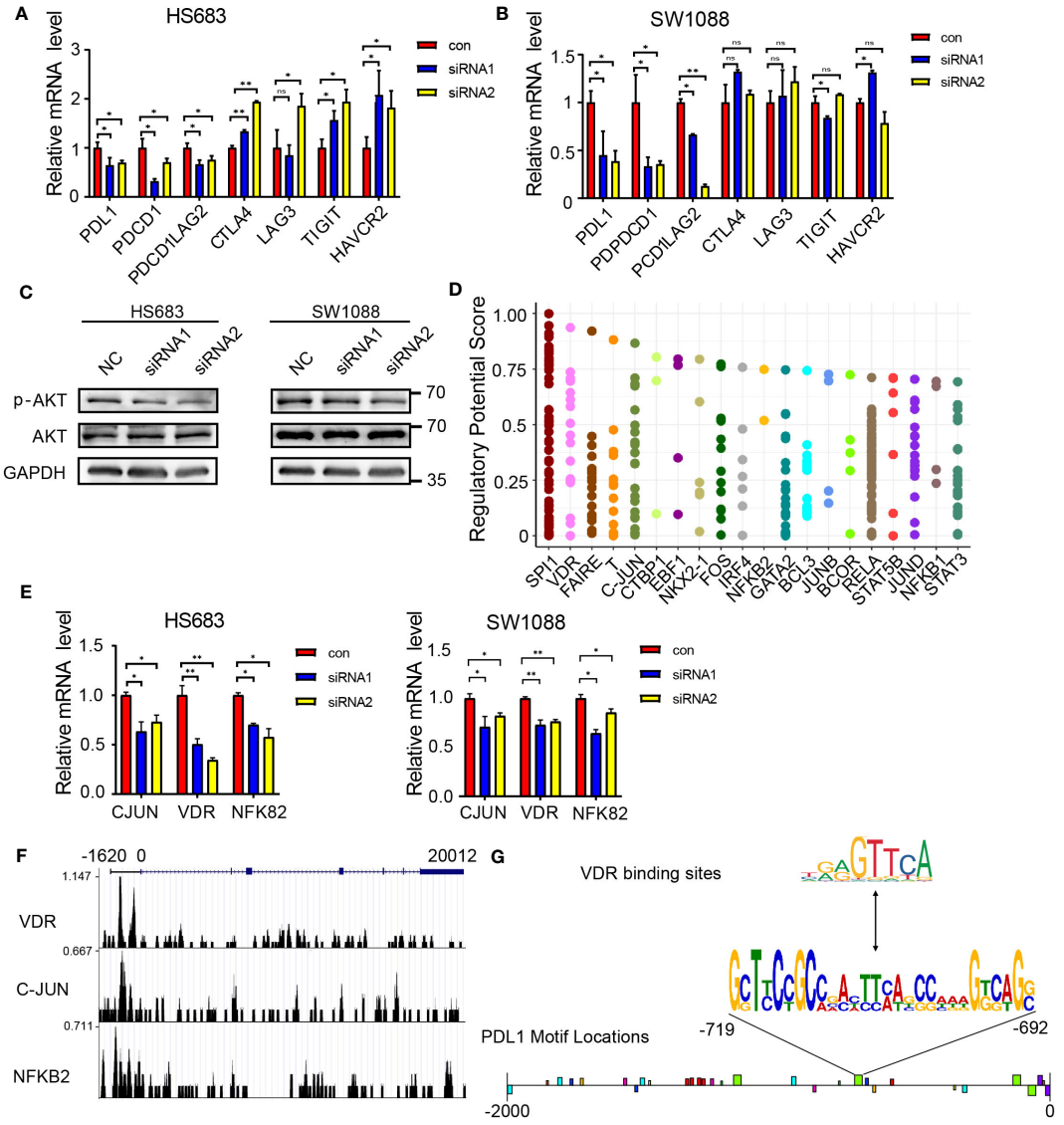


FIGURE 5
JAG1 regulates PDL1 through the PI3K-AKT pathway and VDR. **(A, B)** qPCR analysis reveals the changes in mRNA expression of immune checkpoint genes following JAG1 silencing. **(C)** Western blot analysis demonstrates the protein level alterations of key factors (p-AKT and AKT) in the PI3K-AKT signaling pathway upon JAG1 silencing. **(D)** Prediction of transcription factors regulating PDL1 using cistrome DB. **(E)** qPCR analysis shows the changes in mRNA expression of transcription factors after JAG1 silencing. **(F)** Chip-seq analysis investigates the binding sites of transcription factors with PDL1. **(G)** Motif analysis predicts the binding sites of PDL1 with VDR. *:P<0.05, **:P<0.01, ***P<0.001.

function of Treg cells and increased anti-tumor immunity, further highlighting the crucial role of Notch signaling and its related ligands in immunity (22). The study also showed that silencing JAG1 significantly down-regulated the mRNA levels of PDL1 and PDCD1 in LGG cells. It has been reported that the activation of the PI3K-AKT, Wnt, and EGFR pathways in glioma samples can all promote the upregulation of PD-L1 expression levels (14, 15). Consistent with these findings, we confirmed the upregulation of PD-L1 in LGG cells at the protein level. To investigate the regulatory mechanism of JAG1 on PDL1, we employed cistrome DB to screen for potential transcription factors that could bind to the PDL1 gene. After silencing JAG1, the mRNA levels of JUN, NFKB2, and VDR exhibited a significant decrease. Using the transcription factor prediction website JASPAR, we predicted the binding motifs of VDR with JUN, NFKB2, and VDR, and their binding with the 5' promoter region of PDL1. The results showed multiple predicted binding sites of VDR in the PDL1 promoter region. Overall, our findings suggest that JAG1 may affect the transcription of PDL1 by regulating the expression of VDR, leading to tumor immune escape, promoting tumor cell survival, and shortening patient survival.

Our study has several limitations. Tumors can exhibit diverse characteristics in their external and internal microenvironments. Treating the tumor as a whole may not effectively differentiate the Notch expression levels and immune status across different tumor locations. To address this, future studies can explore the application of single-cell RNA sequencing in combination with spatial transcriptomics analysis. Moreover, it's worth noting that the data

and tissues utilized in this study were obtained from public databases, which may not encompass all the changes occurring in all relevant regions of LGG cases. Therefore, it is crucial to analyze multiple datasets from various sources and validate the results. This should be the focus of future research.

In summary, our LGG classification based on the Notch gene set provides a clear description of the heterogeneity of the immune microenvironment in different LGGs. Our study also demonstrates that JAG1 affects the proliferation of LGG cell lines and PDL1 expression, thus influencing tumor development. This provides valuable insights for the development of therapeutic drugs targeting LGG.

# Materials and methods

## Data collection

In this study, the clinical and RNAseq data of 483 LGG patients was obtained from the TCGA database. As normal brain tissue samples were not available in the TCGA LGG dataset, we downloaded 207 RNA-seq datasets of normal brain tissues as controls from the GTEX database. Therefore, a total of 483 LGG and 207 normal samples were included for the analysis. To mitigate the influence of batch effects, this study employed ComBat from SVA to process the data. The ChIP-seq data is derived from cistrome DB (http://cistrome.org/db/).

## Protein interaction network

This study analyzed the Notch pathway in low-grade glioma (LGG) by selecting 43 relevant genes from the HALLMARK database. Using the R package "Consensus-ClusterPlus" with parameters reps=1000 and pItem=0.8, the 483 LGG patients were clustered based on the mRNA levels of these genes. Principal component analysis (PCA) was conducted to visualize classification differences among the identified clusters. PCA were compared using the R packages "FactoMineR". Survival curves were compared using the R packages "survival" and "jskm". The STRING database was utilized to construct and visualize the interaction interface of the Notch-related gene set, while GeneMania was used to visualize protein connections.

## NotchScore

In this study, the NotchScore for each patient was calculated using unsupervised clustering based on Notch pathway-related gene expression. Common differentially expressed genes (DEGs) were captured between the clustered groups. The Notch Score was defined using the Genomic Grade Index (GGI). It involved multiplying the weights of DEGs with significant differential expression in the Notch pathway-related gene cluster (PC1/PC2) by the GGI ($i$) and summing them to obtain the patient's Notch Score. The NotchScore was then used to assess Notch pathway activity and its relationship with LGG prognosis.

$$\text{NotchScore} = \sum(PC1i + PC2i)$$

## Functional enrichment analysis and TME analysis

This study utilized various analytical techniques to investigate cancer hallmark pathways in LGG patients. The techniques included GSVA and GSEA for pathway analysis, GO and KEGG enrichment analyses for gene annotation, TME analysis using the ESTIMATE package, quantification of immune cell infiltration with ssGSEA, and evaluation of immune checkpoints. The functional enrichment analysis and TME analysis were compared using the R packages "GSEABase", "limma" and "clusterProfiler". The TIDE Score is calculated through the TIDE online calculation website (http://tide.dfci.harvard.edu/).

## Cell culture and treatment

All cell lines were cultured under conditions recommended by product instructions. HS683 (Yaji Biotechnology, Shanghai, China) and SW1088 cell (Tongpai Biotechnology, Shanghai, China) were both cultured in DMEM medium with 10% FBS. The se-quence of siRNA can be found in Supplementary Table S1 (Geneseeq Technology, Su-zhou, China). Each well of the 96-well plate was seeded with 5000 cells and treated with MTT mixed solution on days 0, 2, 4 and 6, followed by 4-hour incubation. After removing the supernatant, 120μl of DMSO was supplied to dissolve the sediment, and the OD value was measured (490 nm wavelength) to detect cell proliferation. When the number of cells reaches 2*106 in the 6-well plate, the cells should be digested, fixed with 70% ethanol, and then incubated with PI dye for detecting the cell cycle using a flow cy-tometer.

## Western blotting

Standard Western blotting assay was performed using rabbit polyclonal anti-JAG1, anti-P27, anti-MCM2, anti-cyclin D1, anti-cyclin E1, and mouse monoclonal anti-GAPDH purchased (Sanying Biotechnology, Wuhan, China). Rabbit polyclonal anti-pAKT and anti-AKT were obtained (Cell Signaling Technology, Massachusetts, USA). The protein levels were normalized, and quantification analysis was executed using ImageJ. The bar graph shows fold changes.

## RNA extraction, reverse transcription, and qPCR

In this study, TRNzol was used to extract total RNA from HS683 and SW1088 cells (Tiangen Biotech, Beijing, China). The extracted

RNA was reverse transcribed into cDNA using HiScript III RT SuperMix with gDNA wiper (Vazyme Biotech, Nanjing, China). RT-QPCR was performed using the ABI 7900 RT-PCR system. The relative mRNA levels of the genes were calculated using the $2^{-\Delta\Delta Ct}$ method, with GAPDH serving as the internal reference. The primers used in the study can be found in Supplementary Table S2.

### Statistical analysis

The statistical analyses were conducted using RStudio. Independent sample t-tests were utilized to analyze normally distributed continuous variables. Apply the Kaplan-Meier method to analyze the survival of the samples. Statistical significance was considered as a p-value< 0.05. In the text, p-values are indicated using asterisks "*". *:P<0.05, **:P<0.01, ***P<0.001. QPCR, cell proliferation and cell cycle experiment were performed three independent times.

## Data availability statement

The original contributions presented in the study are included in the article/Supplementary Materials, further inquiries can be directed to the corresponding author/s.

## Ethics statement

Ethical approval was not required for the studies on humans and animals in accordance with the local legislation and institutional requirements because only commercially available established cell lines were used.

## Author contributions

HS and WD designed this study. BS, FG, LC, YY, XG, RW, ZF, BC, NW, YS, and XL performed the experiments and acquired the data. BS performed the bioinformatic analysis and analyzed experimental data. BS drafted the manuscript. All authors contributed to the article and HS edited and approved the submitted version.

## Funding

The author(s) declare financial support was received for the research, authorship, and/or publication of this article. This study was funded in part by the Startup Foundation for Advanced Talents and Science and Technology Innovation Foundation at Yangzhou University (137011856, HS), postgraduate Research & Practice Innovation Program of Jiangsu Province (SJCX22_1831), the Medical Research Project of Jiangsu Provincial Health Commission (M2022024), the Scientific Research Project of Nantong Municipal Health Commission (MS2022102), Natural Science Foundation of Nanjing University of Traditional Chinese Medicine (no.XZR2020084), Dalian Science and Technology Innovation Fund(2021RJ04). Basic Research Program of Liaoning Province (2022JH2/101300070). The authors gratefully acknowledge the National Natural Science Foundation of China (Grant No. 82371877). Natural Science Foundation of Jiangsu Province of China(BK20201223). Yangzhou society development (YZ20200071). Jiangsu Provincial Health commission(ZDB2020019).

## Conflict of interest

The authors declare that the research was conducted in the absence of any commercial or financial relationships that could be construed as a potential conflict of interest.

## Publisher's note

All claims expressed in this article are solely those of the authors and do not necessarily represent those of their affiliated organizations, or those of the publisher, the editors and the reviewers. Any product that may be evaluated in this article, or claim that may be made by its manufacturer, is not guaranteed or endorsed by the publisher.

## Supplementary material

The Supplementary Material for this article can be found online at: https://www.frontiersin.org/articles/10.3389/fimmu.2023.1247288/full#supplementary-material

## References

1. Kumthekar P, Raizer J, Singh S. Low-grade glioma. *Cancer Treat Res* (2015) 163:75–87. doi: 10.1007/978-3-319-12048-5_5

2. Weller M, Wick W, Aldape K, Brada M, Berger M, Pfister SM, et al. Glioma, nature reviews. *Dis Primers* (2015) 1:15017. doi: 10.1038/nrdp.2015.17

3. Zhou B, Lin W, Long Y, Yang Y, Zhang H, Wu K, et al. Notch signaling pathway: architecture, disease, and therapeutics. *Signal transduction targeted Ther* (2022) 7:95. doi: 10.1038/s41392-022-00934-y

4. Parmigiani E, Taylor V, Giachino C. Oncogenic and tumor-suppressive functions of NOTCH signaling in glioma. *Cells* (2020) 9:2304. doi: 10.3390/cells9102304

5. Kangsamaksin T, Murtomaki A, Kofler NM, Cuervo H, Chaudhri RA, Tattersall IW, et al. NOTCH decoys that selectively block DLL/NOTCH or JAG/NOTCH disrupt angiogenesis by unique mechanisms to inhibit tumor growth. *Cancer Discovery* (2015) 5:182–97. doi: 10.1158/2159-8290.CD-14-0650

6. Yu L, Xia K, Gao T, Chen J, Zhang Z, Sun X, et al. The notch pathway promotes osteosarcoma progression through activation of ephrin reverse signaling. *Mol Cancer Res MCR* (2019) 17:2383–94. doi: 10.1158/1541-7786.MCR-19-0493

7. Jin H, Luo S, Wang Y, Liu C, Piao Z, Xu M, et al. miR-135b Stimulates Osteosarcoma Recurrence and Lung Metastasis via Notch and Wnt/β-Catenin

Signaling, Molecular therapy. *Nucleic Acids* (2017) 8:111–22. doi: 10.1016/j.omtn.2017.06.008

8. Watowich MB, Gilbert MR, Larion M. T cell exhaustion in Malignant gliomas. *Trends Cancer* (2023) 9:270–92. doi: 10.1016/j.trecan.2022.12.008

9. Charles NA, Holland EC, Gilbertson R, Glass R, Kettenmann H. The brain tumor microenvironment. *Glia* (2011) 59:1169–80. doi: 10.1002/glia.21136

10. Fehervari Z. Glioma immune evasion. *Nat Immunol* (2017) 18:487. doi: 10.1038/ni.3736

11. Gieryng A, Pszczolkowska D, Walentynowicz KA, Rajan WD, Kaminska B. Immune microenvironment of gliomas. *Lab investigation; J Tech Methods Pathol* (2017) 97:498–518. doi: 10.1038/labinvest.2017.19

12. Tan AC, Heimberger AB, Khasraw M. Immune checkpoint inhibitors in gliomas. *Curr Oncol Rep* (2017) 19:23. doi: 10.1007/s11912-017-0586-5

13. Tu E, McGlinchey K, Wang J, Martin P, Ching SL, Floc'h N, et al. Anti-PD-L1 and anti-CD73 combination therapy promotes T cell response to EGFR-mutated NSCLC. *JCI Insight* (2022) 7:e142843. doi: 10.1172/jci.insight.142843

14. Liu S, Chen S, Yuan W, Wang H, Chen K, Li D, et al. PD-1/PD-L1 interaction up-regulates MDR1/P-gp expression in breast cancer cells via PI3K/AKT and MAPK/ERK pathways. *Oncotarget* (2017) 8:99901–12. doi: 10.18632/oncotarget.21914

15. Deng X, Liu X, Hu B, Liu J, Fu B, Zhang W. Upregulation of MTHFD2 is associated with PD–L1 activation in bladder cancer via the PI3K/AKT pathway. *Int J Mol Med* (2023) 51:14. doi: 10.3892/ijmm.2022.5217

16. Lastwika KJ, Wilson W 3rd, Li QK, Norris J, Xu H, Ghazarian SR, et al. Control of PD-L1 expression by oncogenic activation of the AKT-mTOR pathway in non-small cell lung cancer. *Cancer Res* (2016) 76:227–38. doi: 10.1158/0008-5472.CAN-14-3362

17. Salama RHM, Faied SMA, Elkholy M, Abd-Elmawgoud NS, Alsanory TA, Alsanory AA, et al. Gene expression of programmed cell death ligand-1 (PDL-1) and vitamin D receptor (VDR) with the serum vitamin D3 in lung cancer. *Egyptian J Bronchol* (2022) 16:65. doi: 10.1186/s43168-022-00168-0

18. Singh RK, Kim K, Rowswell-Turner RB, Hansen JN, Moore RG. Targeting Vitamin-D receptor (VDR) by a small molecule antagonist MeTC7 inhibits PD-L1 but controls THMYCN neuroblastoma growth PD-L1 independently. *bioRxiv* (2020) 252940. doi: 10.1101/2020.08.16.252940

19. Jaiswal A, Murakami K, Elia A, Shibahara Y, Done SJ, Wood SA, et al. Therapeutic inhibition of USP9x-mediated Notch signaling in triple-negative breast cancer. *Proc Natl Acad Sci United States America* (2021) 118:e2101592118. doi: 10.1073/pnas.2101592118

20. Grochowski CM, Loomes KM, Spinner NB. Jagged1 (JAG1): Structure, expression, and disease associations. *Gene* (2016) 576:381–4. doi: 10.1016/j.gene.2015.10.065

21. He Q. *The mechanism of miR-584-5p in glioma and its translational application*. PhD dissertation. Zhengzhou: Zhengzhou University (2019).

22. Yu S, Liu C, Li L, Tian T, Wang M, Hu Y, et al. Inactivation of Notch signaling reverses the Th17/Treg imbalance in cells from patients with immune thrombocytopenia. *Lab investigation; J Tech Methods Pathol* (2015) 95:157–67. doi: 10.1038/labinvest.2014.142

frontiers | Frontiers in Genetics

TYPE Mini Review
PUBLISHED 07 May 2024
DOI 10.3389/fgene.2024.1349612



OPEN ACCESS

EDITED BY
Caroline Chung,
University of Texas MD Anderson Cancer Center, United States

REVIEWED BY
Hemangi Bhonsle,
Virginia Tech Carilion, United States

*CORRESPONDENCE
James Rutka,
james.rutka@sickkids.ca

RECEIVED 05 December 2023
ACCEPTED 22 April 2024
PUBLISHED 07 May 2024

CITATION
Lin C, Smith C and Rutka J (2024), Current immunotherapeutic approaches to diffuse intrinsic pontine glioma.
*Front. Genet.* 15:1349612.
doi: 10.3389/fgene.2024.1349612



# Current immunotherapeutic approaches to diffuse intrinsic pontine glioma

Catherine Lin[1,2,3], Christian Smith[1,2] and James Rutka[1,2,3,4,5]*

[1]Cell Biology Research Program, The Hospital for Sick Children, Toronto, ON, Canada, [2]Arthur and Sonia Labatt Brain Tumour Research Centre, The Hospital for Sick Children, Toronto, ON, Canada, [3]Department of Laboratory Medicine and Pathobiology, University of Toronto, Toronto, ON, Canada, [4]Division of Neurosurgery, The Hospital for Sick Children, Toronto, ON, Canada, [5]Division of Neurosurgery, Department of Surgery, University of Toronto, Toronto, ON, Canada

Diffuse intrinsic pontine glioma (DIPG) is an aggressive brain tumour that occurs in the pons of the brainstem and accounts for over 80% of all brainstem gliomas. The median age at diagnosis is 6–7 years old, with less than 10% overall survival 2 years after diagnosis and less than 1% after 5 years. DIPGs are surgically inaccessible, and radiation therapy provides only transient benefit, with death ensuing from relentless local tumour infiltration. DIPGs are now the leading cause of brain tumour deaths in children, with a societal cancer burden in years of life lost (YLL) of more than 67 per individual, *versus* approximately 14 and 16 YLL for lung and breast cancer respectively. More than 95 clinical drug trials have been conducted on children with DIPGs, and all have failed to improve survival. No single or combination chemotherapeutic strategy has been successful to date because of our inability to identify targeted drugs for this disease and to deliver these drugs across an intact blood-brain barrier (BBB). Accordingly, there has been an increased focus on immunotherapy research in DIPG, with explorations into treatments such as chimeric antigen receptor T (CAR-T) cells, immune checkpoint blockades, cancer vaccines, and autologous cell transfer therapy. Here, we review the most recent advances in identifying genetic factors influencing the development of immunotherapy for DIPG. Additionally, we explore emerging technologies such as Magnetic Resonance-guided Focused Ultrasound (MRgFUS) in potential combinatorial approaches to treat DIPG.

KEYWORDS

**glioma, diffuse intrinsic pontine glioma (DIPG), immunotherapy, brainstem, blood-brain barrier (BBB)**

## Introduction

Diffuse intrinsic pontine glioma (DIPG) is a brain tumour occurring in the pons of the brainstem and accounts for over 80% of all brainstem gliomas (Srikanthan et al., 2021). DIPGs are a subset of diffuse midline gliomas (DMG) and are characterized by the lysine 27 to methionine (K27M) mutation on histone 3 (H3K27M) (International Agency for Research on Cancer, 2022). The median age at diagnosis is 6–7 years old, with less than 1% survival after 5 years (Johung and Monje, 2017; Srikanthan et al., 2021). Its location in the pons makes it impossible to resect the tumour, with chemotherapy and radiotherapy providing only transient benefits. More than 95 clinical drug trials have been conducted on children with DIPGs, and all have failed to improve survival. No single or combination chemotherapeutic strategy has been successful to date because of our inability to identify

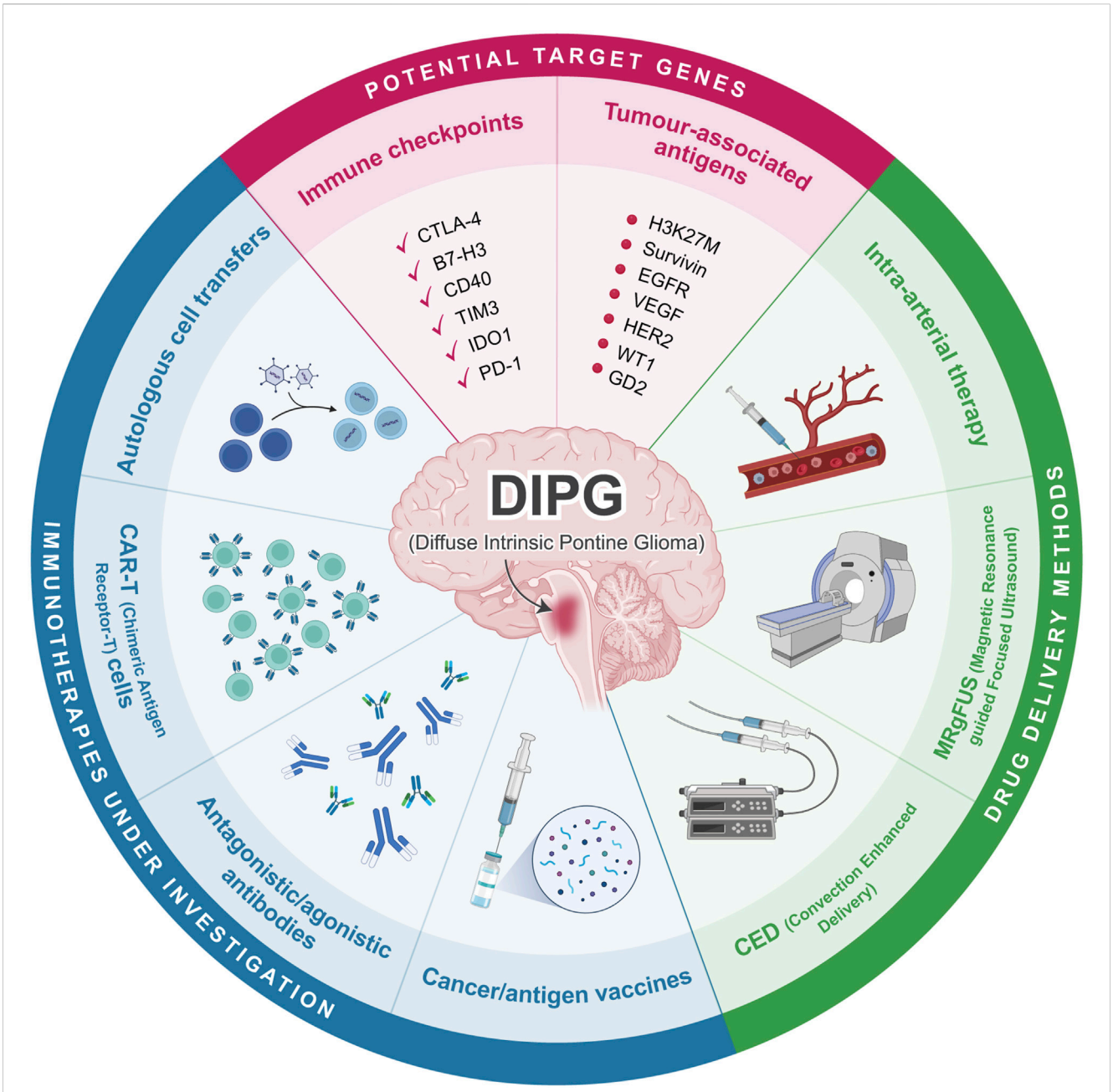


FIGURE 1
Overview of current immunotherapeutic approaches in DIPG. Cancer vaccines, antibodies, CAR-T cells, and autologous cell transfers are currently being investigated as possible immunotherapy for DIPG. Potential target genes include various immune checkpoints and tumour associated antigens. Drug delivery can be conducted through CED, MRgFUS, or intra-arterial therapy. Created with BioRender.com.

targeted drugs for this disease and to deliver these drugs across an intact blood-brain barrier (BBB).

Recent advances in immunology have allowed for improvements to cancer treatment. Immunotherapy focuses on harnessing the individual's immune system to eradicate the tumour, with the characteristics of the tumour-immune microenvironment (TIME) playing a major role in the efficacy of these therapeutics (Waldman et al., 2020). Tumours with higher numbers of immune cells are called "immune-hot" and generally respond better to immunotherapy. In contrast, those with a low immune cell population are "immune-cold," and immunotherapy has minimal effects as these treatments rely on immune activation to clear the tumours (Galon and Bruni, 2019). Past studies have shown DIPG as an "immune-cold" tumour, characterized by a low population of immune cells and reduced expression of immune checkpoint molecules, which poses a significant challenge in immunotherapy treatments in DIPG (Figure 1). In a healthy individual, the balance between inhibitory and stimulatory immune checkpoint pathways is maintained such that inhibitory pathways support self-tolerance and immunosuppression, while stimulatory pathways are focused on activating the immune system against foreign antigens (Marin-Acevedo et al., 2018;

Zhang and Zheng, 2020). In a tumour context, the downregulation of immune stimulatory signals and upregulation of suppressive signals mediated by these checkpoints reduces anti-tumour activity (He and Xu, 2020; Zhang and Zheng, 2020). By modulating the signalling of immune checkpoints, overall immune activation can be increased to kill cancer cells.

## Immune checkpoint approaches

In DIPG patients, Hwang et al. (2018) found that inhibition of PD-1, an immunosuppressive checkpoint molecule, using pembrolizumab resulted in a worsened condition, while Cacciotti et al. (2020) and Dunkel et al. (2023) (NCT03130959) found no significant improvements in survival as well as minimal to no adverse effects. Overall results for the use of anti-PD1 in DIPG do not seem promising (Hwang et al., 2018; Cacciotti et al., 2020; Dunkel et al., 2023). Recent studies have also investigated other checkpoint molecules such as TIM3, B7-H3, and CD40. TIM3 is an inhibitory checkpoint expressed on DIPG cells and immune cells such as microglia and macrophages. Ausejo-Mauleon et al. (2023) reported that using TIM-3 blockades promotes anti-tumour effects in immunocompetent DIPG murine models and found enhanced microglia- and $CD8^+$ T cell-mediated pro-inflammatory immune responses, which ultimately improved survival (Ausejo-Mauleon et al., 2023). The differences in efficacy between anti-PD1 and anti-TIM3 may be attributed to the tumour-immune microenvironment (TIME) composition. Past research indicates that the DIPG TIME has low PD-1 expression, while there is a comparatively higher TIM3 expression (Lin et al., 2018; Ausejo-Mauleon et al., 2023; Chen et al., 2023). This highlights the role that macrophages may play in the TIME and is a potential area for exploration (Lin et al., 2018; Lieberman et al., 2019). B7-H3, also known as CD276, is expressed on both tumour and antigen-presenting cells and inhibits the anti-tumour functions of T cells (Zhang and Zheng, 2020). In the DIPG context, studies have utilized convection-enhanced delivery in combination with the monoclonal B7-H3 antibody, 8H9, as well as the development of anti-B7-H3 CAR-T cells (Souweidane et al., 2018; Vitanza et al., 2023) (NCT04185038). Clinical trials are currently ongoing for various forms of B7-H3-targeting CAR-T cells, such as the single target B7-H3 and the quad-target B7-H3, EGFR806, HER2, and IL13-Zetakine (Quad) CAR-T Cell (NCT04185038, NCT05768880). Preliminary results of the anti-B7-H3 CAR-T cell study showed improved survival (Vitanza et al., 2023). Extended survival was also observed in the 8H9 antibody study, although selection bias may be present due to the study's design (Souweidane et al., 2018).

The indoleamine 2,3-dioxygenase (IDO) pathway is primarily involved in the conversion of tryptophan into kynurenines, but indoleamine 2,3-dioxygenase 1 (IDO1), an enzyme in the pathway, also acts as an immune checkpoint by modulating immunosuppressive responses (Zhai et al., 2018). A clinical trial (NCT02502708) evaluating indoximod, an IDO pathway inhibitor, combined with the chemotherapy drug temozolomide and radiation recently published its results. Overall, the authors concluded that the combination treatment can be tolerated, with variable disease and immune responses observed among the participants. Further studies must be conducted to evaluate treatment efficacy (Johnson et al., 2023). Contrary to the previously mentioned immune checkpoints, CD40 is typically involved in the stimulatory pathway and is expressed on immune cells to promote tumour-killing activity. An agonistic CD40 antibody, APX005M, has been developed to enhance immune activity against the tumour and induce tumour cell apoptosis. Studies have confirmed preliminary safety, with efficacy against DIPG being tested (Lindsay et al., 2020) (NCT03389802).

## Targeting of tumour-associated antigens

Tumour-associated antigens (TAAs) are also potential targets in immunotherapy, ranging from antigens seen across different cancer types to DIPG-specific TAAs. GD2 is a disialoganglioside that is highly expressed in solid tumours, including DIPG, small cell lung cancer, and melanoma; GD2 expression in normal tissue is limited, making GD2 an ideal target for immunotherapy with minimal off-target effects (Mount et al., 2018; Nazha et al., 2020). Clinical trials are ongoing for anti-GD2 CAR-T cells (NCT04196413) and C7R-coexpressing anti-GD2 CAR-T cells (NCT04099797), with clinical and radiological improvements observed in DIPG/DMG patients enrolled in the anti-GD2 CAR-T cells trial (Majzner et al., 2022). Anti-GD2 CAR-T cells and anti-GD2 CAR NK-92 cells are effective in *in vivo* assays using patient-derived DIPG cells and DIPG cell lines (Mount et al., 2018; Mount et al., 2018; Zuo et al., 2023). The Wilms' tumor 1 gene (WT1) is an oncogene in various cancers including leukemia, breast cancer, glioblastoma, and DIPG. Overexpression of WT1 is associated with these cancers, and targeted protein knockdown inhibits cancer growth (Qi et al., 2015). A completed clinical trial that studied DSP-7888, a cancer vaccine that induces WT1-specific T cells, showed improved survival in DIPG patients compared to controls (Fujisaki et al., 2018) (NCT02750891). Separately, an ongoing clinical trial investigates vaccination with WT1 mRNA-loaded autologous monocyte-derived dendritic cells (DCs) as a potential therapeutic for DIPG. It is hypothesized that the DC vaccine will act as an adjuvant to boost anti-tumour immune activity with minimal side effects, given its specificity to WT1-expressing cells (NCT04911621). Epidermal growth factor (EGFR) is another common TAA expressed in tumour cells with limited expression in normal tissue. EGFR mutations leads to constitutive activation of the gene and results in cancer phenotypes, with EGFR overexpression observed in DIPG (Li et al., 2012). More recent studies focus on using nimotuzumab, an anti-EGFR, combined with radiation or radiochemotherapy (Fleischhack et al., 2019) (NCT04532229). While radiation with nimotuzumab does not significantly improve survival compared to radiochemotherapy alone, side effects and adverse events were significantly reduced. Overall, the DIPG patients had an improved quality of life, albeit no changes in survival (Fleischhack et al., 2019). The HER2 protein is a member of the EGFR family, and its overexpression is seen in many solid tumours, including DIPG, with breast cancer being the most notable (Oh and Bang, 2020). Wang et al. (2023a) investigated the use of anti-HER2 CAR-T cells as a therapeutic in DIPG and other DMGs. Results showed HER2-specific immune targeting and cytokine release when co-cultured *in vitro* with patient-derived DIPG cells. Anti-HER2 CAR-T cells also reduce tumour size in *in vivo* DIPG xenografts. The authors concluded that the CAR-T

cells may show efficacy in DIPG patients, although a clinical trial is needed to confirm their hypothesis (Wang et al., 2023a). Vascular endothelial growth factor (VEGF) is a molecule regulating angiogenesis. However, in a tumour context, this is harnessed by the tumour cells to improve tumour angiogenesis and blood vessel accessibility, ultimately supporting tumourigenesis (Shibuya, 2011). A recently completed clinical trial with results published in 2020 showed that the anti-VEGF, bevacizumab, in combination with valproic acid and radiation, was well tolerated but did not improve survival (Su et al., 2020) (NCT00879437). In addition, an ongoing clinical trial will evaluate the survival of DIPG patients when treated with bevacizumab in combination with low-dose radiation (NCT04250064).

Survivin is an inhibitor of the apoptotic pathway and can be found in most cancers (Chen et al., 2016). It is also involved in various cell cycle and signalling pathways such as p53, Wnt, and Notch. Mutations in survivin allow the tumour cells to persist as apoptosis is inhibited (Chen et al., 2016). SurVaxM, a vaccine that immunizes patients with survivin proteins, has been developed. This allows the immune system to recognize survivin-expressing cells as "harmful" and kill the cells, leading to an anti-tumour effect. The clinical trial for SurVaxM is currently in progress and is combined with adjuvant Montanide ISA 51 administration to boost immune responses (NCT04978727). As the hallmark mutation in DIPG, many therapeutic developments have also focused on H3K27M-targetted therapies. This includes the use of H3K27M antigen vaccines (NCT04749641) (Zhang et al., 2023), CAR-T cells (Wang et al., 2023b), and combination therapies with immune checkpoint blockades (NCT02960230) (Grassl et al., 2023). Preliminary data from the NCT04749641 trial testing H3K27M antigen vaccines indicates that survival may be improved compared to other therapies (Zhang et al., 2023). Anti-H3.3K27M CAR-T cells that are specific to HLA-A*02:01 have recently been developed (Wang et al., 2023b). HLAs, also known as human leukocyte antigens, are proteins that bind to peptides and subsequently present them on the cell surface for T cell recognition (Kulski et al., 2022). In this case, the CAR-T cells would only be able to recognize the H3.3K27M peptide in the context of the HLA-A*02:01 complex. Wang et al. (2023b) evaluated the binding and recognition capacity of the CAR-T cells using DIPG cell lines. No binding was detected, and upon further investigation, they found that H3.3K27M peptides were not endogenously presented on HLA-A*02:01 complexes in the DIPG cell lines. The authors concluded that anti-H3.3K27M CAR-T cells specific to HLA-A*02:01 would not be a feasible immunotherapy for DIPG (Wang et al., 2023b). An ongoing clinical trial is investigating the safety and immune activity of a combination therapy using the H3.3.K27M peptide vaccine, poly-ICLC, and the PD-1 blockade antibody nivolumab. Poly-ICLC acts as an adjuvant to boost immune activity. At the same time, nivolumab can block immunosuppressive signalling, which should enhance the anti-tumour activity induced by the H3.3.K27M peptide vaccine (NCT02960230). Separately, Grassl et al. (2023) evaluated the combination therapy of H3K27M peptide vaccines with anti-PD-1 in DMG; some participants had tumours in the pons, indicating DIPG. Due to regulations, the authors could not conduct their study using a consistent anti-PD-1 treatment. Thus, the drugs used were based on availability. Overall, results indicate that the combination therapy is both safe and immunogenic. Additionally, peripheral immune activity decreased over time, along with the observed tumour regression, and tumour progression coincided with decreased immune responses (Grassl et al., 2023).

## Other cell-based therapies

Autologous cellular vaccines and cell transfers allow for targeting of tumour- and patient-specific antigens. In cellular vaccines, the immune cells and tumour lysate containing the antigens are derived from patients. The cells are then incubated or "pulsed" with the lysate to improve tumour antigen-specificity and re-infused into the patient (Alaniz et al., 2014; Yan et al., 2020). Currently, the immunogenicity and safety of cellular vaccines have been shown in non-DIPG gliomas (Yan et al., 2020). An ongoing clinical trial (NCT04837547) is focusing on vaccination with autologous dendritic cells that have been pulsed with total tumour messenger ribonucleic acid (TTRNA-DC) derived from the patient, this allows the dendritic cells to become loaded with the antigens and can present them to T and B cells when re-infused into the patient (Yan et al., 2020). The same trial will stimulate autologous T lymphocytes *ex vivo* using total tumour messenger ribonucleic acid (TTRNA-xALT) and similarly transfer back into the patient. This clinical trial will primarily assess the safety and feasibility of these therapies. Separately, another clinical trial also focuses on vaccination with TTRNA-DC, but in combination with the cytokine GM-CSF as an adjuvant to boost immune response (NCT03396575). Benitez-Ribas et al. (2018) also published preliminary results demonstrating the safety of autologous dendritic cells pulsed with tumour lysates derived from allogenic DIPG cell lines (Benitez-Ribas et al., 2018).

There has also been interest in natural killer (NK) cells for cell transfers other than CAR-T cells. NK cells have increased anti-tumour activity compared to T cells in glioblastoma due to T cell targeting mutations in the tumour (Lieberman et al., 2019; Galat et al., 2023). Galat et al., 2023 differentiated human pluripotent stem cells into NK cells and assessed their cytotoxicity *in vitro* using DIPG cell lines. They found that the cells could successfully engraft in peripheral blood samples and are cytotoxic against DIPG cells. A separate study is focusing on AloCELYVIR, a novel therapy where oncolytic Adenovirus-infected bone marrow-derived allogeneic mesenchymal stem cells are transfused into the patient. These cells can enhance anti-tumour responses and transport oncolytic molecules to various tumour sites, enabling the killing of cancer cells in locations that are more difficult to reach with conventional therapy. Assessments for the safety and efficacy of this therapy in DIPG patients are currently in progress (NCT04758533).

## Combination therapies

There are also studies focusing on combination therapies, with the majority involving immune checkpoint blockades and cancer vaccines. A clinical trial evaluated the efficacy of nivolumab (anti-PD-1) with ipilimumab (anti-CTLA-4). However, no significant improvements in survival compared were noted (NCT03130959) (Dunkel et al., 2023). A novel neo-antigen heat shock protein vaccine (rHSC-DIPGVax)

targeting different DIPG/DMG neo-epitopes has also been developed. Investigation into the vaccine's safety and tolerability in combination with balstilimab (anti-PD-1) and zalifrelimab (anti-CTLA-4) is currently ongoing (NCT04943848). Dual checkpoint inhibitors have been shown to improve objective response rates in cervical cancer compared to standard treatments, although only in patients with PD-1-expressing tumours (O'Malley et al., 2022). Several clinical trials have also investigated combination therapies such as bevacizumab (anti-VEGF) with cetuximab (anti-EGF) (NCT01884740), as well as nivolumab (anti-PD-1) with bempegaldesleukin, which is an immunostimulatory IL2 pathway agonist (NCT04730349), but have since been terminated due to low accrual (NCT01884740) and change in business objectives (NCT04730349). Nivolumab with bempegaldesleukin showed efficacy in various solid tumours regardless of the PD-1 expression levels (Diab et al., 2020); this may be a potential area to explore as DIPG typically has low PD-1 presence (Lin et al., 2018).

## Challenges

A major challenge with DIPG treatments is the delivery method, as the BBB restricts the penetrance of drugs, antibodies, or exogenously administered molecules. More than 95 clinical trials attempted to date have shown no improvements in survival for DIPG patients, likely due to insufficient drug delivery to the target site and, as such, unable to reach therapeutic concentrations. Although recent advances may alleviate this issue, novel delivery methods include convection-enhanced delivery (CED), intra-arterial therapy, and magnetic resonance-guided focused ultrasound (MRgFUS) (Haumann et al., 2020; Pandit et al., 2020). CED utilizes hydraulic pressure to deliver drugs through a microcatheter driven by a pump; pressure allows for homogenous drug distribution throughout the tumour. Several clinical trials have verified the safety and feasibility of this method in DIPG. Still, the invasive nature of the microcatheter insertion and drug leakage into non-target areas may be causes for concern, especially for off-target effects in healthy tissue (Zhou et al., 2017). In intra-arterial therapy, the drug is injected into an artery close to the tumour, followed by a hyperosmolar drug to open the BBB (Haumann et al., 2020; Pandit et al., 2020). An issue with this method is that the opening of the BBB is non-selective and dependent on the brain region, which allows for the passage of other agents as well as increases in brain fluid due to hyperosmotic-like conditions and impaired homeostasis of endothelial cells (Ikeda et al., 2002; Pandit et al., 2020). These side effects may lead to neurological deficits and toxicity (Pandit et al., 2020). However, conflicting evidence indicates that intra-arterial therapy is safe and feasible (Uluc et al., 2022). MRgFUS is a non-invasive method in which microbubbles are intravenously injected and oscillate upon encountering a focused ultrasound field; allowing for safe and transient opening of the BBB (Alli et al., 2018; Haumann et al., 2020; Pandit et al., 2020). The ultrasound beam can be targeted specifically to cover the tumour location, thus minimizing off-target effects. Various therapeutics can be delivered using MRgFUS, including chemotherapy agents, nanoparticles, antibodies, and gene vectors (Haumann et al., 2020). Safety, feasibility, and efficacy using chemotherapy agents have been demonstrated in DIPG mouse models (Alli et al., 2018; Englander et al., 2021; Ishida et al., 2021). In addition, our group has recently initiated a clinical trial evaluating the delivery of doxorubicin, a BBB-excluded drug, to DIPG patients using MRgFUS (NCT05615623). Regarding immunotherapy, MRgFUS has also been shown to affect and modulate the immune system (Kovacs et al., 2017; Choi et al., 2022), although further investigation is needed to characterize the immune changes in DIPG.

## Conclusion

The numerous studies and clinical trials focusing on immunotherapeutics in DIPG open up exciting possibilities for the future. Drug delivery methods can also be assessed in combination with immunotherapeutic approaches to maximize safety and efficacy in prolonging the survival of DIPG patients.

## Author contributions

CL: Conceptualization, Data curation, Writing–original draft, Writing–review and editing. CS: Conceptualization, Project administration, Supervision, Writing–review and editing. JR: Conceptualization, Funding acquisition, Project administration, Resources, Supervision, Writing–review and editing.

## Funding

The author(s) declare financial support was received for the research, authorship, and/or publication of this article. This study was supported by grants from the Canadian Institutes of Health Research (391243); Brain Cancer Canada, Meagan's HUG (Meagan Bebenek Foundation), b.r.a.i.n.child, and the Wiley Fund.

## Conflict of interest

The authors declare that the research was conducted in the absence of any commercial or financial relationships that could be construed as a potential conflict of interest.

## Publisher's note



## References

Alaniz, L., Rizzo, M. M., and Mazzolini, G. (2014). Pulsing dendritic cells with whole tumor cell lysates. *Methods Mol. Biol.* 1139, 27–31. doi:10.1007/978-1-4939-0345-0_3

Alli, S., Figueiredo, C. A., Golbourn, B., Sabha, N., Wu, M. Y., Bondoc, A., et al. (2018). Brainstem blood brain barrier disruption using focused ultrasound: a demonstration of

feasibility and enhanced doxorubicin delivery. *J. Control Release* 281, 29–41. doi:10.1016/j.jconrel.2018.05.005

Ausejo-Mauleon, I., Labiano, S., De La Nava, D., Laspidea, V., Zalacain, M., Marrodan, L., et al. (2023). TIM-3 blockade in diffuse intrinsic pontine glioma models promotes tumor regression and antitumor immune memory. *Cancer Cell* 41, 1911–1926.e8. doi:10.1016/j.ccell.2023.09.001

Benitez-Ribas, D., Cabezon, R., Florez-Grau, G., Molero, M. C., Puerta, P., Guillen, A., et al. (2018). Immune response generated with the administration of autologous dendritic cells pulsed with an allogenic tumoral cell-lines lysate in patients with newly diagnosed diffuse intrinsic pontine glioma. *Front. Oncol.* 8, 127. doi:10.3389/fonc.2018.00127

Cacciotti, C., Choi, J., Alexandrescu, S., Zimmerman, M. A., Cooney, T. M., Chordas, C., et al. (2020). Immune checkpoint inhibition for pediatric patients with recurrent/refractory CNS tumors: a single institution experience. *J. Neurooncol* 149, 113–122. doi:10.1007/s11060-020-03578-6

Chen, X., Duan, N., Zhang, C., and Zhang, W. (2016). Survivin and tumorigenesis: molecular mechanisms and therapeutic strategies. *J. Cancer* 7, 314–323. doi:10.7150/jca.13332

Chen, Y., Zhao, C., Li, S., Wang, J., and Zhang, H. (2023). Immune microenvironment and immunotherapies for diffuse intrinsic pontine glioma. *Cancers (Basel)* 15, 602. doi:10.3390/cancers15030602

Choi, H. J., Han, M., Seo, H., Park, C. Y., Lee, E. H., and Park, J. (2022). The new insight into the inflammatory response following focused ultrasound-mediated blood-brain barrier disruption. *Fluids Barriers CNS* 19, 103. doi:10.1186/s12987-022-00402-3

Diab, A., Tannir, N. M., Bentebibel, S. E., Hwu, P., Papadimitrakopoulou, V., Haymaker, C., et al. (2020). Bempegaldesleukin (NKTR-214) plus nivolumab in patients with advanced solid tumors: phase I dose-escalation study of safety, efficacy, and immune activation (PIVOT-02). *Cancer Discov.* 10, 1158–1173. doi:10.1158/2159-8290.CD-19-1510

Dunkel, I. J., Doz, F., Foreman, N. K., Hargrave, D., Lassaletta, A., Andre, N., et al. (2023). Nivolumab with or without ipilimumab in pediatric patients with high-grade CNS malignancies: safety, efficacy, biomarker, and pharmacokinetics-CheckMate 908. *Neuro Oncol.* 25, 1530–1545. doi:10.1093/neuonc/noad031

Englander, Z. K., Wei, H. J., Pouliopoulos, A. N., Bendau, E., Upadhyayula, P., Jan, C. I., et al. (2021). Focused ultrasound mediated blood-brain barrier opening is safe and feasible in a murine pontine glioma model. *Sci. Rep.* 11, 6521. doi:10.1038/s41598-021-85180-y

Fleischhack, G., Massimino, M., Warmuth-Metz, M., Khuhlaeva, E., Janssen, G., Graf, N., et al. (2019). Nimotuzumab and radiotherapy for treatment of newly diagnosed diffuse intrinsic pontine glioma (DIPG): a phase III clinical study. *J. Neurooncol* 143, 107–113. doi:10.1007/s11060-019-03140-z

Fujisaki, H., Hashii, Y., Terashima, K., Goto, H., Horibe, K., Sugiyama, K., et al. (2018). PDCT-09. Phase 1/2 Study of DSP-7888 in Pediatric Patients with Malignant Glioma. *Neuro-Oncology* 20, vi202. doi:10.1093/neuonc/noy148.839

Galat, Y., Du, Y., Perepitchka, M., Li, X.-N., Balyasnikova, I. V., Tse, W. T., et al. (2023). *In vitro* vascular differentiation system efficiently produces natural killer cells for cancer immunotherapies. *OncoImmunology* 12, 2240670. doi:10.1080/2162402X.2023.2240670

Galon, J., and Bruni, D. (2019). Approaches to treat immune hot, altered and cold tumours with combination immunotherapies. *Nat. Rev. Drug Discov.* 18, 197–218. doi:10.1038/s41573-018-0007-y

Grassl, N., Poschke, I., Lindner, K., Bunse, L., Mildenberger, I., Boschert, T., et al. (2023). A H3K27M-targeted vaccine in adults with diffuse midline glioma. *Nat. Med.* 29, 2586–2592. doi:10.1038/s41591-023-02555-6

Haumann, R., Videira, J. C., Kaspers, G. J. L., Van Vuurden, D. G., and Hulleman, E. (2020). Overview of current drug delivery methods across the blood-brain barrier for the treatment of primary brain tumors. *CNS Drugs* 34, 1121–1131. doi:10.1007/s40263-020-00766-w

He, X., and Xu, C. (2020). Immune checkpoint signaling and cancer immunotherapy. *Cell Res.* 30, 660–669. doi:10.1038/s41422-020-0343-4

Hwang, E., Onar, A., Young-Poussaint, T., Mitchell, D., Kilburn, L., Margol, A., et al. (2018). IMMU-09. Outcome of patients with recurrent diffuse intrinsic pontine glioma (DIPG) treated with pembrolizumab (anti-PD-1): a pediatric brain tumor consortium study (PBTC045). *Neuro-Oncology* 20, i100. doi:10.1093/neuonc/noy059.325

Ikeda, M., Bhattacharjee, A. K., Kondoh, T., Nagashima, T., and Tamaki, N. (2002). Synergistic effect of cold mannitol and Na(+)/Ca(2+) exchange blocker on blood-brain barrier opening. *Biochem. Biophys. Res. Commun.* 291, 669–674. doi:10.1006/bbrc.2002.6495

INTERNATIONAL AGENCY FOR RESEARCH ON CANCER (2022) *WHO classification of tumours of the central nervous system*. Lyon, France: IARC.

Ishida, J., Alli, S., Bondoc, A., Golbourn, B., Sabha, N., Mikloska, K., et al. (2021). MRI-guided focused ultrasound enhances drug delivery in experimental diffuse intrinsic pontine glioma. *J. Control Release* 330, 1034–1045. doi:10.1016/j.jconrel.2020.11.010

Johnson, T. S., Macdonald, T. J., Pacholczyk, R., Aguilera, D., Al-Basheer, A., Bajaj, M., et al. (2023). Indoximod-based chemo-immunotherapy for pediatric brain tumors: a first-in-children phase I trial. *Neuro Oncol.* 26, 348–361. doi:10.1093/neuonc/noad174

Johung, T. B., and Monje, M. (2017). Diffuse intrinsic pontine glioma: new pathophysiological insights and emerging therapeutic targets. *Curr. Neuropharmacol.* 15, 88–97. doi:10.2174/1570159x14666160509123229

Kovacs, Z. I., Kim, S., Jikaria, N., Qureshi, F., Milo, B., Lewis, B. K., et al. (2017). Disrupting the blood-brain barrier by focused ultrasound induces sterile inflammation. *Proc. Natl. Acad. Sci. U. S. A.* 114, E75–E84. doi:10.1073/pnas.1614777114

Kulski, J. K., Suzuki, S., and Shiina, T. (2022). Human leukocyte antigen super-locus: nexus of genomic supergenes, SNPs, indels, transcripts, and haplotypes. *Hum. Genome Var.* 9, 49. doi:10.1038/s41439-022-00226-5

Lieberman, N. A. P., Degolier, K., Kovar, H. M., Davis, A., Hoglund, V., Stevens, J., et al. (2019). Characterization of the immune microenvironment of diffuse intrinsic pontine glioma: implications for development of immunotherapy. *Neuro Oncol.* 21, 83–94. doi:10.1093/neuonc/noy145

Li, G., Mitra, S. S., Monje, M., Henrich, K. N., Bangs, C. D., Nitta, R. T., et al. (2012). Expression of epidermal growth factor variant III (EGFRvIII) in pediatric diffuse intrinsic pontine gliomas. *J. Neurooncol* 108, 395–402. doi:10.1007/s11060-012-0842-3

Lin, G. L., Nagaraja, S., Filbin, M. G., Suva, M. L., Vogel, H., and Monje, M. (2018). Non-inflammatory tumor microenvironment of diffuse intrinsic pontine glioma. *Acta Neuropathol. Commun.* 6, 51. doi:10.1186/s40478-018-0553-x

Lindsay, H., Onar-Thomas, A., Kocak, M., Poussaint, T. Y., Dhall, G., Broniscer, A., et al. (2020). EPCT-02. PBTC-051: First In Pediatrics Phase 1 Study of CD40 Agonistic Monoclonal Antibody APX005M in Pediatric Subjects with Recurrent/Refractory Brain Tumors. *Neuro-Oncology* 22, iii304. doi:10.1093/neuonc/noaa222.127

Majzner, R. G., Ramakrishna, S., Yeom, K. W., Patel, S., Chinnasamy, H., Schultz, L. M., et al. (2022). GD2-CAR T cell therapy for H3K27M-mutated diffuse midline gliomas. *Nature* 603, 934–941. doi:10.1038/s41586-022-04489-4

Marin-Acevedo, J. A., Dholaria, B., Soyano, A. E., Knutson, K. L., Chumsri, S., and Lou, Y. (2018). Next generation of immune checkpoint therapy in cancer: new developments and challenges. *J. Hematol. Oncol.* 11, 39. doi:10.1186/s13045-018-0582-8

Mount, C. W., Majzner, R. G., Sundaresh, S., Arnold, E. P., Kadapakkam, M., Haile, S., et al. (2018). Potent antitumor efficacy of anti-GD2 CAR T cells in H3-K27M(+) diffuse midline gliomas. *Nat. Med.* 24, 572–579. doi:10.1038/s41591-018-0006-x

Nazha, B., Inal, C., and Owonikoko, T. K. (2020). Disialoganglioside GD2 expression in solid tumors and role as a target for cancer therapy. *Front. Oncol.* 10, 1000. doi:10.3389/fonc.2020.01000

Oh, D. Y., and Bang, Y. J. (2020). HER2-targeted therapies - a role beyond breast cancer. *Nat. Rev. Clin. Oncol.* 17, 33–48. doi:10.1038/s41571-019-0268-3

O'Malley, D. M., Neffa, M., Monk, B. J., Melkadze, T., Huang, M., Kryzhanivska, A., et al. (2022). Dual PD-1 and CTLA-4 checkpoint blockade using balstilimab and zalifrelimab combination as second-line treatment for advanced cervical cancer: an open-label phase II study. *J. Clin. Oncol.* 40, 762–771. doi:10.1200/JCO.21.02067

Pandit, R., Chen, L., and Gotz, J. (2020). The blood-brain barrier: physiology and strategies for drug delivery. *Adv. Drug Deliv. Rev.* 165-166, 1–14. doi:10.1016/j.addr.2019.11.009

Qi, X. W., Zhang, F., Wu, H., Liu, J. L., Zong, B. G., Xu, C., et al. (2015). Wilms' tumor 1 (WT1) expression and prognosis in solid cancer patients: a systematic review and meta-analysis. *Sci. Rep.* 5, 8924. doi:10.1038/srep08924

Shibuya, M. (2011). Vascular endothelial growth factor (VEGF) and its receptor (vegfr) signaling in angiogenesis: a crucial target for anti- and pro-angiogenic therapies. *Genes Cancer* 2, 1097–1105. doi:10.1177/1947601911423031

Souweidane, M. M., Kramer, K., Pandit-Taskar, N., Zhou, Z., Haque, S., Zanzonico, P., et al. (2018). Convection-enhanced delivery for diffuse intrinsic pontine glioma: a single-centre, dose-escalation, phase 1 trial. *Lancet Oncol.* 19, 1040–1050. doi:10.1016/S1470-2045(18)30322-X

Srikanthan, D., Taccone, M. S., Van Ommeren, R., Ishida, J., Krumholtz, S. L., and Rutka, J. T. (2021). Diffuse intrinsic pontine glioma: current insights and future directions. *Chin. Neurosurg. J.* 7, 6. doi:10.1186/s41016-020-00218-w

Su, J. M., Murray, J. C., Mcnall-Knapp, R. Y., Bowers, D. C., Shah, S., Adesina, A. M., et al. (2020). A phase 2 study of valproic acid and radiation, followed by maintenance valproic acid and bevacizumab in children with newly diagnosed diffuse intrinsic pontine glioma or high-grade glioma. *Pediatr. Blood Cancer* 67, e28283. doi:10.1002/pbc.28283

Uluc, K., Ambady, P., Mcintyre, M. K., Tabb, J. P., Kersch, C. N., Nerison, C. S., et al. (2022). Safety of intra-arterial chemotherapy with or without osmotic blood-brain barrier disruption for the treatment of patients with brain tumors. *Neurooncol Adv.* 4, vdac104. doi:10.1093/noajnl/vdac104

Vitanza, N. A., Wilson, A. L., Huang, W., Seidel, K., Brown, C., Gustafson, J. A., et al. (2023). Intraventricular B7-H3 CAR T cells for diffuse intrinsic pontine glioma: preliminary first-in-human bioactivity and safety. *Cancer Discov.* 13, 114–131. doi:10.1158/2159-8290.CD-22-0750

Waldman, A. D., Fritz, J. M., and Lenardo, M. J. (2020). A guide to cancer immunotherapy: from T cell basic science to clinical practice. *Nat. Rev. Immunol.* 20, 651–668. doi:10.1038/s41577-020-0306-5

Wang, S. S., Davenport, A. J., Iliopoulos, M., Hughes-Parry, H. E., Watson, K. A., Arcucci, V., et al. (2023a). HER2 chimeric antigen receptor T cell immunotherapy is an effective treatment for diffuse intrinsic pontine glioma. *Neurooncol Adv.* 5, vdad024. doi:10.1093/noajnl/vdad024

Wang, S. S., Pandey, K., Watson, K. A., Abbott, R. C., Mifsud, N. A., Gracey, F. M., et al. (2023b). Endogenous H3.3K27M derived peptide restricted to HLA-A *02:01 is insufficient for immune-targeting in diffuse midline glioma. *Mol. Ther. Oncolytics* 30, 167–180. doi:10.1016/j.omto.2023.08.005

Yan, Y., Zeng, S., Gong, Z., and Xu, Z. (2020). Clinical implication of cellular vaccine in glioma: current advances and future prospects. *J. Exp. Clin. Cancer Res.* 39, 257. doi:10.1186/s13046-020-01778-6

Zhai, L., Ladomersky, E., Lenzen, A., Nguyen, B., Patel, R., Lauing, K. L., et al. (2018). Ido1 in cancer: a Gemini of immune checkpoints. *Cell Mol. Immunol.* 15, 447–457. doi:10.1038/cmi.2017.143

Zhang, Y., Ji, N., Chen, G., Wu, H., Wang, Y., Li, X. O., et al. (2023). H3.3-K27M neoantigen vaccine elicits anti-tumor T cell immunity against diffuse intrinsic pontine glioma: the phase I ENACTING trial. *J. Clin. Oncol.* 41, 2052. doi:10.1200/jco.2023.41.16_suppl.2052

Zhang, Y., and Zheng, J. (2020). Functions of immune checkpoint molecules beyond immune evasion. *Adv. Exp. Med. Biol.* 1248, 201–226. doi:10.1007/978-981-15-3266-5_9

Zhou, Z., Singh, R., and Souweidane, M. M. (2017). Convection-enhanced delivery for diffuse intrinsic pontine glioma treatment. *Curr. Neuropharmacol.* 15, 116–128. doi:10.2174/1570159x14666160614093615

Zuo, P., Li, Y., He, C., Wang, T., Zheng, X., Liu, H., et al. (2023). Anti-tumor efficacy of anti-GD2 CAR NK-92 cells in diffuse intrinsic pontine gliomas. *Front. Immunol.* 14, 1145706. doi:10.3389/fimmu.2023.1145706

# Frontiers in Genetics

**Highlights genetic and genomic inquiry relating to all domains of life**

The most cited genetics and heredity journal, which advances our understanding of genes from humans to plants and other model organisms. It highlights developments in the function and variability of the genome, and the use of genomic tools.

---

## Discover the latest Research Topics

See more →

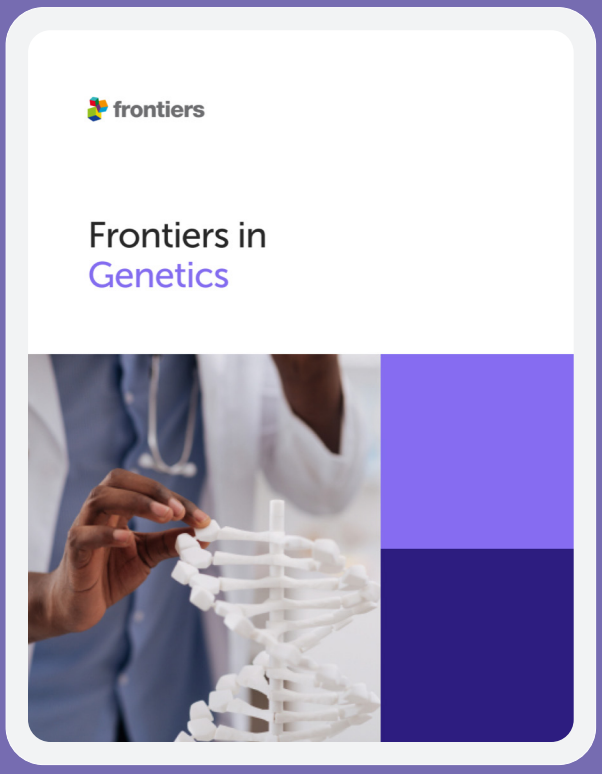


**Frontiers**

Avenue du Tribunal-Fédéral 34
1005 Lausanne, Switzerland
frontiersin.org

**Contact us**

+41 (0)21 510 17 00
frontiersin.org/about/contact